Estimating regional as well as local parameters controlling seismic hazard scenario of the Shillong Plateau

Submitted for the degree of

DOCTOR OF PHILOSOPHY

by

Olympa Baro

DEPARTMENT OF CIVIL ENGINEERING

INDIAN INSTITUTE OF TECHNOLOGY GUWAHATI

GUWAHATI-781039

September-2018

Dedicated to my parents

Naren Chandra Baro and ***Binita Thakuria***

&

my dearest husband

Kaushik Handique

Statement

I do hereby declare that the matter embodied in this thesis is the result of investigations carried out by me in the Department of Civil Engineering, Indian Institute of Technology Guwahati, Guwahati, Assam, India.

In keeping with the general practice of reporting scientific observations, due acknowledgements have been made whenever the work described is based on findings of other investigators.

Place: IIT Guwahati — Olympa Baro

Date: 1st September 2018 — (Enroll no. 146104022)

Certificate

This is to certify that the thesis entitled *"Estimating regional as well as local parameters controlling seismic hazard scenario of the Shillong Plateau"* being submitted by Ms. Olympa Baro, Enrollment number 146104022, to the Indian Institute of Technology Guwahati for the award of the degree of *Doctor of Philosophy* is a record of bonafide research work carried out by her. The thesis work in my opinion has reached the requisite standard for the degree of *Doctor of Philosophy*.

The results embodied in this thesis have not been submitted in any other University/Institute for the award of any Degree or Diploma.

Date:

Place: Guwahati

Dr. Abhishek Kumar
Assistant Professor
Indian Institute of Technology Guwahati,
Assam, India-781039

Acknowledgement

The completion of my PhD research work has been made possible by the generous and unobstructed support from numerous people. I take this opportunity to extend my most sincere gratitude to each and everyone for their unyielding support.

I would like to first of all thank the Indian Institute of Technology Guwahati (IITG) for providing me with an intellectually apt environment to carry out my PhD research. I would also be forever grateful for the financial support provided by the institute.

PhD research for a novice student could be daunting. The guidance provided by the supervisor acts as a guiding light to show the path ahead. For my PhD research, my guiding light has been my supervisor, **Dr. Abhishek Kumar** to whom I express my most sincere and heartfelt gratitude. It has been an honor to be his first Ph.D. student. I appreciate all his contributions of time, ideas and funding to make my Ph.D. experience productive and intellectually stimulating. The passion and enthusiasm he has for his research was contagious and motivational for me, throughout the duration of my PhD work. I am also thankful for the excellent example he has set as a successful geotechnical engineer and professor. His guidance helped me in the time of research and writing of this thesis. I could not have imagined having a better supervisor and mentor for my PhD.

Besides my supervisor, I would also like to thank the rest of my Doctoral committee: **Dr. A. Murali Krishna, Dr. Vinayak Kulkarni** and **Dr. Indu Siva Ranjani G**, for their insightful comments and encouragement, but also for the tough questions, which motivated and inspired me to widen my research from various perspectives.

I gratefully acknowledge the funding from INSPIRE Faculty grant by the Department of Science and Technology, Government of India with my supervisor, towards my Ph.D. research.

I would also like to express my gratitude to the many friends and groups that became a part of my life during my stay in the Indian Institute of Technology Guwahati. I am grateful for their help and support.

Lastly, I would like to thank my parents for all their love and encouragement. I would also like to thank my in-laws for being understanding and supportive. Last but not the least, I would like to extend a special note of thank you to my husband *Kaushik*, who has always been a source of solace and support in the moments of fear or doubt.

Olympa Baro

Abstract

The tectonic plate setup of the crust of the earth makes almost every place on the earth's surface susceptible to earthquake (EQ) occurrences. The places located in the boundary regions of the tectonic plates tend to be more susceptible to EQs due to the continuous tectonic movement. The northeastern region of India is one such region, which is located along not one but two such tectonic plate boundaries. Towards north of the northeastern region is the Eurasian-Indian tectonic plate boundary. Along this plate boundary, the Indian plate is colliding and subducting under the Eurasian tectonic plate. Similar collision is occurring towards the eastern boundary of India, along the Indo-Burmese plate boundary. The collision and subduction process of the tectonic plates began approximately 60 million years ago and is still very much active. As a result of which, the north-eastern region has become a very seismically active region of the world. This tectonic movement has also resulted in the occurrence of several crisscrossing faults within the region. These faults have been responsible for two great EQs in the region namely, the 1897 Assam EQ (M_W-8.1) and the 1950 Assam EQ (M_W-8.7). The movement along the several faults located within the region has also resulted in the formation of the Shillong Plateau (SP) in the southwestern part of the northeastern region. The SP comprises of the Indian state of Meghalaya, which is further sub-divided into 11 districts. The SP is surrounded by the Oldham, Kopili, Dauki and Dhubri faults. Each of these faults has generated EQs in the past which have caused damages in the SP and surrounding areas. Present study aims at understanding the location and orientation of the faults surrounding the plateau. In order words, this study aims at characterizing the seismic sources located in the vicinity of the SP. Hence a seismotectonic province of 500km radius is developed around the SP for identifying and characterizing the potential seismic sources. In support of existing literature as well as past EQ data, comparison of the entire seismotectonic province in terms of past seismicity, tectonic features, geology, thickness of overburden, rupture characteristics, rate of movement and focal depths of EQs is done in the present work. Based on these comparisons, the seismotectonic province is divided into four seismic source zones; 1)

the SP-Assam Valley Zone (SP-AVZ); 2) the Indo-Burma Ranges Zone (IBRZ); 3) the Bengal Basin Zone (BBZ) and 4) the Eastern Himalaya Zone (EHZ). EQ catalogues for each source zone is analyzed for completeness of magnitude and time. Seismic parameter 'b' estimated using maximum likelihood method are found as 0.91±0.03 0.94±0.02, 0.80±0.03 and 0.89 ± 0.03 for SP-AVZ, IBRZ, BBZ and EHZ respectively. The SP-AVZ shows relatively high recurrence rate for 1000 years period. Based on 'b' value and return period, SP-AVZ is found as the zone of high hazard. The maximum potential magnitudes (M_p) that could be generated by the individual faults are estimated. The M_p values are then employed into the Ground Motion Prediction Equations (GMPEs) developed by Toro (2002), NDMA (2010) and Anbazhagan et al. (2013) to perform DSHA. It is observed in this study that variation in hypocentral distance, affects the weights of applicable GMPEs for different sites within the SP. Hence, DSHA is performed for three districts of Meghalaya located within the SP, namely the East Khasi hills, the Ri-Bhoi and the West Garo hills districts rather than the entire plateau. From the DSHA maps it is observed that the northern part of East Khasi hills & West Garo hills and eastern part of Ri-Bhoi districts exhibit the highest PHA values of 0.46g at bedrock level. For Shillong city, Nongpoh and Tura the observed PHA values are 0.36g, 0.46g and 0.33g respectively. The Barapani fault is found to be responsible for the high PHA values within the East Khasi hills and Ri-Bhoi districts. Whereas in the West Garo hills district the Oldham fault gives high PHA values. In addition, obtained response spectra for Shillong city, Nongpoh and Tura indicate the maximum spectral acceleration reaches 0.67g, 0.77g, and 0.64g at 0.1s respectively. PSHA is also performed for the three districts of the East Khasi hills, the Ri-Bhoi and the West Garo hills. In PSHA, similar to DSHA the northern side of East Khasi hills and eastern side of Ri-Bhoi show the highest PHA values. For 2% probability of exceedance with exposure time of 2475 years the highest PHA values at Shillong city and Nongpoh located within the East Khasi hills and Ri-Bhoi districts respectively are estimated as 0.30g and 0.46g respectively. Similarly for 10% probability of exceedance with exposure time for 475 years the highest PHA values at Shillong city and Nongpoh are estimated as 0.20g and 0.33g respectively. Hazard curves developed in this study show that the Barapani fault is responsible for the high PHA values. For the West Garo hills

district however, the southern part shows highest PHA values. For Tura at 2% and 10% probabilities of exceedance the estimated PHA values are 0.22g and 0.13g respectively. Hazard curves developed for Tura in the West Garo hills district show that Dauki and Dhubri faults are responsible for the high PHA values. The difference in DSHA and PSHA results for the West Garo hills district is due to affect of the Oldham fault, which is a source of high seismic hazard with very low probability of EQ occurrence during the design life of a structure. Thus, even though Oldham fault had caused worst seismic scenario as highlighted in DSHA, probability of occurrence of EQ during the design life is very less as observed from hazard curves based on PSHA. Uniform hazard spectra are developed for Shillong city, Nongpoh and Tura which give spectral acceleration values of 0.30g, 0.46g and 0.22g at 2% probability of exceedance respectively and 0.20g, 0.33g and 0.13g at 10% probability of exceedance respectively for 0s. Uniform hazard spectra developed for 50% probability of exceedance at 0s, gives spectral acceleration values of 0.11g, 0.18g and 0.06g at Shillong city, Nongpoh and Tura respectively. Finally, response of local soil in the SP is assessed indirectly by considering different EQs at selected sites in the absence of in situ sub soil characteristics. It is found that since the sites are mostly rocky the ground motion amplification is very less within the SP.

Contents

List of Figures

List of Tables

List of Symbols

$\ln(z)$	Ground motion parameter
$\acute{F}$	Cumulative of a truncated normal distribution
L_0	Length of fault assumed outside of the actual length of fault
M_w	Moment magnitude
$\sum N$	Summation over all (N) seismic sources
m_{min}	Minimum magnitude
m^0	Lower bound magnitude of interest to the calculation
m_0	Certain magnitude value
m^u	Maximum magnitude event that can occur on the source
n_0	Largest seismic events
r_j	Distance from the site
t_0	Certain time interval
v_β	Vectorconsisting of the coefficients of variation of the unknown $\bar{\beta}$
v_λ	Vectorconsisting of the coefficients of variation of the unknown $\bar{\lambda}$

w_j	Weight of GMPE model
x_i	Number of EQ events in a unit time interval
$\bar{\beta}$	Mean value of parameter β
ε_a	Aleatory uncertainty
ε_e	Epistemic uncertainty
$\bar{\lambda}$	Mean value of the activity rate
σ_λ	Standard deviation
μ	Mean (expectation) of the normal distribution
C_β	Normalizing co-efficient of β
E_f	Expected value from a given model
f	Probability distribution resembling “true” observations
g	Probability distribution representing a selected GMPE model
m_{max}	Regional maximum magnitude
M_{obs}	Maximum observed EQ magnitude
M_p	Maximum possible magnitude
R_{JB}	Joyner-Boore distance

T	Sample length
β	2.303b
σ^2	Variance
$E[ln(z)]$	Mean log ground motion level given by the GMPE
L	Length of the fault
R	Minimum distance from the site to the fault rupture,
$S[\ln(z)]$	Standard error of the log of ground motion level obtained from the GMPE
$X(m_i)$	Rupture length in kilometers for the event of magnitude m_i
Z	Ground motion level
a	Seismic activity of a region
b	Relative likelihood of large and small EQs
$\alpha(m^0)$	Frequency of occurrence of events of magnitude m^0 and larger
λ	Unbiased mean
$\lambda(m_i)$	Annual frequency of occurrence of EQs of magnitude m_i (above a certain minimum size of EQ) on seismic source n

List of Abbreviations

AD	Anno Domini
AF	Amplification Factor
AVZ	Assam Valley Zone
BBZ	Bengal Basin Zone
BNS	Bangong Nujiang Suture
BSSC	Building Seismic Safety Council
BTF	Bame Tutin Fault (BTF)
CMF	Churachandpur–Mao Fault
CNDM	Centre for Natural Disaster Management
COSMOS	Consortium of Organization for Strong Motion Observation System
CWPRS	Central Water and Power Research Station
DBF	Debagram-Bogra Fault
DSHA	Deterministic Seismic Hazard Analysis
DSI	Data Support Index
DSRC	Dynamic Soil Response Curve
EBZ	Eastern Boundary Zone
EHZ	Eastern Himalayas Zone
EMS	European Macroseismic Scale
EPRI	Electric Power Research Institute
EQ	Earthquake
GKF	Garhmayna–Khanda Ghosh Fault
GMPE	Ground Motion Prediction Equations
GPS	Global Positioning System

G-R	Gutenberg-Richter
GSHAP	Global Seismic Hazard Assessment Program
GSI	Geological Survey of India
HFT	Himalayan Frontal Thrust
IBRZ	Indo-Burma Ranges Zone
IITR	Indian Institute of Technology Roorkee
IMD	India Meteorological Department
ISR	Institute of Seismological Research
IST	Indus Suture thrust
JGF	Jangipur–Gaibandha Fault
KNF	Katihar Nailphamari fault
LLH	Log Likelihood
MAXC	Maximum Curvature Method
MBT	Main Boundary Thrust
MBZ	Mishmi Block Zone
M_C	magnitude of completeness
MCT	Main Central Thrust
M_L	Local magnitude
MMI	Modified Mercalli Intensity
m_{min}	Minimum Magnitude Threshold Limits
MRMF	Munger-Saharsha Ridge Marginal Fault
Mya	Million years ago
NDMA	National Disaster Management Authority
NEHRP	National Earthquake Hazard Reduction Program
NGRI	National Geophysical Research Institute

ONGC	Oil and Natural Gas Corporation
PDF	Probability Density Function
PF	Pingla Fault
PGA	Peak Ground Acceleration
PHA	Peak Horizontal Acceleration
PSHA	Probabilistic Seismic Hazard Analysis
R_{HYPO}	Hypocentral distance
R_{JB}	Joyner-Boore distance
RLD	Rupture Length
R_{RUP}	Rupture distance
SA	Spectral Acceleration
SBF	Sainthia–Bahmani Fault
SHZ	Shillong Zone
SP	Shillong Plateau
TP	Tibetan Plateau
TSI	Topographical Survey of India
UHS	Uniform Hazard Spectra
UNISDR	United Nations International Strategy for Disaster Reduction
USGS	United States Geological Survey

Chapter 1 - Introduction

1.1 Background

Earthquakes (EQs) are a form of natural hazards which are unpredictable in nature. This unpredictable nature of EQs makes them relatively more damaging compared to other forms of natural hazards. Historical records across the world provide proof of the damaging nature of EQs, one such example is the 1755 Lisbon EQ ($9.0 \leq M_L \leq 8.5$). This EQ generated a tsunami destroying several monasteries, convents and the Royal Palace (Maxwell 2006). As per Zitellini (1999) the 1755 Lisbon EQ had killed 10,000 people out of which 1000 casualties were caused by the tsunami. The 1783 Calabria EQ is another European EQ which had caused landslides, liquefaction and subsidence. Thirty thousand people were reportedly killed by this EQ (Galli and Bosi 2002). These damage reports of the past EQs bring to light the seismically active regions of Europe. In Asia, Japan is a highly seismic region with immense reports of damaging EQs. One such EQ is the 1923 Kanto EQ (M_W-7.9) which had caused major devastations in the city of Tokyo and Yokohama and killed approximately 140000 people (Pollitz et al. 2005). The 1964 Niigata EQ (M_W-7.5) of Japan damaged somewhere around 11,000 houses. Again in 1995 the Kobe EQ (M_W-6.9) hit Japan, causing sand boils, lateral movement and excessive settlement of the soil (Cubrinovski et al. 2001). In recent times, the 2011 Tohoku EQ (M_W-9.0) created tsunami which had killed 15,534 people (EERI 2011). The reason behind the high seismicity of Japan is due to the location of the country at the junction of several tectonic plates. The Himalayas is another region within Asia which is located at the junction of two plates, viz. the Indian and the Eurasian plates. The continuous tectonic movement between the two plates has made the Himalayas the main source of seismic activity in India. The Himalayas can be broadly divided into three segments the North-western & Western Himalaya, the Central & Eastern Himalaya and the Northeastern Himalaya (Kayal 2008). In 1555, the North-Western Himalaya was hit by a devastating EQ (Avouac et al. 2006). Based on the damage reports, the EQ magnitude was estimated to be greater than or equal to 8 (Bilham 2004). In 1803, another EQ ($M>7.0$) had occurred in the western Himalayas. According to

Dasgupta and Mukhopadhyay (2014), the 1803 EQ was felt across the Indo-Gangetic plains from the western to the eastern boundaries of the country. The upper stories of the Qutub Minar, situated in Delhi, were also damaged during this EQ (Dasgupta and Mukhopadhyay 2014). In 1905 the Kangra EQ (Ms-7.83) hit the Indian state of Himachal Pradesh located in the North-western Himalayas (Ambraseys and Bilham, 2000). As per (Thakur et al. 2000) at the epicentral zone, in Kangra, an intensity of X was reported on the Rossi-Forel scale. Another North-western Himalayan EQ is the 2005 Kashmir EQ (M_W- 7.6). The EQ had originated in the western syntaxis zone where the Himalayan arc meets the Karakorum, the Pamir and the Hindu Kush mountain ranges (Avouac et al. 2006). As per Avouac et al. (2006) the EQ caused severe damages and killed at least 80,000 people. The Central & Eastern Himalayan segment has also experienced several major ($7.0 \leq M_W \leq 7.9$) and one great ($M_W \geq 8.0$). The EQs which have originated in the Central & Eastern Himalayan segment, have mostly affected Nepal and the state of Bihar in India. The 1833 Nepal EQ ($7.5 < M < 7$), 1934 Bihar-Nepal EQ (M_L- 8.4) and the very recent 2015 Nepal EQ (M_W-7.8) are such examples. The 1833 Nepal EQ triggered a number of landslides and rock falls which blocked several of the passes to Tibet and built a temporary dam in the Kamla River. The natural dam broke after four days and flooded the nearby villages (Bilham 1995). During the 1934 Bihar-Nepal EQ the maximum damages were reported from the southern border of Nepal and the Monghyr town in Bihar, India (Pandey and Molnar 1988). In Nepal at several places the ground had slumped, tilted and fissured. In Bihar, India the local site effects due to the presence of thick alluvium soil caused extensive damage to the buildings. The 2015 Nepal EQ caused violent shaking which led to the destruction of several houses in the Himalayas. The death toll reported in Nepal from this EQ was 10,000. The seismicity of the North-eastern Himalayan segment is low compared to the other two sections of the Himalayas. In the North-eastern Himalayan segment only two significant EQs have occurred till date the first in 1941 near Tezpur, Assam ($M > 7.0$) and the second in 1947 in Arunachal Pradesh ($M_S > 7.7$) (CNDM).Very limited information is available about both the events. However, further east in the syntaxis zone of the Himalayas and the Indo-Burma ranges the tectonic movement of the plates had generated the 1950 Assam EQ (M_W-8.7). During this EQ maximum damages were caused in Upper Assam, the

Abor hills and the Mishmi Hills. Large fissures, landslides, liquefaction and formation of sand vents were reported at many places.

In comparison to the Himalayan segment, however, the rest of the north-eastern region of India has experienced high seismicity. Some of the damaging EQs that had occurred in this region include; before 600AD (M≥7.0), 700-1050 AD (M≥7.0),1450-1650 A.D (M≥7.0) (Sukhija et al. 2006), 1869 Cachar EQ(M_W-7.5), 1897 Assam EQ(M_W-8.1), 1923 Meghalaya EQ(M_S-7.1), 1930 Dhubri EQ(M_S-7.1), 1943 Assam EQ(M_S-7.2), 1947 Arunachal Pradesh EQ (M_S-7.7), 1950 Assam EQ(M_W-8.7), 1988 Manipur EQ(M_S-7.3), 2009 Assam EQ (M_W-5.1), 2011 Sikkim EQ (M_W 6.9) and the recent 2016 Imphal EQ(M_W-6.7). It has been observed that the sources of the majority of the above mentioned EQs are located towards the south western region of northeast India. As per Bilham and England (2001), movement along these faults also led to the formation of a plateau in the south western part of the region, known as the Shillong Plateau (SP). The SP is spread over approximately 25,000km^2 and comprises mostly of the Indian state of Meghalaya. Past EQs such as 1869 Cachar EQ, 1897 Assam EQ, 1923 Meghalaya EQ, the 1930 Dhubri EQ, 1943 Assam EQ and 2009 Assam EQ, which had originated in the faults around the SP, have caused intense and widespread damages. As per Oldham (1882), 1869 Cachar EQ caused significant damages to public and governmental buildings in Shillong and Nongpoh. Shillong and Nongpoh are located within the East Khasi hills and Ri-Bhoi districts of the state of Meghalaya respectively. The 1897 Assam EQ also caused wide spread damages. According to Bilham (2008), during the 1897 Assam EQ, many buildings were significantly damaged or destroyed in Shillong and in Cherrapunji, also located in the East Khasi hills district. In addition, numerous landslides were triggered by the same EQ in Nongpoh and Tura. Tura is located within the West Garo hills district of Meghalaya. Another damaging EQ for the SP was the 1930 Dhubri EQ. During this EQ, Cherrapunji and Shillong were shaken up to intensity VII (Rossi Forel scale) and in Tura up to intensity VIII; poor construction of the houses in Cherrapunji led to severe damages, even majority of government buildings had witnessed wall cracks leading to damage (Gee 1934).

From the above discussion, it is clear that past EQs have caused damages across the SP particularly at the sites of Shillong, Cherrapunji, Nongpoh and Tura. To prevent similar damages from future EQs, it is essential to understand the seismic hazard potential of the SP. However, till this date, seismic hazard analysis considering regional parameters has not been attempted for the SP in particular. In addition, most of the past studies performed for the northeastern region are limited to the seismic hazard assessment at the bedrock level, either due to limitations with ground motion records or subsoil properties or both. Hence, in this study, a regional level seismic hazard analysis at bedrock and a new methodology for indirect estimation of the soil response is attempted for the SP.

1.2 Organization of the thesis

This thesis is divided in seven chapters and a brief discussion on each of these chapters is given below.

Chapter 1 introduces the motivation behind the present work by providing a background for the purpose of this study. **Chapter 2** deals with the literature review done to understand the origin, tectonics and damages cause by EQs in the study area. The critical appraisal of the literature is also included in this chapter, based on which the objectives for the study are stated. **Chapter 3** presents the seismotectonic province developed for the SP by identifying the potential seismic sources located within a radius of 500km from the centre of SP. In addition, within this chapter, an attempt is made to understand the effect of the identified seismic sources on the seismic hazard potential of the SP. In **Chapter 4** the maximum possible EQ magnitude on each fault is estimated, based on an incremental method (an addition of a constant value to the maximum observed EQ magnitude). Numerous suitable Ground Motion Prediction Equations (GMPEs) are selected using the average sample log-likelihood (LLH) approach. As the variation in hypocentral distances can affect the ranks or weights of selected GMPEs, deterministic seismic hazard analysis (DSHA) is performed separately for the districts of East Khasi hills, Ri-Bhoi and West Garo hills of Meghalaya located within the SP. DSHA only provides the worst-case scenario without considering the uncertainties associated with EQ magnitude, hypocentral distance and ground motion exceedance of

a particular value at a site for a known exposure period. These shortcomings of DSHA are addressed by Probabilistic Seismic Hazard Analysis (PSHA) and hence in this study, PSHA is also performed for the districts of East Khasi hills, Ri-Bhoi and West Garo hills as presented in **Chapter 5**. Both the DSHA and PSHA performed in this study are at the bedrock level. Use of these hazard values is very limited until the response of the local soil is also taken into account. The quantification of local site effects needs a number of field and laboratory tests, estimation of dynamic soil properties and input bedrock motion for future EQs which is not readily available for the SP at present. Hence, in **Chapter 6,** the response of local soil is studied indirectly by taking into account the surface level of ground shaking during various past as well as recent EQs observed at different locations. **Chapter 7** summarizes major conclusions derived from the study.

Chapter 2- Literature Review

2.1 Introduction

The origin of the SP can be traced back to approximately 60 million years ago (Mya) when the Indian Plate was undergoing collision and subduction along the northern and eastern boundaries of present day India. There are several theories about the origin and uplift of the SP, one of the theories given by Khattri et al. (1983) suggest, that the plateau rose to the present height due to thermal disturbance in the upper mantle. In another theory Kailasam (1979) suggested that the SP had originated as a result of isostatic adjustment. However, the most popular theory for the origin of the SP is the popping up of the plateau due to tectonic movement along faults. This theory has gained popularity due to the presence of a number of faults in the close vicinity of the plateau. Simultaneously, the presence of these faults has led to a complex tectonic setting of the SP. The geological setup of the SP is also a very diverse one, consisting of an array of rocks formed in different geological eons. The geological and tectonic setup of the SP is discussed in details below.

2.2 Geology of the Shillong Plateau

The SP is an isolated Precambrain (4,600-541 Mya) cratonic block of the Indian plate. This cratonic block was formed as a result of tectonic detachment of the SP from the Indian plate by the Garo-Rajmahal tectonic graben (Kakati 2015). This turned the SP into a horst consisting of an assortment of rock formations from different geological time periods. As per Kakati (2015) the geological time scale of rock formations in the SP range from the Archean - Proterozoic (4000 to 541 Mya) to the Pleistocene (2,588,000 to 11,700 years ago). The major rock formations found in the SP are Cretaceous–Tertiary (145.5-2.588 Mya) sediments, the Sylhet trap, Lower Gondwana rocks, Shillong Group of rocks, Precambrian gneissic complex (Basement gneiss) (http://megdmg.gov.in/features.html). The Precambrian basement gneisses of the SP comprises of amphibolite–granulite rock, which is unconformably overlain by the Shillong Group. The Shillong group was formed of greenschist facies intra-cratonic

sandy and clayey rocks (Nandy 2001). The Sylhet Traps are the youngest igneous rocks found within the SP which cut across all the previous magmatic and metamorphic rock. The Cretaceous –Tertiary sediments were deposited in the southern and eastern peripheries of the SP which were later uplifted (Kakati 2015).

2.3 Tectonic setting of the Shillong Plateau

The formation of the SP through the different geological eons and the ongoing plate tectonic movements has led to the development of a series of faults surrounding the plateau. The SP is bounded in the south by the east-west trending 320km long Dauki fault as shown in Figure 2.1. According to Murthy et al. (1969), the Dauki fault is a system of four faults, which dip towards north on surface level and then continue further below the surface. However as per Srinivasan (2003), the Dauki fault is a south dipping normal fault with a strike slip component. Further, as per Srinivasan (2005) the Dauki fault is a single fault and not a system of faults. A northwest extension of the Dauki fault is the Dapsi thrust (Figure 2.1) which exists within the plateau along the northwest-southeast direction and is 90~100km long. It is a reverse fault with a strike slip component (Kayal 2008). The Dapsi thrust acts as a boundary between the SP and the alluvial plains to the southwest of the plateau. To the west of the SP, lies the north south trending Dhubri fault as shown in Figure 2.1, this fault was the source for the 1930 Dhubri EQ. Figure 2.1 also shows the south dipping reverse fault called the Oldham fault which lies to the north of the SP (Bilham and England 2001). According to Bilham and England (2001), the SP was uplifted due to the movement along the Oldham fault and the Dauki fault. With the help of geodetic and GPS data, Bilham and England (2001) found that the 1897 Assam EQ had originated as a result of 16m slip along the Oldham fault. However, Rajendran et al. (2004) questioned the existence of the Oldham fault and suggested that the SP was instead uplifted due to the presence of the Brahmaputra fault and the Dauki fault. As per Rajendran et al. (2004), the Brahmaputra fault lies further north of the SP in the alluvial plains of the Assam Valley. The Assam Valley extends from north-northeast to southeast of the SP, and was formed as a result of the sediments carried by the rivers Brahmaputra and Barak. A prominent fault of the SP- Assam Valley region is the Kopili fault (Figure 2.1). This fault is 300-

400km long and 50km wide extending in the north up to the Main Boundary Thrust (MBT) in the Himalayas. As per Kayal et al. (2010), the Kopili fault is a strike slip fault with a dip in the northeast direction. The Kopili fault was the source for the 1869 Cachar EQ and the 1943 Assam EQ. Kumar et al. (2016) had conducted paleoseismic investigations along the Kopili fault and found that apart from 1869 Cachar EQ and 1943 Assam EQ, three other major EQs ($7.0 \leq M_W \leq 7.9$) had also occurred along this fault. Kumar et al. (2016) concluded that the Kopili fault has been seismically active since the past 900 years. According to Kayal et al. (2010), the Kopili fault is at present an active fault of the SP- Assam Valley region. Other faults in and around the SP include Samin fault, Dudhnoi fault, Barapani fault and Kulsi fault (Angelier and Baruah, 2009; Kayal et al. 2006) as shown in Figure 2.1.

2.4 Uplift of the Shillong Plateau

The above discussion clearly highlights the complex tectonic setting of the SP, which helps support the theory of uplift by tectonic movement. However, the existence of a number of faults has also led to various opinions about which faults were actually responsible for the uplift of the plateau. Several researchers have given different views on the uplift of the SP which are discussed in this section.

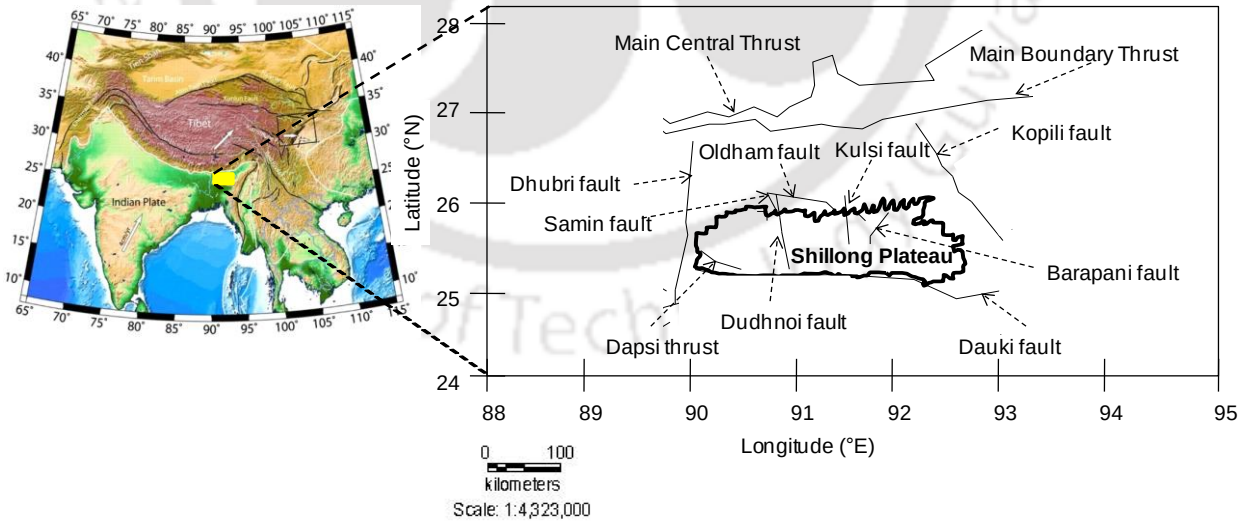

Figure 2.1: Seismic sources located in the vicinity of the Shillong Plateau

Kayal (1987) and Kayal et al. (2006) performed microearthquake studies in the SP and Assam Valley during the periods 1982-1984 and 2001- 2003 respectively to study the complex tectonic model of the SP. As per the above studies, the seismicity was found to be highest in the western part of the SP. Kayal et al. (2006) concluded that the uplift of the SP was due to the Dapsi thrust in the west and the Brahmaputra Fault. The fault plane solutions obtained by Kayal et al. (2006) inferred that the Dapsi thrust and the Brahmaputra faults were the two boundary faults of the SP. The sections taken along the depth of the SP and the fault plane solutions for the EQs recorded revealed that the north-east dipping Dapsi thrust in the western part of the plateau is seismically active.

In another study performed by Rao and Kumar (1997), it was proposed that the complex tectonic setting of the SP had lead to compressive forces which resulted in "pop-up" mechanism of the SP. Further, Rao and Kumar (1997) suggested that the "pop-up" structure was facilitated by the Dauki fault in the south, the Brahmaputra fault in the north, the Dhubri fault in the west and the Disang thrust in the east of the SP.

Bilham and England (2001) proposed another theory for the uplift of the SP. According to Bilham and England (2001), the Himalayas in the north and the thick sediments of the Bengal Basin to the south and east of the SP had added weight to the region around the plateau. Along with this, the westward movement of the Indo-Burma range towards the Bengal Basin added more weight to the Indian plate resulting in flexure of the Indian Plate below the SP. In order to relieve these bending stresses, the Indian plate popped-up between two faults, the Oldham fault to the north and the Dauki fault to the south. As per Bilham and England (2001), the Oldham fault is a 110km long, 57° south dipping reverse fault beneath the northern edge of the SP. With the help of geodetic and GPS data Bilham and England (2001) concluded that the 1897 Assam EQ had occurred as a result of slip of 16m along the Oldham fault. As a result, the northern edge of the SP had risen by 11m during 1897 Assam EQ. Bilham and England (2001) also concluded that the return period for EQs similar to 1897 Assam EQ in the SP is 3000 years.

According to Rajendran et al. (2004), the Oldham fault does not exist and the SP was uplifted by the Brahmaputra and the Dauki faults. The Brahmaputra fault lies to the north of the SP and was the source of the 1897 Assam EQ (Rajendran et al. 2004). Rajendran et al. (2004) conducted gravity survey and observed a gravity anomaly ranging from -80 to -200 mGal in the Assam Valley. This variation in the gravity anomaly was concluded to be due to the Brahmaputra fault. Rajendran et al. (2004) also conducted paleo-liquefaction studies near Dilma and Jira in the Assam Valley. The paleo-liquefaction studies showed that the area had undergone multiple liquefactions during previous EQs indicating the presence of a fault (the Brahmaputra fault) within the river basin. Rajendran et al. (2004) also found several other historical records as indications of past EQ damages in the Assam Valley. On the basis of the gravity survey, paleo-liquefaction studies and historical evidences, Rajendran et al. (2004) suggested that EQs similar to 1897 Assam EQ must have occurred in the Assam Valley due to the Brahmaputra fault. Rajendran et al. (2004) also suggested that the return period of great EQs in the Assam Valley is approximately 1200 years, contradicting the speculative time of 3000 years as suggested by Bilham and England (2001).

Morino et al. (2011) however did not agree with the findings of Rajendran et al. (2004) and pointed out that the variation in the gravity anomaly found below the Assam Valley was too weak and did not support the presence of the Brahmaputra fault. Morino et al. (2011) also concluded that the paleo-liquefaction associated with the 1897 Assam EQ had occurred on both north and south sides of the SP. Hence, the claim of Rajendran et al. (2004) that the Brahmaputra fault was the cause of the maximum intensity in the Assam valley was found questionable by Morino et al. (2011). Later, Sukhija et al. (2006) also raised doubts about the presence of Brahmaputra fault. Sukhija et al. (2006) highlighted that the existence of the Brahmaputra fault was deduced without taking into account the triangulation studies done after the 1897 Assam EQ (Strahan 1891; Bond 1899; Burrard 1909; Wilson 1939). The triangulation studies had stated that no slip had occurred during the 1897 Assam EQ at the present day proposed location of the Brahmaputra Fault. Further, according to Sukhija et al. (2006), there exists no remote sensing evidence of the Brahmaputra fault to support the work by Rajendran et al. (2004).

In another study, Srinivasan (2003) performed remote sensing surveys to understand the mechanics behind the uplift of the SP. In the digital images obtained from remote sensing survey, it was found that the eastern and western parts of the SP are at a higher topographic level than the central part. The eastern part of the SP was found to be at a height of 1200m to 1900m and the western part at 1200m to 1400m, whereas in the central part, the topographic height drops to approximately 300m. Srinivasan (2003) also observed that the density of tectonic fractures in the central portion of the SP is relatively higher than in the eastern and western parts. From these observations, Srinivasan (2003) concluded that the SP had undergone differential uplift in the eastern and western portions with respect to the central part. This differential uplift of the plateau was assumed to be caused by the vertical movement of deep seated faults trending perpendicular to the Oldham fault of Bilham and England (2001). The remote sensing studies conducted by Srinivasan (2003) did not support the existence of any major faults in the northern boundary of the SP. Hence, the uplift of the plateau was solely inferred to be due to the differential uplift.

2.5 Damages in the Shillong Plateau due to historic as well as recent EQs

The intricate network of faults in the SP has not only led to difference in opinions about the origin and uplift of the plateau, but also have been the source of several EQs in the past. Well documented reports on the EQ damages that have occurred since the 1869 Cachar EQ is available. However very little to no information is available about the EQs that had occurred prior to the 1869 Cachar EQ. Only historical and archaeological records shed some light on the occurrence of EQs in and around the SP, in terms of the damages to the structures of those times.

To obtain more information about EQs that had occurred prior to1869 Cachar EQ, several researchers have conducted paleo-liquefactions in the vicinity of the SP. One such study was conducted by Sukhija et al. (1999a) and Sukhija et al. (1999b). The paleo-liquefaction studies were conducted at various sites in the valley of the Krishnai and the Dudhnai rivers. The first site was at Jira south of the Krishnai River, where at a depth of 8m, Sukhija et al. (1999a) and Sukhija et al. (1999b) found 30cm thick sand dykes breaking into the overlying clay layer of 1m height. The samples collected from

this clay layer supported the occurrence of a "Modern" EQ approximately ≤50 years ago. Similar results were obtained from the Ronghaminchi site in Meghalaya. The corresponding EQ for these alterations was deduced to be the 1897 Assam EQ. At another site at Bedabari, near the Krishnai River, clear signs of shaking and faulting of alternating clay and sand subsurface layers were found. At the Kharidhara site, sand dykes of 2m height intruding the silt layer above the sand reservoir were found. At the Dainadubi site, along the Dudhnai River, organic samples were found at sedimentary beds, which had deformed due to seismic shaking. Testing all the samples from the sites of Bedabari, Kharidhara and Dainadubi, Sukhija et al. (1999a) and Sukhija et al. (1999b) concluded that a major EQ had occurred during 1450-1650 AD. Samples were also collected from Beltaghat near the Krishnai River where, Sukhija et al. (1999a) and Sukhija et al. (1999b) found evidence of another major EQ dating back to 700-1050 AD. Carbon dating of two dead tree trunks found buried underground at the bank of the Mora-Krishnai River and another from the Mendipathar area further supported the occurrence of this event. At a site located 200m downstream of Beltaghat, Sukhija et al. (1999a) and Sukhija et al. (1999b) found a peat sample, which upon examination indicated another major EQ that had occurred before 600AD. Based on these findings, Sukhija et al. (1999a) and Sukhija et al. (1999b) concluded from the paleo-liquefaction studies that the SP has experienced three major EQs and one great EQ till date. The first major EQ dates before 600A.D, the second EQ during 700-1050 A.D and the third EQ during 1450-1650 A.D. Based on these results, Sukhija et al. (2006) concluded that the return periods of major and great EQs in the SP is 400-600 years and 500 years respectively.

Similar to the above studies, in another attempt, paleo-liquefaction studies were conducted by Rastogi (1993) wherein, four trenches 5-10m long, 4-5m wide and 5m deep were dug. The first trench was located 0.5km south of Jira, where Rastogi (1993) found a sand dyke from a dried riverbed. The sand dyke was found to intrude the upper alternate layers of sand and clay. This observation was confirmed by the second trench dug by Rastogi (1993) near the first trench. The third trench was dug further south of the first two trenches. In the third trench, inclined sand dykes which had cut through alternating sand and clay layers were found. As a result, slumping of clay layers was

observed. The fourth trench was dug near Mendipathar, Meghalaya where a dead tree trunk at a depth of 4m below the ground surface was found. Based on carbon dating of the tree trunk, it was found that the tree had died 1200 to 1300 years ago. Further, at the base of the trench, a dried river bed consisting of alternating clay and sand layers was found. The study of the sand dykes and the slumping of the clay layers indicated the occurrence of liquefaction phenomenon in the area due to major to great EQs in the past. From the field investigations, Rastogi (1993) concluded that the presence of the sand dykes in all the four trenches and the finding of a 1200 year old dead tree was a clear indication of occurrence of a major to great EQ approximately 1200±100 years ago in the SP region.

These discussions are related to various investigations in general performed by different researchers highlighting the occurrence of EQs in prehistoric times (1000 AD or before). Detailed discussion about the observed damage scenario from 1869 Cachar EQ onwards is presented in the sections below.

2.5.1 1869 Cachar EQ

The 1869 Cachar EQ (M_W-7.5), had originated 9.4 km north of Kumbhirgram, Assam (CNDM). The rupture area of this EQ was found to be located within the Kopili fault (Dasgupta, 2011). This EQ caused wide spread damages extending from Dibrugarh in the north, to Manipur in the east, Patna in the west and Kolkata in the south. Damages due to this EQ were reported by Captain Godwin-Austen, surveyor of Topographical Survey of India (TSI) and by Thomas Oldham, the Superintendent of the Geological Survey of India (GSI) under the British rule (Austen 1869; Oldham 1882). In Guwahati, Assam clear cracks were visible on the walls and arches of the city jail (Oldham 1882). Brick buildings in the city had also undergone damages. In the Khasi Hills to the west of Shillong city in Meghalaya, public buildings had undergone moderate to severe damages. The arches and the walls of the Overseer's bungalow and Deputy Commissioner's courthouse were cracked. Oldham (1882) also reported of severe shocks in Nongpoh which is located 48km south of Guwahati city. Damage reports collected by Oldham (1882) from Manipur highlighted the complete damage of the Manipuri King's two-storied brick house. Ground fissures and sand vents were

reported, along the banks of the Jiri River in Assam and the Surma River in Bangladesh as shown in Figure 2.2. Austen (1869) reported that the river Barak had flowed backwards for almost an hour and the depth of the river bed became shallower due to this EQ. A number of ground fissures and sand vents were also reported to have occurred in this area. Figure 2.3 present a typical case of ground fissures occurrence during 1869 Cachar EQ.

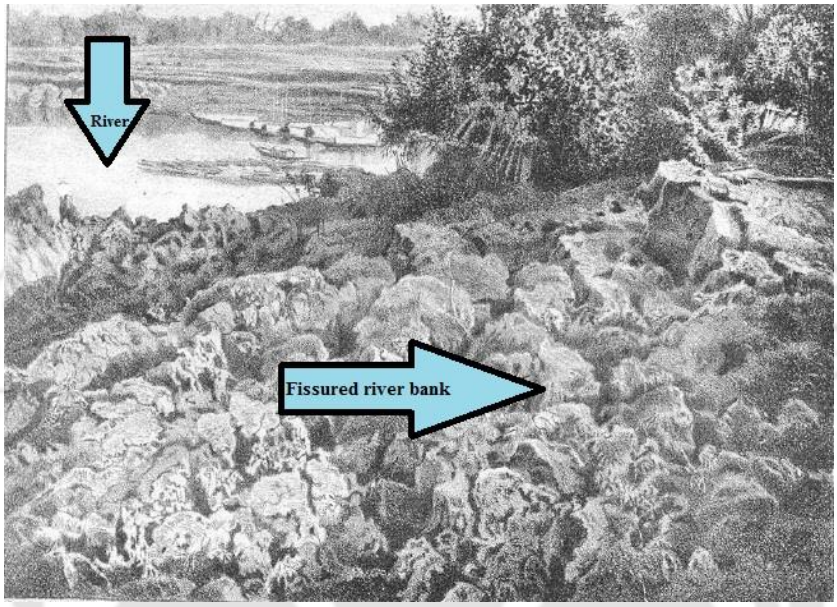

Figure 2.2: Fissured ground on a river bank after the 1869 Cachar EQ (modified after Oldham 1882)

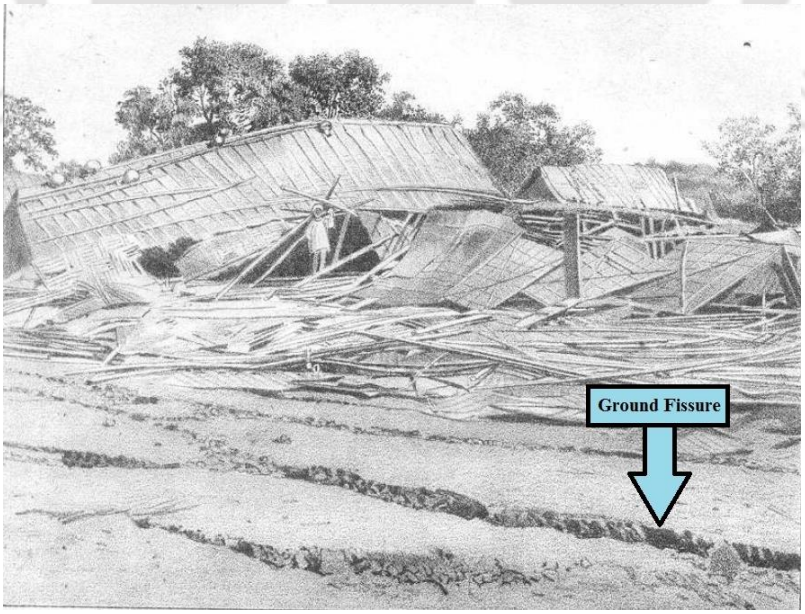

Figure 2.3: Fissures seen on the bazaar road in Cachar after the 1869 Cachar EQ (modified after Oldham 1882)

2.5.2 1897 Assam EQ

On 12th June 1897, the SP and its neighboring areas were hit by an intraplate EQ. Estimated magnitude of this EQ as per Bilham and England (2001) was Mw 8.1. This EQ was powerful enough to cause damage to buildings located in Kolkata and triggered seiches in Myanmar. The shaking due to this EQ was felt at several places across the Indian subcontinent (CNDM). Large fissures of 18 to 30m length ran parallel to the banks of the Brahmaputra River and its various tributaries. The Dhubri bazaar in Dhubri, Assam was severely affected by fissuring. East of Dhubri at Rowmari, sand vents had formed which ejected sand and mud up to a height of 1m above the ground level (Oldham 1899). A typical case of sand vents reported at Rowmari during this EQ is shown in Figure 2.4. The EQ had occurred at the peak of the monsoon season which had increased the number of sand vents and liquefied sites. The monsoon season also caused flooding and landslides at several places throughout the Assam Valley. The water level in the Brahmaputra River had risen to a height of 7.6m along with a reversal in the flow direction during this EQ. Due to liquefaction; the abutments of the bridge on Grand trunk road west of Guwahati were moved forward while one of the piers was tilted over. Shaking from the EQ, also gave rise to standing waves in the Brahmaputra River up to a height of 3m above the existing water level. As a result, the bazaars and the houses along the banks of the rivers were flooded (Oldham 1899). Numerous landslides were reported at Nongpoh and Tura in Meghalaya (Bilham 2008). At Tura most of the masonry houses were severely damaged due to collapse of the masonry plinth. The ground had cracked and slid at places blocking water courses and forming lakes at various locations. As per Bilham (2008), fissures and landslides occurred along the Guwahati-Shillong road turned the houses and bridges in these areas to rubble. According to Bilham (2008) in Shillong city, the bazaar, masonry houses, Government house, local church and the Telegraph Office were destroyed. In Cherrapunji, similar damages to the houses, roads and tombstones had occurred and 500 to 600 people died mainly due to landslides (Bilham 2008). Due to the severe damages reported in the SP during this EQ, Ambraseys and Bilham (2003) attributed an intensity of X on the Rossi-Forel scale to the plateau.

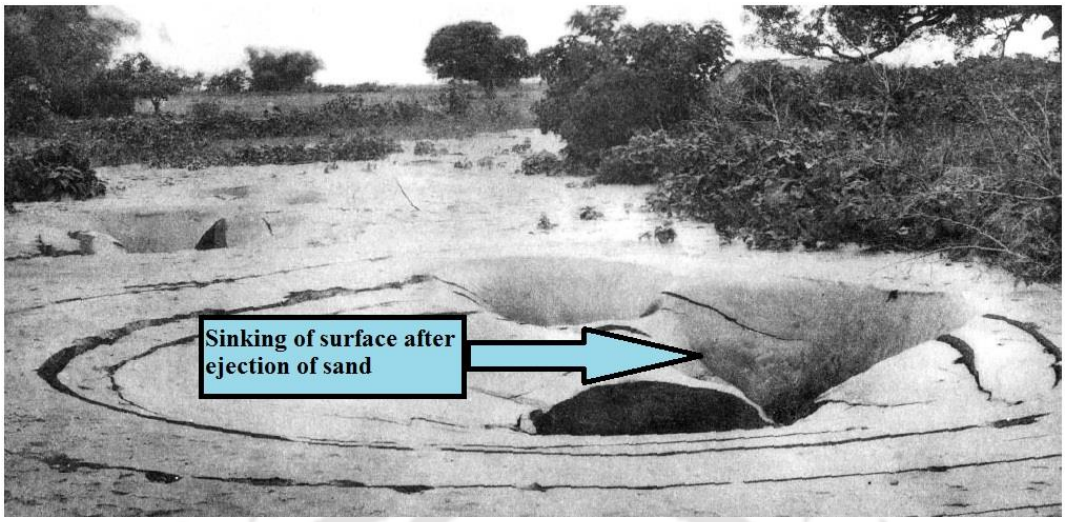

Figure 2.4: Sand vents created near Rowmari after the 1897 Assam EQ (modified after Oldham 1899)

2.5.3 1923 Meghalaya EQ

The 1923 Meghalaya EQ (M_S-7.1) had occurred on the Dauki fault (CNDM). Very limited information is available about this EQ. The intensity of this EQ was felt across the state of Meghalaya, at Sivasagar and Borjuli in Assam and Nagrakata in West Bengal. Towards south the shaking was felt across Srimangal, Barisal, Chittagong, Midnapore and Narayanganj in Bangladesh. Heavy damages were also reported in Mymensingh in Bangladesh, and Cherrapunji& Guwahati in India (CNDM).

2.5.4 1930 Dhubri EQ

The 1930 Dhubri EQ (M_S-7.1) had originated in the Dhubri fault (Kayal 2008). The intensity of this EQ was felt from Dibrugarh and Manipur in the east, Kolkata in the south, Patna in the west and Nepal, Bhutan and Sikkim in the north (Kayal 2008). The damages that occurred during this EQ were reported by Gee (1934). As per Gee (1934), the Dhubri town lying in close proximity to the Dhubri fault, was the worst affected region. The Dhubri town experienced an intensity of IX on the Rossi Forel scale. Tura in Meghalaya, south of Dhubri in the SP, was shaken with an intensity of VIII. Most of the government buildings were affected; some suffered minor damages like cracked walls as shown in Figure 2.5 and peeling of plasters off the walls while others underwent severe damages. In Gauripur near Dhubri, fissures and sand vents were observed as shown in Figure 2.6. As per Gee (1934) Goalpara and Guwahati in Assam

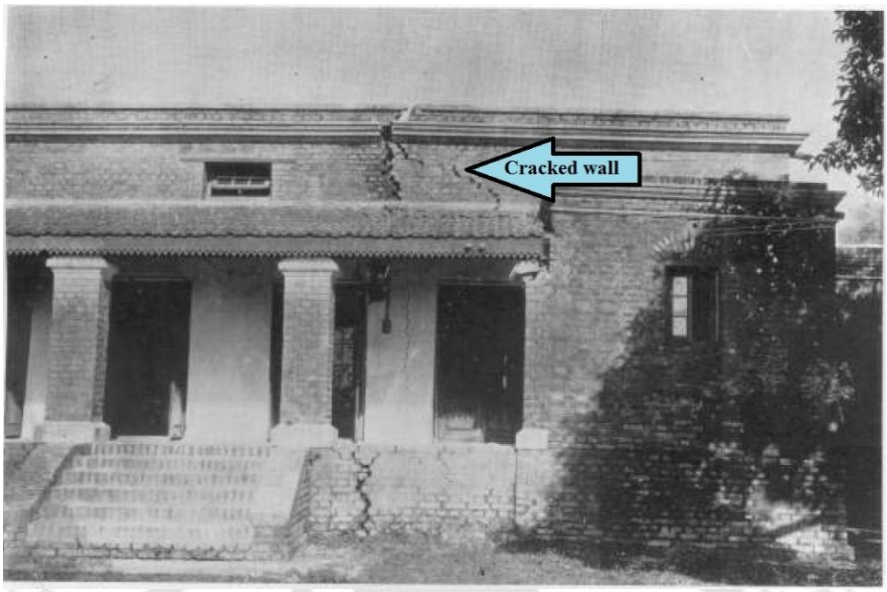

Figure 2.5: Walls of houses cracked after the 1930 Dhubri EQ (modified after Gee 1934)

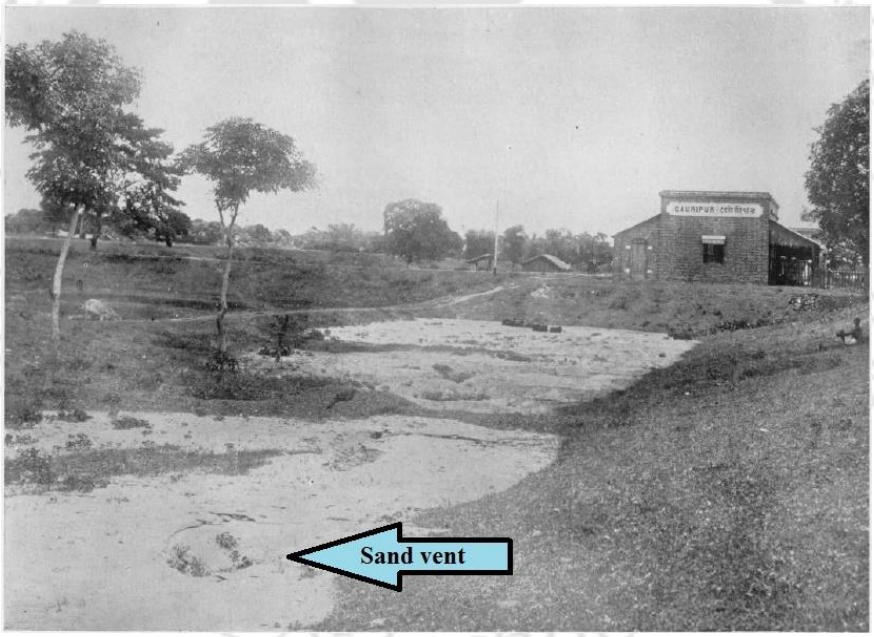

Figure 2.6: Sand vents in Gauripur near Dhubri, Assam after the 1930 Dhubri EQ (modified after Gee 1934)

were shaken by an intensity of VII and Cherrapunji and Shillong in the SP were shaken by an intensity of VI on the Rossi Forel scale.

2.5.5 1943 Assam EQ

Continuing the seismic experience of the past, the area in close proximity to the SP was again hit by the 1943 Assam EQ (M_S-7.2) on 23rd of October 1943. Studies found that

the source fault for this EQ was the Kopili fault, which had previously caused the 1869 Cachar EQ (CNDM). Limited information is available about the 1943 Assam EQ. The only information is about intense shaking brought by the EQ that woke-up people in the night and the report of a rumbling noise. Fissures and unevenness of the ground, falling of trees and damaged buildings due to the EQ were also reported (CNDM).

2.5.6 2009 Assam EQ

In recent times, on 19th August 2009, an EQ of magnitude Mw 5.1 was recorded on the Kopili fault. The epicenter for this EQ was located at latitude 26°56'00"N and longitude 92°48'00"E and the focal depth was approximately 10km. According to Kayal et al. (2010), during this EQ, the Kopili fault had undergone a right lateral strike slip movement. On 21st September 2009 another EQ (M_W-6.3) located approximately 100km north of the 2009 Assam EQ was felt in Bhutan known as the 2009 Bhutan EQ. This EQ too was traced back to the Kopili fault. This EQ had similar focal depth and focal mechanism as that of the 2009 Assam EQ. Kayal et al. (2010) suggested that the 2009 Assam EQ must have been the foreshock of the 2009 Bhutan EQ.

2.6 Indian standard code IS 1893 (Part1):2016

From the above discussion on past EQ damages, it can be concluded that the seismic potential of faults located within northeast India is very high. Similar seismic activities have been observed in other parts of India as well, such as the Himalayan mountain belt, parts of the Indo-Gangetic basin and parts of western India. Taking into account the regular occurrence of EQs across the country and the risks associated with such events, the government of India has developed a seismic zonation map. The idea behind the development of the seismic zonation map was to provide a guideline for engineers for construction of EQ resistant structures in seismically active regions. The first zonation map was developed by Tandon (1956), where the country was divided into three zones of Severe hazard, Light hazard and Minor hazard, based on distribution of EQ occurrences across the country. This map was improved in 1962 by the Bureau of Indian Standards. As per the IS 1893:1962, the country was divided into seven zones from 0 (no damage) to VI (extensive damage). This zonation map was later revised in 1970 after the occurrence of the 1967 Koyna EQ (M_W-6.6), as this EQ had occurred in the Deccan Plateau which was earlier

considered to be a stable part of the Indian subcontinent. The Deccan Plateau was earlier put in zone 0, but after the 1967 Koyna EQ it was realized that no region can be considered to be free of seismic activity. Hence, the new code IS 1893:1970, divided the country into five zones namely from I to V, where zone I showed least amount of seismic activity and zone V showed the highest level of seismic activity. In 1984, the zonation map was again revised to take into account regions of different seismogenic potential, identified on the basis of past EQs and regional faults (Mahopatra and Mohanty 2010). In the year 2002 after the 1993 Latur EQ (M_W-6.2), the zonation map was again revised. Latur was previously placed in zone I, which was zone of low seismic activity. The most recent revision of the code has been done in the year 2016. The IS 1893:2016 consists of four source zones from II to V, where zone II shows the least seismic activity and zone V gives the highest level of shaking as shown in Figure 2.7. The entire northeastern region of the country and parts of Bihar, Uttarakhand, Himachal Pradesh, Jammu and Kashmir, Rann of Kutch and Andaman and Nicobar islands has been placed in zone V. The next lower level of seismic intensity is seen in the seismic zone IV which includes most of the northern belt of the country from Jammu and Kashmir in the west to Sikkim in the east and some parts of Rajasthan. Zone III with moderate level of shaking includes parts of Punjab, Uttar Pradesh, Rajasthan, Maharashtra, Latur, Telangana, Andhra Pradesh, and Kerala. Zone II with the least seismic activity includes most parts of southern India and also a major portion of Madhya Pradesh and Rajasthan. The current zonation map of India, though revised, is not free from limitations. As per the IS 1893(Part1):2016, the zones II, III, IV and V have fixed Zone Factors (Z) of 0.10, 0.16, 0.24 and 0.36 respectively. These zone factors are assigned for vast areas extending for more than hundreds of kilometers. For example; the northeastern region of India which extends for 262230 km² is grouped under zone V. Several studies have highlighted that northeast India is a diverse region varying vastly in terms of geology and tectonics. This infers that the IS 1893(Part1):2016 has not looked into the details of the geology and tectonics of the region before including it into a single zone. The zonation map of IS 1893(Part1):2016 also lacks in detailed information about active seismic sources located within a zone, past EQ data, site classification and return period of past damaging EQs. Owing to the limitations of the IS 1893(Part1):2016, several researchers have performed regional level seismic hazard analysis for different regions of India. Past studies

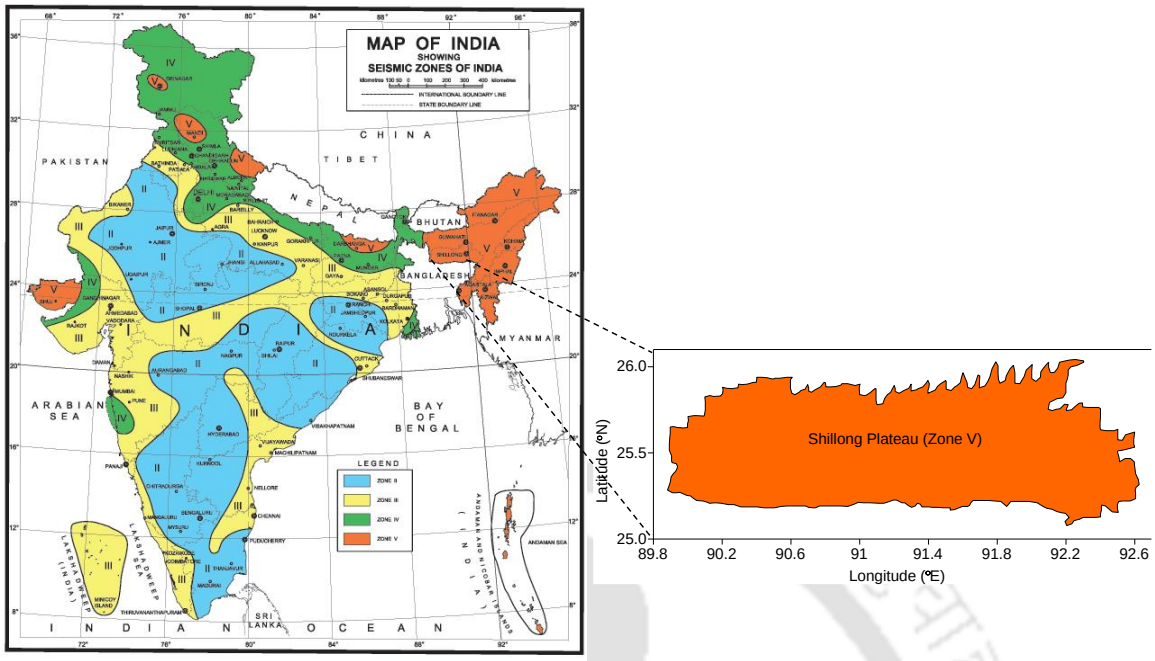

Figure 2.7: Seismic zonation map of India with magnified area of the SP (modified after IS 1893(Part1):2016)

have also used Eurocode 8 and NEHRP (BSSC 2004) for microzonation site classification studies across India. The subsequent section provides a brief discussion on the Eurocode 8, the NEHRP (BSSC 2004) and some of the seismic hazard studies performed in India.

2.7 Eurocode 8

The Eurocode 8 was developed for the design of EQ resistance structures in Europe. The code contains rules for buildings. The Eurocode 8 identifies different ground types and seismic zones. For the purpose of seismic zonation Eurocode 8 divides territories on the basis of local hazard. As per Eurocode 8, hazard is described in terms of a single parameter a_{gR}, which is the reference peak ground acceleration on Type A ground. Ground type A is described as Rock or other rock-like geological formation with shear wave velocity Vs30> 800 (m/s). An importance factor Υ_1 is multiplied with the parameter a_{gR} to obtain the design ground acceleration a_g on type A ground. This design ground acceleration (a_g) is employed in the development of the horizontal elastic response spectrum (S_eT) shown in Figure 2.8. The equations for estimation of S_eT at different time periods as per the Eurocode 8 are given below

$$0 \le T \le T_B : S_c(T) = a_g . S . \left[1 + \frac{T}{T_B} . (\eta . 2.5 - 1)\right] \quad (2.1)$$

$$T_B \leq T \leq T_C: S_e(T) = a_g.S.\eta.2.5 \quad (2.2)$$

$$T_C \leq T \leq T_D: S_e(T) = a_g.S.\eta.2.5\left[\frac{T_C}{T}\right] \quad (2.3)$$

$$T_D \leq T \leq 4s: S_e(T) = a_g.S.\eta.2.5\left[\frac{T_C T_D}{T^2}\right] \quad (2.4)$$

where, $S_e(T)$ is the elastic response spectrum

T is the vibration period of a linear single-degree-of-freedom system

a_g is the design ground acceleration on type A ground ($a_g = \gamma_1 a_{gR}$)

T_B is the lower limit of the period of the constant spectral acceleration branch

T_C is the upper limit of the period of the constant spectral acceleration branch

T_D is the value defining the beginning of the constant displacement response range of the spectrum

S is the soil factor

η is the damping correction factor with a reference value of η = 1 for 5% viscous damping

The values of the above mentioned parameters are specified in the Eurocode 8 for different ground types. Eqs. 2.1-2.4 are used in this study to develop response spectra at different sites within the study area for the purpose of comparison. Detailed discussion on the comaprision between the response spectrum developed in this study and the ones developed using Euroode 8 is given in Chapter 4.

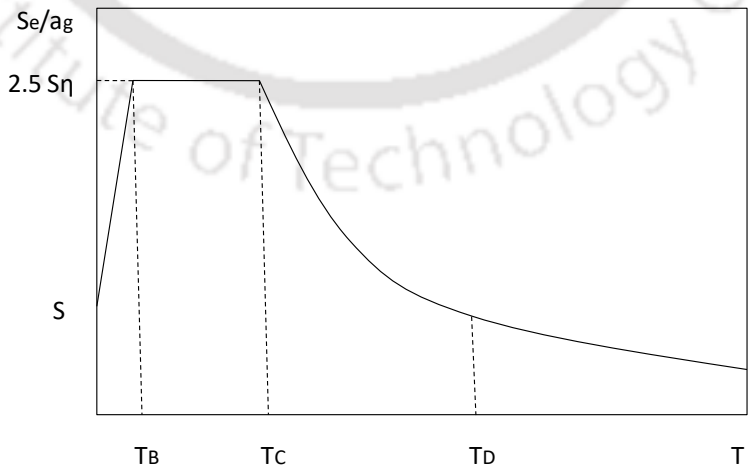

Figure 2.8: Shape of the elastic response spectrum as given in Eurocode 8

2.8 NEHRP site classification (BSSC 2004)

The National Earthquake Hazard Reduction Program (NEHRP) has provided site classification for seismic design. As per the NEHRP guidelines, a site can be classified as types A, B, C, D, E and F based on the shear wave velocity ($\overline{Vs}$), standard penetration resistance value (N) and undrained shear strength (*Su*). Table 2.1shows the various site classes as per NEHRP guidelines.

Table 2.1: Site classification as per NEHRP

Site class	Soil profile name	Soil profile in top 30m		
		Shear wave velocity, $\overline{Vs}$ (ft/s)	Standard penetration resistance, N	Undrained shear strength, *Su* (psf)
A	Hard rock	$\overline{Vs}$ > 5000	-	-
B	Rock	2500 < $\overline{Vs}$ ≤ 5000	-	-
C	Very dense soil and soft rock	1200 < $\overline{Vs}$ ≤ 2500	N>20	*Su*>2000
D	Stiff soil	600≤ $\overline{Vs}$ ≤ 1200	15≤N≤50	1000≤*Su*≤2000
E	-	$\overline{Vs}$ <600	N<15	*Su*<1000
F	-	1. Soils vulnerable to potential failure or collapse under seismic loading such as liquefiable soils, quick and highly sensitive clays, collapsible weakly cemented soils. 2. Peat and/or highly organic clays (*H* > 10 ft [3 m] of peat and/or highly organic clay, where *H* = thickness of soil) 3. Very high plasticity clays (*H* > 25 ft [8 m] with *PI* > 75) 4. Very thick, soft/medium stiff clays (*H* > 120 ft [36 m]) with *Su*< 1,000 psf (50 kPa)		

In this study the above mentioned NEHRP site classification is used for checking the suitability of GMPEs for the study area.

2.9 Seismic hazard studies in northeast India

Seismic hazard analysis is an essential step for assessment of realistic seismic hazard potential of a region. At present, two basic methods of seismic hazard assessment are in use: deterministic and probabilistic. Deterministic Seismic Hazard Analysis (DSHA) identifies the most damaging EQ sources located at minimum distance which could cause maximum intensity of shaking at the site. DSHA only considers the worst case scenario which could lead to uneconomic results for regular structures. Hence, Cornell (1969) introduced the concept of Probabilistic Seismic Hazard Analysis (PSHA). PSHA provides a more realistic and economic seismic hazard scenario as this method takes into account the uncertainties associated with magnitude, hypocentral distance and ground motion exceedance of a particular value. The steps required for performing DSHA and PSHA are given below referring to Figures 2.9 (a-d) and 2.10 (a-d) respectively.

Steps for performing DSHA

- **Step 1:** Collection of EQ data and information on tectonic features available within 500km radius around the SP (Figure 2.9a).
- **Step 2:** Estimation of minimum source to site distance (Figure 2.9b).
- **Step 3:** Selection of maximum possible EQ which can produce the maximum level of shaking by each of the identified sources (Figure 2.9c).
- **Step 4:** Estimation of seismic hazard at the sites of interest using applicable GMPEs using Logic-tree approach (Figure 2.9d).

Steps for performing PSHA

- **Step 1:** Identification of seismic sources and characterizations of each source in terms of probability distribution of both potential rupture locations we well as hypocentral distances (Figure 2.10a).
- **Step 2:** Estimation of frequency of occurrence of various magnitude values on each source using the Gutenberg-Richter recurrence relation (Figure 2.10b).
- **Step 3:** Combination of uncertainties in EQ location, size, and ground motion parameter to obtain the probability of ground motion exceedance for applicable GMPEs, within a certain time period in terms of hazard curve (Figure 2.10c).
- **Step 4:** Estimation of seismic hazard from total hazard curves (Figure 2.10d).

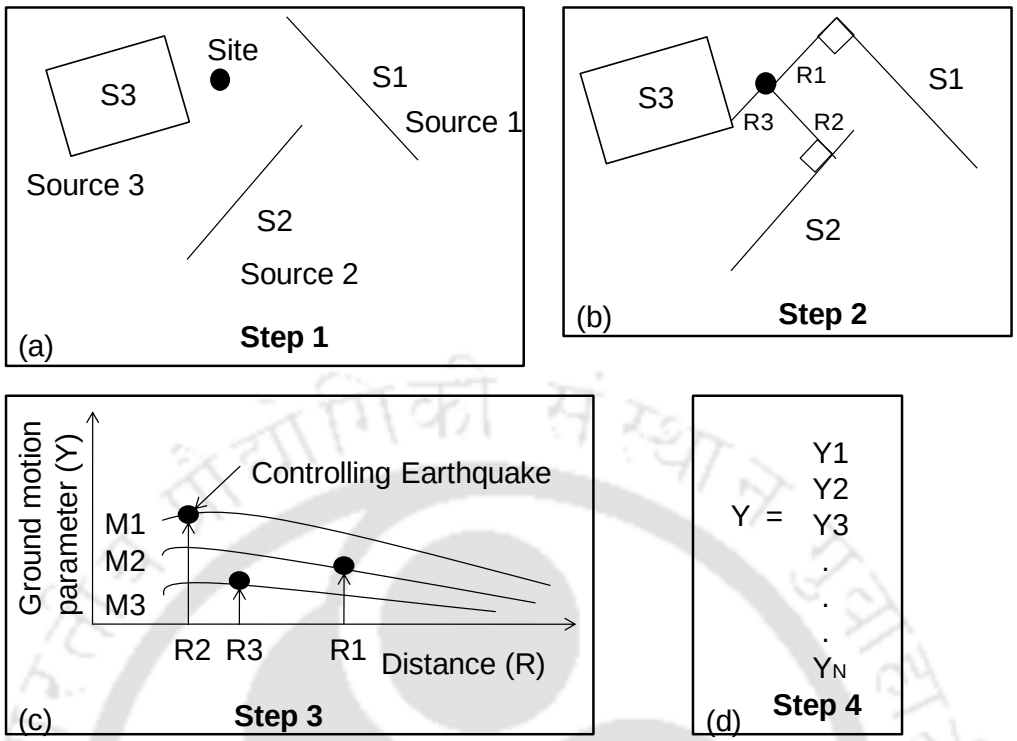

Figure 2.9: Steps in the Deterministic seismic hazard analysis (modified after Reiter 1990)

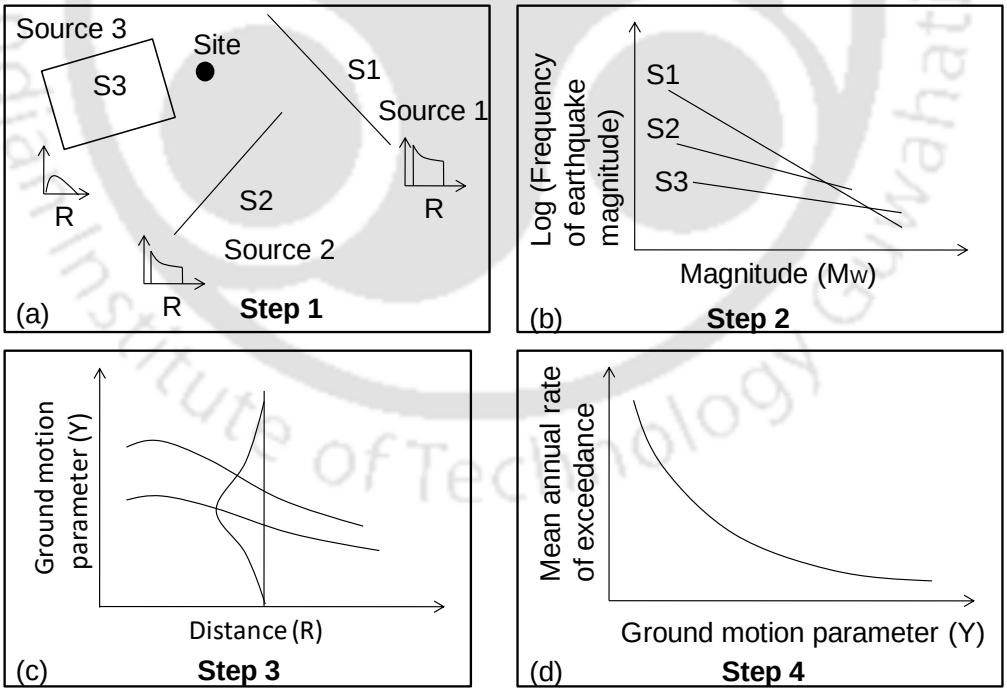

Figure 2.10: Steps in the Probabilistic seismic hazard analysis (modified after Reiter 1990)

Both DSHA and PSHA have found their numerous applications for various regions in India. One such study was done by Khattri et al. (1983), where PSHA was performed for India and its adjoining regions. Khattri et al. (1983) developed a Peak Ground Acceleration (PGA) based hazard map corresponding to 10% probability of exceedance in 50 years. The hazard map was developed based on the GMPE developed by Algermissen and Perkins (1976). Khattri et al. (1983) found that the Himalayan region in the northern boundary, Arakan-Yoma in the eastern boundary and Shillong massif in northeast India showed high probabilistic accelerations.

Similar hazard map for the entire country and adjoining regions was developed by Bhatia et al. (1999), under the Global Seismic Hazard Assessment Program (GSHAP). Bhatia et al. (1999) performed PSHA for 10% probability of exceedance in 50 years. Bhatia et al. (1999) used the attenuation relation developed by Joyner and Boore (1981). From the seismic hazard analysis, Bhatia et al. (1999) found that the Himalayan region and the Tibet Plateau further north showed high hazard values of 0.25g. Even higher values of 0.35-0.40g were observed in the Burmese arc, northeast India and Hindukush region. Both Khattri et al. (1983) and Bhatia et al. (1999) concluded that northeast India shows high seismic hazard potential. The high seismic activity of northeast India is also evident from the past EQ damages discussed earlier in this chapter. Hence, in the later years, several seismic hazard studies were performed for northeast India either state wise or for the entire region.

One such study for the entire northeast region was performed by Sharma and Malik (2006). Sharma and Malik (2006) performed PSHA for northeast India by dividing the region into four seismogenic zones. These four zones were further sub divided into ten seismogenic zones. Sharma and Malik (2006) estimated the hazard parameters of b-values, maximum magnitude and return periods for M_W-6.0 for each of the ten zones. The hazard parameters were then employed into the GMPEs developed by Sharma and Bungum (2006) & Youngs et al. (1997) to developed hazard maps for 10% and 20% probability of exceedance in 50 years. Sharma and Malik (2006) concluded that the PGA values for 10% and 20% exceedance in 50 years ranged from 0.05g to 0.6g and 0.01g to 0.4g respectively.

In another study, Raghukanth et al. (2009) performed DSHA for Imphal city in Manipur, by developing a stochastic finite-fault seismological model to estimate the rock

level acceleration time history. Non-linear soil response analysis was also performed to estimate the amplification of the local soil. Raghukanth et al. (2009) tested the simulated model to obtain the ground motion acceleration at Imphal city for the 1869 Cachar EQ. It was found that during the 1869 Cachar EQ the PGA value in Imphal city had ranged from 0.14-0.18g. Raghukanth et al. (2009) also tested the model for a hypothetical EQ in the Indo-Burmese Arc of M_W-8.1, for which the PGA in Imphal ranged from 0.25 g to 0.33 g.

In 2010, the National Disaster Management Authority (NDMA) of India published a report on PSHA for India which is referred as NDMA (2010) in this thesis. The entire country was divided into 32 seismic source zones based on historical seismicity, tectonic feature and geology. NDMA (2010) estimated the "b" parameter for each of these zones using maximum likelihood method. NDMA (2010) also developed a GMPE for the entire country along with different sets of coefficients for seven different regions identified within the country. Employing this GMPE, NDMA (2010) developed hazards maps for the country considering different probabilities of exceedance.

Following the DSHA study done by Raghukanth et al. (2009) for Imphal city, Pallav et al. (2012) performed PSHA for the state of Manipur. Referring to the work by Goswami and Sarmah (1982) and Nandy (2001), Pallav et al. (2012) divided the region into seven different seismic source zones based on geology as well as tectonic setting. Pallav et al. (2012) estimated b parameters for each of the seven source zones based on maximum likelihood procedure of Kijko and Graham (1998). Among the seven source zones, the b parameters for SP and Assam Valley zones were the lowest i.e. these two zones were found to be most seismically active. Pallav et al. (2012) used the GMPEs by Atkinson and Boore (2003) & Boore and Atkinson (2008) to develop Uniform Hazard Response Spectra for nine district headquarters of Manipur, corresponding to return periods of 100, 500 and 2500 years. Pallav et al. (2012) found major portions of Manipur to be vulnerable to severe seismic hazard. Among the nine districts, the highest level of hazard was observed in the districts of Ukhrul, Senapati, Imphal east and Imphal west.

In another study, Sil et al. (2013) performed PSHA for the northeastern states of Tripura and Mizoram. For this study, Sil et al. (2013) identified a seismotectonic region of 500km radial distance which was later divided into six source zones. Sil et al. (2013)

estimated the b parameter for each of the six seismic source zones using G-R recurrence law. The b parameter values inferred that the Naga thrust and Mishmi thrust were the most seismically active zones among the six seismic source zones. The GMPEs by Atkinson and Boore (2003) & Gupta (2010) were used to develop Uniform Hazard Response Spectra for 2% and 10 % probability of exceedance in 50 years. Sil et al. (2013) found that the northern part of Tripura showed the highest level of seismic hazard.

2.10 Effect of local soil

In addition to seismic hazard analysis, which is performed at the bedrock level, the assessment of the effect of local soil is equally important to decide the surface level of ground shaking. As building damages at a site during an EQ is a function of both the seismic activity of the controlling EQ sources as well as the presence of subsoil beneath the building. The presence of subsoil between the bedrock and the surface alters the ground motion generated during an EQ once it reaches the surface. This phenomenon is known as the local site effect and has considerable influence in changing the ground motion characteristics namely amplitude, frequency content and duration of motion between the bedrock and the surface (Anbazhagan et al. 2010). Depending upon the subsoil characteristics, the amount of damage during an EQ may vary from epicentral region to distant locations as reported worldwide. In order to explore the importance of local site in controlling the induced effects of EQ, the determination of subsoil characteristics is very much required. These subsurface characteristics can be very complex in nature and hence, in order to account for local site effects, a number of field investigations are desired. Other challenges include estimation of dynamic soil properties and input bedrock motion for the future EQ. Determination of dynamic soil properties requires a number of representative soil samples to be tested under cyclic loading for a wide range of strains. So far, very limited attempts to determine dynamic properties of regional soils have been made. Hence, use of dynamic soil properties of one region for site response study of other region is common. Input motion is also an important parameter for an assessment of local site effects during an EQ. In India, recorded ground motions are only available from 1986 with no major to great EQs having occurred since then. Thus, similar to the dynamic soil properties, ground motions recorded in other parts of the world are frequently used in the absence of regional

ground motion records for site response analysis. In spite of the challenges mentioned above, local site effects were estimated worldwide with suitable assumptions in dynamic soil properties and bedrock motions. Anbazhagan et al. (2011) performed site response analyses of typical sites at Dehradun, Lalru and Najibabad located in Uttarakhand, India using synthetic ground motions in the absence of regional ground motion records. Based on the work, the surface level of PGA was found comparable to the felt intensities during 1999 Chamoli EQ (Anbazhagan et al. 2011). Kumar et al. (2012) performed a site response analysis of a typical site at Lucknow (Uttar Pradesh) considering regional ground motion records from COSMOS (Consortium of Organization for Strong Motion Observation System) in order to arrive at the amplification factor (AF) values. Anbazhagan et al. (2010) focused on understanding the response of the Lucknow soil considering an EQ scenario in the western and central seismic gap in the Himalayas. Desai and Choudhury (2014) performed the site response analysis of two typical sites located in nuclear power plant as well as in port areas of Mumbai. In the absence of regional ground motion records, ground motions recorded during the 2001 Bhuj EQ were modified using wavelet method to match the uniform hazard spectrum and were used for site response of above locations (Desai and Choudhury 2014). Phanikanth et al. (2011) used ground motion records from the 2001 Bhuj EQ, the 1989 Loma Prieta EQ, the 1989 Loma Gilroy EQ and the 1995 Kobe EQ in order to perform site response of typical sites in Mumbai in the absence of regional ground motion records. Based on preceding discussion, it can be highlighted that the input motion, subsoil information and the dynamic soil properties are important components of any site response analysis.

2.11 Critical appraisal of the Literature

Based on the above discussions, an attempt has been made in this study to quantify (based on available information about seismicity and subsoil information), seismic hazard due to various active sources surrounding the SP. Taking into account the past literature on seismicity of the SP and the adjoining regions, need for the present study is understood. Referring to IS 1893(Part1):2016, limitation in terms of no detailed information about the geology, tectonics, site classification and return period of past damaging EQs in the SP or the regions located in its vicinity is witnessed. In addition, IS 1893(Part1):2016 clubs the entire

northeastern region into a single seismic zone of V and thus variation of seismicity on regional scale within the northeast India is not covered. Highlighting such shortcoming in seismic zonation map of country as per national code, several researchers have performed seismic hazard studies for various parts of the country including northeast India. These include work by Khattri et al. (1983) which performed PSHA for India and its adjoining regions. However, a major limitation of Khattri et al. (1983)'s study is the use of a single GMPE developed by Algermissen and Perkins (1976) for the entire study area. This limitation can be observed in the study done by Bhatia et al. (1999) as well, where only the GMPE developed by Joyner and Boore (1981) was used to develop hazard map for the entire country and adjoining regions. In later years, Sharma and Malik (2006) while performing PSHA for northeast India used two GMPEs given by Sharma and Bungum (2006) & Youngs et al. (1997). However, Sharma and Malik (2006) have not clearly mentioned the weights given to each of the GMPEs during the analysis. NDMA (2010) performed PSHA for the entire country by identifying 32 seismic zones and developing a new GMPE for the study area. However, NDMA (2010) only gave 7 sets of coefficients for the entire country, which indicates that several of the 32 source zones were considered as a single region for the analysis including the entire northeast India. Pallav et al. (2012) while performing PSHA for Manipur used the GMPEs developed by Atkinson and Boore (2003) and Boore and Atkinson (2008). However, similar to the limitations of the earlier studies, Pallav et al. (2012) did not mentioned as to what or how the weights were assigned to the GMPEs used for the region. Further, in the study performed by Pallav et al. (2012), it was not clearly highlighted as to what methodology was adopted for the assignment of maximum possible magnitude to each fault. Sil et al. (2013) performed PSHA for Tripura and Mizoram and used the GMPEs given by Atkinson and Boore (2003) & Gupta (2010). Sil et al. (2013) also had also not mentioned what weights have been assigned to the GMPEs selected for their study area. Further, Sil et al. (2013) had used the Gutneburg–Richter law (G-R law) for estimation of the hazard parameters. Previous studies have highlighted that the G-R law is infused with several short comings. Hence, several studies such as NDMA (2010) and Pallav et al. (2012) used the maximum likelihood method for a better estimation of seismic hazard potential of the respective study areas.

Further, most of the above mentioned studies had performed seismic hazard studies at the bedrock level and not taken into account the effect of the local soil. However, for the applicability of the seismic hazard results in the design of structure, it is essential to take into consideration the local soil effect. Further, it has to be mentioned here that though several seismic hazard studies were performed for the entire country, no seismic hazard studies have been performed for the SP considering regional parameters till now. Hence, this study is an attempt to understand the seismic hazard potential of the SP by taking in account the regional and local parameters. The objectives of this study are stated in the next section.

2.12 Objectives of the study

This thesis is focused on performing seismic hazard analysis for selected regions within the SP. It has been mentioned in Chapter 1 that during past EQs most damages within the SP were reported from Shillong located in the East Khasi hills district, Nongpoh in the Ri-Bhoi district and Tura in the West Garo hills district. Based on these damage reports, this study attempts to perform both deterministic and probabilistic seismic hazard analysis for the districts of East Khasi hills, Ri-Bhoi and West Garo hills at the bedrock level. This study also aims to understand the response of the soil above the bedrock and hence, in-direct estimation of local soil response is also performed for the SP. The objectives of this study are;

1. Review on the origin, tectonic setting and past damages of the SP.
2. Seismic source characterization of the study area.
3. Deterministic seismic hazard analysis of the districts of East Khasi hills, Ri-Bhoi and West Garo hills.
4. Probabilistic seismic hazard analysis of the districts of East Khasi hills, Ri-Bhoi and West Garo hills.
5. In-direct estimation of local soil response for the SP.

Chapter 3 - Seismic source characterization

3.1 Introduction

The northeastern region of India is a hot bed of seismic activity. Observing the occurrence of several EQs in the past and the extent of damages caused by each of these EQs, several studies have attempted to estimate the seismic hazard potential of specific regions in the northeast India. While performing the seismic hazard analysis, each of the previous studies had identified and characterized the seismic source zones which can potentially control the seismicity of northeast India. Sharma and Malik (2006) analyzed the seismic hazard potential of northeast India by identifying four seismic source zones namely; (i) East west trending zone comprising of Main Boundary Thrust (MBT) and Main Central Thrust (MCT), (ii) Eastern Syntaxis, (iii) Shillong Massif and (iv) north south trending tectonic features consisting of Arakan Yoma ranges and eastern boundary Thrust. Further, Pallav et al. (2012) performed seismic hazard analysis of Manipur in the northeast India and identified seven seismic source zones based on geology and tectonic features. In another work, Sil et al. (2013) identified six seismic source zones based on seismicity, tectonic features and fault rupture characteristics while assessing the seismic hazard potential of Tripura and Mizoram states in the northeast India.

Similar to the above mentioned studies, the present study attempts to develop the seismotectonic map for the SP. Taking into account the seismic characteristics of the surrounding region, which may directly or indirectly control the seismic activity of the SP, the following steps are proposed/ followed in this study.

- **Step 1:** Collection of EQ data and information on tectonic features available within 500km radius around the SP.
- **Step 2:** Identification of seismic source zones within 500km radius around the SP.
- **Step 3:** Development of seismotectonic region of 500km radius around the SP.
- **Step 4:** Check for completeness of collected data with respect to magnitude and time.

- **Step 5:** Estimation of *b*-value.
- **Step 6:** Estimation of return periods within different seismic source zones for various magnitudes.

Thus, as per Step 1, while developing seismotectonic map, past EQ events as well as the seismic sources located within a radial distance of the SP have to be identified. Several past studies such as Tavakoli and Ashtiany (1999), Gupta (2002), Raghukanth and Iyengar (2006), Kumar et al. (2013), Anbazhagan et al. (2013), etc. developed seismotectonic maps for different regions across the globe. The radii of these seismotectonic regions vary from 300 to 900km. In case of regions with history of major ($7.0 \leq M_W \leq 7.9$) or great ($M_W \geq 8.0$) EQs, past studies such as Pallav et al. (2012), Sil et al. (2013), Sitharam and Sill (2014) and Anbazhagan et al. (2015) considered the radius of the seismotectonic region as equal to or greater than 500km. SP considered in this study is also located in a zone of high seismicity as discussed earlier. Further, past damage reports have highlighted that EQs originating at distances greater than 300km had caused moderate to severe damages in the SP. Hence, in this study a seismotectonic region is identified for the SP with a radius of 500km. The centre of the seismotectonic region is taken within the SP at 25.63°N latitude and 91.25°E longitudes. This seismotectonic region covers most of the north-eastern region of India, parts of the eastern Himalayas and the plains of Bengal & Bangladesh. Discussion and comparison in terms of tectonic features, geology and overburden thickness by means of existing literature is presented here in order to understand the difference in tectonic settings of different part of the seismotectonic region.

3.2 Tectonic setting of the seismotectonic region

The tectonic setting of the SP is discussed in details in Chapter 2, hence in this chapter only a brief discussion is provided. The SP is composed of crystalline rock basement and covered with Tertiary (60 to 2.6 mya) sediments (Angelier and Baruah 2009). To the south of the SP is the Dauki fault which is a south dipping normal fault with a strike slip component (Srinivasan 2003). To the west of the SP is the north south trending Dhubri fault. North of the SP is the Oldham or the Brahmaputra fault, which was responsible for the 1897 Assam EQ (M_W-8.1). As per Rajendran et al. (2004), the

Brahmaputra fault lies further north of the SP in the plains of the Assam Valley. East of the SP is the 300-400 km long and 50 km wide, northwest dipping Kopili fault which was the source fault for the 1869 Cachar EQ (M_W-7.5) and the 1943 Assam EQ(M_S-7.2). Figure 3.1 shows the faults located in the vicinity of the SP as well as within the rest of the seismotectonic region in the form of a source map.

To the east and southeast of the Assam Valley lays the Indo Burmese Ranges at an elevation of 1000m. The Indo Burmese Ranges came into existence due to the subduction of the Indian plate under the Burmese plate. Towards the north, these mountain ranges trend in the northeast-southwest direction where it is also known as the

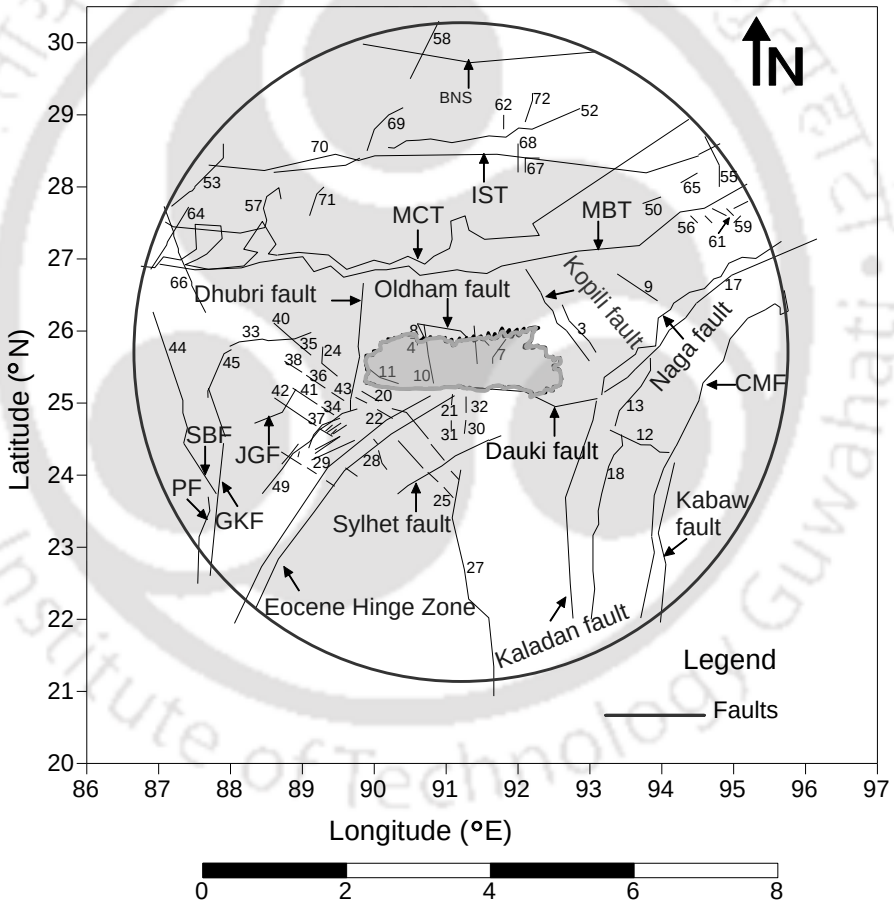

Figure 3.1: Source map showing the faults within the seismotectonic region (IST –the Indus Suture thrust, BNS – the Bangong Nujiang Suture, MCT –the Main Central Thrust, MBT – the Main Boundary Thrust, CMF – the Churachandpur–Mao Fault, GKF – the Garhmayna–Khanda Ghosh Fault, JGF – the Jangipur–Gaibandha Fault, PF – the Pingla Fault, and SBF – the Sainthia–Bahmani Fault. The fault numbers correspond to those in column 1 of Table 3.1.)

Naga Hills having a complex tectonic setting of more than eight thrust faults riding over each other (Kayal 2008). As the mountains trend towards south, the direction changes to northwest-southeast. Towards south, the Indo Burmese Ranges comprise of a series of north-south trending folds which are known as the Tripura fold belt. The intensity of these folds decreases from east to west (Jena et al. 2012). Thick sedimentary deposits dating back to approximately 145 to 34 Mya exist in the Indo Burmese Ranges (Angelier and Baruah 2009). Above subduction process led to the formation of various faults in this region such as the Kaladan fault, Naga thrust, Eastern boundary thrust or the Churachandpur–Mao Fault (CMF) and the Kabaw fault as shown in Figure 3.1. As per Sikder and Alam (2003), the Kaladan fault is a thrust fault extending from the Arakan coast in the south to Nagaland in the north. According to Maurin and Rangin (2009) however, the northern portion of the Kaladan fault shows strike slip faulting and to the south, 23°N thrust focal mechanism is observed on the Kaladan fault. Towards the north of the Kaladan fault is the Naga thrust, the trace of which is found along the Naga Hills (Wang et al. 2014). As per Wang et al. (2014), the Naga thrust is a 400km long active thrust fault with a 23° dip which decreases with depth. The Churachandpur–Mao Fault (CMF) is located to the east of the Naga thrust in the Imphal valley. From GPS measurement studies Kundu and Gahalaut (2013) concluded that the CMF is a thrust fault which presently behaves as a strike slip fault. As per Wang et al. (2014), the CMF is a 170km long strike slip fault having potential to produce an EQ of M_W-7.6 in the future. Further east of the CMF is the 280km long Kabaw fault. Wang et al. (2014) with the help of remote sensing studies concluded that the Kabaw fault is a strike slip fault with a 45° dip which is currently active and has potential to produce an EQ of M_W-8.4 in the future.

Towards the western boundary of the Indo Burmese Ranges, the Tripura fold belt culminates into the alluvial plains of Bengal and Bangladesh. This entire region is a like a trough composed of sedimentary rock strata (Pallav et al. 2012). The trough was filled with sediments carried by the River Ganges and the River Brahmaputra since 60 to 2.6 Mya. The depth of the sediments in these plains increases towards east and reaches up to 20km in Bangladesh (Mohanty and Walling 2008). As per Kayal (2008),

the thick sediment deposit along with the occurrence of only intra plate EQs leads to lesser seismic activity in this region. A prominent fault of the Bengal and Bangladesh alluvium is the northeast-southwest trending strike slip Sylhet fault as shown in Figure 3.1 (Kayal 2008).The Sylhet fault was the source of the 1918 Srimangal EQ (m_b-7.6). Another prominent tectonic feature of the Bengal and Bangladesh alluvium is the Eocene Hinge Zone which is located in northeast-southwest direction (Figure 3.1) (Nath et al. 2014). The Eocene Hinge Zone is 500km long and 25km wide, located at a depth of 4.5km beneath the Kolkata city (Nath et al. 2014; Kayal 2008). The Eocene Hinge Zone was responsible for the 1935 Pabna EQ (M_W-6.2). As per Curray et al. (1982), the Eocene Hinge Zone demarcates the boundary between the continental crust in the north and oceanic crust in the south below the Bengal and Bangladesh plains. As per Mohanty et al. (2013), other important faults existing in this region are the Garhmayna–Khanda Ghosh Fault (GKF), Jangipur–Gaibandha Fault (JGF), Pingla Fault (PF) and Sainthia–Bahmani Fault (SBF) as shown in Figure 3.1.

The eastern part of the Bengal and Bangladesh plain extend in the north up to the Himalayan mountain ranges. The collision and subduction of the Indian plate below the Eurasian plate which brought the Himalayas into existence about 60mya also led to the formation of several folds, faults and thrusts in the Himalayan region. These faults are spread from the north to south including; the Indus Suture thrust (IST), the MCT, the MBT and the Himalayan Frontal Thrust (HFT). According to Kayal (2008), the Himalayan mountain range from west to east can be divided into three segments namely (i) the North-western and the Western Himalaya which includes Jammu and Kashmir, Himachal Pradesh, Garhwal and Kumaun Himalaya, (ii) the Central and the Eastern Himalaya which includes Nepal, Sikkim and Darjeeling Himalaya and (iii) the North-eastern Himalaya which includes Bhutan and Arunachal Pradesh Himalaya. Further, Kayal (2008) based on the thrust system of the Himalayas, divided the North-eastern Himalaya into the Trans-Axial Himalaya, Central Himalaya, Lesser Himalaya and the Outer Himalaya. The Outer Himalaya is separated from the Lesser Himalaya by the east-west trending MBT (Ni and Barazangi 1984). The MBT extends throughout the length of the Himalayas and is seismically active (Angelier and Baruah 2009; Ni and Barazangi 1984). It can be observed from Figure 3.1 that to the north of the MBT is the

MCT. The MCT also extends through the entire length of the Himalayas. From east to west, the MCT separates the Lesser Himalayas from the Central Himalaya (Kayal 2008). As per Mukhopadhyay (2011), the MCT is active only in some segments along its length. Events such as 1991 Uttarkashi EQ(M_W-6.8), 1999 Chamoli EQ(M_W-6.6) and 1980 Gangtok EQ(M_W-6.3) had occurred on the western segment of the MCT (Mukhopadhyay 2011). However, other studies have concluded that the 1991 Uttarkashi EQ and the 1999 Chamoli EQ sources were located to the south of the MCT and hence the MCT is presently in a dormant state (Ni and Barazangi 1984; Kayal 2014). Figure 3.1 shows that further north of MCT is the IST which separates the Trans-Axial Himalaya from the Central Himalaya. To the north of the IST, the Himalayas extend into the Tibetan Plateau (TP). One of the major faults in the southern TP is the Bangong Nujiang Suture (BNS) (Figure 3.1), which is a 1200km long strike–slip fault (Gen-ru et al. 2010). In the North-eastern Himalayan segment of the MBT and MCT, no major EQs have been reported in recent times. Mittal et al. (2012) concluded that a seismic gap known as the "Northeast Seismic Gap" exists in this region between the epicentres of 1950 Assam EQ and the 1934 Bihar-Nepal EQ. As per Srivastava et al. (2015), this seismic gap has the potential to produce an EQ of M_W-8.5 in the near future.

In the present work, all the tectonic features within the seismotectonic region of 500km radius are identified from various past studies such as Mukhopadhyay and Dasgupta (2015); Anbazhagan et al. (2015); Kundu and Gahalaut (2013); Morino et al. (2013); Mohanty et al. (2013); Zhou et al. (2011); NDMA (2010); Angelier and Baruah (2009); Mohanty and Walling (2008); Socquet et al. (2006); Yin (2006); Yin (2000); SEISAT (2000) as well as Choudhury (1993) and complied into a source map. A total of 72 tectonic sources are collected within 500km radial distance.

3.3 Identification of Seismogenic zones

The diversity in the tectonic features, geology and overburden thickness across the seismotectonic region is already discussed in the previous section. Taking into account the differences mentioned in the previous section, various regions within the seismotectonic map can be identified. It can be observed that the SP and Assam Valley region, the Indo Burmese mountain ranges, the plains of Bengal and Bangladesh and

finally the Eastern Himalayan terrain differ from each other in terms of geology and seismotectonics. Further, in this study additional parameters of rupture characteristics and rate of movement for each of these regions are discussed to clearly identify and characterise the seismic source zones affecting the seismicity of the SP. The difference in the rupture characteristics of each of these regions is identified with the help of the declustered EQ data. Determination of the rupture characteristics for each of the four regions is discussed next.

3.3.1 Rupture characteristics

Past studies have highlighted that during an EQ only a segment of a fault ruptures, instead of the entire length of the fault (Stein et al. 2012). This percentage of the rupture length (RLD) within a fault governs the energy released or the magnitude of earthquake. To determine the percentage rupture of various faults across the seismotectonic region, the ratio of the RLD to the total length of the faults is estimated. RLD of each fault is estimated using the Wells and Coppersmith (1994) empirical relations between the moment magnitude (M_W) and the RLD based on maximum magnitude of EQ on each fault. Table 3.1 presents the percentage rupture estimated for each fault within the seismotectonic region.

Table 3.1: Percentage ruptures of faults across the seismotectonic region

Fault no.	Fault name	Fault type	(Mw)	RLD (km)	Actual length (km)	Percent rupture (%)	Reference
1	Oldham	reverse	8.1	-	110	-	Bilham and England (2001)
2	Dhubri	all	7.1	47.8	198.5	24.1	SEISAT (2000)
3	F91-93	all	6.5	18.4	91.4	20.1	Angelier and Baruah (2009)
4	Samin	reverse	4.2	0.6	4	15.3	Angelier and Baruah (2009)
5	Kopili	normal	7.2	38.9	300	13	SEISAT (2000)
6	Dauki	reverse	7.1	41	320	12.8	NDMA (2010)
7	Barapani	reverse	5.6	4.7	40	11.6	Angelier and Baruah (2009)

8	Chedrang	reverse	5.2	2.6	24	10.8	Angelier and Baruah (2009)
9	Bomdila	all	5.5	3.8	74.9	5	Angelier and Baruah (2009)
10	Dudhnoi	all	5.5	3.8	91.9	4.1	Angelier and Baruah (2009)
11	Dapsi	reverse	5.5	4	100	4	Angelier and Baruah (2009)
12	F110-113	all	7.2	56	100.9	55.5	Angelier and Baruah (2009)
13	F96-99	all	6.7	25.3	54.7	46.3	Angelier and Baruah (2009)
14	CMF	strike slip	7.3	71.1	300	23.7	Angelier and Baruah (2009)
15	Kaladan	reverse	7.5	73.3	338.5	21.6	Kundu and Gahalaut (2013)
16	Kabaw	strike slip	7.2	60	280	21.4	Kundu and Gahalaut (2013)
17	Disang	reverse	7	35.5	480	7.4	Angelier and Baruah (2009)
18	F100-109	all	6.1	9.7	295.3	3.3	Angelier and Baruah (2009)
19	Naga	reverse	5.5	4	400	1	Angelier and Baruah (2009)
20	F144	all	6.5	18.4	30.7	60	Choudhury (1993)
21	F154	all	6.1	9.7	17	57.3	Choudhury (1993)
22	F145	all	6.4	15.7	27.9	56.3	Choudhury (1993)
23	Sylhet	strike slip	7.6	118.6	234	50.7	Angelier and Baruah (2009)
24	F116	all	6.3	13.4	27.4	48.9	Choudhury (1993)
25	F152	all	6	8.3	21.9	37.9	Choudhury (1993)
26	Eocene Hinge Zone	all	7.8	145.2	500	29	Mohanty and Walling (2008)
27	Arakan	all	7.5	90.2	367	24.6	Socquet et al. (2006)
28	Madhupur	all	5.9	7.1	36.3	19.5	Morino et al. (2013)
29	F132	all	6.2	11.4	73.6	15.5	Choudhury (1993)

30	F156	all	5.3	2.7	21.4	12.8	Choudhury (1993)
31	F157	all	5	1.7	14.7	11.6	Choudhury (1993)
32	F155	all	5.1	2	25	8	Choudhury (1993)
33	KNF	all	6	8.3	127.6	6.5	Mohanty et al. (2013)
34	F122	all	4.9	1.4	23.2	6.2	Choudhury (1993)
35	F115	all	5	1.7	32.5	5.2	Choudhury (1993)
36	F119	all	5	1.7	35.8	4.7	Choudhury (1993)
37	F124	all	4.6	0.9	19.4	4.6	Choudhury (1993)
38	F118	all	4.9	1.4	32.2	4.5	Choudhury (1993)
39	GKF	all	6	8.3	206	4	Mohanty et al. (2013)
40	F114	all	4.6	0.9	26.9	3.3	Choudhury (1993)
41	F121	all	4.9	1.4	45.8	3.1	Choudhury (1993)
42	F123	all	4.8	1.2	46.6	2.6	Choudhury (1993)
43	F117	all	4.5	0.8	31.4	2.4	Choudhury (1993)
44	MRMF	all	5.5	3.8	211.2	1.8	Mohanty et al. (2013)
45	Kishanganj	all	4.9	1.4	86.1	1.7	Anbazhagan et al. (2015)
46	JGF	all	4.8	1.2	87.2	1.4	Mohanty et al. (2013)
47	SBF	all	4.2	0.5	92.2	0.5	Mohanty et al. (2013)
48	Pingla	all	4.2	0.5	137.9	0.3	Mohanty et al. (2013)
49	DBF	all	4	0.3	200	0.2	Mohanty et al. (2013)
50	F94	all	6.4	15.7	30.3	51.8	Mukhopadhyay and Dasgupta (2015)
51	BNS	strike slip	7.7	140.6	323	43.5	Zhou et al. (2011)
52	Kakahtang	thrust	7.7	97.9	313	31.3	Yin (2006)
53	Dudhkosi	all	5.2	2.3	11.7	19.9	Anbazhagan et al. (2015)
54	Indus suture	all	7.7	123.9	701	17.7	Zhou et al. (2011)

55	BTF	all	6.5	18.4	105	17.5	Mukhopadhyay and Dasgupta (2015)
56	F72	all	5.3	2.7	15.7	17.4	Mukhopadhyay and Dasgupta (2015)
57	Munsiari	thrust	7	35.5	248	14.3	Yin (2006)
58	F9	all	6.3	13.4	99.3	13.5	Yin (2000)
59	F77	all	5	1.7	15.7	10.8	Mukhopadhyay and Dasgupta (2015)
60	MBT	thrust	7.7	97.9	973.2	10.1	Mohanty et al. (2013)
61	F75	all	4.6	0.9	15.7	5.7	Mukhopadhyay and Dasgupta (2015)
62	F7	all	4.8	1.2	22	5.6	Yin (2000)
63	MCT	thrust	7.2	47.4	1326	3.6	Mohanty et al. (2013)
64	Arun	all	5.2	2.3	113	2.1	Anbazhagan et al. (2015)
65	F95	all	4.3	0.6	30.1	1.8	Mukhopadhyay and Dasgupta (2015)
66	Purnea	all	5.2	2.3	176.9	1.3	Anbazhagan et al. (2015)
67	F1-2	all	4.8	1.2	31.4	3.9	Yin (2000)
68	F3-4	all	4.5	0.8	44.4	1.7	Yin (2000)
69	F10-12	all	6.3	13.4	86.7	15.5	Yin (2000)
70	F13-14	all	5.1	2	135	1.5	Yin (2000)
71	F15-16	all	6.1	9.7	49.6	19.7	Yin (2000)
72	F5-6	all	5.5	3.8	45.8	8.2	Yin (2000)

Note that names of some of the faults are unknown in the literature, and hence marked in this Table as FXXX (Figure 3.1 shows the location of the faults).

It has been mentioned earlier that a total of 72 seismic sources are found within the seismotectonic region as listed in Table 3.1. Certain faults were nomenclature by previous researchers as mentioned in Table 3.1 while others have been nomenclature in

this work as shown in Table 3.1 for ease in referring them. It can be observed from Table 3.1 that the percent rupture of the faults range between 0.2% and 60%. For comparison, this variation in the percentage rupture is divided into six bins of 10% rupture each, ranging from 0 to 60%. Figure 3.2 presents a plot of frequency versus percentage rupture of faults within the seismotectonic region. It can be observed from Figure 3.2 that Bengal and Bangladesh region shows a considerable variation in the percentage rupture. While in the first bin (0-10 % rupture), Bengal and Bangladesh region has the highest frequency. In the last bin (50-60 % rupture) as well, this region shows the highest percentage rupture compared to other regions. Overall the region of Bengal and Bangladesh shows the highest frequency corresponding to 0 to 10% rupture compared to other regions as shown in Figure 3.2. The Eastern Himalaya range show the next higher rupture percentage between 0 to 10% and 10 to 20% which is lower than the Bengal and Bangladesh region but significantly higher than the SP and Assam Valley region and the Indo Burmese mountain ranges as shown in Figure 3.2. In case of the Indo Burmese ranges, a frequency value of 3 is obtained for first and third bins which further drops to 1 in the fifth and sixth bins showing that chances of this region undergoing greater than 20% rupture is significantly less. For the SP and Assam Valley region, the percentage rupture is confined to first three bins i.e. the percentage rupture in this zone does not exceed 30% and frequency values range from 0 to 5 as shown in Figure 3.2. Higher percentage rupture is an indication that the faults in a region can produce larger EQs and high frequency of larger percentage rupture is an indication of possibility of frequently occurring larger EQs. Based on the above comparison in terms of percentage rupture as well as frequency of occurrence, it can be concluded that Bengal and Bangladesh region has highest chances to produce larger magnitude EQ (sixth bin) in the future. It has to be mentioned here that the rupture percentage of the Oldham fault is not shown in Table 3.1. It is found in this study that using Wells and Coppersmith (1994) empirical relations, the RLD for the Oldham fault is more than the actual length of the fault given by Bilham and England (2001). Taking the ratio of the RLD to the actual length thus gives a rupture percentage of more than 100% which is impractical. Further, as no other study has commented on the actual length of the fault, the rupture percentage of the Oldham fault is not estimated in this study.

3.3.2 Slip-rates

Another parameter used in this study to highlight the clear distinction among the regions of the SP and Assam Valley, the Indo Burmese mountain ranges, the plains of Bengal and Bangladesh and the Eastern Himalayas is the rate of movement. This work takes into account the Global Positioning System (GPS) based studies performed by various researches to highlight the same. Figure 3.3 shows the rate of movements across the different parts of the seismotectonic region based on previous studies. As per Paul et al. (2001) the SP is moving south with respect to the Indian plate at a rate of 6.3±3.8mm/yr. Similar conclusion was drawn by Banerjee et al. (2008) stating that the SP with respect to the Indian plate has a southward motion of 4-7mm/yr. However, Jade et al. (2007) found that the state of the present day deformation within the SP is almost negligible (1.5±1mm/yr). Jade et al. (2007) concluded that the Oldham fault and the Dauki fault bordering the SP are presently in locked state. The SP is presently acting as a rigid body coupled to the Indian plate and is moving along with the Indian plate in the N51°E direction. Towards the north of the SP as well, a very limited deformation was observed (Jade et al. 2007). However, towards the northeast of the SP in the Assam Valley, the Kopili fault is undergoing active deformation. Kundu and Gahalaut (2013) with the help of GPS measurement observed that at present a slip of 2.9 ± 1.5mm/year is occurring across the Kopili fault. Recently, Vernant et al. (2014) observed that the SP

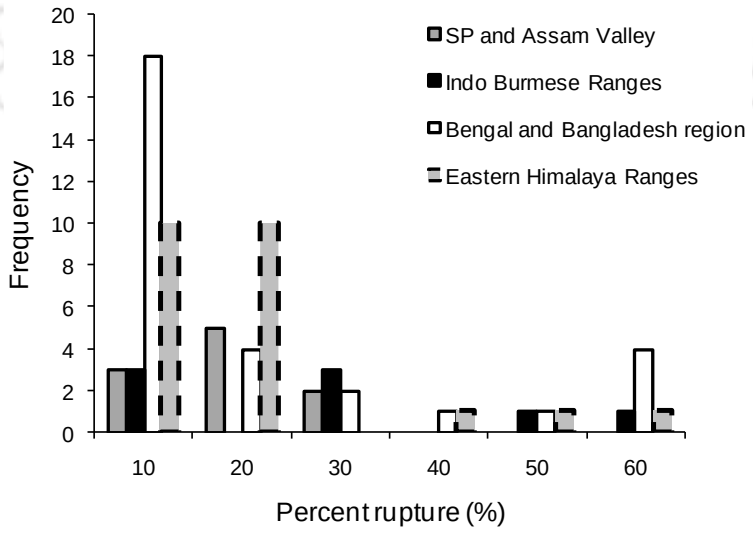

Figure 3.2: Frequency vs. percentage rupture plot showing the variation of rupture percentage of faults during past EQs across the seismotectonic region

and the Assam Valley regions have broken off from the Indian plate. As per Vernant et al. (2014), the SP and the area to the north of the SP in the Assam Valley are actually situated on a rigid block known as the Shillong block and the area to the east of the Kopili fault in the Assam Valley is another rigid block called the Assam block. Both these blocks were found to rotate separately in a clockwise direction with respect to the Indian plate. It was found that the Shillong block and the Assam block rotate at rate of approximately 1.1°/Million yr (Vernant et al. 2014).

The tectonic movement across the neighbouring Indo-Burmese mountain ranges is however very different. Kundu and Gahalaut (2013) and Jade et al. (2007) found that

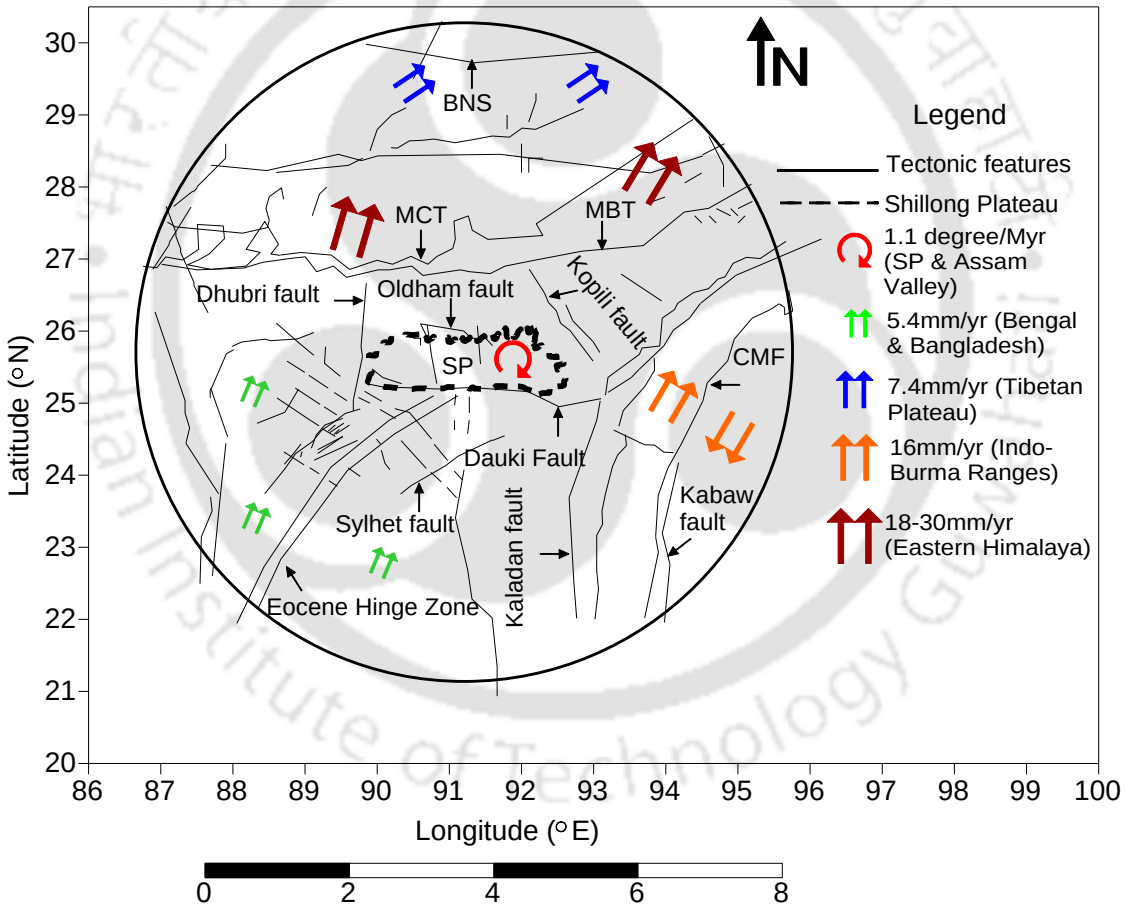

Figure 3.3: Source map showing the direction of movement of different regions within the seismotectonic region with coloured arrows

at present most of the faults in this region exhibits strike slip movement. Kundu and Gahalaut (2013) further emphasised that the Indo Burmese ranges could be broadly divided into eastern and western blocks along the two sides of the CMF. The eastern

block was found moving south to southwest with respect to the Indian plate, whereas the western block is moving in northward direction with respect to the Sunda plate which lies to east of the Indian plate. The Indian plate and the Sunda plate are found to be moving relative to each other at a rate of 36mm/yr out of which 16mm/yr is accommodated in the CMF fault in the Indo Burmese ranges (Kundu and Gahalaut 2013).

Very limited information is available about the rate of movement of the plains of Bengal and Bangladesh. As per Krishna and Sanu (2000) convergence along N33° at the rate of 5.4±2.8mm/yr is occurring in this region.

In the Eastern Himalayan mountain ranges the plate convergence movement is still dominant. As per Jade et al. (2007), the convergence rate across the Eastern Himalayan ranges is 15mm/yr. Banerjee et al. (2008) also found similar convergence rates of 15-20mm/yr across this region. Vernant et al. (2014) found that the rate of convergence increased within the region from 18mm/yr in the eastern Nepal Himalayas to 31mm/yr in eastern Assam. In the southern region of the TP, to the north of the Eastern Himalayan ranges, the north south converging movement is replaced by an east-west tectonic extension (Gan et al. 2007). Along the BNS, the TP is undergoing strike slip movement at the rate of 7.4±0.8mm/yr (Gen-ru et al. 2010).

Based on the above discussions it can be observed that in terms of tectonic features, geology, thickness of overburden, rupture characteristics and rate of movement, the entire seismotectonic region cannot be considered as one seismic source but, a combination of different source zones. Hence, for further analysis in the present work, the entire seismotectonic region is divided into four seismic source zones as;

a) Shillong Plateau-Assam Valley Zone (SP-AVZ)

b) Indo-Burma Ranges Zone (IBRZ)

c) Bengal Basin Zone (BBZ)

d) Eastern Himalayas Zone (EHZ)

Figure 3.4 shows the four seismic source zones with the tectonic features and the past EQs within the seismotectonic region. Figure 3.4 also shows the years of occurrence of some of the major EQs within each of the sour seismic source zones.

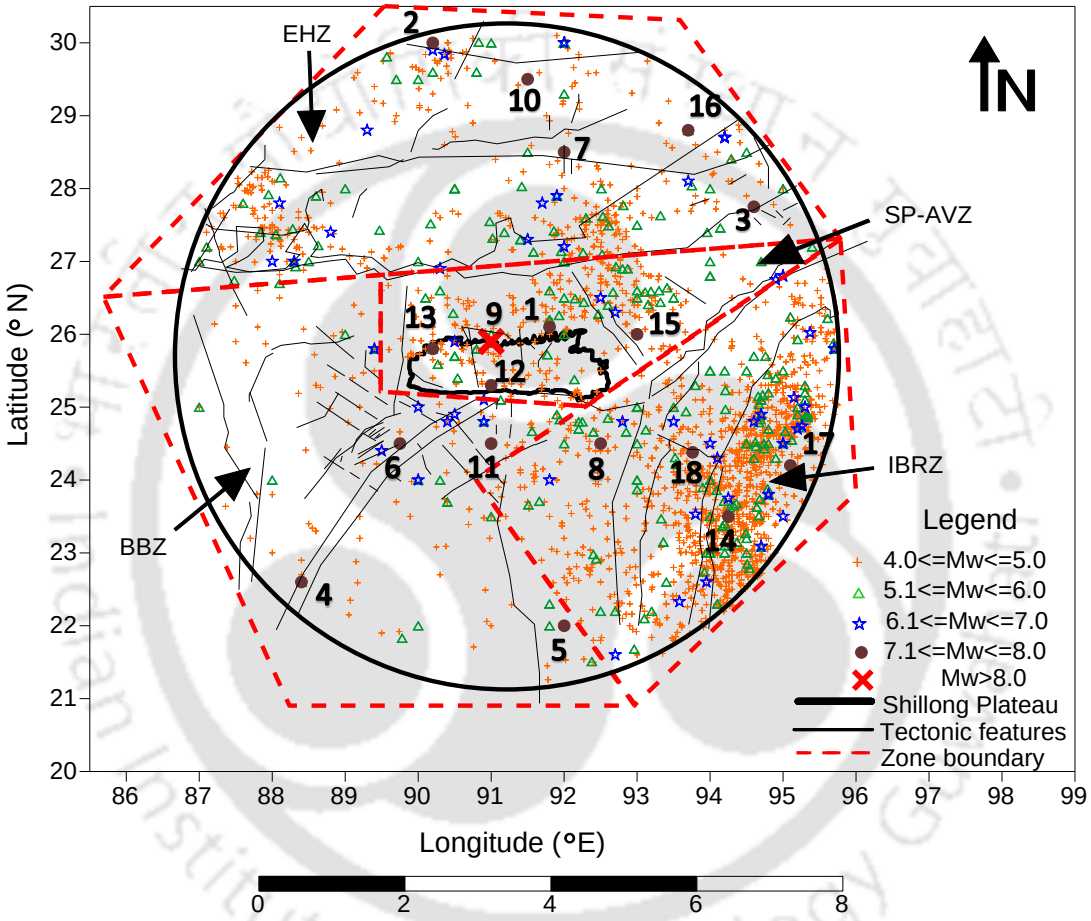

Figure 3.4: Seismotectonic map of the SP showing the four seismic source zones, past EQs from the declustered catalogue, and active faults. (Note: numbers in figure represent past major EQs; 1- 825EQ (M-8.0); 2-1411EQ (M-7.7); 3-1697EQ (M-7.2);4-1737EQ (M-7.2); 5-1762EQ (M-7.5); 6-1787EQ (M-7.8); 7-1806EQ (M-7.7); 8-1869EQ (M-7.5); 9-1897EQ (M-8.1); 10-1915EQ (M-7.1); 11-1918EQ (M-7.6); 12- 1923EQ (M-7.1); 13-1930EQ (M-7.1); 14-1938EQ (M-7.2); 15-1943EQ (M-7.2); 16-1947EQ (M-7.7); 17-1954EQ (M-7.7); 18-1957EQ (M-7.0))

3.4 Earthquake catalogue and its completeness

To estimate the seismic hazard potential of the SP, information about past EQs that had occurred within the seismotectonic region of 500km radius is collected here. These EQ data are collected from three sources namely; United States Geological Survey (USGS Earthquake Hazards Program) (http://earthquake.usgs.gov/earthquakes/search/), India Meteorological Department (IMD Preliminary Earthquake Report) (http://www.imd.gov.in/pages/earthquake_prelim.php) and National Disaster Management Authority (NDMA 2010). NDMA (2010) in turn has collected the EQ data from IMD, Geological Survey of India (GSI), National Geophysical Research Institute (NGRI), Central Water and Power Research Station (CWPRS), Institute of Seismological Research (ISR), Indian Institute of Technology Roorkee (IITR) and Oil and Natural Gas Corporation (ONGC) among other organizations. Archive of past EQs by USGS consists of the various EQ events that have occurred around the world. Information about the origin time, location, date of occurrence, focal depth and magnitude for each of the EQ events is available in these archives. USGS reports past EQs in moment magnitude scale (M_W) and body wave magnitude scale (m_b). For the present study, past EQs for the period of 1915 to 2015 within 500km radial distance (21.09°-30.16°N, 86.71°-95.79°E) are collected from USGS. Since other magnitude scales saturate for higher magnitude and also to arrive at a homogeneous EQ catalogue, all the EQs collected above are converted from m_b to M_W using the following empirical relation based on worldwide data by Scordilis (2006);

$$M_W = 0.85m_b + 1.03 \tag{3.1}$$

Eq. (3.1) is used to convert m_b to M_W for EQ data collected from USGS. Additional information about past EQs within the study area is collected from IMD. Archive by IMD contains pre-instrumental as well as instrumentally recorded significant EQs which occurred around the globe. Each EQ data consists of origin time, location, focal depth and magnitude. All the EQ events in IMD catalogue are recorded in Local magnitude (M_L) scale. Baruah and Baruah (2011) found that, for the SP and adjoining regions EQ data recorded in Local magnitude (M_L) scale is approximately equivalent to

moment magnitude scale. Thus, the Local magnitude (M_L) scale EQ data collected from IMD is used as M_W data in this study.

As another source, NDMA (2010) developed EQ catalogue for entire Indian subcontinent comprising of EQ events having $M_W \geq 4$ from various sources including USGS, ISC, IMD and existing literature. NDMA (2010) catalogue contains EQ events from 2474 B.C to 2008 A.D for India. For the present work, EQs that had occurred between the periods of 1411 A.D. to 2008 A.D. are collected from NDMA (2010) within 500km radial distance. All the EQ data collected based on NDMA (2010) were in M_W scale and thus no correlation is used for homogenization. A single EQ catalogue is developed by merging the EQ data from NDMA (2010), USGS and IMD. Since NDMA (2010) also had EQ data from IMD, the repeated EQ events are removed from the catalogue. After removing the repeated EQ events, a total of 2660 EQs for the periods 1411 A.D. to 2015 A.D. remained in the revised EQ database developed for the study area. This revised catalogue has a collection of main EQ events, foreshocks and aftershocks. Foreshocks and aftershocks are events which occur in clusters and are temporally and spatially dependent on the main EQ event (Christophersen et al. 2011). In order to understand the true potential of a seismic source, it is essential to remove dependent events. In this study, the above collected EQ events are declustered using static window method. As per the method, EQ events which had occurred within 30km distance of each other and within a time span of 30.5 days can be grouped together into a cluster. The EQ event with maximum magnitude within that cluster is identified as the main event. Remaining EQs are dependent events of the main event i.e. foreshocks and aftershocks, which should be removed. Applying the above method on the catalogue, the numbers of EQ events within the 500km radius are reduced from 2660 to 2359 within the entire seismotectonic region.

Based on the geographical location, the above data are distributed among the four seismic source zones. For each of the four EQ catalogues completeness analyses, both with respect to magnitude as well as time are done here, as discussed in subsections below;

3.4.1 Completeness with respect to magnitude

Completeness with respect to magnitude is checked by estimating the minimum magnitude of the catalogue or the magnitude of completeness (M_C). To check for the completeness of the EQ catalogue the maximum curvature method (MAXC) of Wiemer and Wyss (2000) is used in this work. As per MAXC method, the maximum curvature point is defined by estimating the maximum value of the first derivative of the frequency magnitude curve. The point of the maximum curvature gives the M_C value. Figures 3.5 (a-e) show the magnitudes of completeness plots for each of the four seismic source zones and the entire EQ catalogue as well. It can be observed from Figures 3.5 (a-e) that the M_C values for EQ catalogues corresponding to the SP-AVZ, IBRZ, BBZ, EHZ and the entire catalogue are found as 4.0. Hence, beyond magnitude value of 4.0, all the five EQ catalogues are found complete with respect to magnitude.

3.4.2 Completeness with respect to time

To estimate the recurrence rate of EQs in each of the four seismic source zones, it is essential that the declustered EQ catalogues should be complete. Hence, to check the completeness of each of the four EQ catalogues with respect to time, Stepp (1972) methodology is adopted. The four EQ catalogues of the seismic source zones are further divided into four magnitude classes; 1) $4.0 \leq M_W \leq 5.0$; 2) $5.1 \leq M_W \leq 6.0$; 3) $6.1 \leq M_W \leq 7.0$ and 4) $7.1 \leq M_W \leq 8.0$. As per Stepp (1972) method, the EQ catalogue should be divided into time bins. Each of these bins is then treated as a single process which occurs in acertain interval of time. Time interval should be taken such that the recurrence rate of the EQ events is stable during that time period. Further, time interval is so chosen that a large number of EQ events are available in each bin so as to minimise the variance. In order to maintain an efficient variance for the EQs, Stepp (1972) method assumes that the EQ events follow the Poisson distribution model. As per the Poisson distribution model, if x_1, x_2, x_3, ……., x_n are the number of EQ events in a unit time interval then the unbiased mean rate for each time interval of this dataset is given as;

$$\lambda = \frac{1}{n}\sum_{i=1}^{n} x_i \tag{3.2}$$

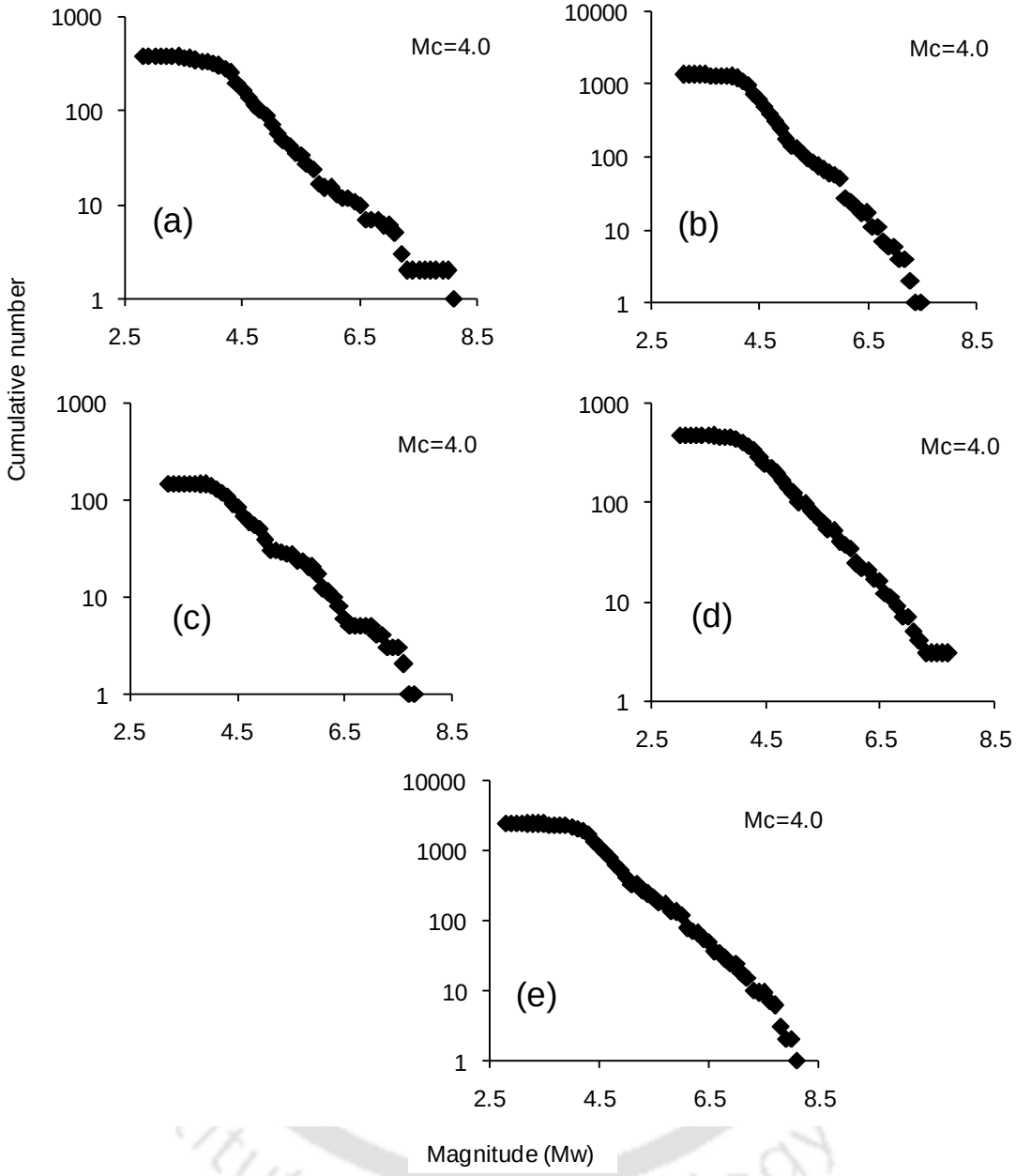

Figure 3.5: Cumulative frequency distribution plots showing the M_C values for separate EQ catalogues of (a) SP-AVZ, (b) IBRZ, (c) BBZ, (d) EHZ and (e) entire catalogue of the seismotectonic region respectively. (For each of the plots x-axis shows the M_W and y-axis shows the cumulative number of EQs)

In this case, the variance is given as:

$$\sigma_{\lambda}^{2} = \frac{\lambda}{n} \tag{3.3}$$

Where, n is the number of unit time intervals. In Eq. (3.3), if the time interval is 1 year, then the standard deviation (σ_{λ}) of the estimated mean (λ) is given as;

$$\sigma_\lambda = \frac{\sqrt{\lambda}}{\sqrt{T}} \tag{3.4}$$

Where, T is the sample length. Stepp (1972) concluded that if λ is constant for each magnitude class then σ_λ is equal to $\frac{1}{\sqrt{T}}$ for each time interval.

Using Stepp (1972) method explained above, completeness analyses of all the four EQ catalogues corresponding to all the four seismic source zones are done in this study. Figures 3.6 (a-d) show the plot of σ_λ versus time interval for the SP-AVZ, IBRZ, BBZ and EHZ respectively. For each of the seismic source zones, σ_λ is plotted versus $1/\sqrt{T}$ for various magnitude classes. The extent up to which the σ_λ for a magnitude class is found parallel to the $1/\sqrt{T}$ line, EQ catalogue for that duration is considered complete. Table 3.2 shows the years of completeness for different magnitude classes in each of the four seismic source zones. It can be observed from Table 3.2 that for magnitude class $7.1 \leq M_W \leq 8.0$, EQ catalogues are complete in the range of 120 to 160 years. Similarly for magnitude class $4.0 \leq M_W \leq 5.0$, for each of the four seismic source zones, EQ catalogues are found complete for last 40 years.

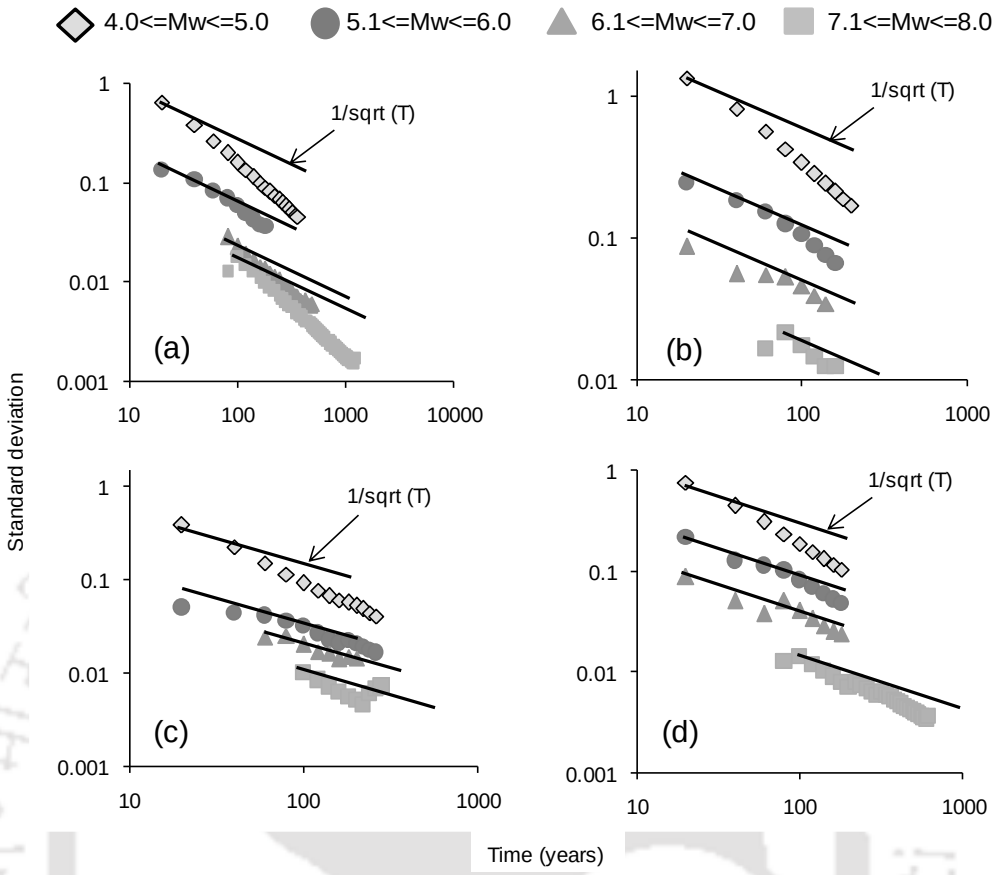

Figure 3.6: Standard deviation versus time interval plots for different magnitude classes for (a) SP-AVZ, (b) IBRZ, (c) BBZ and (d) EHZ respectively.(For each of the plots x-axis shows the time in years and y-axis shows standard deviation)

Table 3.2: Years of completeness for different magnitude classes for the four seismic source zones

Seismic source zone	Magnitude class	Years of completeness (years)
SP-AVZ	$4.0 \leq M_W \leq 5.0$	40
	$5.1 \leq M_W \leq 6.0$	100
	$6.1 \leq M_W \leq 7.0$	120
	$7.1 \leq M_W \leq 8.0$	140
IBRZ	$4.0 \leq M_W \leq 5.0$	40
	$5.1 \leq M_W \leq 6.0$	80
	$6.1 \leq M_W \leq 7.0$	100
	$7.1 \leq M_W \leq 8.0$	120
BBZ	$4.0 \leq M_W \leq 5.0$	40
	$5.1 \leq M_W \leq 6.0$	100
	$6.1 \leq M_W \leq 7.0$	120
	$7.1 \leq M_W \leq 8.0$	140

EHZ	4.0≤ M_W≤5.0	40
	5.1≤ M_W≤6.0	100
	6.1≤ M_W≤7.0	120
	7.1≤ M_W≤8.0	160

3.5 Seismicity Analysis

Once the completeness analyses of EQ catalogues for the four seismic source zones are done, complete part of EQ catalogues are further used to estimate the 'b' parameter in each of the four source zones. The 'b' parameter can be estimated using the Gutenberg Richter (G-R) recurrence law as well as Kijko et al. (2016) method. The G-R recurrence law follows the method of least-square fitting for estimation of the 'b' parameter. Gutenberg and Richter (1956) proposed the following recurrence law based on exponential distribution of EQ event on each fault;

$$Log_{10}(N) = a - bM \tag{3.5}$$

where, *N* is the number of EQs of magnitude *M*, 'a' represents the seismic activity of a region and 'b' denotes the relative likelihood of large and small EQs.

As mentioned earlier, the G-R recurrence law is a least-square fitting method which does not take into account M_C which is an essential parameter in seismic hazard analysis. Further, as per Marzocchi and Sandri (2003), the comprehensiveness of the G-R recurrence law was questioned by several researchers in the past. Hence, in the present study to estimate the mean annual activity rate (λ), 'b' and maximum regional magnitude (m_{max}), a new method proposed by Kijko et al. (2016) based on maximum likelihood is used. Maximum likelihood method as per Kijko et al. (2016) considers mixed dataset containing pre-instrumental EQ events and instrumentally recorded EQ events. The pre-instrumental dataset is nomenclature as the extreme catalogue and the instrumentally recorded dataset as the *s* sub-catalogues. Different minimum magnitude threshold limits (m_{min}) are assigned to both the extreme and *s* sub-catalogues. For the extreme catalogue Kijko et al. (2016) assumed a time span of t_0 consisting of n_0 largest seismic events, of magnitude $\geq m_0$. The value of m_0 has to be either larger or equal to

the overall minimum magnitude of interest for the whole catalogue i.e. m_{min}. The likelihood function for the extreme catalogue is given by the equation shown below

$$L_H(\theta|m_0, t_0, v) \equiv L_H(\theta) = \prod_{k=1}^{n_0} f_M^{max}\left(m_{0k}|v_\beta, m_0, t_{0k}\right) \tag{3.6}$$

where vectors $\boldsymbol{m_0}$ and $\boldsymbol{t_0}$ are respectively defined as the (n_0 × 1) vectors, consisting of the n_0 largest EQ magnitudes m_{0k}, associated with time intervals t_{0k}, when k=1,…, n_0. The vector v= (v_λ,v_β) consists of the coefficients of variation of the unknown $\bar{\lambda}$ and $\bar{\beta}$. For the *s* sub-catalogues Kijko et al. (2016) assumed that each sub-catalogue has a time span t_i (i=1,…,s) and is complete, starting from the known magnitude $m_{min}^{(i)}$. For each sub-catalogue *i*, the vector $\boldsymbol{m_i}$ denotes n_i observed seismic-event magnitudes m_{ik} such that $m_{ik} \geq m_{min}^{(i)}$ in which k=1,…,n_i. Kijko et al. (2016) considered the magnitude of the EQs to be independent of their number and obtained the likelihood function for each sub-catalogue as the product of the likelihood functions of $\bar{\lambda}$ and $\bar{\beta}$. The likelihood function of $\bar{\lambda}$ is given by the equation below

$$L_i\left(\bar{\lambda}|n_i, t_i\right) = \left(\bar{\lambda}^{(i)}t_i + q_\lambda\right)^{-q_\lambda}\left(\frac{\bar{\lambda}^{(i)}t_i}{\bar{\lambda}^{(i)}t_i + q_\lambda}\right)^{n_i} \tag{3.7}$$

where,

$$q_\lambda = \frac{\bar{\lambda}^2}{\sigma_\lambda^2} \tag{3.8}$$

such that $\bar{\lambda}$ denotes the mean value of the activity rate λ, $\bar{\lambda}^{(i)}$ is the mean EQ activity rate corresponding to the magnitude level of completeness $m_{min}^{(i)}$ and is defined as

$$\bar{\lambda}^{(i)} = \bar{\lambda}\left[1 - F_M\left(m_{min}^{(i)}|v_\beta, m_{min}\right)\right] \tag{3.9}$$

where $F_M(.|.)$ is defined as;

$$F_M\left(m|v_\beta, m_{min}\right) = C_\beta\left[1 - \left(\frac{q_\beta}{q_\beta + \bar{\beta}(m - m_{min})}\right)^{q_\beta}\right] \tag{3.10}$$

where, $\bar{\beta}$ is the mean value of parameter β, C_β = normalizing co-efficient of β and is defined as;

$$C_\beta = \left[1 - \left(\frac{q_\beta}{q_\beta + \bar{\beta}(m_{max} - m_{min})}\right)^{q_\beta}\right]^{-1} \quad (3.11)$$

$$q_\beta = \frac{\bar{\beta}^2}{\sigma_{\bar{\beta}}^2} \quad (3.12)$$

where, σ_β is the standard deviation of $\bar{\beta}$. Similarly the likelihood function of $\bar{\beta}$ is given by the equation below;

$$L_i(\bar{\beta}|\boldsymbol{m_i}) = \left[C_\beta \bar{\beta}\right]^{n_i} \prod_{k=1}^{n_i} \left[1 + \frac{\bar{\beta}}{q_\beta}\left(m_{ik} - m_{min}^{(i)}\right)\right]^{-(q_\beta+1)} \quad (3.13)$$

Thus the likelihood function of θ, based on all *s* complete sub-catalogues is obtained by taking the product of Eq. (3.7) and Eq. (3.13) as shown below;

$$L_c(\theta) = \prod_{i=1}^{s} L_i(\bar{\lambda}|n_i, t_i) L_i(\bar{\beta}|m_i) \quad (3.14)$$

The joint likelihood function for the entire catalogue is the product of the likelihood functions of the extreme and *s* sub-complete catalogues (Kijko et al. 2016) which is shown by the equation below;

$$L(\theta) = L_H(\theta) \times L_C(\theta) \quad (3.15)$$

Maximization of the joint likelihood function estimates the hazard parameters of 'λ' and 'b'. However, the estimation of the hazard parameters of 'λ' and 'b' is also a function of m_{max}. Kijko et al. (2016) proposed calculating m_{max} by the equation given in Kijko (2004) which is shown below

$$m_{max} = m_{max}^{obs} + \frac{\delta^{\frac{1}{q}} exp\left[\frac{nr^q}{1-r^q}\right]}{\bar{\beta}}\left[\Gamma\left(-\frac{1}{q}, \delta r^q\right) - \Gamma\left(-\frac{1}{q}, \delta\right)\right] \quad (3.16)$$

where, m_{max}^{obs}= maximum observed magnitude, δ = nC_β, n = number of recorded magnitudes,

$$r = \frac{p_\beta}{(p_\beta + m_{max} - m_{min})} \quad (3.17)$$

$$p_\beta = \frac{\bar{\beta}}{\sigma_{\bar{\beta}}^2} \tag{3.18}$$

$\Gamma(.,.)$ is the complementary incomplete gamma function. As m_{max} is on both sides of Eq.(3.16) the estimator is calculated through iterative procedure. Thus, maximization of the joint likelihood function and iterative solution of m_{max} provides the hazard parameter of λ, b and m_{max} for a region. Based on the method proposed, Kijko et al. (2016) developed a computer program to estimate the above mentioned hazard parameters. For the present study, same computer program received from Prof A. Kijko (based on personal communication) is used to estimate 'λ', 'b' and m_{max} values. It has been mentioned earlier that according to Kijko et al. (2016) method, the entire EQ catalogue needs to be divided into extreme and *s* sub-complete catalogues. Hence, the earlier developed EQ catalogues for each of the four seismic source zones are divided into one extreme and two sub-complete catalogues. A minimum magnitude threshold value for each of the extreme and sub-complete catalogues is estimated by the MAXC method of Wiemer and Wyss (2000). Similar to NDMA (2010), magnitude uncertainties of 0.5 and 0.3 for the magnitude values of the extreme and sub-complete catalogues respectively are taken for the present analysis. The values of 'λ', 'b' parameter, β (β=2.303b) and m_{max} obtained from the analyses for each of the four seismic source zones are reported in Table 3.3. Further, comparisons are made in terms of 'b' value estimated in the present study and the ones obtained during past studies for region under study as shown in Table 3.3.

Table 3.3: Hazard parameters for four seismic source zones estimated in the present work and comparison of b-value with past studies

Seismic source zone	λ	β	b-value	m_{max}
SP-AVZ	2.49± 0.30	2.09 ± 0.08	0.91±0.03 (Present work) 0.67±0.07 (Pallav et al. 2012) 0.73±0.04 (NDMA, 2010) 1.00±0.09 (Thingbaijam and Nath, 2008)	8.50 ±0.47

IBRZ	16.44±2.14	2.17 ± 0.04	0.94±0.02 (Present work) 0.86±0.03 (Pallav et al. 2012) 0.80±0.02 (NDMA, 2010) 1.17±0.04 (Thingbaijam and Nath, 2008)	7.58 ± 0.26
BBZ	1.65± 0.20	1.84 ± 0.08	0.80±0.03 (Present work) 0.69±0.08 (Pallav et al. 2012) 0.74±0.04 (NDMA, 2010) 0.82±0.12 (Shankar and Sharma, 1998)	8.41 ± 0.66
EHZ	5.84 ± 0.79	2.06 ± 0.07	0.89±0.03 (Present work) 0.70±0.04 (Pallav et al. 2012) 0.71±0.04 (NDMA, 2010) 1.05±0.06 (Thingbaijam and Nath, 2008)	7.78 ± 0.26

Thingbaijam and Nath (2008) attempted determination of m_{max} values of four seismic source zones covering almost the entire northeast India. As per Thingbaijam and Nath (2008), the entire area was divided into four seismic source zones namely; Eastern Himalayan Zone (EHZ), Mishmi Block Zone (MBZ), Eastern Boundary Zone (EBZ) and Shillong Zone (SHZ). In comparison to the present work, b values found by Thingbaijam and Nath (2008) using tapered G-R recurrence law (Vere-Jones et al. 2001, Kagan 2002) as presented in Table 3.3 are higher for three zones namely SP-AVZ, IBRZ and EHZ. It has to be mentioned here that the seismic zonation done in the present study is completely different from the zonation done by Thingbaijam and Nath (2008) which may be an attribute for different b values between the two studies. In addition, Thingbaijam and Nath (2008) findings were based on EQ catalogue between 1964 and 2006 while EQ catalogue in the present work is complete itself up to 160 years as presented in Table 3.2. Difference in the duration of EQ catalogue might also be the reason for difference in the b values.

In a separate work, National Disaster Management Authority, Government of India developed probabilistic seismic hazard map of entire India which is referred here as NDMA (2010). NDMA (2010) developed EQ catalogue by combining three different kinds of EQ data namely; instrumental, historic and the one obtained from paleoseismic studies. Further, collected data were homogenized and declustered before the analysis. NDMA (2010) divided the entire country into 32 seismic source zones based on historical seismicity, tectonic feature and geology. A careful observation of Figure 2.3 as per NDMA (2010) shows that the geographical extent of seismic zones 4, 5, 8, 9 and 10 covers an area bigger than the seismotectonic region of 500km radial distance which is considered in the present work. Thus, in comparison to the present work, the EQ catalogue used by NDMA (2010) was completely different. Moreover, NDMA (2010) used computer program by Kijko and Graham (1998) to determine b parameter, after dividing entire catalogue into extreme and complete part, which is different from Kijko et al. (2016) used in the present work. Thus, even though present study as well as NDMA (2010) found b values for similar seismic source zones, above mentioned reasons might be the attributes for different b values obtained from the two studies as listed in Table 3.3.

Pallav et al. (2012) attempted probabilistic seismic hazard of Manipur which is located south-east of the present study area of the SP. Referring to the work by Goswami and Sarmah (1982) and Nandy (2001), Pallav et al. (2012) considered the entire seismotectonic region to consist of seven different seismic source zones based on geology as well as tectonic setting. Work by Pallav et al. (2012) considered Naga thrust, Mishmi thrust as separate source zones while present work considers Naga thrust within SP-AVZ, and Mishmi thrust as a part of EHZ, thus clearly differentiating the definition of seismic source zones by Pallav et al. (2012) in comparison to the present study. In addition, after data completeness based on Stepp (1972), Pallav et al. (2012) estimated b parameters for each of the seven source zones based on Kijko and Graham (1998) method while present study uses Kijko (2016) method to determine b values. Thus, findings by Pallav et al. (2012) are slightly different from the present work due to different source zonation as well as different method of seismic parameter determination as presented in Table 3.3.

In another work, while performing probabilistic seismic hazard analysis of Tripura and Mizoram states, Sil et al. (2013) developed seismotectonic map covering 500km radial distance around both the states collectively, thus covering entire north-east India, whole part of Bangladesh, west part of Burma and south part of China. Based on seismicity, fault mechanism and tectonic features, the entire seismotectonic region was divided into six source zones as per Sil et al. (2013). Further based on EQ catalogue ranging between the year 1710 and 2010, Sil et al. (2013) determined b parameter for each of the six seismic source zones using G-R recurrence law. It has to be mentioned here that no demarcations of the boundary of six seismic source zones were mentioned by Sil et al. (2013) which made comparison of b value difficult with the present findings. However, it has to be highlighted here that the center of 500km radial distance in the present work is located within SP which is completely different from the center of 500km taken by Sil et al. (2013); clearly suggesting different EQ catalogues in both the studies. Further, present study uses maximum likelihood method by Kijko et al. (2016) while findings by Sil et al. (2013) were based on least square fitting law of G-R relation. Above two reasons might be the attributes for different findings by the present work and the one found by Sil et al. (2013).

Based on the 'b' values obtained in this work (Table 3.3), it can be concluded that the BBZ shows high seismic activity in comparison to other three seismic source zones. In addition to 'b' parameter determination, number of studies, such as by Parvez and Ram (1997), Shanker and Sharma (1998), Das et al. (2006), Sharma and Malik (2006), Nath et al. (2008), Nath et al. (2009), NDMA (2010), Raghukanth and Das (2010), Pallav et al. (2012), Nath et al. (2014) etc. attempted seismic hazard analysis for northeast India as a whole or for different regions within northeast. The seismic hazard potential of a region is also a function of the return period of different magnitude EQs within a certain time period. Thus, in addition to the determination of 'b' values for each seismic source zone, the return periods versus magnitude for the four seismic source zones considering a magnitude interval of 0.1 are also estimated in this study using the above computer program developed by Kijko. Figures 3.7 (a-d) present the return periods versus M_W for SP-AVZ, IBRZ, BBZ and EHZ respectively. It can be observed from Figures 3.7 (a-d) that for M_W=6, the return period increases in the order of IBRZ, EHZ, SP-AVZ and

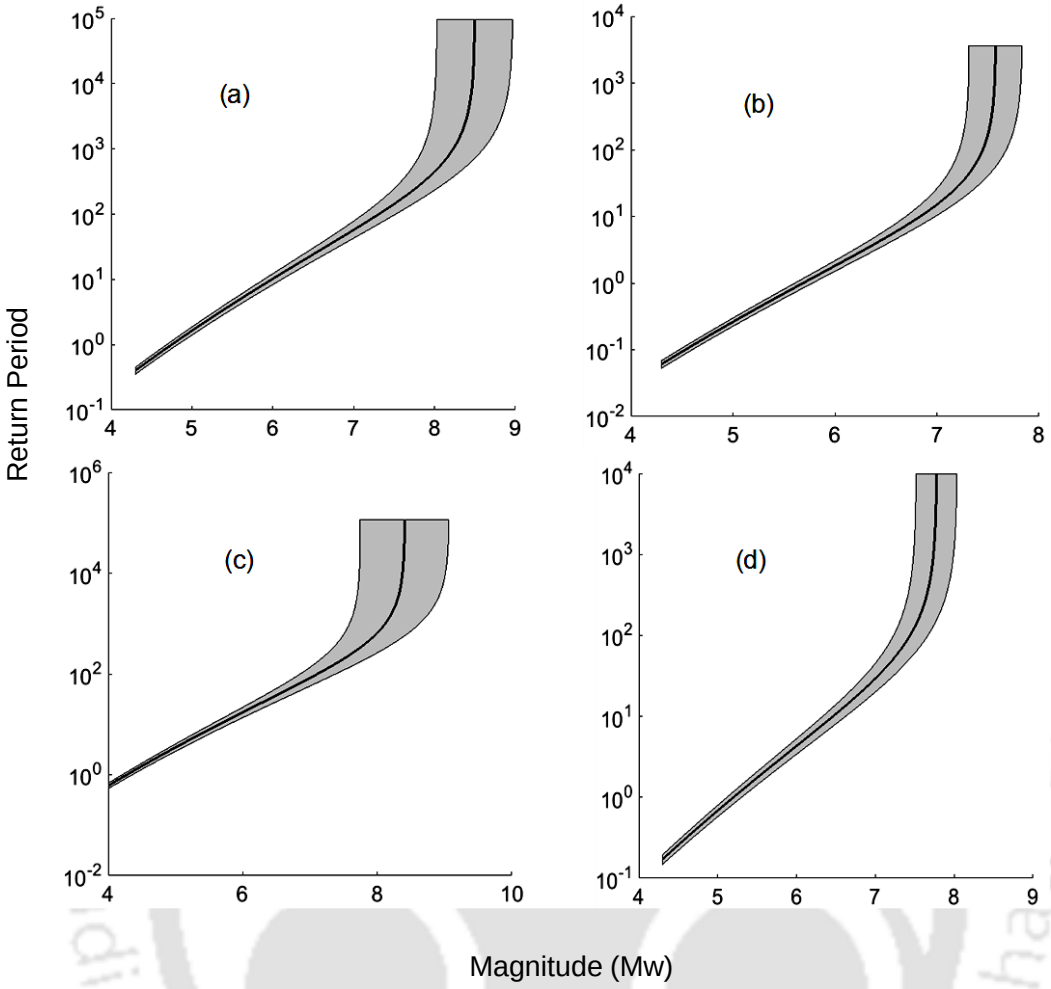

Figure 3.7: The plots of return periods of different magnitude EQs for (a) SP-AVZ, (b) IBRZ, (c) BBZ and (d) EHZ respectively. (For each of the plots x-axis shows magnitude (M_W) and y-axis shows the return period in years. Further, the solid line in each plot represents the return period with respect to magnitude and the shaded area indicates the standard deviation in the return period)

BBZ. This indicates that M_W=6.0 EQ is more frequent in the order of BBZ<SP-AVZ<EHZ<IBRZ. Similarly considering m_{max} of each source zone into account, the return periods increase in the order of BBZ>SP-AVZ>EHZ>IBRZ for M_W-8.4, 8.5, 7.8 and 7.6 respectively. In other words, frequency of maximum potential EQ to occur in a seismic source zone is in the order of BBZ>SP-AVZ> EHZ>IBRZ. From Table 3.3 as well it can be observed that λ value is highest for IBRZ and lowest for the BBZ. This implies that the mean seismic activity rate is highest for IBRZ and lowest for BBZ. Further, obtained return period here are compared with existing literature. Based on the present work, for $M_W \geq 6.0$, the return periods for the zones SP-AVZ, IBRZ and EHZ are found as 10.2 years, 1.81 years and 4.31 years respectively. As per Thingbaijam and

Nath (2008) however, the return periods for the same regions were found as 7.7 years, 3.3 years and 7.2 years. Similarly, for BBZ, return period for $M_W \geq 6.0$ based on the present work is obtained as 17.4 years in comparison to 32 years as reported by Shankar and Sharma (1998). It has to be highlighted here that the above differences between the return periods estimated in the present work and the return periods obtained from the previous studies may be the attributes of difference in choice of seismic source zone boundaries and the duration of EQ data considered in the analyses.

Based on known values of return period versus magnitude, it is difficult to understand the probability of a particular magnitude to occur within a period. Thus, plot of probability of exceedance versus magnitude is important. Figures 3.8 (a-c) present probability of exceedance versus magnitude plots, for each of the four seismic source zones for 50, 100 and 1000 years respectively. It can be observed from Figure 3.8 (a) that up to $M_W \leq 6.0$, each of the four seismic source zones has 100% probability to produce at least one EQ within 50 years. However, for $M_W > 6.0$ the decrease in the probability of exceedance in 50years is in the order of IBRZ>EHZ>SP-AVZ>BBZ. Similarly, it can be observed from Figures 3.8 (b) and 4.8 (c) that for $M_W > 6.2$ and $M_W > 7.2$ respectively, the probability of exceedance in 100 and 1000 years is in the decreasing order of IBRZ>EHZ>SP-AVZ>BBZ. This observation is analogous to the order of return periods for $M_W \geq 6.0$ obtained for the four zones in the previous discussion. Thus, these observations imply that IBRZ has the highest recurrence rate while BBZ has the lowest recurrence rates for $M_W > 6.0$. However, Table 3.3 shows that m_{max} for IBRZ, EHZ, SP-AVZ and BBZ are 7.6, 7.8, 8.5 and 8.4 respectively. Thus, even though IBRZ shows a high recurrence rate for EQs with $M_W \leq 7.4$ in 50 years and 100 years among all four zones, this zone cannot produce a great EQ based on the present work. In addition, SP-AVZ which is capable of producing EQs of $M_W \leq 8.5$ shows a relatively high recurrence rate for 1000 years period. Hence, collectively it can be concluded that the SP-AVZ is a zone of high hazard zone (less recurrence rate and high probability of exceedance of $M_W = 8.5$) and IBRZ is a low hazard.

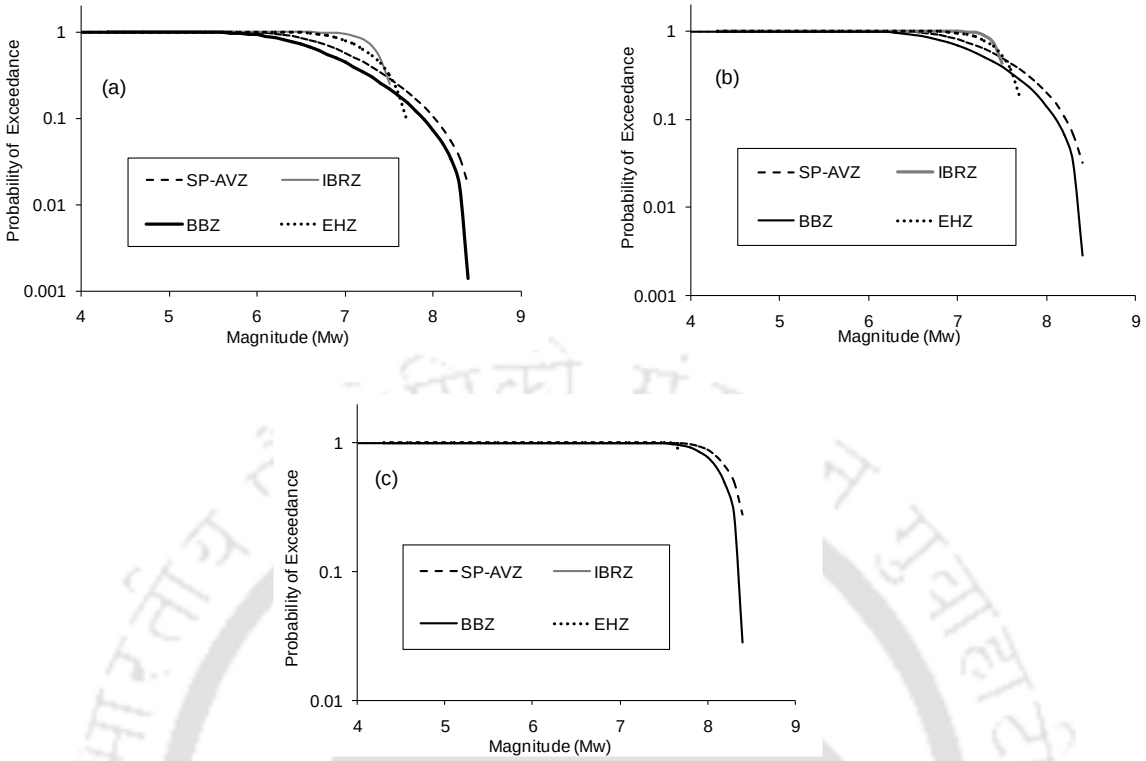

Figure 3.8: Probability of occurrence of different magnitude EQs in four seismic source zones for the return periods (a) 50 years, (b) 100 years and (c) 1000 years

3.6 Summary

This chapter presents a detailed study on identification and characterization of potential seismic sources located in the vicinity of the SP. All the tectonic features located within a radial distance of 500km from the centre of the SP are identified from past literature. In addition, information about past EQs originating within the 500km radius of the SP is also collected from various sources. These linear tectonic features and the past EQs are then compiled into a seismotectonic map. From the seismotectonic map it is observed that the EQ events are not uniformly distributed. Further based on tectonic features, geology, thickness of overburden, rupture characteristics and rate of movement, the entire seismotectonic map is divided into four seismic source zones namely; SP-AVZ, IBRZ, BBZ and EHZ. Further, in order to determine 'b' parameter, declustered EQ catalogues are assessed for completeness with respect to magnitude as well as time. With respect to magnitude, EQ catalogue for SP-AVZ, IBRZ, BBZ, EHZ as well as the entire catalogue are found complete for $M_W \geq 4.0$. Similarly, completeness analyses with

respect to time suggests EQ catalogue for different source zones are found complete for different durations. Based on complete dataset, 'b' values as per the maximum likelihood method, estimated for the SP-AVZ, IBRZ, BBZ and EHZ are 0.91±0.03, 0.94±0.02, 0.80±0.03 and 0.89±0.03 respectively. Based on the 'b' values obtained, BBZ is found to be the seismically most active source zone among the above four zones. Obtained 'b' values are found within the available spectra for 'b' values for each of the seismic source zones obtained by previous literatures. Further, return period versus M_W are obtained for each of the four seismic source zones. For source zones IBRZ, BBZ and EHZ, return periods based on existing literature are found lower that values reported in the literature. For SP-AVZ, present study finds an increase in return period in comparison to existing literature. Further, the analysis is extended to develop plots of probability of exceedance versus M_W within different periods. Based on probability of exceedance of different magnitudes it is found from the present work that even though IBRZ shows a high recurrence rate for obtained EQs with $M_W \leq 7.4$ in 50 years and 100 years among all four zones, this zone cannot produce a great earthquake. Similarly, SP-AVZ which is capable of producing EQs of $M_W \leq 8.5$ shows a relatively high recurrence rate for 1000 years period.

Chapter 4 - Deterministic Seismic Hazard Analysis

4.1 Introduction

Seismic hazard can be defined as a seismic phenomenon that "may cause loss of life, injury or other health impacts, property damage, loss of livelihoods and services, social and economic disruption, or environmental damage" (https://www.unisdr.org/we/inform/terminology). In seismological and EQ engineering community, seismic hazard is assessed using strong ground motion parameters, such as, peak ground acceleration and/or seismic intensity. The assessment is based on the knowledge of seismic wave excitation at the source, seismic wave propagation, its attenuation, and site effect in the region under consideration. Meanwhile, a comprehensive seismic hazard assessment should combine the results of seismological, geomorphological, geological, and tectonic investigations and modeling (e.g. Ismail-Zadeh 2014).

At present, two basic methods of seismic hazard assessment are in use: probabilistic and deterministic. The probabilistic seismic hazard analysis determines the rates of exceedance of certain levels of ground motion estimated over a specified period of time, and considers uncertainties in EQ source, magnitude, path, and site conditions (e.g., Cornell 1968). Meanwhile there is some criticism of the probabilistic assessment, and it is related to the validity of a point source model, ground motion uncertainties in the mathematical formulation of the method, and incapability to correctly model the dependencies between large numbers of uncertain random parameters (Panza et al. 2010). Deterministic Seismic Hazard Analysis (DSHA) is based on specified EQ scenarios. Namely, for a given earthquake, the attenuation of seismic energy with distance is assessed to determine the level of ground motion at a particular site using the available knowledge on EQ sources and wave propagation processes. Although the occurrence frequency of the ground motion is usually not addressed in DSHA, the method is considered to be robust for an assessment of hazard and useful for decision-making (Babayev et al. 2010).

The origins of DSHA could be traced back to nuclear power industry applications. It is in association with the fact that ground shaking due to a scenario-based EQ in the vicinity of critical infrastructure (e.g., nuclear power plants, dams, etc.) is to be seriously considered. DSHA performance includes, identification of seismic sources located around a site of interest which could influence the hazard scenario at the site. In DSHA, an EQ is assumed to occur at the point of the fault closest to the site of hazard assessment. Thus, the shortest distance from the site to the source is calculated. Based on the information of past EQs, which had occurred around the site, the maximum possible EQ magnitude is determined. Considering the identified sources, the shortest distance, and the maximum possible magnitude earthquake, the ground motions, which could occur at the site, are estimated.

Several researchers have performed DSHA studies across India. Desai and Choudhury (2014) performed DSHA for Greater Mumbai. DSHA for Lucknow city was performed by Kumar et al. (2013). Parvez et al. (2003) performed DSHA for the entire country and the adjoining areas. In this study DSHA is performed for the SP.

4.2 Estimation of maximum possible magnitude

Ground shaking due to an EQ is influenced by its magnitude, and hence, an assessment of the maximum possible EQ magnitude (*Mp*) is of importance in seismic hazard analysis. In this study *Mp* is estimated for each of the 72 seismic sources. There are several statistical methods for *Mp* assessments at a fault using EQ catalogues (e.g., Kijko and Sellevoll 1989; Kijko and Graham 1998). Unfortunately, the number of EQ associated with individual faults does not allow for a reliable assessment of the *Mp* using statistical methods. Moreover, *Mp* cannot be solely determined from EQ catalogues (e.g., Holschneider et al. 2011), and thus an additional information should be used for this aim. This information includes the fault plane geometry and the maximum observed displacement on the fault; long-term geological and paleo-seismological assessments to reduce the errors in calculations of *Mp*; and others. In addition, numerical modeling of regional fault dynamics is a powerful alternative to overcome the shortcomings associated with the short time duration (about 100+ years) of recorded EQ catalogues (e.g., Sokolov and Ismail-Zadeh et al. 2015; Ismail-Zadeh et al., 2017).

Hence, the simplest approach to calculate *Mp* i.e. by adding a constant to the maximum observed EQ magnitude (M_{obs}) is used. In this study, constant 0.4 is added, if M_{obs}<5; 0.5, if 5≤ M_{obs}<8; and 0.6 otherwise (NDMA 2010; Kumar et al. 2013). Table 4.1 lists M_{obs} and *Mp* on each fault. The fault numbers in Table 4.1 correspond to the fault numbers in Figure 4.1.

Table 4.1: Faults considered in this study and their characteristics

Source Zone	Fault name	Fault no.	M_{obs}	M_p	Focal depth (km)
SP-AVZ	Oldham	1	8.1	8.7	60
	Dhubri	2	7.1	7.6	60
	F91-93	3	6.5	7.0	180
	Samin	4	4.2	4.6	51
	Kopili	5	7.2	7.7	35
	Dauki	6	7.1	7.6	60
	Barapani	7	5.6	6.1	10
	Chedrang	8	5.2	5.7	42
	Bomdila	9	5.5	6.0	33
	Dudhnoi	10	5.5	6.0	60
	Dapsi	11	5.5	6.0	60
IBRZ	F110-113	12	7.2	7.7	35
	F96-99	13	6.7	7.2	68
	CMF	14	7.3	7.8	150
	Kaladan	15	7.5	8.0	150
	Kabaw	16	7.2	7.7	41
	Disang	17	7.0	7.5	120
	F100-109	18	6.1	6.6	60
	Naga	19	5.5	6.0	56
BBZ	F144	20	6.5	7.0	50
	F154	21	6.1	6.6	50
	F145	22	6.4	6.9	50
	Sylhet	23	7.6	8.1	50
	F116	24	6.3	6.8	50
	F152	25	6.0	6.5	50
	Eocene Hinge Zone	26	7.8	8.3	50
	Arakan	27	7.5	8.0	50
	Madhupur	28	5.9	6.4	30
	F132	29	6.2	6.7	50

	F156	30	5.3	5.8	39
	F157	31	5.0	5.5	36
	F155	32	5.1	5.6	10
	KNF	33	6.0	6.5	50
	F122	34	4.9	5.3	39
	F115	35	5.0	5.5	50
	F119	36	5.0	5.5	50
	F124	37	4.6	5.0	50
	F118	38	4.9	5.3	50
	GKF	39	6.0	6.5	50
	F114	40	4.6	5.0	50
	F121	41	4.9	5.3	50
	F123	42	4.8	5.2	50
	F117	43	4.5	4.9	50
	MRMF	44	5.5	6.0	50
	Kishanganj	45	4.9	5.3	50
	JGF	46	4.8	5.2	50
	SBF	47	4.2	4.6	50
	Pingla	48	4.2	4.6	50
	DBF	49	4.0	4.4	50
EHZ	F94	50	6.4	6.9	70
	BNS	51	7.7	8.2	70
	Kakahtang	52	7.7	8.2	70
	Dudhkosi	53	5.2	5.7	1
	Indus suture	54	7.7	8.2	70
	BTF	55	6.5	7.0	70
	F72	56	5.3	5.8	22
	Munsiari	57	7.0	7.5	70
	F9	58	6.3	6.8	140
	F77	59	5	5.5	21
	MBT	60	7.7	8.2	70
	F75	61	4.6	5.0	33
	F7	62	4.8	5.2	85
	MCT	63	7.2	7.7	70
	Arun	64	5.2	5.7	33
	F95	65	4.3	4.7	59
	Purnea	66	5.2	5.7	70
	F1-2	67	4.8	5.2	85
	F3-4	68	4.5	4.9	73

	F10-12	69	6.3	6.8	70
	F13-14	70	5.1	5.6	10
	F15-16	71	6.1	6.6	35
	F5-6	72	5.5	6.0	29

4.3 Ground motion prediction equations (GMPEs)

An important step while performing seismic hazard analysis is to assess the level of ground shaking at the site of interest in terms of ground motion parameters. As regional EQ ground motion measurements are scarce and influenced by soil conditions, these ground motion parameters are obtained using appropriate ground motion prediction equations (GMPEs). Different region specific GMPEs have been developed so far to estimate the ground motion parameters (or seismic hazard level) at a site. Nath et al. (2005), Das et al. (2006), Raghukanth and Iyengar (2007), Sharma et al. (2009), Nath et al. (2009), Baruah et al. (2009), Gupta (2010), NDMA (2010) and Anbazhagan (2013) developed GMPEs for the Himalayas and northeast India considering recorded or synthetic EQ data as well as their combination. The existence of several GMPEs could lead to the uncertainty associated with the degree of suitability of the GMPE for the study area. This uncertainty could be addressed by applying the logic tree approach, wherein appropriate weights or ranks suitable for the study area are added to the GMPEs (Delavaud et al. 2009). Nath and Thingbaijam (2011) point out that several of the earlier studies had paid little attention to the proper selection of GMPEs. Thus, Nath and Thingbaijam (2011) adopted the efficacy test method by Scherbaum et al. (2009) for the selection and ranking of the most suitable GMPEs applicable to different regions of India.

Following Nath and Thingbaijam (2011), initially several best suitable GMPEs for northeast India consisting of GMPEs by Hwang and Huo (1997), Toro (2002), Atkinson and Boore (2006), Raghukanth and Iyengar (2007) and Nath et al. (2009) were selected. The above mentioned GMPEs were checked for their applicability within the seismotectonic region of radius 500 km, consisting of EQ events of magnitude ranging from 4.0 to 8.7. Except for the GMPE by Toro (2002), the remaining GMPEs have either been developed for shorter distance ranges or for lesser magnitude ranges.

Therefore, for the present seismic hazard analysis the GMPE developed by Toro 2002 is used which is shown below;

$$\ln(y) = A_1 + A_2(M-6) + A_3(M-6)^2 - A_4 \ln R_M - (A_5 - A_4)\max\left[\ln\left(\frac{R_M}{100}\right), 0\right] - A_6 R_M + \varepsilon_e + \varepsilon_a \quad (4.1)$$

where $R_M = R_f + 0.089\exp(0.6M)$

R_f is the hypocentral distance, y is the spectral acceleration (in g); M is the moment magnitude; ε_e is epistemic uncertainty; ε_a is aleatory uncertainty; and A_1 to A_6 are the constants (presented in Table 2 by Toro et al. 1997).

Nath and Thingbaijam (2011) had also suggested that the GMPE developed by Kanno et al. (2006) for Japan is suitable for the Himalayan and the Indo-Myanmar regions. As these regions are fall within the seismotectonic region, hence Kanno et al. (2006) is selected for this study

$$\log_{10}(y) = B_1 M_w + B_2 r - \log_{10}(r) + B_3 + \varepsilon_2 \quad (4.2)$$

where r is the hypocentral distance in km; B_1, B_2, and B_3 are the regression coefficients; and ε_2 is the error between observed and predicted values. Values of these coefficients for different oscillation periods are taken from Kanno et al. (2006).

In addition, two other GMPEs developed by NDMA (2010) and by Anbazhagan et al. (2013) are used in this study. GMPE proposed by NDMA (2010) is represented as;

$$\ln(y/g) = C_1 + C_2 M + C_3 M^2 + C_4 r + C_5 \ln(r + C_6 e^{C_7 M}) + C_8 \log_{10}(r) f_0 + \ln(\varepsilon_3) \quad (4.3)$$

where, g is the acceleration due to gravity; C_1 to C_8 are the coefficients specific for northeast India; $f_0 = \max\left(\ln\left({}^{r}/_{100}\right), 0\right)$, and ε_3 is the standard error. Values of the coefficients for different periods are taken from NDMA (2010). Anbazhagan et al. (2013) developed a GMPE for the Himalayan region considering both recorded and synthetically generated ground motion data for 14 significant EQs, occurred at different segments of the Himalayan belt. Synthetic ground motions were developed for the past EQs with no ground motion records, which also included the 1897 Assam EQ. The GMPE developed by Anbazhagan et al. (2013) is as follows;

$$\log_{10}(y) = D_1 + D_2 M - b\log_{10}(r + e^{D_3 M}) + \sigma \quad (4.4)$$

where, b is a decay parameter;D_1, D_2, and D_3 are regression constants; and σ represents the standard error. Values of the coefficients for different periods are taken from Anbazhagan et al. (2013).Table 4.2 lists the GMPEs used in the present study with the magnitude range and distance range up to which each of the selected GMPE is valid.

Table 4.2: Summary of GMPEs used in the study

Model	Region	Magnitude	Distance (km)
Toro (2002)	Eastern North America	5.0-8.0	R_{JB}<1000
Kanno et al. (2006)	Japan, USA, Turkey	5.5-8.2	R_{RUP} (also R_{HYPO}) ≤450
NDMA (2010)	India	4.0-8.5	R_{HYPO}≤500
Anbazhagan et al. (2013)	Himalayan region	5.3-8.7	R_{HYPO}≤300

Note-R_{JB} is Joyner-Boore distance, R_{RUP} is rupture distance and R_{HYPO} is hypocentral distance.

The GMPEs considered in this study were developed on the basis of limited ground motion data, and for this reason, the equations have a standard error term. Logic tree approach provides a possibility to select more than one GMPE in seismic hazard analysis so that the standard error in the proposed seismic hazard value can be minimized. However, a relative weightage of selected GMPEs will influence the standard error term, and hence, a suitable weight should be assigned to each selected GMPE before using the logic tree (Delavaud et al.2009). Scherbaum et al. (2009) proposed to assess the appropriateness of each selected GMPE in terms of the Kullback–Leibler divergence D, which is the measure of how one probability distribution (e.g., for the "true" ground motion) diverges from an expected probability distribution (e.g., for the ground motion predicted by a GMPE model) as;

$$D(f,g) = E_f[log_2(f)] - E_f[log_2(g)] \quad (4.5)$$

where f is the probability distribution resembling "true" observations, which are actually unknown; g is the probability distribution representing a selected GMPE model, E_f is the expected value from a given model. The Kullback–Leibler divergence becomes

smaller with the probability distribution g approaching the probability distribution f. Scherbaum et al. (2009) suggested to calculate the second term in Eq. (4.5) using the average sample log likelihood (*LLH*);

$$LLH(g,x) = -\frac{1}{N}\sum_{i=1}^{N} log_2[g(x_i)] \tag{4.6}$$

where, $x = \{x_i\}$, i=1,…,N are samples of ground motion values obtained using a GMPE model $g(x_i)$. The model $g(x_i)$ follows a normal distribution with the probability density function (*PDF*) over range of x_i (i=1,…,N), as;

$$PDF = \left(\frac{1}{\sqrt{2\pi}\sigma}\right)^N \exp\left(-\sum_{i=1}^{N}\frac{(x_i-\mu)^2}{2\sigma^2}\right) \tag{4.7}$$

where μ is the mean (expectation) of the normal distribution, σ is the standard deviation, and σ^2 is the variance. For this *PDF*, the value of *LLH* can be estimated as;

$$LLH = log_2(\sqrt{2\pi}) + log_2(\sigma) + \frac{log_2(e)}{N}\sum_{i=1}^{N}\frac{(x_i-\mu)^2}{2\sigma^2} \tag{4.8}$$

Using the *LLH* value for each GMPE model, the Data Support Index (DSI) can be calculated for each GMPE. The DSI is a measure of the percentage by which the weight of a model is increased (positive DSI) or decreased (negative DSI) by the data used (Delavaud et al. 2012). The weight (w_j) of GMPE model g_j (j= 1, …, M) can then be calculated as;

$$w_j = 2^{-LLH(g_j,x)} \Big/ \sum_{k=1}^{k=M} 2^{-LLH(g_k,x)} \tag{4.9}$$

and the DSI of model g_j as;

$$DSI_j = 100\frac{w_j - w_{unif}}{w_{unif}} \tag{4.10}$$

where, w_{unif} is the uniform weight $w_{unif} = 1/M$, and M = 4 in this study.

To generate a set $\{x_i\}$ of the ground motion parameter (PHA) using a selected GMPE, the following procedure is used. For each of three cities located in the districts of East-Khasi Hill, Ri-Bhoi and West Garo – the Shillong city (25.57°N, 91.89°E), Nongpoh (25.87°N, 91.83°E) and Tura (25.51°N, 90.20°E) (1) a minimal distance

(referred to as 'epicentral distance') between the city and the nearest fault within each of four seismic source zones is calculated; (2) the maximal epicentral distance is assumed to be the radius of the seismotectonic region (i.e. 500km) for each of four source zones; and (3) $\{x_i\}$values (PHA values) are calculated from relevant GMPEs based on the range of hypocentral distances(based on above range of epicentral distance and known information on focal depth) and on the highest possible EQ magnitude (*Mp*) within each seismic source zone. (From Table 4.1, the highest *Mp* is 8.7, 8.0, 8.3, and 8.2 for SP-AVZ, IBRZ, BBZ, and EHZ, respectively.

For example, for the Shillong city, the minimal epicentral distance from the IBRZ, BBZ, and EHZ source zones are 120 km, 60 km, and 160 km, respectively. Since the Shillong city is located within SPAVZ, the minimal epicentral distance is 30 km (the distance from the Shillong city to the Barapani fault). Hence, for the calculation of $\{x_i\}$ values, the range of hypocentral distances for the Shillong city is taken as 30 to 500km, 120 to 500km, 60 to 500km, and 160 to 500km from the SP-AVZ, IBRZ, BBZ, and EHZ seismic source zones, respectively. Similarly, the set of values $\{x_i\}$ is generated in the case of Nongpoh and Tura; the minimum hypocentral distance within SP-AVZ is calculated from Nongpoh and Tura with respect to the Dapsi fault and the Barapani fault, respectively.

Based on the $\{x_i\}$ values so obtained, the LLH value for the GMPE model g_j as well as w_j and DSI_k are calculated using Eqs. (4.8)-(4.10). Only those GMPEs, which give positive DSI values, are identified and ranked in the order of the highest to the lowest DSI values. New $w_i$values are then calculated for the GMPE models having positive DSI to obtain the weights for relevant GMPEs, which are used for seismic hazard assessments within each of four seismic source zones. Tables 4.3, 4.4 and 4.5 present the LLH values, DSI values, ranks and weights $w_i$of different GMPEs obtained for each seismic source zone for the East Khasi hills, Ri-Bhoi and West Garo hills districts, respectively.

Table 4.3: Log likelihood (LLH) value, Data Support Index (DSI) value, rank and weight of the employed GMPEs for the East Khasi hills district

Zone	GMPEs	LLH values	DSI value	Rank	Weights
SP-AVZ	Toro (2002)	35.34	1.53	2	0.39
	Kanno et al. (2006)	36.63	-58.41	4	-
	NDMA (2010)	34.69	60.03	1	0.61
	Anbazhagan et al. (2013)	35.41	-3.15	3	-
IBRZ	Toro (2002)	25.29	14.26	3	0.32
	Kanno et al. (2006)	26.70	-56.01	4	-
	NDMA (2010)	25.23	19.22	2	0.33
	Anbazhagan et al. (2013)	25.18	23.53	1	0.35
BBZ	Toro (2002)	30.70	11.21	3	0.31
	Kanno et al. (2006)	32.05	-56.39	4	-
	NDMA (2010)	30.44	33.23	1	0.38
	Anbazhagan et al. (2013)	30.69	11.96	2	0.31
EHZ	Toro (2002)	19.06	12.82	3	0.31
	Kanno et al. (2006)	20.53	-59.47	4	-
	NDMA (2010)	19.03	14.79	2	0.32
	Anbazhagan et al. (2013)	18.83	31.85	1	0.37

Table 4.4: Log likelihood (LLH) value, Data Support Index (DSI) value, rank and weight of the employed GMPEs for the Ri-Bhoi district

Zone	GMPEs	LLH values	DSI value	Rank	Weights
SP-AVZ	Toro (2002)	36.08	46.00	1	0.51
	Kanno et al. (2006)	38.18	-65.93	4	-
	NDMA (2010)	36.11	42.37	2	0.49
	Anbazhagan et al. (2013)	36.99	-22.45	3	-
IBRZ	Toro (2002)	23.74	14.20	3	0.32
	Kanno et al. (2006)	25.17	-57.55	4	-
	NDMA (2010)	23.70	17.41	2	0.33

	Anbazhagan et al. (2013)	23.60	25.94	1	0.35
BBZ	Toro (2002)	29.15	11.71	3	0.31
	Kanno et al. (2006)	30.53	-56.85	4	-
	NDMA (2010)	28.94	30	1	0.37
	Anbazhagan et al. (2013)	29.11	15.15	2	0.32
EHZ	Toro (2002)	22.18	13.05	3	0.31
	Kanno et al. (2006)	23.63	-58.59	4	-
	NDMA (2010)	22.12	18.02	2	0.33
	Anbazhagan et al. (2013)	22.01	27.51	1	0.36

Table 4.5: Log likelihood (LLH) value, Data Support Index (DSI) value, rank and weight of the employed GMPEs for the West Garo hills district

Zone	GMPEs	LLH values	DSI value	Rank	Weights
SP-AVZ	Toro (2002)	33.00	4.94	2	0.29
	Kanno et al. (2006)	34.34	-58.39	4	-
	NDMA (2010)	32.49	50.37	1	0.42
	Anbazhagan et al. (2013)	33.03	3.07	3	0.29
IBRZ	Toro (2002)	18.28	13.63	2	0.32
	Kanno et al. (2006)	19.76	-59.24	4	-
	NDMA (2010)	18.30	12.14	3	0.31
	Anbazhagan et al. (2013)	18.04	33.46	1	0.37
BBZ	Toro (2002)	31.48	10.90	2	0.31
	Kanno et al. (2006)	32.81	-56.12	4	-
	NDMA (2010)	31.19	34.86	1	0.38
	Anbazhagan et al. (2013)	31.48	10.36	3	0.31
EHZ	Toro (2002)	20.62	12.96	3	0.31
	Kanno et al. (2006)	22.08	-59.04	4	-
	NDMA (2010)	20.58	16.34	2	0.33
	Anbazhagan et al. (2013)	20.42	29.74	1	0.36

For the three districts within the source zones of IBRZ, BBZ and EHZ, the GMPEs developed by Toro (2002), NDMA (2010) and Anbazhagan et al. (2013) are found to be suitable. Within SP-AVZ, the GMPEs developed by Toro (2002) and NDMA (2010) are suitable for the East Khasi hills and Ri-Bhoi districts, and the GMPEs by Toro (2002), NDMA (2010), and Anbazhagan et al. (2013) are suitable for the West Garo hills district. It has to be noted here that the GMPEs by Toro (2002), NDMA (2010), and Anbazhagan et al. (2013) were developed for the site conditions with the shear wave velocity (Vs) of 1.8 km s^{-1}, 3.6 km s^{-1}, and 3.6 km s^{-1}, respectively. According to the NEHRP site classification scheme (BSSC 2004), the sites with Vs> 1.5km s^{-1} are considered to belong to site class A (hard rock).

The ground motion predicted by the GMPE can be compared to that recorded during EQs to select the suitable prediction equations, when both the recorded and predicted data are assessed at the bedrocks. Unfortunately, despite the existing ground motion recordings in the India, the site information about the recording stations is incomplete (e.g. Anbazhagan et al. 2013; Harinarayan and Kumar 2018a, b).Therefore, unless proper site information is known, the recorded ground motion can be used neither for developing GMPEs nor for site-specific ground response analysis.

4.4 Peak Horizontal Acceleration (PHA)

The M_p values obtained in this work are employed in the selected GMPEs to perform DSHA for the study area. To obtain an unbiased measure of minimum hypocentral distances between the faults and study area, the SP is divided into 58 x 21 cells along the longitude and latitude respectively. The size of each cell is 0.05° x 0.05°. The minimum hypocentral distances between the 72 faults and the top left corner of each cell are determined. These minimum hypocentral distances and M_p values are then employed in the selected GMPEs. The PHA values are estimated at the bedrock level from the selected GMPEs at the top left corners of each cell. The PHA values are calculated taking into account the weights assigned to each of the GMPEs from the LLH calculations as discussed earlier. Because the seismotectonic region consists of four seismic source zones, four sets of PHA values are obtained in this study at each cell based on weights of each GMPE for that seismic source zone. The highest PHA

value among the four is assigned to each cell to produce a PHA contour map. Figures 4.1 (a-c) present the results of the DSHA for three districts of (a) East Khasi hills, (b) Ri-Bhoi, and (c) West Garo hills. The maximum PHA values at Shillong city, Nongpoh, and Tura are 0.36g, 0.46g, and 0.33g respectively. It can be observed from Figure 4.1a that the highest PHA value of 0.46 g within the East Khasi hills district is obtained on the northern side of the district. For the Ri-Bhoi district the highest PHA value of 0.46g is obtained on the eastern part of the district (Figure 4.1b). These high PHA values are found to be due to the presence of the Barapani fault at that location. However, at other locations within the two districts, the Oldham fault is found to influence significantly the PHA values. Similarly, for the West Garo hills district the Oldham fault is found to be responsible for the high PHA value towards the north. However, towards south of the district, the Dauki fault is found to influence the PHA values. The Barapani fault, the Oldham fault and the Dauki fault are all located within the SP-AVZ. This shows that the tectonic and geological setting of the SP-AVZ is such, that this zone has the potential to cause the highest seismic hazard among the four seismic source zones. This is comparable to the results obtained in Chapter 4, where a similar conclusion was derived.

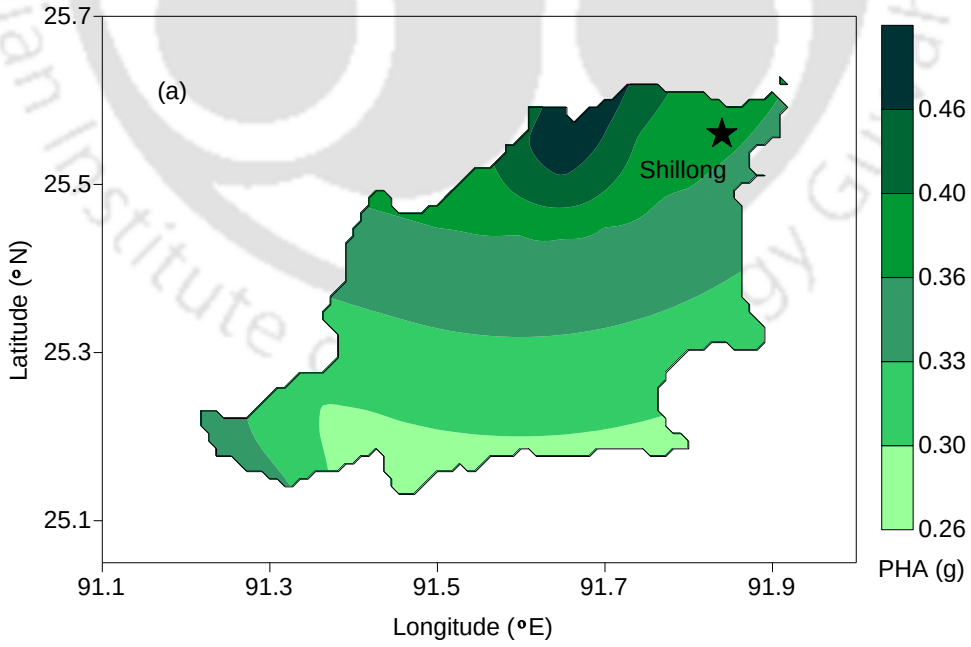

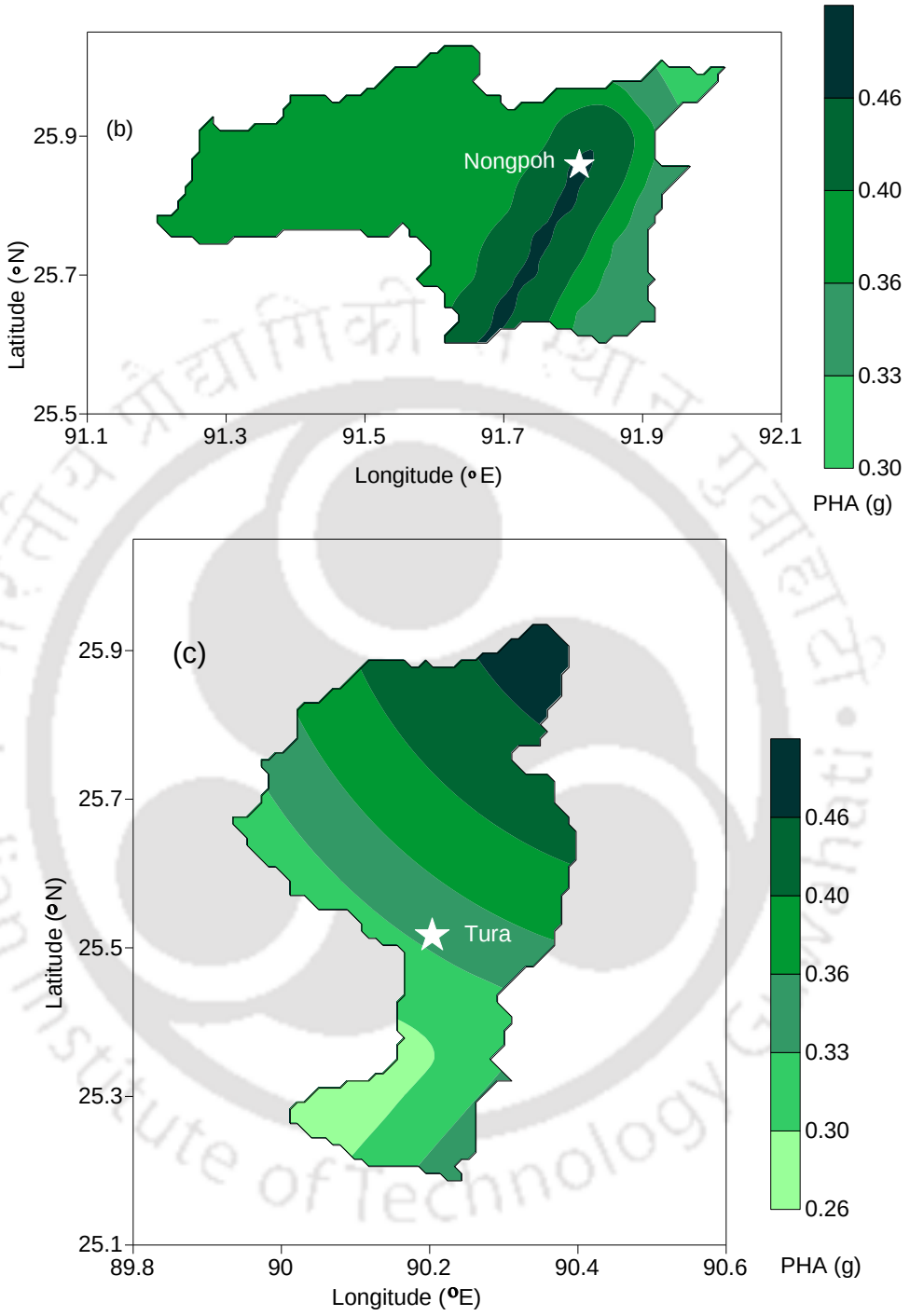

Figure 4.1: Peak horizontal accelerations for the (a) East Khasi hills, (b) Ri-Bhoi, and (c) West Garo hills districts

The PHA values obtained on the basis of DSHA are juxtaposed with PHA contours maps developed by the NDMA (2010) based on Probabilistic Seismic Hazard Analysis (PSHA). It should be mentioned that while DSHA assesses the worst scenario

and presents the values of the ground motion related to the worst scenario, PSHA allows determining the rates of exceedance of the specified ground motion within a desired time. Therefore, a direct comparison between the DSHA and PSHA results is meaningless.

The NDMA (2010) contours over the SP gave PHA values of 0.40g, 0.45g and 0.55g at 2%, 1% and 0.5% probabilities for the oscillation period of 0s. It has to be noted here that the contours developed by NDMA (2010) are for the entire SP at different percentages of probability of exceedance and not for individual cities as attempted in this study. The PHA values estimated in this study are further compared to the hazard maps for Manipur (an Indian state east to Meghalaya) developed by Pallav et al. (2012) at 0.02 probability of exceedance in 50 years. Pallav et al. (2012) found that the PHA values for 11 districts of Manipur range from 0.4 to 1.1g.

4.5 Response spectra

Further, attempts are made to develop response spectra for the Shillong city (25.57°N, 91.89°E), Nongpoh (25.87°N, 91.83°E) and Tura (25.51°N, 90.20°E). The response spectra are calculated at top left corners of the cells at the minimum hypocentral distances from each of the 72 faults and for the corresponding M_p values. The hypocentral distance and M_p are then used in selected GMPEs with their appropriate weights. The coefficients in GMPEs (Eqs. 5.1-5.4) are the function of the period of oscillations. This way, DSHA is performed for different periods, and the response spectra are developed for above mentioned three locations. Developed response spectra at bedrock level for the Shillong city, Nongpoh and Tura are shown in Figure 4.2. At period 0s, the spectral acceleration (SA) value is 0.36g for Shillong city, which matches well with the value assigned to seismic zone V of the Seismic Zones of India (IS1893 Part 1:2016). The SA at Nongpoh at 0s, 0.1s and 0.2s are 0.46g, 0.77g and 0.55g respectively, which are the highest values among the three sites. An increase in the SA values can be observed after 0.2s at Tura.

The response spectra developed in this study is in agreement with those developed earlier (e.g., Eurocode 8; NDMA 2010) as shown in Figures 4.3 (a-c). For example, the Eurocode 8 is matching well up to 0.1s for all the above three locations.

However, the predicted SA at 0s obtained for Nongpoh is higher than those estimated on the basis of Eurocode 8. For the Shillong city, the response spectra from NDMA (2010) give SA values of 0.45 g and 0.80 g at 0 s and 0.1 s, respectively, which are higher than the values obtained in this study. Again for periods greater than 0.1 s the NDMA (2010) SA values match well with the results of the present study (Figure 4.3 a). A similar trend can be observed for Nongpoh (Figure 4.3 b), where the higher values of 0.59 g and 0.93 g are attained at 0 s and 0.1s, respectively, and a closer match with the present studies is obtained for the periods greater than 0.2 s. For Tura (Figure 4.3 c), the SA values of 0.35 g and 0.63g at 0 s and 0.1 s, respectively are similar to the present study, while not well matching the results of the present study at the periods greater than 0.2 s.

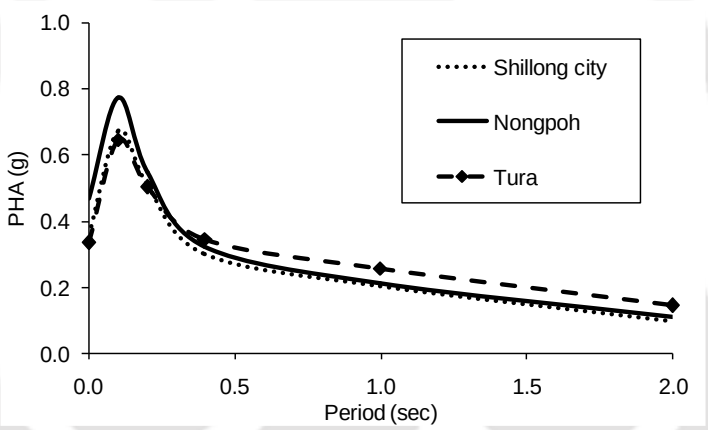

Figure 4.2: Response spectra at Shillong city, Nongpoh and Tura based on DSHA

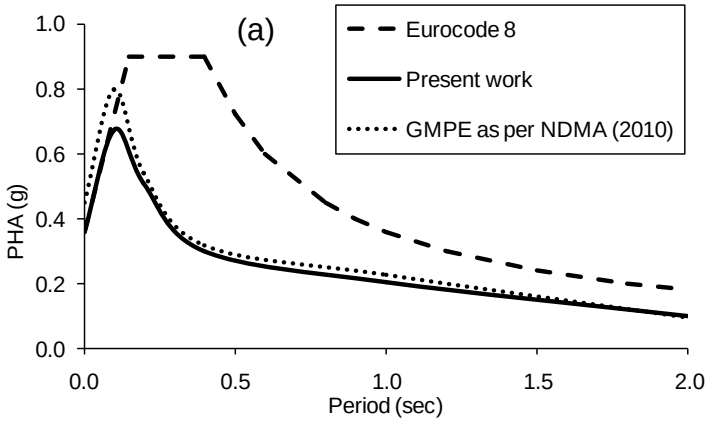

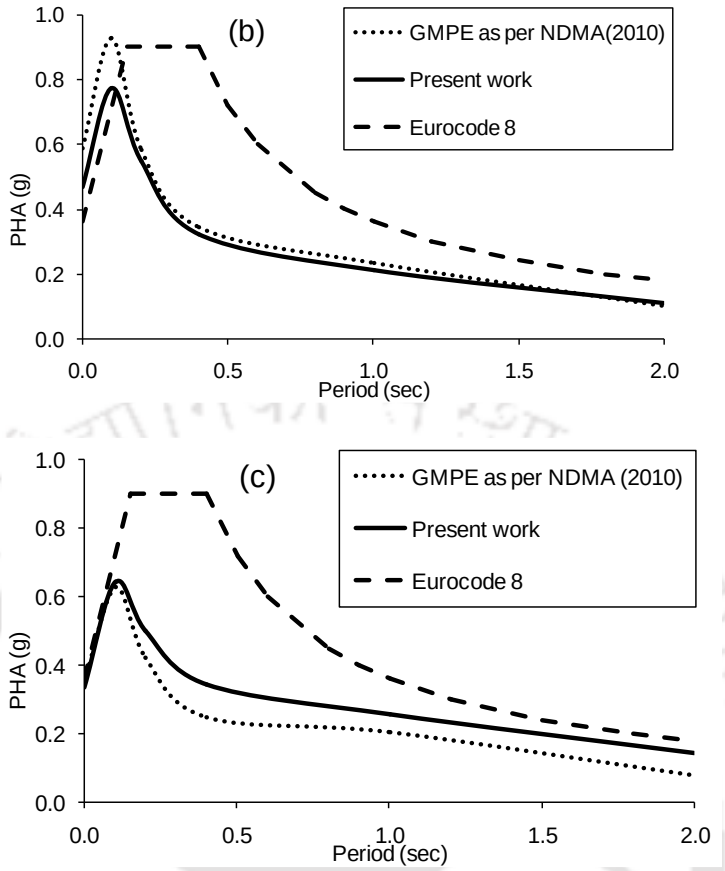

Figure 4.3: Comparison of different response spectra at (a) Shillong city, (b) Nongpoh and (c) Tura

4.6 Summary

DSHA is performed for the three districts –East Khasi hills, Ri-Bhoi, and West Garo hills within the SP. The PHA values obtained range from 0.26g to 0.46g within these districts. For the East Khasi hills and the West Garo hills districts, the northern parts show higher PHA values of 0.46g. For the Ri-Bhoi district, higher PHA value of 0.46g is observed in its eastern part. It is considered in this study that the higher PHA values in the eastern part of the Ri-Bhoi district and the northern part of the East Khasi hills district are due to the Barapani fault. Meanwhile, the Oldham fault influences the PHA values for the remaining areas within the two districts. The higher PHA value in the northern part of the West Garo hills district is also assumed to be due to the Oldham fault.

The DSHA maps for the East Khasi hills, Ri-Bhoi and West Garo hills districts are compared to the PHA contours maps developed by NDMA (2010) and Pallav et al.

(2012), and the comparisons show a reasonable agreement. The response spectra developed for the Shillong city, Nongpoh and Tura are also compared to the response spectra developed using Eurocode 8 and the GMPE given by NDMA (2010). Except of some deviations in the response spectra associated with the use of multiple GMPEs and LLH weights in this work, the comparison shows a good match.

Chapter 5 - Probabilistic Seismic Hazard Analysis (PSHA)

5.1 Introduction

EQs are natural hazards which are associated with uncertainties related to location, size and ground motion exceedance. PSHA addresses these uncertainties and provides an unambiguous picture of future EQ scenario at a site (Cornell 1969). PSHA is particularly helpful in case of sites with complex tectonic setting such as the SP. It has been mentioned earlier that the SP is affected by the seismotectonic setting of four seismic source zones identified in Chapter 4. The tectonic features, geology, thickness of overburden, rupture characteristics and rate of movement of each of the four seismic sources zones are varying widely. This wide variation among the seismic sources zones provide a particularly challenging task at hand to estimate the future seismic hazard potential of the SP. For example, faults lying within both the BBZ and the IBRZ have produced major EQs in the past. However, within the IBRZ a large cluster of M_W<7.0 EQs can also be observed, which is absent within the BBZ (Figure 4.4). Thus the consideration of only the minimum hypocentral distance and the maximum magnitude EQ, as in DSHA, might provide somewhat reasonable results for the BBZ however, for the IBRZ the seismic hazard potential would be severely underestimated. Further, from DSHA it is clear that the consideration of only the minimum hypocentral distance and the maximum magnitude results in the highest possible values of ground motion parameters. This means that presence of the Oldham fault, with past record of M_W-8.1 EQ, within SP-AVZ would result in the highest value of ground motion parameter at a site located in the vicinity of the fault. However, the probability of exceedance of this high value of ground motion parameter during the design life of a structure is very thin, as with the increase in the size of the EQ, the probability of occurrence of the event decreases. Similarly, from DSHA results no information is available about the occurrences of major EQs within other seismic source zones during the design life of a structure. Hence, taking into account the above mentioned observations, it can be concluded that performing PSHA for sites with complex tectonic such as the SP, is essential to arrive at reasonable seismic hazard values. It has been mentioned earlier that

during the past EQs, most damages were reported from the districts of East Khasi hills, Ri-Bhoi and West Garo hills. Hence, previously DSHA has been performed for the above mentioned districts. In this chapter, PSHA is attempted for the same three districts as discussed in detail in subsequent sections. The methodology adopted in this study to perform PSHA is already discussed in Chapter 3.

5.2 Uncertainties in PSHA

As mentioned earlier, PSHA takes into account the uncertainties associated with magnitude, hypocentral distance and ground motion exceedance of a particular source. The combination of the above mentioned uncertainties gives a frequency of ground motion exceedance at a site, during a certain time period due to that source. The probability of exceedance $p_E(z)$ of a ground motion level *z*, for an exposure time period *t*, at a site is given by the Poisson distribution model as shown below;

$$P_E(z) = 1 - e^{-(v_z.t)} \tag{5.1}$$

where, v_z is the annual frequency of ground motion exceedance at the site of interest. The uncertainties related to magnitude, hypocentral distance and ground motion exceedance of a particular value is addressed by v_z, which is given by (EM-1110 1999);

$$v(z) = \sum_{n=1}^{N} \sum_{m_i=m^0}^{m_i=m^u} \lambda_n(m_i) \left[\sum_{r_j=r_{min}}^{r_j=r_{max}} P_n\left(R = r_j | m_i\right) P(Z > z | m_i r_j)\right] \tag{5.2}$$

where, $\sum_N$ = summation over all (*N*) seismic sources

$\lambda_n(m_i)$ = annual frequency of occurrence of EQs of magnitude m_i (above a certain minimum size of EQ) on seismic source *n*

$P\left(R = r_j | m_i\right)$ = probability of an EQ of magnitude m_i on source *n* occurring at a certain distance r_j from the site

$P(Z > z | m_i r_j)$= probability that ground motion level z will be exceeded, given an EQ of magnitude m_i on source *n* at distance r_j from the site

Various probabilities of exceedance mentioned above are discussed in details in the next subsections.

5.2.1 Fault Deaggregation

The $\lambda_n(m_i)$ in Eq. (5.2) is obtained by discretizing the cumulative recurrence relationship at a specified discretization step size, Δm. The cumulative EQ recurrence relationship is given by the truncated exponential distribution of the Gutenberg and Richter recurrence law (EM-1110 1999) as shown below;

$$N(M > m) = \alpha(m^0).\frac{10^{-b(m-m^0)}-10^{-b(m^u-m^0)}}{1-10^{-b(m^u-m^0)}} \tag{5.3}$$

where, m^0 = lower bound magnitude of interest to the calculation

m^u = maximum magnitude event that can occur on the source

$\alpha(m^0)$ = frequency of occurrence of events of magnitude m^0 and larger

The value of $N(M > m)$ thus obtained is then used to estimate $\lambda(m_i)$ using the following equation (EM-1110 1999);

$$\lambda_n(m_i) = N\left(m > m_i - \frac{\Delta m}{2}\right) - N\left(m > m_i + \frac{\Delta m}{2}\right) \tag{5.4}$$

In this study, the value of Δm for each fault in Eq. (5.4) is calculated as $\frac{1}{6}(m^u - m^0)$. Further, Eq. (5.4) is given for an entire region. To differentiate between near and distant sources and to obtain the activity rates of each source, it is required to estimate $\lambda_n(m_i)$ for individual sources. Iyengar and Ghosh (2004) used the heuristic principle of conservation of seismic activity for deaggregation from entire region to individual fault. As per this approach, the number of EQs per year with $m > m^0$ in the region denoted by $N(m_0)$, should be equal to the sum of number of events possible on different faults denoted by $N_i(m_0)$ (i=1,2,..., N_i) where "*i*" represents total number of faults. Governing equation by Iyengar and Ghosh (2004) gave the following relation;

$$N_i(m_0) = 0.5(\alpha_i + \delta_i)N(m_0) \tag{5.5}$$

where, $$\alpha_i = \frac{L_i}{\sum L_i} \tag{5.6}$$

$$\delta_i = \frac{Number\ of\ EQs\ close\ to\ the\ source}{Total\ number\ of\ EQs\ in\ the\ region} \quad (5.7)$$

where, L_i is the length of the i^{th} fault.

The values of $\alpha_i$and δ_i obtained in this study following the above approach along with a typical calculation for the frequency of EQ magnitude for the Oldham fault are shown in Table 5.1.

Table 5.1: Typical calculation of frequency of exceedance of various magnitudes to occur for Oldham fault

m_i	α_i	δ_i	$\Delta m/2$	$m_i-\Delta m/2$	$m_i+\Delta m/2$	$N(mi>m-\Delta m/2)$	$N(mi>m+\Delta m/2)$	$N_i(m_0)$
4.0	0.0097	0.0093	0.3917	3.6083	4.3917	0.8102	0.1576	0.65261
4.8	0.0097	0.0093	0.3917	4.3917	5.1750	0.1576	0.0306	0.12695
5.6	0.0097	0.0093	0.3917	5.1750	5.9583	0.0306	0.0059	0.02470
6.4	0.0097	0.0093	0.3917	5.9583	6.7417	0.0059	0.0011	0.00480
7.1	0.0097	0.0093	0.3917	6.7417	7.5250	0.0011	0.0002	0.00093
7.9	0.0097	0.0093	0.3917	7.5250	8.3083	0.0002	0.0000	0.00018
8.7	0.0097	0.0093	0.3917	8.3083	8.7000	0.0000	0.0000	0.00002

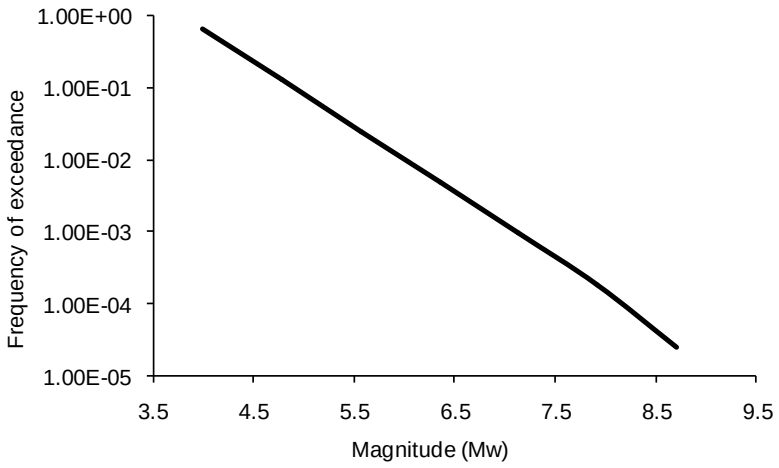

Figure 5.1: Frequency of exceedence of various magnitudes for Oldham fault

Figure 5.1 shows the frequency of exceedance versus magnitude curve for Oldham fault which is located to the north of the SP. As per Bilham and England (2001), the Oldham fault was responsible for the 1897 Assam EQ (M_W-8.1). It can be observed from Figure 5.1 that the frequency of exceedance reduces with increase in the magnitude. For an EQ event of M_W-8.7, the frequency of exceedance on Oldham fault is 0.0002 or return period for this event would be at least one event in every 5000 years.

5.2.2 Uncertainty in hypocentral distance

For the estimation of the uncertainty associated with hypocentral distance, the approach given by Kiureghian and Ang (1977) is used in the present work, following works by Anbazhagan et al. (2009); NDMA (2010); Pallav et al. (2012) and Kumar et al. (2013). Kiureghian and Ang (1977) had given the following equations for the cumulative probability distribution, for ruptured segment uniformly distributed along a well-defined fault.

$$P(R < r) = 0 \text{ for } R < (D^2 + L_0^2)^{1/2} \tag{5.8}$$

$$P(R < r) = \frac{(r^2 - D^2)^{1/2} - L_0}{L - X(m_i)} \text{ for } (D^2 + L_0^2)^{1/2} \leq R < \{D^2 + [L + L_0 - X(m_i)]^2\}^{1/2} \tag{5.9}$$

$$P(R < r) = 1 \text{ for } R > \{D^2 + [L + L_0 - X(m_i)]^2\}^{1/2} \tag{5.10}$$

where, L = length of the fault,

L_0= length of fault assumed outside of the actual length (L)

$X(m_i)$= rupture length in kilometers for the event of magnitude m_i.

Figure 5.2 shows the notations used by Kiureghian and Ang (1977) to estimate conditional probability in hypocentral distance. Following Anbazhagan et al. (2009) and Kumar et al., (2013), $X(m_i)$ is calculated using the following equation given by Wells and Coppersmith (1994) in absence of precise information about fault mechanism available on the faults in the study region.

$$X(m_i) = \min[10^{-2.44+0.59(m_i)}, L] \tag{5.11}$$

where, L = the length of the fault.

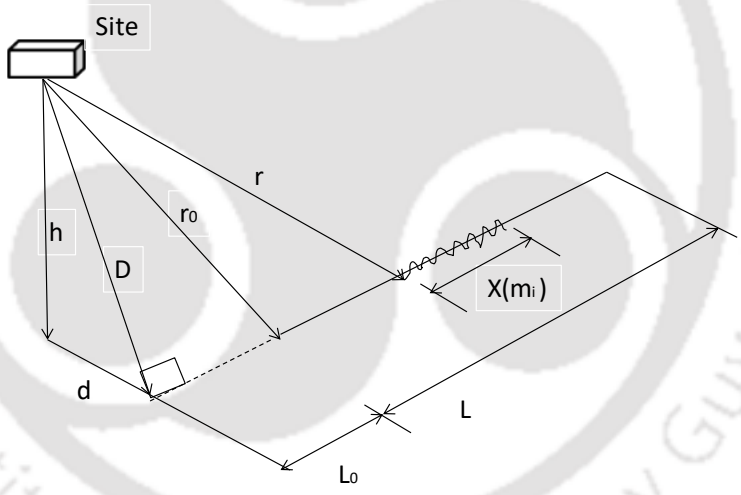

Figure 5.2: Notations used by Kiureghian and Ang (1977) to estimate conditional probability in hypocentral distance

In the present study, each of the 72 faults identified within the seismotectonic region are divided into14 sub-faults each. The three districts are also divided into 0.05° x 0.05° grids. The distances between the top left corners of these grids to the end-point coordinates of each of the sub-faults are calculated. The probability density function of hypocentral distance of the various sub faults of the 72 faults are estimated using the Eqs. (5.8), (5.9) and (5.10). Figure 5.3 shows a typical probability density function of hypocentral distance at Shillong city (25.57°N, 91.89°E) due to the Barapani fault. It can be observed from Figure 5.3 that the probability density function attains a high value of 0.0825 at 25km hypocentral distance between Barapani fault and Shillong city (25.57°N, 91.89°E). This implies that at 25km distance from Shillong city (25.57°N, 91.89°E), the probability of rupture to occur on the Barapani fault is the highest.

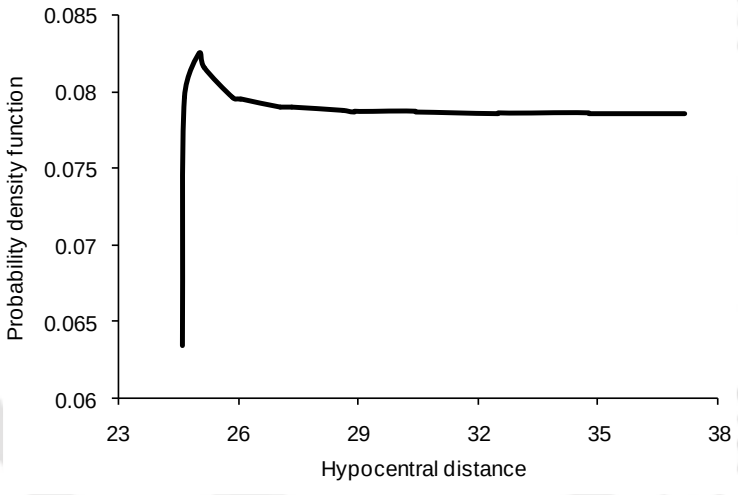

Figure 5.3: Probability density function for Hypocentral distance calculated for the Barapani fault

5.2.3 Uncertainty in ground motion exceedance

It has been mentioned earlier that regional GMPEs are developed based on a limited number of ground motion records. As a result of which ground motions proposed based on such GMPEs are associated with some level of error. This error is taken into account in PSHA by estimating the probability of exceedance of the ground motion parameter beyond a threshold value, for a given m_i and r_j. As per EM-1110 (1999), the conditional probability distribution $P(Z > z|m_i r_j)$ is estimated using lognormal distribution as given below;

$$P(Z > z|m_i r_j) = 1.0 - \acute{F}\left\{\frac{\ln(z) - E[ln(z)]}{S[\ln(z)]}\right\} \quad (5.12)$$

where,$\ln(z)$is the ground motion parameter, $E[ln(z)]$ is the mean log ground motion level given by the attenuation relationship, $S[\ln(z)]$ is the standard error of the log ground motion level obtained from the GMPE used and $\acute{F}$ is the cumulative of a truncated normal distribution.

5.3 Hazard curve

In this study, $\ln(z)$ is obtained from the selected GMPEs at 0.05° x 0.05° grids of each district after application of appropriate weights as per Tables 5.3(a-c) given in Chapter 5. The frequency of ground motion exceedance in accordance with Eqs. 5.1 and 5.2 are estimated at a constant interval of 0.025g for ground motion ranging from 0.025g to 0.8g for each of the seismic source, at each of the grid corner, for each of the three districts. The various probabilities of exceedance estimated in the study are combined to obtain the hazard curve. As per Kumar et al. (2013) a hazard curve defines the frequency of exceedance for various levels of ground motions due to a fault at a site. Figures 6.4 (a-c) show the 12 hazard curves for 12 typical sources at Shillong city (25.57°N, 91.89°E), Nongpoh (25.87°N, 91.83°E) and Tura (25.51°N, 90.20°E).

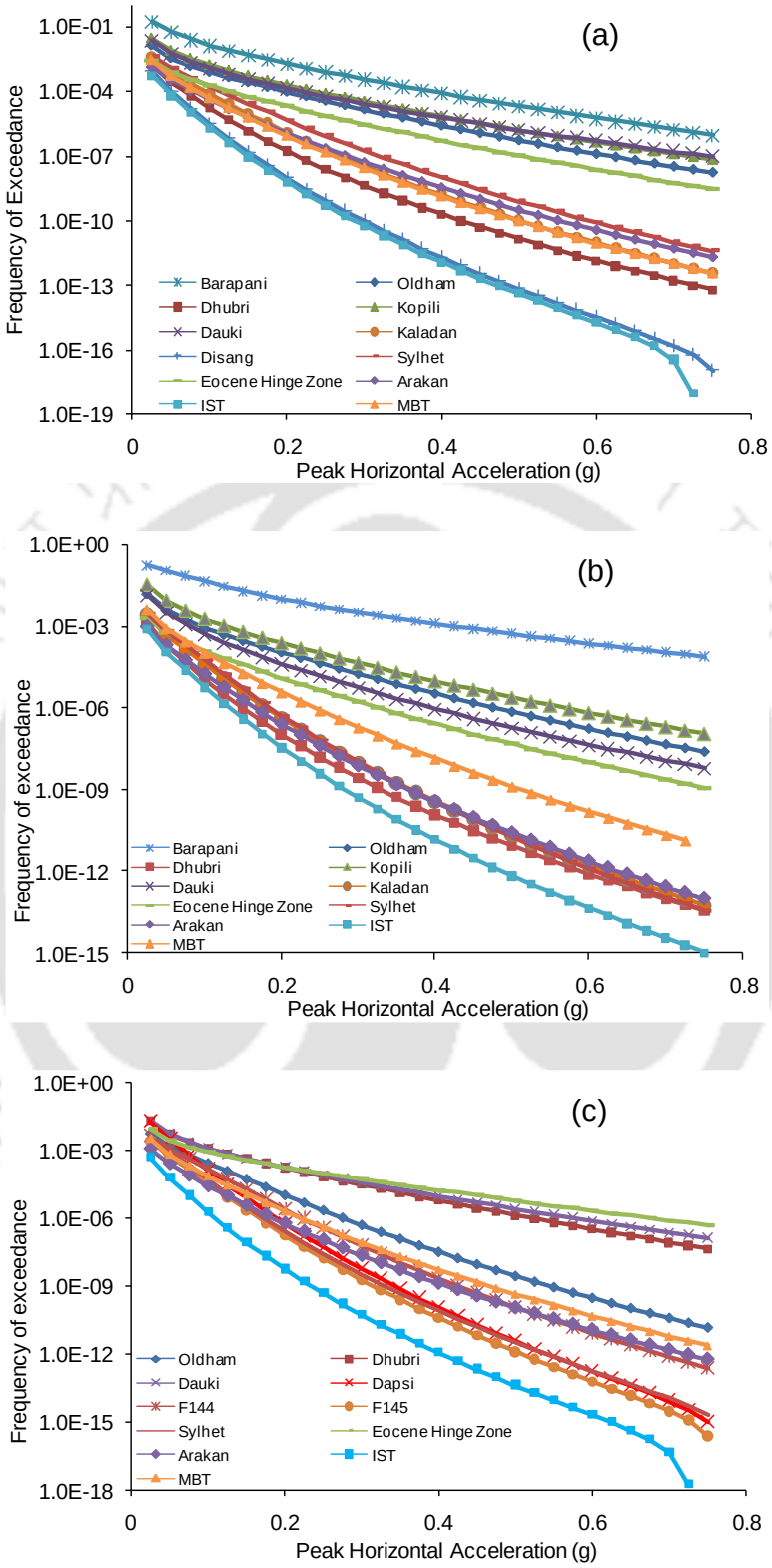

Figure 5.4: Hazard curves from typical sources at (a) Shillong city (b) Nongpoh and (c) Tura

It can be observed from Figure 5.4(a) that at Shillong city, the Barapani fault possesses the highest frequency of exceedance for entire range of ground motions considered followed by the Dauki fault, Kopili fault, Oldham fault, Eocene Hinge Zone and so on. Similarly, Figure 5.4(b) shows that at Nongpoh, the Barapani fault is the highest hazard causing fault. It can be observed from Figure 5.4(c) that at Tura, till 0.175g, both the Dauki and the Dhubri faults show the highest frequency of exceedance. Beyond 0.175g however, the Eocene Hinge Zone shows a high level of frequency of exceedance. As the frequencies of exceedance of both the Dauki and the Dhubri faults overlap till 0.175g, it can be concluded that both of these fault have the same potential of causing seismic hazard at Tura.

PSHA summarizes all the possible contributions from each source in determination of seismic hazard at a site. The percentage contribution to seismic hazard, possible by a fault, from various combinations of magnitudes and hypocentral distances, can be estimated by deaggregation (NDMA 2010; Pallav et al. 2012; Kumar et al. 2013). In this study, the percentage contributions to seismic hazard by the highest hazard causing faults at Shillong city (25.57°N, 91.89°E), Nongpoh (25.87°N, 91.83°E) and Tura (25.51°N, 90.20°E) are shown in Figures 5.5(a- d). It can be observed from Figure 5.5(a) that the Barapani fault provides the highest contribution of 13.7% at Shillong city if an EQ of M_W-6.1 occurs at 24.67km hypocentral distance. Similarly, Figure 5.5(b) concludes that at Nongpoh, the highest contribution from Barapani fault is 13.9% due to an EQ of M_W-6.1, occurring

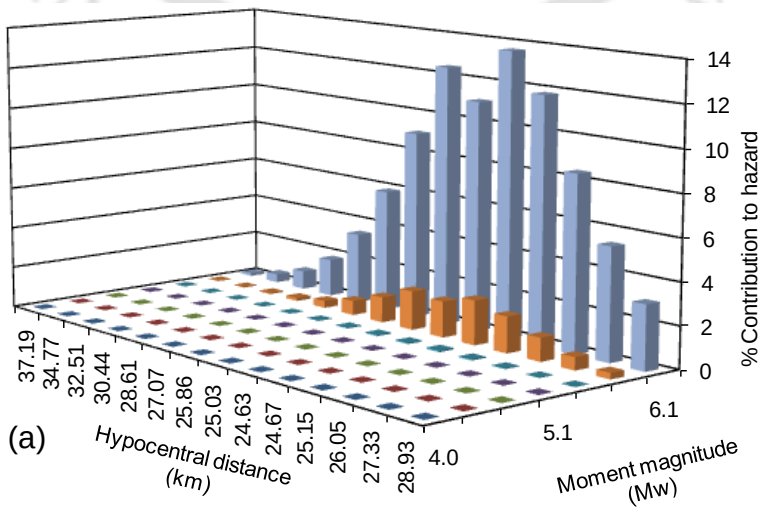

(a)

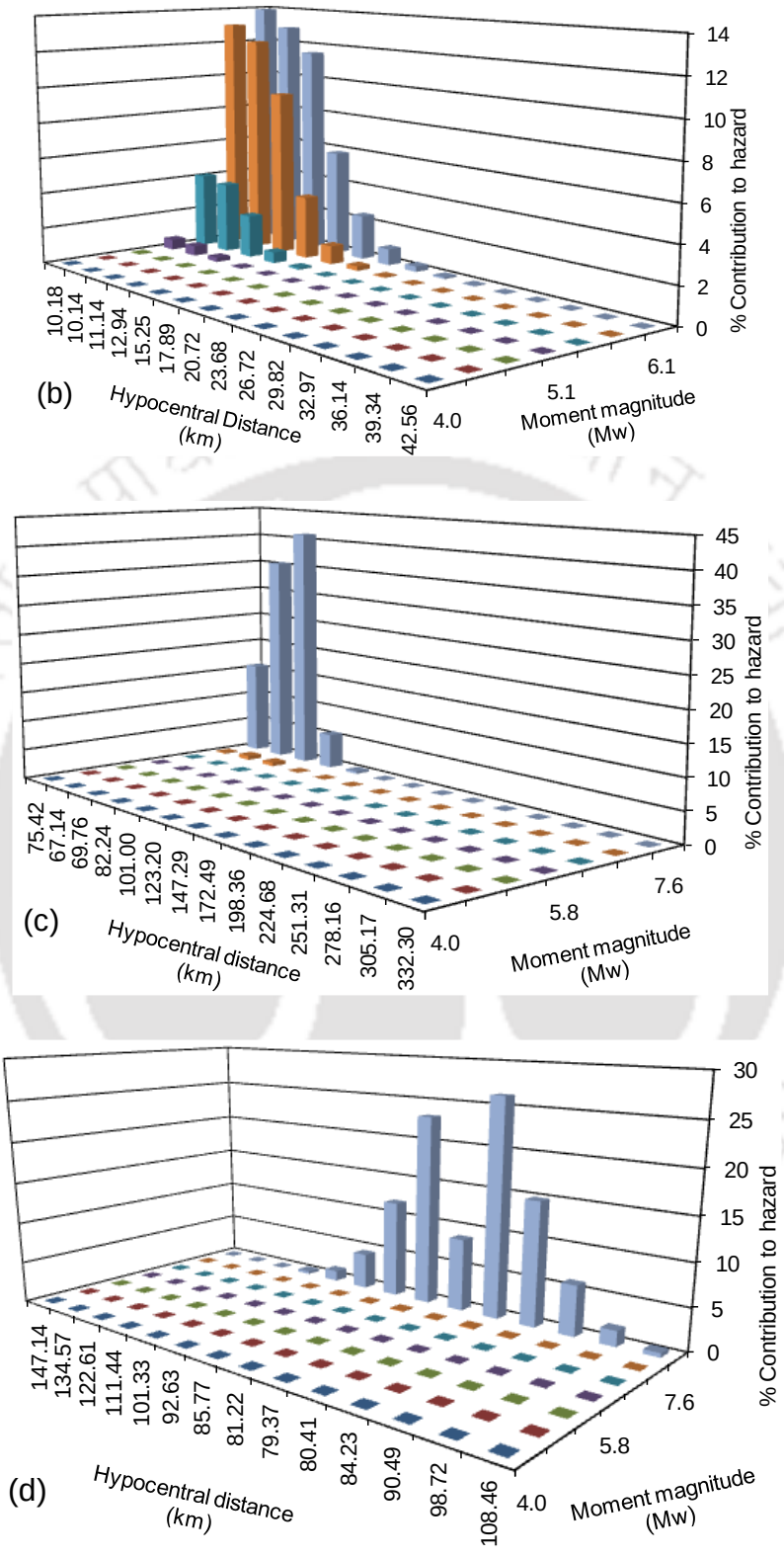

Figure 5.5: Deaggregation plot for (a) Barapani fault at Shillong city, (b) Barapani fault at Nongpoh (c) Dauki fault at Tura and (d) Dhubri fault at Tura

at 10.18km hypocentral distance. Further, from Figure 5.5(c) it can be observed that at Tura, the highest contributions of 41.1% from Dauki fault is possible due to EQ of M_W-7.6 occurring at 69.76km hypocentral distance. Considering Dhubri fault, a contribution of 26.3% is possible at Tura due to an event of M_W-7.6 occur at 80.41km hypocentral distance as can be observed from Figure 5.5(d).

Summation of hazard curves from all the 72 sources, developed for a site gives the total hazard curve indicating the overall frequency of exceedance of a particular ground motion considering all available sources. Figures 5.6 (a-c) show the total hazard curves at 0s, 0.4s, 1s and 2s for Shillong city (25.57°N, 91.89°E), Nongpoh (25.87°N, 91.83°E) and Tura (25.51°N, 90.20°E). It can be observed from Figure 5.6(a) that at 0s for 0.2g, frequency of exceedance is 0.0022, which gives a return period of 438 years. Thus, the probability of exceedance of 0.2g at Shillong city in the next 50 years is 10.79%. Similarly, at 0.4s, 1s and 2s, the frequency of exceedance are found as 0.000763, 0.00028 and 1.35E-06 respectively. Thus, accordingly the probability of exceedance in 50 years at 0.4s, 1s and 2s are 3.74%, 1.40% and 0.006% respectively. Similar observations can be made from Figures 5.6(b) and 6.6(c) for Nongpoh and Tura respectively.

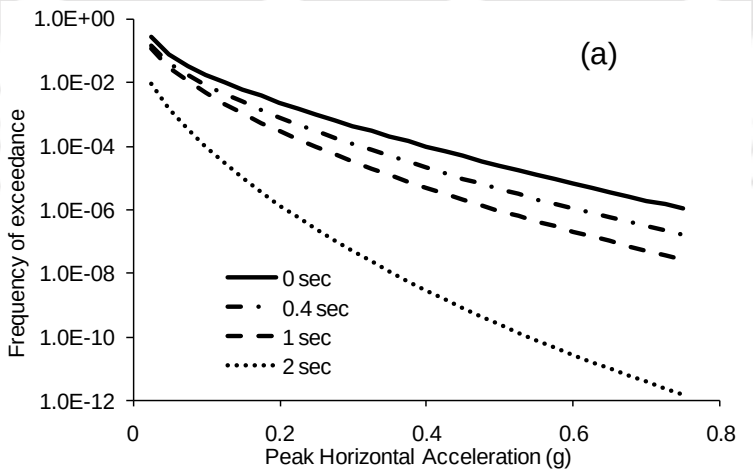

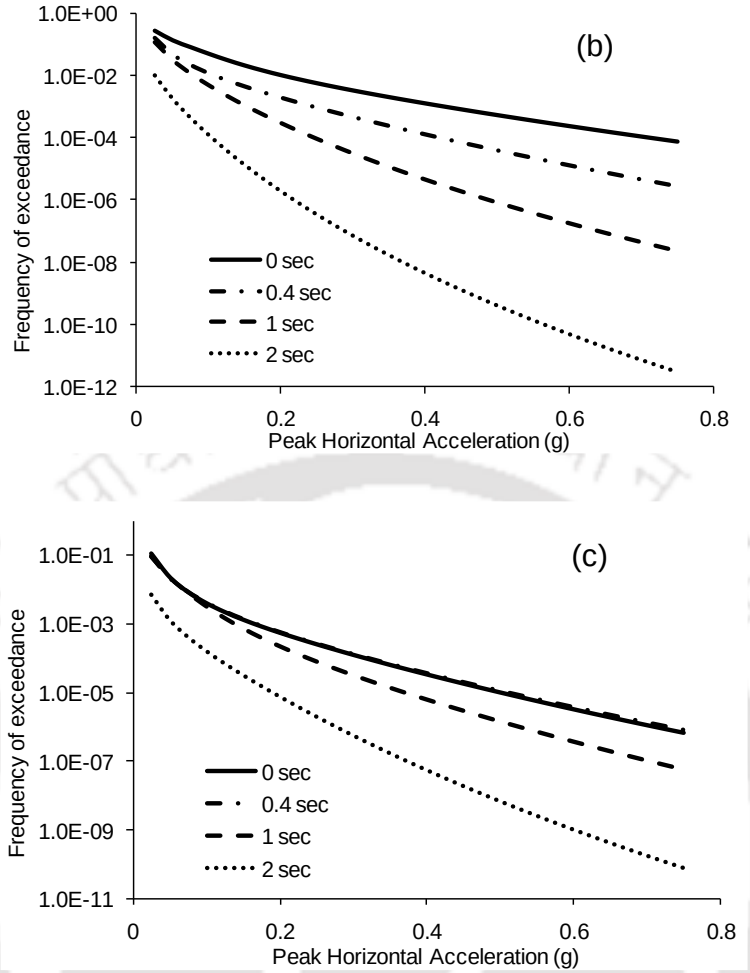

Figure 5.6: Total hazard curves at 0s, 0.4s, 1s and 2s at (a) Shillong city, (b) Nongpoh and (c) Tura

5.4 PSHA maps

Once hazard curves and total hazard curves are known, PSHA based seismic hazard value for known probability of exceedance, in desired period can be estimated. Repeating this exercise for all the grids would help to develop PSHA maps for the areas of interest. In this section, PSHA maps are developed for the districts of East Khasi hills, Ri-Bhoi and West Garo hills. To develop these PSHA maps, a MATLAB code is developed, which estimates the PHA value for East Khasi hills, Ri-Bhoi and West Garo hills comprising of 247, 273 and 323 grid points respectively laid out in a grid of 0.05° x 0.05°. Developed code is validated with the outcomes of Kumar et al., (2013). Figures 5.7 (a-c) show the PSHA based maps for the districts of East Khasi hills, Ri-Bhoi and West Garo hills for 2% probability of exceedance with exposure period of 2475 years. It

can be observed from Figures 5.7 (a and b) that for East Khasi hills and Ri-Bhoi districts, the northern and eastern regions respectively, show highest PHA value of 0.46g. This indicates that the northern and eastern regions are more prone to highest seismic hazard in the above regions. Figure 5.7 (c) shows that for the West Garo hills district, the southern part has a high PHA value of 0.24g. The PHA values at Shillong, Nongpoh and Tura are 0.30g, 0.46g, and 0.22g respectively.

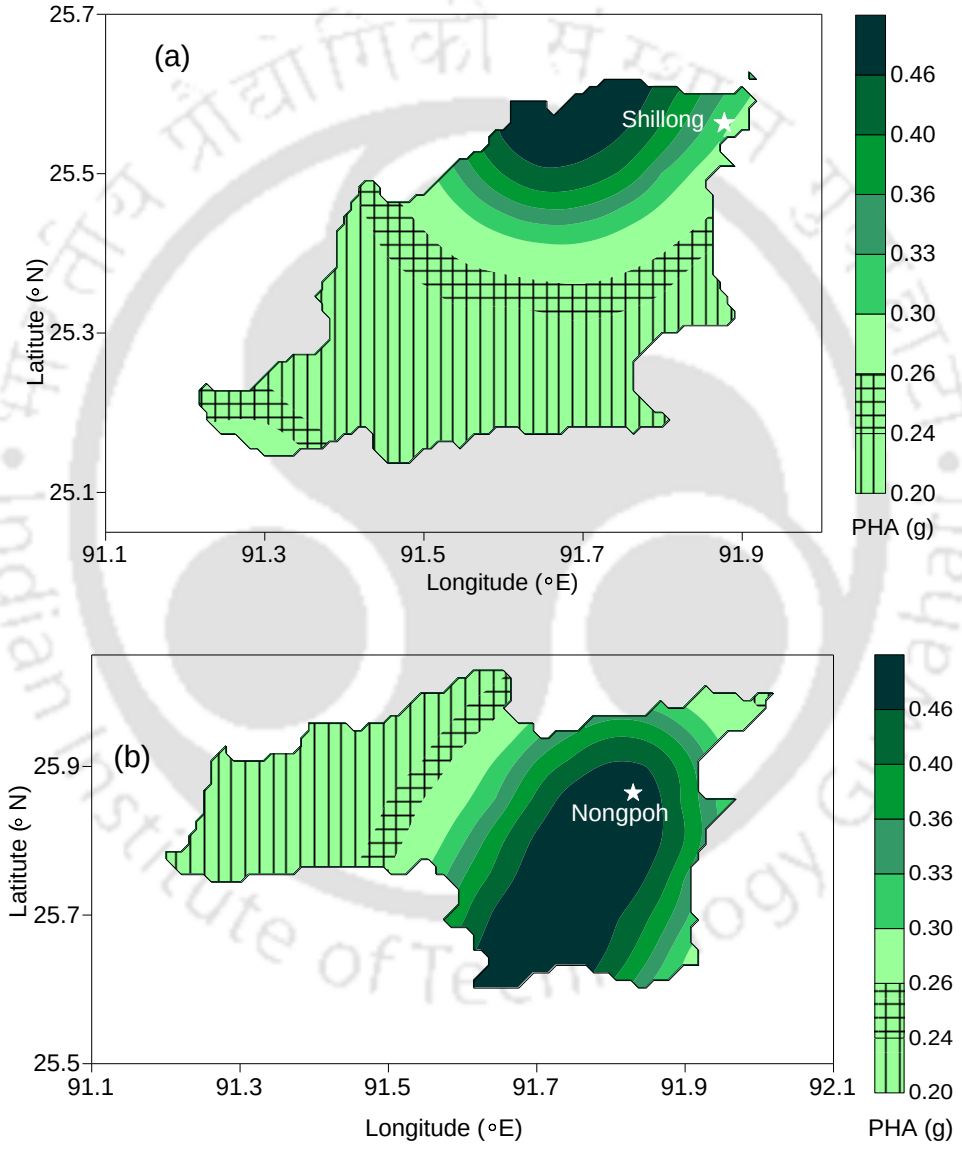

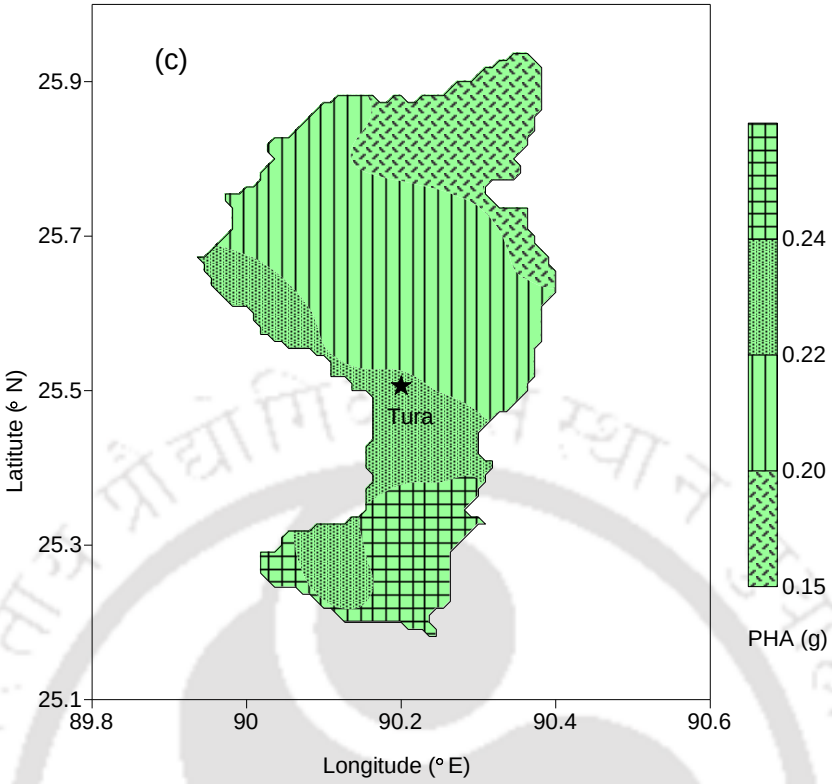

Figure 5.7: PSHA maps for (a) East Khasi Hills (b) Ri-Bhoi and (c) West Garo hills districts for 2 % probability of exceedance in 50 years

Figures 5.8 (a-c) show the PSHA based maps for the three districts at 10% probability of exceedance with exposure period of 475 years. It can be observed from Figures 5.8 (a-c) that similar to Figures 5.7 (a-c), the northern and eastern regions of the East Khasi hills & Ri-Bhoi districts and the southern region of the West Garo hills district are more prone to seismic hazard. The maximum PHA values at Shillong city, Nongpoh and Tura for 10% probability of exceedance are found as 0.20g, 0.33g, and 0.13g respectively.

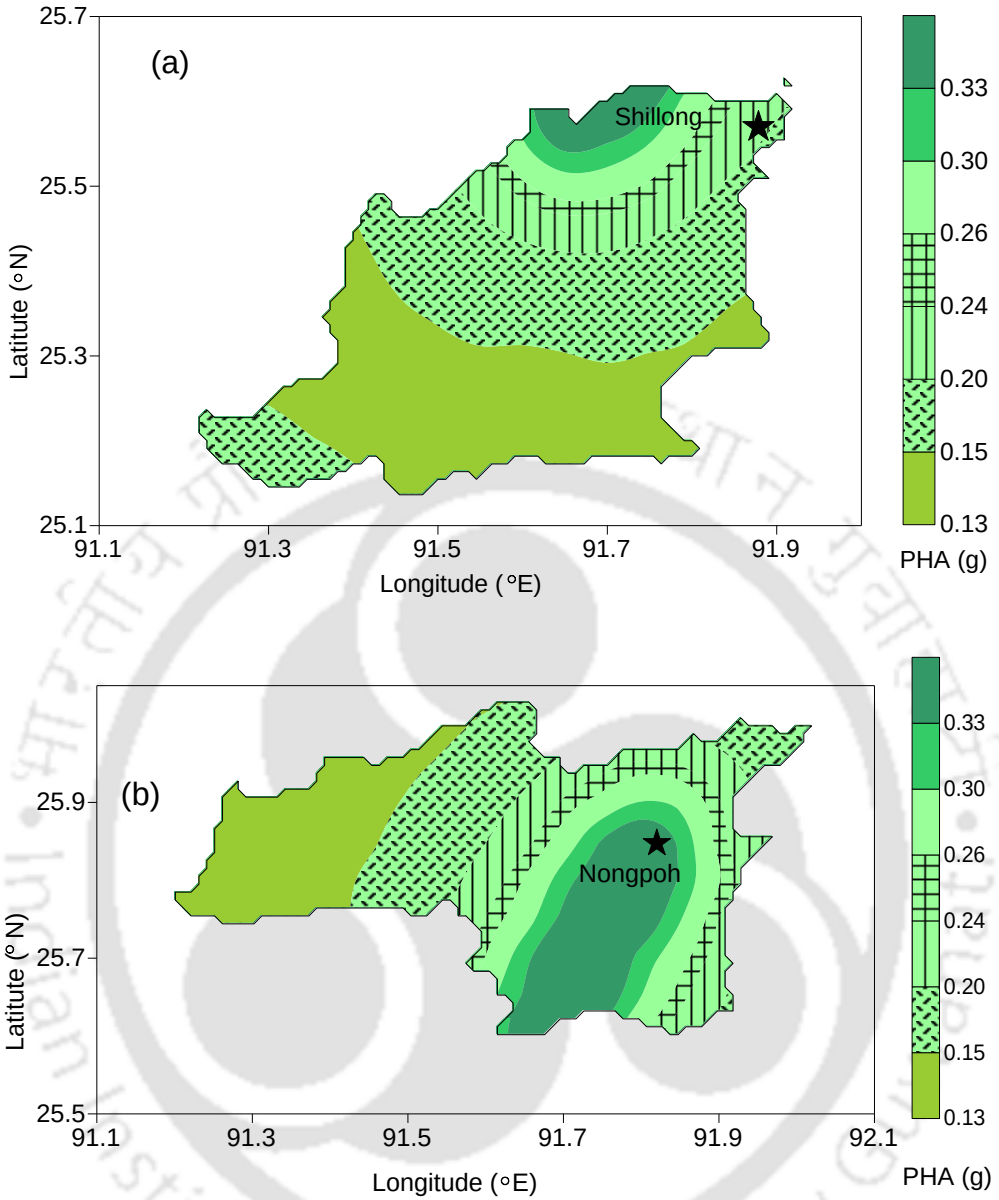

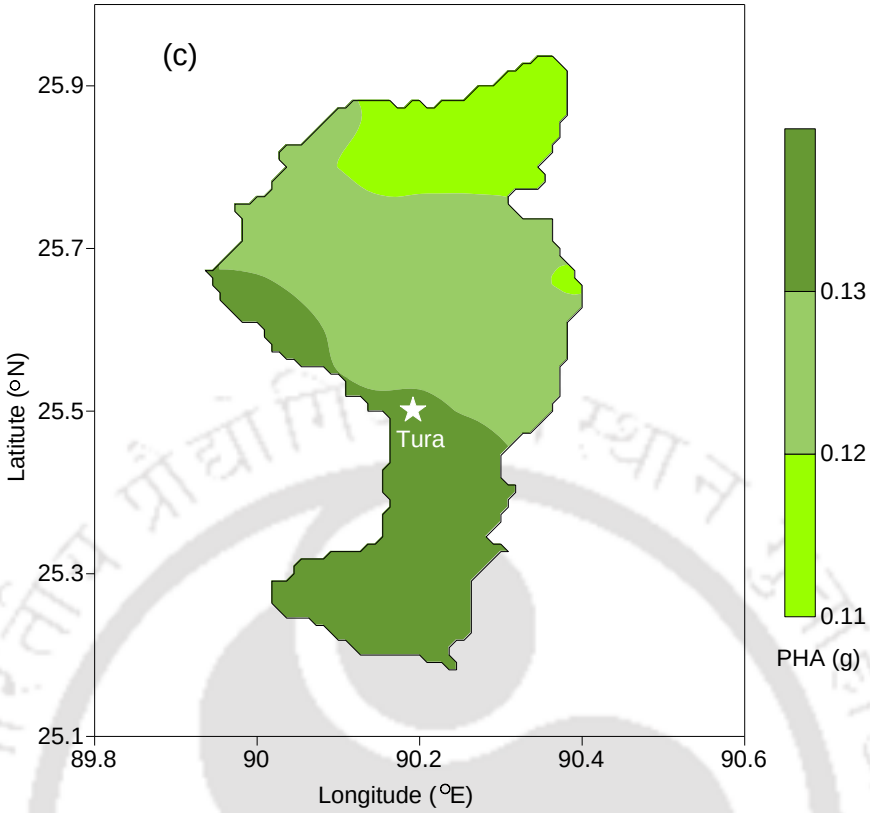

Figure 5.8: PSHA maps for (a) East Khasi Hills (b) Ri-Bhoi and (c) West Garo hills districts for 10 % probability of exceedance in 50 years

As discussed earlier, seismic hazard studies for the northeastern region were also attempted during previous studies. Most of such available studies; such as Bhatia et al. (1999) and NDMA (2010) developed PSHA maps for 10% probability of exceedance. As per Bhatia et al. (1999), the PHA values over the SP at 10% probability of exceedance is in the range of 0.25-0.30g. NDMA (2010) contours passing over the SP at 10% probability of exceedance gives PGA values of 0.25g. Thus, the PHA values obtained in this study are found comparable to previous studies considering 10% probability of exceedance in 50 years. At 2% probability of exceedance, NDMA (2010) report shows a 0.4g PGA contour over the SP region, which is found comparable to the PHA value obtained in this study.

Once total hazard curves at different periods of interest are known (Figures 5.6 a-c), Uniform Hazard Spectra (UHS) are developed at Shillong city (25.57°N, 91.89°E), Nongpoh (25.87°N, 91.83°E) and Tura (25.51°N, 90.20°E) as shown in Figures 5.9 (a-

c). UHS give the variation in spectral acceleration values at different period for the same probabilities of exceedance. It can be observed from Figure 5.9(a) that at period 0s, the Spectral Acceleration (SA) values at Shillong city for 2%, 10% and 50% probabilities of exceedance are 0.30g, 0.20g and 0.11g respectively. Figure 5.9(a) also shows that the peak SA values for 2%, 10% and 50% probabilities of exceedance are attained at period 0.1s as 0.53g, 0.35g and 0.19g respectively. After 0.1s a gradual decrease in the SA plots can be observed. Figure 5.9(b) shows UHS developed at Nongpoh, where the SA values at period 0s are 0.46g, 0.34g and 0.18g for 2%, 10% and 50% probabilities of exceedance respectively. It can be observed from Figure 5.9(c) that the 0s SA values at Tura for 2%, 10% and 50% probabilities of exceedance are 0.22g, 0.13g and 0.06g respectively. As per NDMA (2010) at 0s, 0.2s, 0.5s, 1s and 1.25s the spectral acceleration values for the SP for 2% probability of exceedance are 0.40g, 0.40g, 0.20g, 0.11g and 0.12g respectively. Similarly, for 10% probability of exceedance the spectral acceleration values at 0s, 0.5s and 1.25s are 0.25g, 0.12 and 0.08g. Hence, the SA values obtained in the present study are found comparable with those of NDMA (2010).

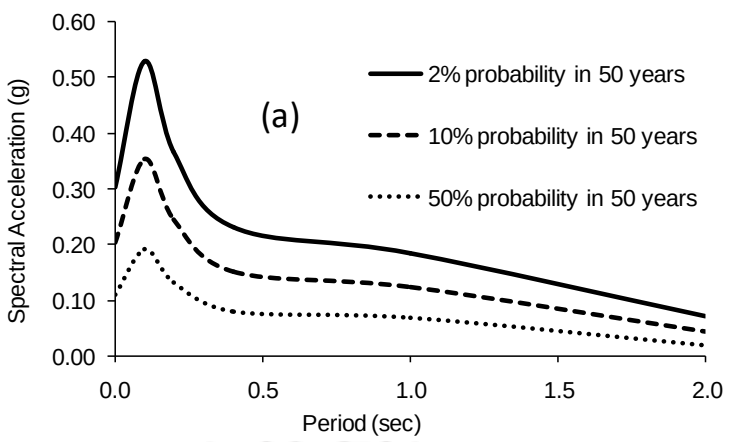

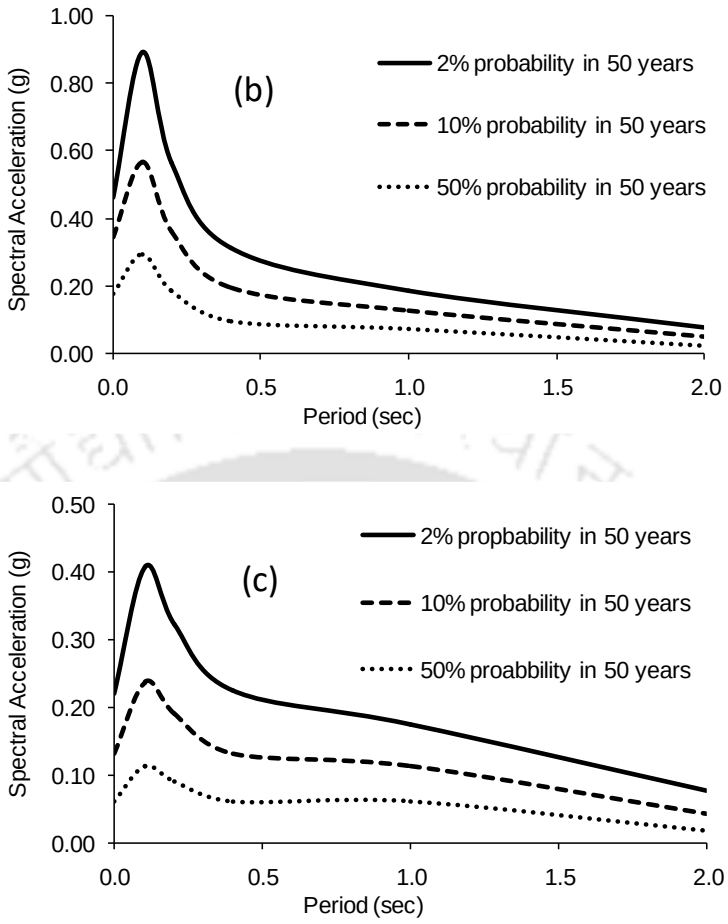

Figure 5.9: Uniform hazard spectra for (a) Shillong city, (b) Nongpoh and (c) Tura

5.5 Comparison between DSHA and PSHA

In Chapter 4 DSHA maps for the districts of East Khasi hills, Ri-Bhoi and West Garo hills have been developed. Comparison between DSHA map shown in Figure 4.1(c) of Chapter 4 and PSHA maps obtained in this chapter for West Garo hills district (Figures 5.7c and 5.8c) show a complete reversal of the seismic hazard variation within the district. It is found in Chapter 4 that the northern portion of the West Garo hills district is more prone to seismic hazard. In Chapter 4 it is considered that the Oldham fault is responsible for the high seismicity of the northern portion of the district. However, using the same EQ catalogue, 'b' parameter, M_p values, GMPEs, etc. as Chapter 4, it is found in the present chapter that the southern part of the West Garo hills district has higher seismic hazard. It is also found that instead of the Oldham fault, the Dhubri and the Dauki faults are responsible for the high seismic hazard for the West Garo hills

district. A close observation of DSHA performed in Chapter 4 suggests that those findings were mostly governed by seismic hazard from the Oldham fault which, among all the 72 faults is located closest to the West Garo hills district. Maximum reported EQ on this fault was M_W-8.1 and is located north of the SP. As widely accepted, DSHA results resemble worst scenario without considering the chances of its repetition during the design life. Observing the hazard curve due to Oldham fault at Tura (25.51°N, 90.20°E) from Figure 5.4(c), it can be concluded that, even though Oldham fault has experienced Mw-8.1 EQ, its frequency of occurrence is lower than Eocene hinge zone, Dauki fault and Dhubri fault. This clearly indicates that though the Oldham fault has produced M_W-8.1 EQ in the past, its probability of occurrence in the future is significantly lower. This observation shows that outcomes of DSHA are valid only in case of worst scenarios, but considering very low probability of such scenarios to occur during the design life of a structure, the findings from PSHA may not get affected significantly.

Even though DSHA and PSHA findings cannot be compared directly as approaches are completely different, this comparison is just to understand the relative application of outcomes from DSHA and PSHA. In order to validate above observation, a revised DSHA is done in the present chapter using same inputs of Chapter 4 but not considering Oldham fault in the analysis taking into account its low probability of occurrence as observed from PSHA. Figure 5.10 presents the DSHA based revised PHA map for West Garo hills district without considering the Oldham fault. It can be observed form Figure 5.10 that after the removal of the Oldham fault from the analysis, the DSHA and PSHA results for the West Garo hills district show similar trend of highest seismic hazard towards the south with gradually decreasing seismic hazard towards north. Hence, it can be concluded from this observation that the effect of a high seismic hazard fault is prominent in DSHA, which only considers the worst-case scenario. However, in case of PSHA, the probability of rupture from source such as the Oldham fault during the design life of a structure is very less.

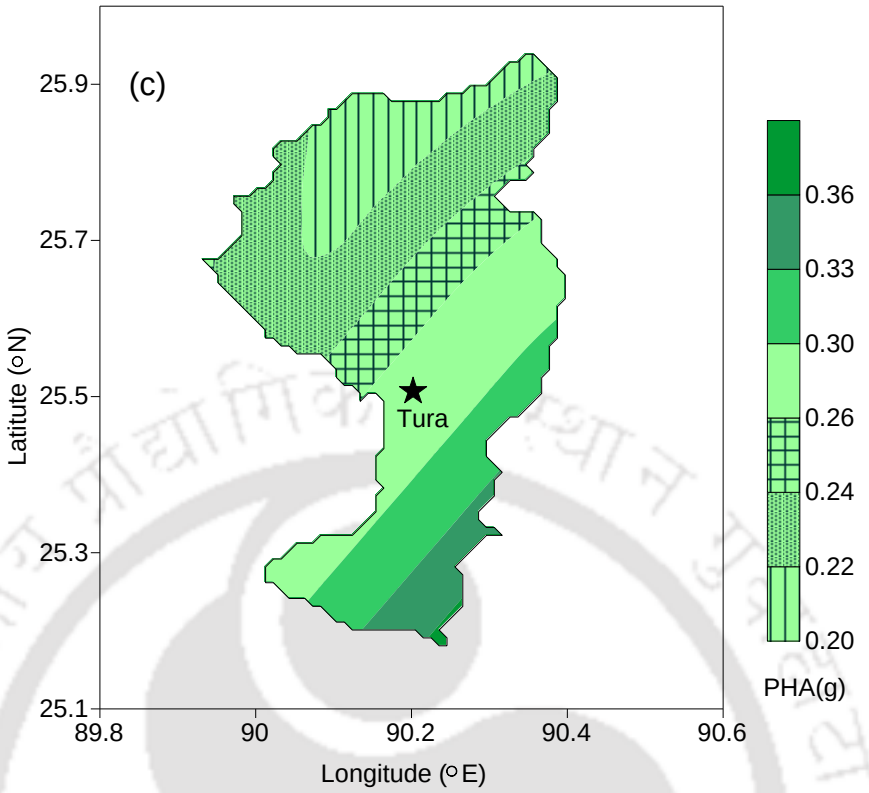

Figure 5.10: DSHA map of West Garo hills without Oldham fault as a source

5.6 Summary

PSHA is performed for the districts of East Khasi hills, Ri-Bhoi and West Garo hills located within the SP. Hazard curves are developed at the sites of Shillong city, Nongpoh and Tura located within the East Khasi hills, Ri-Bhoi and West Garo hills districts respectively. Hazard curves show that the Barapani fault possesses the highest frequency of exceedance at Shillong city and Nongpoh. At Tura, both Dauki and Dhubri faults are found to be the highest hazard causing faults. The northern part of East Khasi hills district, eastern part of Ri-Bhoi district and southern part of the West Garo hills district are found to show high PHA value. Within the three districts the PHA values range from 0.15g to 0.46g at 2% probability of exceedance in 50 years. Similarly at 10% probability of exceedance in 50 years the PHA values range from 0.11g to 0.33g. The PSHA maps developed for the three districts are compared to the contours maps developed by Bhatia et al. (1999) and NDMA (2010) which show reasonable agreement. Uniform Hazard Spectra are developed for Shillong city, Nongpoh and

Tura. The SA values obtained in this study are found to be comparable with the values given in NDMA (2010). The West Garo hills district DSHA map developed in Chapter 4 is compared to the PSHA map developed in the present chapter. The comparison shows the effect of Oldham fault, which is prominent only in the case of DSHA in case of PSHA little to no effect, is observed.

Chapter 6 - In-direct estimation of local soil response

6.1 Introduction

The seismic hazard maps developed in the previous chapters are at the bedrock level. The surface level of ground shaking is however, a function of both the bedrock level of ground motion and its alteration due to local soil. Hence, the application of the hazard maps for design of EQ resistant structures is very limited until the response of the local soil is also taken into account. However, quantification of local site effects requires a number of field and laboratory tests, estimation of dynamic soil properties and input bedrock motion for future EQs. Further, for majority of locations around the world, above mentioned information is not readily available. Similarly, regional ground motion data, which is also an important parameter for an assessment of local site effects, during an EQ, is not always readily available. This is due to the fact that instrumental recording of ground motion records is a very recent phenomenon, especially in countries like India where the records are only available from 1986 onwards. Further, after the beginning of instrumental ground motion recording, no major or great EQs have occurred in the SP. Hence, the data of a major or great EQ ground motion record is not readily available for the quantifying the local soil response of the SP.

In the year 2015, the neighboring country of Nepal suffered a major EQ of M_W-7.8. During this EQ several stations around the world recorded the ground motion records. These ground motion records available from the 2015 Nepal EQ are used in this study to quantify the response of the local soil of a number of sites across Nepal. For the estimation of the response of the local soil an Amplification Factor (AF) versus PHA curve called as the Dynamic Soil Response Curve (DSRC) is developed in this work. Using the DSRC curve the response of the soil for a known bedrock motion, can be estimated at a site. Once it is observed that using DSRC reasonable results are obtained for Nepal, the same principle of in-direct estimation of the local soil with the help of a DSRC curve is also employed for the SP.

6.2 DSRC for Nepal

The database used for this study consists of ground motions both from pre-instrumental EQs in terms of MMI values as well as recorded ground motions during 2015 Nepal EQ at the selected sites. Collected MMI values are converted to PGA. In the existing literature, so many correlations between MMI and PGA are available for various regions across the globe. For Nepal, however, no such regional correlation between MMI-PGA exists at present. In order to develop such a correlation in this work, firstly both the MMI and PGA values from 12 selected stations, during 2015 Nepal EQ, are collected as reported by the United States Geological Survey (USGS) (Mw-7.8, 2015 Nepal EQ). The MMI values vary from VII to IX for the stations considered here. Details of all 12 selected stations are given in Table 6.1.

Table 6.1: Summary of selected stations considered for PGA-MMI correlation

Station number	Latitude (°N)	Longitude (°E)	Epicentral Distance (km)	PGA (g)	MMI
1	28.28	84.29	48.17	0.61	VIII
2	27.68	84.41	63.04	0.30	VII
3	27.94	85.46	87.53	1.32	IX
4	28.28	84.31	45.65	0.61	VIII
5	28.22	84.80	12.04	1.30	IX
6	28.20	84.74	5.27	1.31	IX
7	28.06	84.92	26.81	1.33	IX
8	27.97	85.18	57.77	0.97	IX
9	27.92	85.14	55.57	0.98	IX
10	27.92	85.13	54.62	0.98	IX
11	27.89	85.14	57.47	0.99	IX
12	27.93	85.32	73.46	0.71	VIII

Since the objective is to quantify the effect of local soil for the Nepal region, stations located in different parts of Nepal, with recorded ground motions available in the USGS database are selected. The MMI and PGA values obtained from the 12 stations are used

to develop a MMI versus PGA as shown in Figure 6.1. The variation between PGA-MMI follows a clear trend between MMI of VII and IX. Based on the variation observed in Figure 6.1, a new correlation between PGA and MMI is proposed in this work for Nepal. The functional form of the proposed correlation is chosen to minimize root mean square (RMS) errors between the observations and the model curve. Since limited dataset of MMI and PGA for each site is available for the 2015 Nepal EQ, correlations considering other variables such as epicentral distance, magnitude are not attempted in this work.

It has to be highlighted here that the proposed correlation is completely based on MMI and PGA values from Nepal region, reported as per (USGS) (Mw-7.8, 2015 Nepal EQ) and thus does not require any validation. While the seismicity of the Himalayas is vibrant due to the convergence between Indian and Eurasian plate happening at a rate of 5 cm/ year, the seismicity of western coast of USA is high due to convergence of the Jaun de Fuca plate underneath the North American plate at a rate of 4 cm/year. Detailed comparison between the western coast of USA and the Himalayas in terms of seismicity, age of the origin of both the plate boundaries, etc., was presented by Walter et al. (2005). Wald et al. (1999) proposed correlation between MMI (in the range of V to VIII) and PGA based on records from eight significant EQs in the western USA including the 1971

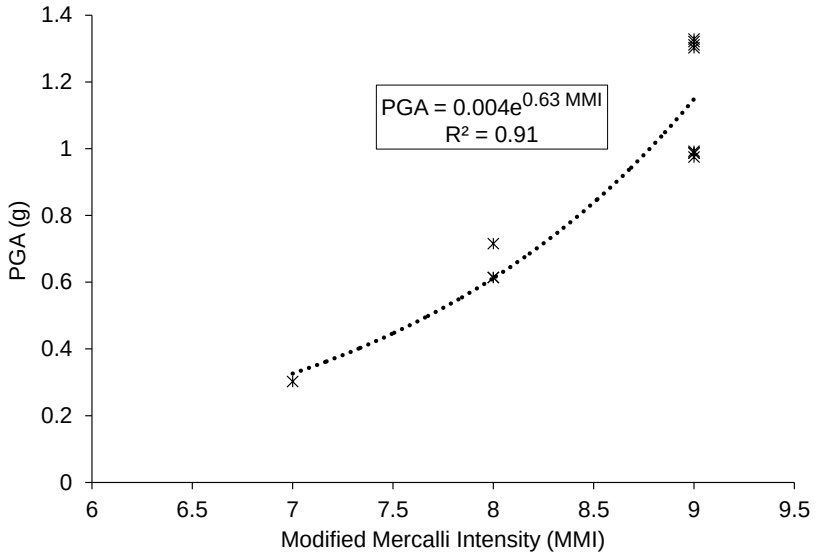

Figure 6.1: PGA versus MMI correlation based on ground motion data from selected sites as given in Table 6.1

San Fernando EQ (M_W-6.7), the 1979 Imperial valley EQ (M_W-6.6), the 1994 Landers EQ (M_W-7.3), etc. Comparison between the proposed correlation developed in this study and the one given by Wald et al. (1999) is shown in Figure 6.2.

It can be observed from Figure 6.2 that both the correlations show a close match. For MMI of V, proposed correlation and the one by Wald et al. (1999) estimate PGA as 0.07 and 0.09 g, respectively. Similarly for MMI of VIII, PGA values estimated by proposed correlation and by Wald et al. (1999) are 0.60 and 0.45 g, respectively. Another correlation between MMI with PGA for western USA was developed by Hershberger (1956) which is also used here for comparison. Again it can be observed from Figure 6.2 that for MMI of IX, PGA of 1.1 and 0.86 g are obtained as per the proposed correlation and the one by Hershberger (1956), respectively. Two other correlations developed considering EQ records from USA, Japan and Europe, developed by Murphy and O'Brien (1977); Trifunac and Brady (1975) are also compared with the proposed correlation. As per Sanjay et al. (2013), the correlation by Murphy and O'Brien (1977) was found applicable for Sikkim, Nepal and the adjoining regions. Similarly, Umut (2004) used correlation by Trifunac and Brady (1975) for seismic microzonation of Lalitpur, Nepal. Thus, both of correlations by Murphy and O'Brien (1977), Trifunac and Brady (1975) were highlighted suitable for Nepal. Figure 6.2 shows that the proposed correlation falls in between the correlations given by Murphy and O'Brien (1977) and Trifunac and Brady (1975).

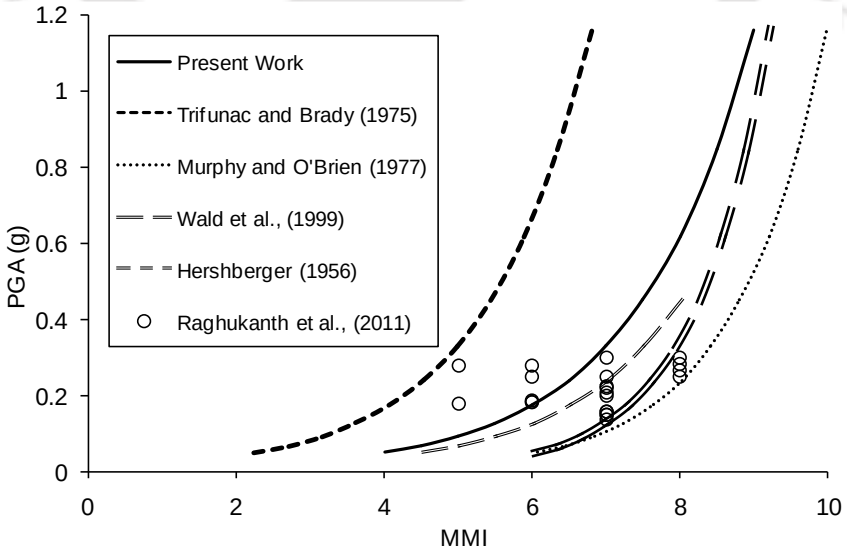

Figure 6.2: Comparison of proposed MMI-PGA correlation with various correlations

In another work, Raghukanth et al. (2011) developed PGA during 2011 Sikkim EQ based on stochastic modeling and compared with observed MMI. PGA-MMI dataset given by Raghukanth et al. (2011) for Sikkim is also compared as shown in Figure 6.2. It can be observed that the proposed correlation falls in between the data range given by Raghukanth et al. (2011). In general, Raghukanth et al. (2011) highlighted that PGA-MMI correlations are often based on randomly distributed records and thus considerable variation is possible. A large variation in the database used for developing the correlation was also shown by Wald et al. (1999) while comparing with MMI-PGA correlation by Trifunac and Brady (1975). Thus, comparison shown in this section is considered satisfactory since the proposed correlation is closely matching with correlations developed for western USA and the dataset for 2011 Sikkim EQ. In addition, the proposed correlation falls in between two different correlations which were developed considering dataset from same regions.

6.3 Estimation of Peak Ground Acceleration (PGA) and Peak Horizontal Acceleration (PHA) for Nepal

In order to assess the effect of local soil during an EQ, five typical stations namely Kathmandu (27.72°N, 85.33°E), Patan (27.67°N, 85.31°E), Bhaktapur (27.67°N, 85.43°E), Pokhara (28.22°N, 83.99°E) and Bharatpur (27.68°N, 84.43°E) are selected in this work. All these stations are located in the western, central and southern parts of Nepal, respectively. The MMI values based on reported damages during 1833 Nepal EQ (M-7.7) and 1934 Bihar-Nepal EQ (M-8.1) at all the above stations is collected as per Bilham (1995). During 2015 Nepal EQ (M_W-7.8), the MMI values at the above five locations are taken as per USGS (M_W-7.8, 2015 Nepal EQ). The summary of MMI values at each of the above five stations during the 1833 EQ, the 1934 EQ and the 2015 EQ are presented in Table 6.2. Further, based on the range of hypocentral distance from each station during the above three EQs, it can be said that the MMI values are available over a wide range of hypocentral distance from 66km to 360km as shown in Table 6.2. Similarly, at each station, different values of MMI were observed during various EQs. For example, Kathmandu had experienced MMI of VIII and IX during the above mentioned EQs. Similarly, for Pokhara, the observed values of MMI during the

above EQs were varying from VII to VIII as listed in Table 6.2. Using the proposed correlation as per Figure 6.1, above MMI values at Kathmandu, Patan, Bhaktapur, Pokhara and Bharatpur are used to calculate PGA values during all the three EQs as listed in Table 6.2.

A number of attenuation relations are available at present for the Himalayan belt based on recorded as well as synthetic ground motions. In this study, the GMPE given by Anbazhagan et al. (2013) for the Himalayan region is used for estimation of the bedrock level PHA values at Kathmandu, Patan, Bhaktapur, Pokhara and Bharatpur during 1833 Nepal EQ, 1934 Bihar-Nepal EQ and 2015 EQ. The PHA values estimated at the five stations during each of the above mentioned three EQs are shown in Table 6.2.

It can be observed from Table 6.2 that the PHA values during 1833 Nepal EQ are varying from 0.04to 0.23 g for all the stations. Similarly, during the 2015 EQ, the PHA variation is observed from 0.17 to 0.31 g. At Pokhara station, the PHA value is varying from as low as 0.03g during 1934 Bihar-Nepal EQ to as high as 0.24 g during 2015 Nepal EQ. Large variation in PHA during all the EQs is an attribute of large variation in the hypocentral distance among the selected stations as listed in Table 6.2.

Table 6.2: Summary of PHA, MMI and PGA values for selected five sites during the three EQs

Site [Lat. (°N), Long. (°E)]	EQ	M_W	Epicenter Coordinates		Hypo. Dist. (km)	PHA (g)	MMI	PGA (g)	AF
			Lat. (°N)	Long. (°E)					
Kathmandu (27.72, 85.33)	1833	7.7	28.00	86.00	83.21	0.20	VIII	0.62	3.03
	1934	8.1	26.60	86.80	206.12	0.08	VIII	0.62	7.79
	2015	7.8	28.17	84.70	86.97	0.21	VIII	0.62	2.89
Patan (27.65, 85.32)	1833	7.7	28.00	86.00	87.39	0.19	VIII	0.62	3.26
	1934	8.1	26.60	86.80	202.41	0.08	VIII	0.62	7.56
	2015	7.8	28.17	84.70	90.84	0.20	VIII	0.62	3.08

Bhaktapur (27.67, 85.32)	1833	7.7	28.00	86.00	75.76	0.233	VIII	0.62	2.64
	1934	8.1	26.60	86.80	193.77	0.08	VIII	0.62	7.05
	2015	7.8	28.17	84.70	99.29	0.17	VIII	0.62	3.52
Pokhara (28.22, 84.00)	1833	7.7	28.00	86.00	224.71	0.04	VII	0.33	5.28
	1934	8.1	26.60	86.80	360.16	0.03	VII	0.33	6.29
	2015	7.8	28.17	84.70	80.04	0.24	VII	0.33	1.36
Bharatpur (27.66, 84.43)	1833	7.7	28.00	86.00	181.74	0.06	VIII	0.62	10.22
	1934	8.1	26.60	86.80	291.67	0.05	VII	0.33	5.79
	2015	7.8	28.17	84.70	66.30	0.31	VII	0.33	1.04

Once the values of PHA and PGA at all the five locations are estimated, the values of AF are determined as the ratio of PGA to PHA as listed in Table 6.2. It can be observed from Table 6.2 that the values of AF are showing a wide variation from as low as 1.04 to as high as 10.22. Referring to the works of EPRI (1993) and Romero and Rix (2005) value of AF or amplification in bedrock motion at a station is related to the PHA value at that station in the form of AF versus PHA plot as shown in Figure 6.3. It can be deciphered from Figure 6.3 that the variation of AF with PHA is following a consistent relation for all the sites. For lesser values of PHA (<0.08 g), AF as high as 10 is obtained as shown in Figure 6.3. The value of AF reduces drastically for PHA of 0.15 g onwards. Large values of AF for low amplitude PHA and vice versa were observed by EPRI (1993). For PHA greater than 0.5 g, no amplification to de-amplification was reported by EPRI (1993). These observations were also supported by Romero and Rix (2005) based on the observations made during1989 Loma Prieta EQ and 1985 Michaocan EQ. Romero and Rix (2005) attributed large accelerations to large strains. At these large strains the soil behavior is governed by its high damping ratio which results in low AF. Thus, higher values of AF for low PHA and vice versa as calculated in the present work are consistent with those determined earlier.

For correlating AF with PHA, out of exponential and power regression, power regression is found to be giving highest R^2 value at each of the station. For this reason, power model is chosen for correlating AF to PHA. The correlations between AF and

PHA are developed based on the power trendlines as shown in Figure 6.3.The AF versus PHA plot is coined as DSRC for Nepal in the present study. In order to validate the proposed correlation, comparison with the findings of EPRI (1993) and Ashford et al. (2000) is done as shown in Figure 6.4. It can be seen from Figure 6.4 that the average AF-PHA correlation obtained in this work is consistent with the findings of EPRI (1993) and Ashford et al. (2000). For low PHA values, the present work shows slightly higher values of AF in comparison with the other works. This maybe the attributes of large thickness of overburden in Nepal compared to the other studies. A deeper soil layer may yield higher values of AF at lower PHA as depicted in Figure 6.4. Overall it can be concluded that the AF-PHA variation obtained in the present work is in accordance with the recorded data as well as numerical studies in different parts of the world. Thus, based on the correlation given in Figure 6.1, the value of AF between the bedrock and the surface and subsequently the PGA values can be determined based on PHA for Nepal.

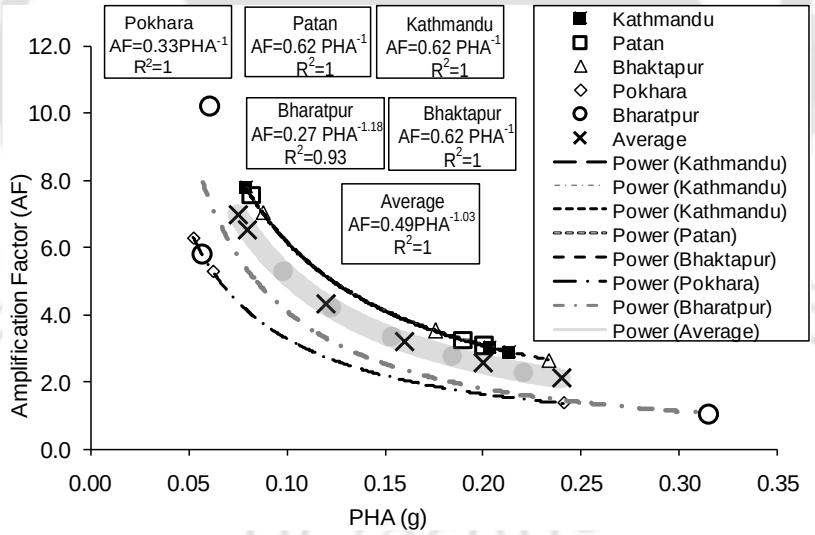

Figure 6.3: Plot of AF versus PHA for five selected sites of Nepal during different EQs

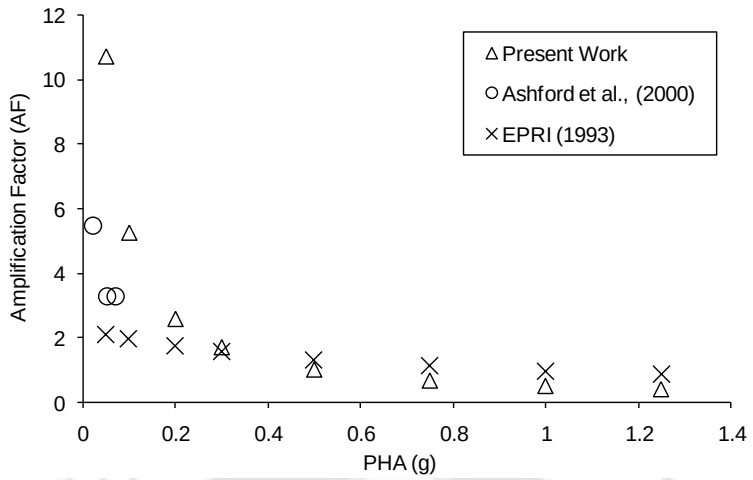

Figure 6.4: Comparison of proposed AF-PHA correlation in present work with existing literature

6.4 Estimation of PGA and PHA for the SP

Based on the above discussion, it can be concluded that soil response for a site where the information about the subsoil is limited, in-direct estimation of the local soil with the help of a DSRC curve can be done. Following the same principal, in-direct estimation of the local soil for the SP is also estimated in this study. Similar to Nepal, a correlation is developed between MMI and PGA in the absence of any correlation existing at present for the SP. To develop this correlation MMI and PGA values obtained during the 2016 Myanmar EQ (M_W-6.9) and the 2016 Imphal EQ (M_W-6.7) as per United States Geological Survey (USGS) (https://www.usgs.gov/) are used. Even though these two EQs had not occurred on the faults surrounding the SP, the shaking due to the EQs was felt within the plateau. Further, as mentioned earlier there are no recent major to great EQs in the vicinity of the SP to develop such a correlation. Using the MMI and PGA values reported during the above mentioned EQs a MMI versus PGA plot is developed as shown in Figure 6.5. Figure 6.5 also shows the correlation developed between MMI and PGA for the SP. The developed correlation shown in Figure 6.5 is used to estimate PGA values during 1885 Bengal EQ (M_L-7.0), 1869 Cachar EQ (M_W-7.5), 1918 Srimangal EQ (M_S-7.6), and 1930 Dhubri EQ (M_S-7.1) based on reported MMI values. It has to be highlighted here that above mentioned four EQs had originated on faults lying at a close vicinity of the SP and had caused damages

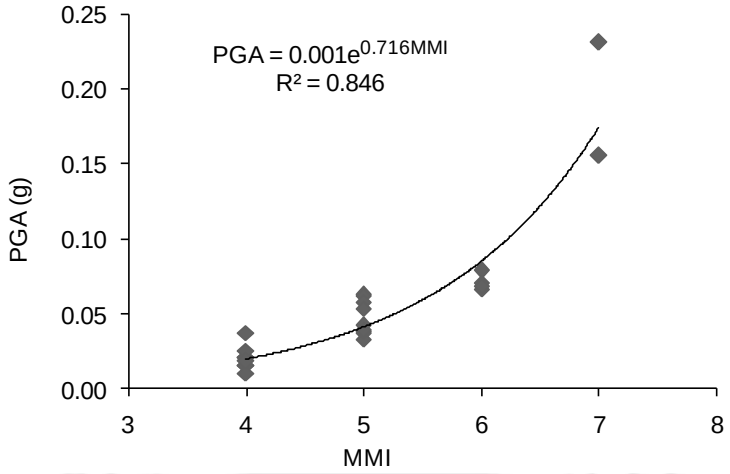

Figure 6.5: Correlation between MMI and PGA for the SP

in the SP. The MMI felt within the SP during the above mentioned past EQs are collected from isoseismal maps. The isoseismal maps were developed by the Geological Survey of India. The Geological Survey of India developed the isoseismal maps for each of these EQs in different intensity scales. Sabri (2002) re-evaluated the intensities for each of the EQs and redrew the isoseismal maps using the European Macroseismic Scale (EMS). In this study the isoseismal maps developed by Sabri (2002) are used and the EMS scale is converted to MMI scale as per Musson et al. (2010). It was observed from the isoseismal maps that during the various past EQs different sites across the SP experienced different shaking intensities. MMI of VI and V were felt across Shillong city (25.57°N, 91.89°E) during the 1869 Cachar EQ and 1918 Srimanagal EQ respectively. Similarly, during the same 1918 Srimanagal EQ, MMI of VI was felt in Cherrapunji (25.27° N, 91.73° E). Further, MMI of V and VI during the 1885 Bengal EQ and the 1930 Dhubri EQ respectively were reported in Cherrapunji. At Tura (25.51° N, 90.20° E) as well, MMI of V was reported during the 1885 Bengal EQ. It can be observed from Figure 6.5 that the proposed correlation is valid only till a MMI value of 7. For this reason, the PGA value for the 1897 Assam EQ is not estimated using the proposed correlation since a MMI of X was reported due to this EQ within the SP. Thus employing various MMI values from the isoseismal maps into the proposed correlation, PGA values at the surface level across the SP are estimated.

It has been mentioned earlier that unlike Nepal, in SP strong ground motion records for recent major or great EQs is not available. Hence, unlike Nepal the PHA

values at bedrock level are not estimated at any particular recording stations, instead PHA values are estimated at Shillong city(25.57°N, 91.89°E), Tura (25.51° N, 90.20° E) and Cherrapunji (25.27° N, 91.73° E). To estimate the PHA values at the above mentioned sites the GMPEs developed by Toro (2002), NDMA (2010) and Anbazhagan et al. (2013) are used in this study. These three GMPEs have been found suitable for the SP in the previous chapters and hence are employed to estimate the PHA values. The PHA values obtained using the above mentioned three GMPEs are listed in Table 6.3. It can be observed from Table 6.3 that a wide range of PHA from 0.02g to 0.14g is available in the present work, representing a wide range of ground motion scenario. Taking into account PHA estimated using each of the three selected GMPEs and above estimated PGA, AF is estimated. Table 6.3 lists PHA and AF values estimated at the sites Shillong city, Tura and Cherrapunji during different EQs.

Table 6.3: PHA and AF values estimated for the past EQs in the SP

Site		Shillong city	Shillong city	Tura	Cherrap-unji	Cherrap-unji	Cherrap-unji
EQ / GMPEs		1869 Cachar	1918 Srimangal	1885 Bengal	1885 Bengal	1918 Srimangal	1930 Dhubri
Toro (2002)	PHA	0.04	0.04	0.02	0.01	0.05	0.02
	AF	1.90	1.01	1.81	3.00	1.48	3.73
NDMA (2010)	PHA	0.02	0.11	0.05	0.03	0.14	0.05
	AF	3.86	0.34	0.66	1.04	0.52	1.34
Anbazhagan et al. (2013)	PHA	0.07	0.06	0.03	0.02	0.09	0.03
	AF	1.08	0.56	1.30	2.11	0.78	2.61

Similar to Nepal a PHA versus AF plot is developed for the SP as shown in Figure 6.6, using the PHA and AF values obtained in Table 6.3. It can be observed from Figure 6.6 that for higher PHA values lower values of AF is obtained. This is in accordance to the findings of EPRI (1993), Romero and Rix (2005) and analysis done for Nepal previously in this chapter. EPRI (1993) reported that for PHA higher than 0.5g

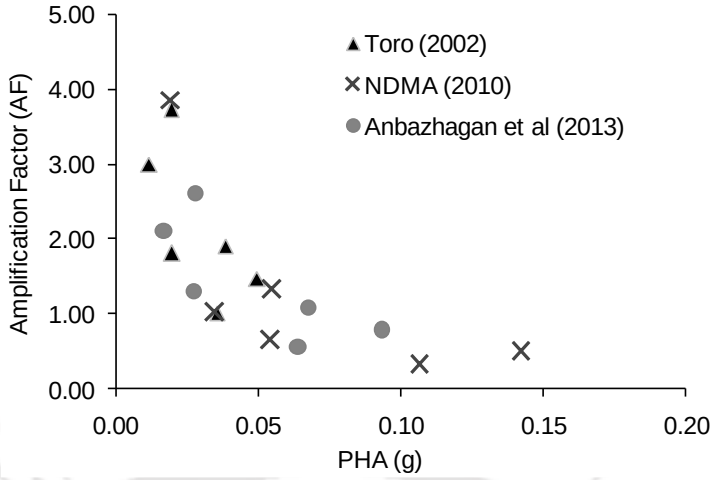

Figure 6.6: PHA versus AF for the SP

deamplification of AF occurs. From Figure 6.3 it can be observed that for Nepal, the value of AF reduces drastically from PHA of 0.15 g onwards. Similarly, it can be observed from Figure 6.6 that deamplification of AF starts to occur at 0.05g. It has to be highlighted here that most of the sites across the SP are of site classes of A (firm or hard rocks) or B (soft to firm rocks) as per Mittal et al. (2012). The sites Shillong city, Tura and Cherrapunji chosen in this study are of site classes A, B and A respectively. Since the sites are mostly rocks the ground motion amplification is very less within the SP. Hence in Figure 6.6 as the PHA value begins to increase the AF starts to decrease.

6.5 Summary

Local soil always plays an important role in deciding the response of the superstructure as well as the induced effects during an EQ. However, most of the available seismic hazard studies map the probable level of ground shaking at the bedrock and not at the surface. Thus, the outcome of such seismic hazard studies has limitations for use in building design and quantification of induced effects. To address the current limitations in the site response practices, a new method of indirect assessment of the local soil response for Nepal and the SP is proposed in this chapter. In case of Nepal, a new correlation is developed between MMI-PGA based on recorded data at different sites during the 2015 Nepal EQ, which is found to match well with similar correlations available for western USA. Using the proposed correlation, felt MMI values during 1833 Nepal EQ and 1934 Bihar-Nepal EQ at selected locations are converted to PGA

values. In addition, ground motion records at these sites during the 2015 Nepal EQ are also considered. Based on the datasets of recorded ground motions as well as MMI values, variation of AF versus PHA is found for all the selected sites. Following the approach used for Nepal, for the SP also a new correlation is developed between MMI-PGA based on MMI and PGA values obtained during 2016 Myanmar EQ and 2016 Imphal EQ. This correlation developed for the SP is used to estimate the PGA values at Shillong city, Tura and Cherrapunji during the 1885 Bengal EQ, 1869 Cachar EQ, 1918 Srimangal EQ and 1930 Dhubri EQ. At the same sites, PHA values at the bedrock level are estimated with the help of suitable GMPEs. Using the AF and PHA values obtained for the SP, a DSRC plot is proposed for the SP, which is found to show similar trend as the DSRC plot developed for Nepal.

Chapter 7 - Conclusions

The SP located within north-eastern region of India, has experienced a number of damaging EQs in the past. This seismic activity of the plateau can be attributed to the presence of an intensive network of seismically active faults located in the vicinity of the SP. In this study, an attempt has been made to understand and characterizing the seismic sources located around the SP. Once an understanding of the seismic sources located around the SP have been made possible, this study is further extended into performing deterministic and probabilistic seismic hazard analysis for the plateau. Seismic hazard studies are however performed at the bedrock level, which is not very useful for design purposes at the ground surface level. Hence in this study, the response of local soil of the SP is assessed indirectly considering different EQs at selected sites in the absence of in situ sub soil characteristics. The salient conclusions obtained from this study are presented in the following sub headings.

7.1 Seismic source characterization

1. Based on tectonic features, geology, thickness of overburden, rupture characteristics and rate of movement, the entire seismotectonic map is divided into four seismic source zones namely; SP-AVZ, IBRZ, BBZ and EHZ
2. Using maximum likelihood methodology, *b*-values obtained for the seismic source zones SP-AVZ, IBRZ, BBZ and EHZ are 0.91±0.03, 0.94±0.02, 0.80±0.03 and 0.89±0.03 respectively.
3. Based on *b*-value, return period and probability of exceedance, SP-AVZ is found as zone of high hazard zone while IBRZ is a low seismic hazard zone.

7.2 Deterministic Seismic Hazard Analysis (DSHA)

1. It is found that variation in hypocentral distance, affects the weights of applicable GMPEs for different sites within the SP (based on information theoretic approach).

2. Hence DSHA is performed for three districts namely East Khasi hills, Ri-Bhoi and West Garo hills rather than the entire SP.
3. The PHA values obtained from the GMPEs are used to develop DSHA maps for the three districts. It is found that the PHA values range from 0.26g to 0.46g for the East Khasi hills and West Garo hills districts. For the Ri-Bhoi district the PHA values range from 0.30g to 0.46g.
4. Higher PHA values on the eastern part of the Ri-Bhoi district, northern part of the East Khasi hills district and northern part of the West Garo hills district indicate the higher seismic hazard potential within these districts.
5. The higher PHA values in the eastern part of the Ri-Bhoi district and the northern part of the East Khasi hills district are assumed to be associated with the Barapani fault.
6. The higher PHA value in the northern part of the West Garo hills district is assumed to be due to the Oldham fault.

7.3 Probabilistic Seismic Hazard Analysis (PSHA)

1. Based on the variation in hypocentral distance and the effect on the weights of applicable GMPEs for different sites within the SP, PSHA is performed for the districts of East Khasi hills, Ri-Bhoi and West Garo hills rather than the entire SP.
2. PSHA results are obtained in the form of hazard curves. For each of the three districts individual hazard curves of potential faults affecting each of the districts is obtained.
3. From the hazard curves developed for the Ri-Bhoi and the East Khasi hills districts Barapani fault is found as the most hazardous fault within these two districts. For the West Garo hills district, the Dhubri fault and Dauki fault are found to be the most hazardous faults.
4. From PSHA maps at 2% and 10% probabilities of exceedance in 50 years it is inferred that for the East Khasi hills district and the Ri-Bhoi district, the northern and eastern parts respectively are prone to high seismic hazard. The southern region of the West Garo hills district is more prone to seismic hazard.

5. Comparison between the seismic hazard potential maps of the DSHA and PSHA maps, highlight the stark contract for the West Garo hills district. It is assumed that the Oldham fault, a high seismic hazard source with very low probability of occurrence is responsible for the high seismic hazard potential reflected in the DSHA map. As DSHA considers the worst case scenario, the affect of Oldham fault is prominently observed in the results. However, in case of PSHA little to no effect of the Oldham fault is observed in the results.

7.4 In-direct estimation of local soil response

1. A new method of indirect assessment of the local soil response for Nepal and the SP is proposed in this study.
2. The response of the local soil for Nepal is computed indirectly from the AF versus PHA, DSRC curve.
3. Similar approach is applied to the SP, where response of local soil is computed indirectly from the DSRC curve.
4. From DSRC, it is found that deamplification of AF starts to occur 0.15 g onwards. For the SP, deamplification of AF starts at 0.05g. This is due to the fact that sites chosen within the SP are of class A (firm or hard rocks) or B (soft to firm rocks).
5. From DSRC it can also be concluded that the response of the soil changes with change in input ground motion characteristics.

7.5 Major contributions of the present study

1. Four seismic source zones affecting the seismic hazard potential of the SP are identified on the basis of tectonic features, geology, thickness of overburden, rupture characteristics and rate of movement.
2. Effect of the variation of hypocentral distances on the weights of GMPEs is identified and analyzed in this study.
3. Findings from the present work show that in case of seismic hazard analysis of significantly larger area such as the SP; the analysis is to be done in parts and

not as a single study area due to the variation in weights of same or different GMPEs.

4. Effect of a high potential seismic hazard source with low probability of occurrence is clearly highlighted in the seismic hazard results obtained for the West Garo hills district.
5. A new method of indirect assessment of the local soil response for Nepal and the SP is proposed in this study

7.6 Limitations of the present study

1. Estimated return period is based on available EQ catalogue. If in the future more EQs are unearthed in the nearby faults, the EQ catalogue could be updated and thereby the results.
2. Presence of hidden faults may always be a source of uncertainty in the present findings. Thus, if more numbers of sources are found, the seismic hazard values may change.
3. Present study considers the 1897 Assam EQ to occur on the Oldham fault as per Bilham and England (2001). However, other studies exists which doubt the existence of the Oldham fault.
4. Postulate of the Assam Seismic Gap as suggested by limited literature has not been considered in the present work.
5. AF versus PHA plot obtained for the SP is only applicable to sites classes A and B. For other site classes borehole data is needed.
6. In the absence of information on great EQs that has occurred in the study area prior to 1411, the present seismic hazards results maybe an underestimation of the real scenario. As in the case of 2011 Tohoku EQ (M_W-9.0) of Japan, where due to no prior information on great EQs, the region was considered to be less seismically active.

7.7 Recommendation for future scope

1. Paleoseismic investigations can be attempted to ascertain the seismicity and return periods of significant hazard causing faults and the present findings can be updated.
2. In-situ ground response analysis and liquefaction assessment can be attempted.
3. Knowing the building classification, studies related to seismic vulnerability and risk can be performed.

भारतीय प्रौद्योगिकी संस्थान गुवाहाटी
Indian Institute of Technology Guwahati

References

1. Algermissen, S. T., & Perkins, D. M. (1976). *A probabilistic estimate of maximum acceleration in rock in the contiguous United States*. U.S. Geological Survey open-file Report, 76–416. Retrieved from https://www.nrc.gov/docs/ML1302/ML13022A452.pdf

2. Ambraseys, N., & Bilham, R. (2000). A note on the Kangra M s = 7. 8 earthquake of 4 April 1905.*Current Science*, *79*(1), 45–50.

3. Anbazhagan, P., Vinod, J. S., & Sitharam, T. G. (2009). Probabilistic seismic hazard analysis for Bangalore. *Natural Hazards, 48*(2), 145-166. doi:10.1007/s11069-008-9253-3

4. Anbazhagan, P., Kumar, A., & Sitharam, T. G. (2010). *Site response of Deep soil sites in Indo-Gangetic plain for different historic earthquakes.* Proceedings of 5th international conference on recent advances in geotechnical earthquake engineering and soil dynamics, San Diego, California

5. Anbazhagan, P., Kumar, A., & Sitharam, T. G. (2011). *Amplification factor from intensity map and site response analysis for the soil sites during 1999 Chamoli earthquake.* Proceeding of 3rd Indian Young Geotechnical Engineers Conference, New Delhi, India

6. Anbazhagan, P., Kumar, A., & Sitharam, T. G. (2013). Ground motion prediction equation considering combined dataset of recorded and simulated ground motions. *Soil Dynamics and Earthquake Engineering, 53*, 92-108. doi:10.1016/j.soildyn.2013.06.003

7. Anbazhagan, P., Smitha, C., Kumar, A., & Chandran, D. (2013). Estimation of design basis earthquake using region-specific Mmax, for the NPP site at Kalpakkam, Tamil Nadu, India. *Nuclear Engineering and Design, 259*, 41-64. doi:10.1016/j.nucengdes.2013.02.047

8. Anbazhagan, P., Bajaj, K., & Patel, S. (2015). Seismic hazard maps and spectrum for Patna considering region-specific seismotectonic parameters. *Natural Hazards, 78*(2), 1163-1195. doi:10.1007/s11069-015-1764-0

9. Angelier, J., & Baruah, S. (2009). Seismotectonics in Northeast India: A stress analysis of focal mechanism solutions of earthquakes and its kinematic implications. *Geophysical Journal International, 178*(1), 303-326. doi:10.1111/j.1365-246x.2009.04107.x

10. Ashford, S. A., Warrasak, J., & Panitan, L. (2000). *Amplification of earthquake ground motions in Bangkok*. Proceedings of 12th world conference on earthquake engineering, Auckland, New Zealand. Retrieved from http://www.iitk.ac.in/nicee/wcee/article/1466.pdf

11. Atkinson, G. M., & Boore, D. M. (2003) Empirical ground-motion relations for subduction zone earthquakes and their application to Cascadia and other regions. *Bulletin of the Seismological Society of America, 93*, 1703-1729

12. Atkinson, G. M., & Boore, D. M. (2006). Earthquake Ground-Motion Prediction Equations for Eastern North America. *Bulletin of the Seismological Society of America, 96*(6), 2181-2205. doi:10.1785/0120050245

13. Austen, G. (1869). *Earthquake in the Cachar Hills, Extracts from Letters*. Proceedings of the Royal Geographical Society, Vol. XIII, 1868-69.

14. Avouac, J. P., Ayoub, F., Leprince, S., Konca, O., & Helmberger, D. V. (2006). The 2005, Mw 7.6 Kashmir earthquake: Sub-pixel correlation of ASTER images and seismic waveforms analysis. *Earth and Planetary Science Letters, 249*(3-4), 514–528.

15. Babayev, G., Ismail-Zadeh, A., & Mouël, J. L. (2010). Scenario-based earthquake hazard and risk assessment for Baku (Azerbaijan). *Natural Hazards and Earth System Science, 10*(12), 2697-2712. doi:10.5194/nhess-10-2697-2010

16. Banerjee, P., Bürgmann, R., Nagarajan, B., & Apel, E. (2008). Intraplate deformation of the Indian subcontinent. *Geophysical Research Letters, 35*(18). doi:10.1029/2008gl035468

17. Baruah, S., Baruah, S., Gogoi, N. K., Erteleva, O., Aptikaev, F., & Kayal, J. R. (2009). Ground motion parameters of Shillong plateau: One of the most seismically active zones of northeastern India. *Earthquake Science, 22*(3), 283-291. doi:10.1007/s11589-009-0285-2

18. Baruah, S., & Baruah, S. (2011). Moment Magnitude – Local Magnitude Relationship for the Earthquakes of Shillong- Mikir Plateau of Northeast India Region. *Memoir of the geological society of India,* 77,141-148

19. Bhatia, S., Kumar, M., & Gupta, H. (1999). A probabilistic seismic hazard map of India and adjoining regions. *Annals of Geophysics*, 42(6). http://dx.doi.org/10.4401/ag-3777

20. Bilham, R. (1995). Location and magnitude of 1833 Nepal earthquake and its relation to the rupture zones of contiguous great Himalayan earthquakes. *Current Science, 69*(2),101–128

21. Bilham, R. (2004). Earthquakes in India and the Himalaya: tectonics,geodesy and history. *Annals of Geophysics, 47*, 839–858.

22. Bilham, R. (2008). Tom La Touche and the Great Assam Earthquake of 12 June 1897: Letters from the Epicenter. *Seismological Research Letters,* 79(3), 426-437. doi:10.1785/gssrl.79.3.426

23. Bilham, R., & England, P. (2001). Plateau pop-up in the great 1897 Assam earthquake. *Nature, 410*(6830), 806-809. doi:10.1038/35071057

24. Bond, J. (1899). Narrative Account of the Assam Revisionary Triangulation, in Strahan, C., Annual Report of triangulation 1897-1898, *Survey of India Department*, Part II, xii-xiii, Calcutta

25. Boore, D. M. & Atkinson, G. M. (2008) Ground-Motion Prediction Equations for the Average Horizontal Component of PGA, PGV, and 5%-Damped PSA at Spectral Periods between 0.01 s and 10.0 s. *Earthquake Spectra, 24* (1), 99-138.

26. Building Seismic Safety Council National Institute of Building Sciences (BSSC). (2004). *NEHRP Recommended Provisions for Seismic Regulations for new Buildings*

and Other Structures (FEMA 450). Building Seismic Safety Council National Institute of Building Sciences, Washington, D.C. 2004. Retrieved from http://www.nehrp.gov/pdf/fema450provisions.pdf.

27. Burrard, S. G. (1909). *Great Trigonometrical Survey of India*. Synoptical Volume 35, North East Longitudinal Series, Dehra Dun.

28. Centre for Natural Disaster Management (CNDM) (2002) *Scenario of seismic hazard in Assam*. A report by the Assam Administrative Staff College, Guwahati, Assam, India. Retrieved from https://aasc.assam.gov.in/sites/default/files/swf_utility_folder/departments/aasc_webcomindia_org_oid_4/portlet/level_2/SCENARIO%20OF%20SEISMIC%20HAZARD%20IN%20ASSAM.pdf

29. Choudhury, J. R. (1993) *Bangladesh-Seismicity in Bangladesh*. Incede Report, Bangkok

30. Christophersen, A., Gerstenberger, M. C., Rhoades, D. A., & Stirling, M. W. (2011) *Quantifying the effect of declustering on probabilistic seismic hazard.* Proceedings of the Ninth Pacific Conference on Earthquake Engineering, Auckland, New Zealand. Retrieved from https://www.nzsee.org.nz/db/2011/206.pdf

31. Cornell, C. A. (1968). Engineering seismic risk analysis. *Bulletin of the Seismological Society of America*, 58(5), 1583–1606. Retrieved from http://dx.doi.org/

32. Cubrinovski, M., Ishihara, K., & Kijima, T. (2001). *Effects of liquefaction on seismic response of a storage tank on pile foundations.* Fourth International Conference on Recent Advances in Geotechnical Earthquake Engineering and Soil Dynamics and Symposium in Honor of Professor W.D. Liam Finn, San Diego, California. Retrieved from https://scholarsmine.mst.edu/cgi/viewcontent.cgi?article=3657&context=icrageesd

33. Curray, J. R., Emmel, F. J., Moore, D. G., & Raitt, R. W. (1982). Structure, Tectonics, and Geological History of the Northeastern Indian Ocean. In A. E. M.

Nairn & F. G. Stehli (Eds.), *The Ocean Basins and Margins: The Indian Ocean*. Boston, MA: Springer US. doi:10.1007/978-1-4615-8038-6_9

34. Das, S., Gupta, I. D., & Gupta, V. K. (2006). A Probabilistic Seismic Hazard Analysis of Northeast India. *Earthquake Spectra, 22*(1), 1-27. doi:10.1193/1.2163914

35. Dasgupta, S., & Mukhopadhyay, B. (2014). 1803 Earthquake in Garhwal Himalaya – archival materials with commentary. *Indian Journal of History of Science*, *49*(1), 21–33.

36. Delavaud, E., Scherbaum, F., Kuehn, N., & Riggelsen, C. (2009). Information-Theoretic Selection of Ground-Motion Prediction Equations for Seismic Hazard Analysis: An Applicability Study Using Californian Data. *Bulletin of the Seismological Society of America, 99*(6), 3248-3263. doi:10.1785/0120090055

37. Desai, S., & Choudhury, D. (2014). Deterministic Seismic Hazard Analysis for Greater Mumbai, India. *Geo-Congress 2014 Technical Papers*. doi:10.1061/9780784413272.038

38. Earthquake Engineering Research Institute (EERI) (2011). *Learning from Earthquakes: The March 11, 2011, Great East Japan (Tohoku) Earthquake and Tsunami: Societal Dimensions.* An EERI Special Earthquake Report. Retrieved from http://www.eqclearinghouse.org/2011-03-11-sendai/files/2011/03/Japan-SocSci-Rpt-hirez-rev.pdf

39. Engineer Manual (EM) 1110 (1999). *Response spectra and seismic analysis for concrete hydraulic structures*. Department of Army, U.S. Army corps of Engineers, Washington DC-20314-1000. Retrieved from http://citeseerx.ist.psu.edu/viewdoc/download?doi=10.1.1.9.3905&rep=rep1&type=pdf

40. Electric Power Research Institute, EPRI (1993). *Guidelines for determining design basis ground motion*. Palo Alto, CA, 1, EPRI TR-102293

41. Eurocode 8. (2004). *Design of structures for earthquake resistance – part 1: General rules, seismic actions and rules for buildings*. European Committee for

Standardization, Brussels. Retrieved from http://civil.emu.edu.tr/courses/civl471/1998-3-2005.pdf

42. Galli, P., & Bosi, V. (2002). Paleoseismology along the Cittanova fault: Implications for seismotectonics and earthquake recurrence in Calabria (southern Italy). *Journal of Geophysical Research*, *107*(B3), 1–19.
43. Gan, W., Zhang, P., Shen, Z. K., Niu, Z., Wang, M., Wan, Y., Zhou, D., Cheng, J. (2007). Present-day crustal motion within the Tibetan Plateau inferred from GPS measurements. *Journal of Geophysical Research*, *112*(B8). doi:10.1029/2005jb004120
44. Gee, E. R. (1934). The Dhubri earthquake of the 3rd July 1930. *Memoirs of the. Geological Survey of India*, *65*(1), 1-106.
45. Goswami, H. C., & Sarmah, S. K. (1982). Probabilistic earthquake expectancy in the northeast Indian region. *Bulletin of Seismological Society of America*, *72*(3), 999–1009.
46. Gupta, I. D. (2002). The state of the art in seismic hazard analysis. *ISET Journal of Earthquake Technology*, *39*(4), 311–346. doi:10.1.1.539.7022
47. Gupta, I. D. (2010). Response spectral attenuation relations for intraslab earthquakes in Indo- AC 536 Burmese subduction zone. *Soil Dynamics and Earthquake Engineering*, *30*, 368–377
48. Gutenberg, B., & Richter, C. F. (1956). Magnitude and energy of EQs. *Annals Of Geophysics*,*9*, 1-15
49. Harinarayan, N. H., & Kumar, A. (2018a). Determination of NEHRP Site Class of Seismic Recording Stations in the Northwest Himalayas and Its Adjoining Area Using HVSR Method. *Pure and Applied Geophysics*, *175*(1), 89-107. doi:10.1007/s00024-017-1696-6
50. Harinarayan, N. H., & Kumar, A. (2018b). Seismic Site Classification of Recording Stations in Tarai Region of Uttarakhand, from Multiple Approaches. *Geotechnical and Geological Engineering*. doi:10.1007/s10706-017-0399-1
51. Hershberger, J. (1956). A comparison of earthquake acceleration with intensity ratings. *Bulletin of Seismological Society of America*, *46*, 317–320

52. Holschneider, M., Zoller, G., and Hainzl, S. (2011). Estimation of the Maximum Possible Magnitude in the Framework of a Doubly Truncated Gutenberg-Richter Model. *Bulletin of Seismological Society of America, 101*(4), 1649-1659. doi:10.1785/0120100289
53. Hwang, H., & Huo, J. (1997). Attenuation relations of ground motion for rock and soil sites in eastern United States. *Soil Dynamics and Earthquake Engineering, 16*(6), 363-372. doi:10.1016/s0267-7261(97)00016-x
54. Indian Meteorological Department, IMD. Retrieved from http://www.imd.gov.in/pages/earthquake_prelim.php
55. IS1893 (Part 1): 2016. *Criteria for Earthquake Resistant Design of Structures, Part 1: General Provisions and Buildings*. Bureau of Indian Standards, New Delhi. Retrieved from https://archive.org/details/1893Part12016
56. Ismail-Zadeh, A. (2014). Extreme seismic events: From basic science to disaster risk mitigation. *Extreme Natural Hazards, Disaster Risks and Societal Implications,* 47-60. doi:10.1017/cbo9781139523905.007
57. Ismail-Zadeh, A., Soloviev, A., Sokolov, V., Vorobieva, I., Muller, B., Schilling, F. (2017). Quantitative modeling of the lithosphere dynamics, earthquakes and seismic hazard. *Tectonophysics*. http://doi.org/10.1016/j.tecto.2017.04.007.
58. Iyenger, R. N., & Ghosh, S. (2004). Microzonation of earthquake hazard in Greater Delhi area. *Current Science*, 87(9),1193–1202
59. Jade, S., Mukul, M., Bhattacharyya, A. K., Vijayan, M. S. M., Jaganathan, S., Kumar, A., Tiwari, R. P., Kumar, A., Kalita, S., Sahu, S.C., Krishna, A.P., Gupta, S. S., Murthy, M.V. R. L., & Gaur, V. K. (2007). Estimates of interseismic deformation in Northeast India from GPS measurements. *Earth and Planetary Science Letters, 263*, 221–34. doi:10.1016/j.epsl.2007.08.031
60. Jaiswal, K., & Sinha, R. (2007). Probabilistic Seismic-Hazard Estimation for Peninsular India. *Bulletin of Seismological Society of America, 97*(1B), 318-330. doi:10.1785/0120050127
61. Jena, A. K., Haldia, B. S., Solomon, R., Sahoo, A. K., Bhanja, A. K., & Samanta, A. (2012). *Exploration Strategy in Tripura Fold Belt, Assam & Assam Arakan Basin , India - Some Contemporary Approach.* 9th Biennial International Conference &

Exposition on Petroleum Geophysics, Hyderabad. Retrieved from https://www.spgindia.org/spg_2012/spgp458.pdf

62. Joyner, W. B. & Boore, D. M. (1981). Peak horizontal acceleration and velocity from strong motion records including records from the 1979 Imperial Valley California earthquake. *Bulletin of Seismological Society of America*, *71*, 2011-2038
63. Kagan, Y. Y. (2002). Seismic moment distribution revisited: I. Statistical results. *Geophysical Journal International*, *148*(3), 520-541. doi:10.1046/j.1365-246x.2002.01594.x
64. Kailasam, L. N. (1979). Plateau uplift in peninsular India. *Techtonophysics, 61*,243-269.
65. Kakati, P. (2015). *Microstructural Behaviour of Lower Metapelitic Formation of the Proterozoic Shillong Basin, Meghalaya, India* (Doctoral thesis). Retrieved from http://shodhganga.inflibnet.ac.in/handle/10603/50841
66. Kanno, T., Narita, A., Morikawa, N., Fujiwara, H., Fukushima, Y. (2006). A new attenuation relation for strong ground motion in Japan based on recorded data. *Bulletin of Seismological Society of America, 96*, 879–897. doi: 10.1785/0120050138
67. Kayal, J. R. (2008). *Microearthquake Seismology and Seismotectonics of South Asia*. McGraw Hill Publication, India
68. Kayal, J. R., Arefiev, S. S., Baruah, S., Tatevossian, R., Gogoi, N., Sanoujam, M., Gautam, J. L., Hazarika, D., & Borah, D. (2010). The 2009 Bhutan and Assam felt earthquakes (M_W 6.3 and 5.1) at the Kopili fault in the northeast Himalaya region. *Geomatics, Natural Hazards and Risk, 1*(3), 273-281. doi:10.1080/19475705.2010.486561
69. Kayal, J. R. (2014). Seismotectonics of the great and large EQs in Himalaya. *Current Science,106* (2),188-197
70. Khattri, K. N. & Tyagi, A. K., (1983). Seismicity pattern in the Himalayan plate boundary and identification of the area of high seismic potential, *Tectonophysics, 9*, 281-297.

71. Khattri, K., Rogers, A., Perkins, D., & Algermissen, S. (1984). A seismic hazard map of India and adjacent areas. *Tectonophysics, 108*(1-2), 93-134. doi:10.1016/0040-1951(84)90156-2
72. Kijko, A. (2004). Estimation of the Maximum Earthquake Magnitude, m max. *Pure and Applied Geophysics, 161*(8), 1655-1681. doi:10.1007/s00024-004-2531-4
73. Kijko, A., & Sellevoll, M.A. (1989). Estimation of earthquake hazard parameters from incomplete data files. Part I. Utilization of extreme and complete catalogs with different threshold magnitudes. *Bulletin of Seismological Society of America, 79*,645–654.
74. Kijko, A., & Graham, G. (1998). Parametric-historic Procedure for Probabilistic Seismic Hazard Analysis Part I: Estimation of Maximum Regional Magnitude m max. *Pure and Applied Geophysics, 152*(3), 413-442. doi:10.1007/s000240050161
75. Kijko, A., Smit, A., & Sellevoll, M. A. (2016). Estimation of Earthquake Hazard Parameters from Incomplete Data Files. Part III. Incorporation of Uncertainty of Earthquake-Occurrence Model. *Bulletin of Seismological Society of America, 106*(3), 1210-1222. doi:10.1785/0120150252
76. Kiureghian, D. A., & Ang, A. H-S. (1977). A fault rupture model for seismic risk analysis. *Bulletin of Seismological Society of America* ,67,1173–1194
77. Krishna, M. R., & Sanu, T. (2000). Seismotectonics and rates of active crustal deformation in the Burmese arc and adjacent regions. *Journal of Geodynamics, 30*(4), 401-421. doi:10.1016/s0264-3707(99)00074-5
78. Kumar, A., Anbazhagan, P., & Sitharam, T. G. (2013). Seismic hazard analysis of Lucknow considering local and active seismic gaps. *Natural Hazards, 69*(1), 327-350. doi:10.1007/s11069-013-0712-0
79. Kumar, A., & Mondal, J. K. (2017). Newly developed MATLAB based code for Equivalent linear site response analysis. *Geotechnical and Geological Engineering*. doi 10.1007/s10706-017-0246-4.
80. Kumar, D., Reddy, D., & Pandey, A. K. (2016). Paleoseismic investigations in the Kopili Fault Zone of North East India: Evidences from liquefaction chronology. *Tectonophysics, 674*, 65-75. doi:10.1016/j.tecto.2016.02.016

81. Kundu, B., & Gahalaut, V. K. (2013). Tectonic geodesy revealing geodynamic complexity of the Indo-Burmese arc region, North East India. *Current Science, 104* (7), 920-933
82. Mahopatra, A. K., & Mohanty, W. K. (2010). *An Overview of Seismic Zonation Studies in India*. Indian Geotechnical Conference, Mumbai, India. Retrieved from https://gndec.ac.in/~igs/ldh/conf/2010/articles/043.pdf
83. Marzocchi, W., & Sandri, L. (2003). A review and new insights on the estimation of the b -value and its uncertainty. *Annals of Geophysics, 46*(6), 1271-1282. doi: 10.4401/ag-3472
84. Maurin, T., & Rangin, C. (2009). Structure and kinematics of the Indo-Burmese Wedge: Recent and fast growth of the outer wedge. *Tectonics, 28*(2). doi:10.1029/2008tc002276
85. Maxwell, K. (2006). *Lisbon 1755 : The First "Modern" Disaster (but if modern, how is it so ?)*. The Treaty of Windsor and 620 Years of Anglo-Portuguese Relations, St. Peter's College. Retrieved from http://www.mod-langs.ox.ac.uk/files/windsor/5_maxwell.pdf
86. Mittal, H., Kumar, A., & Ramhmachhuani, R. (2012). Indian National Strong Motion Instrumentation Network and Site Characterization of Its Stations. *International Journal of Geosciences, 3*(06), 1151-1167. doi:10.4236/ijg.2012.326117
87. Mohanty, W. K., & Walling, M. Y. (2008). Seismic hazard in mega city Kolkata, India. *Natural Hazards, 47*(1), 39-54. doi:10.1007/s11069-007-9195-1
88. Mohanty, W. K., Verma, A. K., Vaccari, F., & Panza, G. F. (2013). Influence of epicentral distance on local seismic response in Kolkata City, India. *Journal of Earth System Science, 122*(2), 321-338. doi:10.1007/s12040-013-0275-1
89. Mondal, J. K., & Kumar, A. (2015). *Impact of Frequency Content of input motion upon local site effect*. 50th Indian Geotechnical Conference, Pune, Maharashtra, India. Retrieved from https://www.researchgate.net/publication/283343654_IMPACT_OF_FREQUENCY_CONTENT_OF_INPUT_MOTION_UPON_LOCAL_SITE_EFFECT
90. Mondal, J. K., & Kumar, A. (2016). Impact of Higher Frequency Content of Input Motion upon Equivalent Linear Site Response Analysis for the Study Area of Delhi. *Geotechnical and Geological Engineering*. doi 10.1007/s10706-016-0153-0.

91. Morino, M., Kamal, A. S. M. M., Muslim, D., Ali, R. M. E., Kamal, M. A., Rahman, M. Z., & Kaneko, F. (2011). Seismic event of the Dauki Fault in 16th century confirmed by trench investigation at Gabrakhari Village, Haluaghat, Mymensingh, Bangladesh. *Journal of Asian Earth Sciences*, *42*, 492–498.
92. Morino, M., Kamal, A. S. M. M., Ali, R. M. E., Talukder, A., Khan, M.H. (2013). *Report of active fault mapping in Bangladesh : Paleo-seismological study of the Dauki fault and the Indian-Burman plate boundary fault*. Comprehensive Disaster Management Program, Ministry of Disaster Management and Relief. Retrieved from https://www.scribd.com/document/261700908/Report-Active-Fault-Mapping-Paleo-seismological-Study-of-the-Dauki-Fault-and-the-Indian-Burman-Plate-Boundary-Fault-2013
93. Mukhopadhyay, B. (2011). Clusters of Moderate Size Earthquakes along Main Central Thrust (MCT) in Himalaya. *International Journal of Geosciences, 2*(03), 318-325. doi:10.4236/ijg.2011.23034
94. Mukhopadhyay, B., & Dasgupta, S. (2015). Earthquake swarms near eastern Himalayan Syntaxis along Jiali Fault in Tibet: A seismotectonic appraisal. *Geoscience Frontiers, 6*(5), 715-722. doi:10.1016/j.gsf.2014.12.009
95. Murphy, J. R., & O'Brien, L. J. (1977). The correlation of Peak ground acceleration amplitude with seismic intensity and other physical parameters. *Bulletin of Seismological Society of America, 67*, 877–915
96. Musson, R. M. W., Grünthal, G., & Stucchi, M. (2010). The comparison of macroseismic intensity scales. *Journal of Seismology*, *14*(2), 413–428
97. Nandy, D. R. (2001). *Geodynamics of Northeastern India and the Adjoining Region*. Kolkata: ABC Publications.
98. Nath, S. K. (2005). A seismic hazard scenario in the Sikkim Himalaya from seismotectonics, spectral amplification, source parameterization, and spectral attenuation laws using strong motion seismometry. *Journal of Geophysical Research, 110*(B1). doi:10.1029/2004jb003199
99. Nath, S. K, Vyas, M., Pal, I., & Sengupta, P. (2005). A seismic hazard scenario in the Sikkim Himalaya from seismotectonics, spectral amplification, source parameterization, and spectral attenuation laws using strong motion seismometry. *Journal of Geophysical Research, 110*(B1). doi:10.1029/2004jb003199

100. Nath, S. K., Thingbaijam, K. K., & Raj, A. (2008). Earthquake hazard in Northeast India — A seismic microzonation approach with typical case studies from Sikkim Himalaya and Guwahati city. *Journal of Earth System Science, 117*(S2), 809-831. doi:10.1007/s12040-008-0070-6

101. Nath, S. K., Raj, A., Thingbaijam, K. K., & Kumar, A. (2009). Ground Motion Synthesis and Seismic Scenario in Guwahati City--A Stochastic Approach. *Seismological Research Letters, 80*(2), 233-242. doi:10.1785/gssrl.80.2.233

102. Nath, S. K., & Thingbaijam, K. K. (2011). Peak ground motion predictions in India: An appraisal for rock sites. *Journal of Seismology, 15*(2), 295-315. doi:10.1007/s10950-010-9224-5

103. Nath, S. K., Adhikari, M. D., Maiti, S. K., Devaraj, N., Srivastava, N., & Mohapatra, L. D. (2014). Earthquake scenario in West Bengal with emphasis on seismic hazard microzonation of the city of Kolkata, India. *Natural Hazards and Earth System Science, 14*(9), 2549-2575. doi:10.5194/nhess-14-2549-2014

104. National Disaster Management Authority (NDMA) (2010). *Development of Probabilistic Seismic Hazard Map of India.* Technical report by National Disaster Management Authority, Government of India

105. Ni, J., & Barazangi, M. (1984). Seismotectonics of the Himalayan Collision Zone: Geometry of the underthrusting Indian Plate beneath the Himalaya. *Journal of Geophysical Research: Solid Earth, 89*(B2), 1147-1163. doi:10.1029/jb089ib02p01147

106. Oldham, R.D. (1899). Report on the Great Earthquake of 12 June 1897. *Memoirs of the Geological Survey of India,29*,1-379

107. Oldham, T. (1882). The Cachar earthquake of 10th January, 1869, by the late Thomas Oldham edited by Oldham RD. *Memoirs of the Geological Survey of India,19*,1-98

108. Pallav, K., Raghukanth, S. T., & Singh, K. D. (2012). Probabilistic seismic hazard estimation of Manipur, India. *Journal of Geophysics and Engineering, 9*(5), 516-533. doi:10.1088/1742-2132/9/5/516

109. Pandey, M. R., & Molnar, P. (1988). The distribution of intensity of the Bihar-Nepal earthquake of 15 January 1934 and bounds on the extent of the rupture zone. *Journal of Nepal Geological Society, 5*(1), 22-44.

110. Panza, G. F., Irikura, K., Kouteva, M., Peresan, A., Wang, Z., & Saragoni, R. (2010). Advanced Seismic Hazard Assessment. *Pure and Applied Geophysics, 168*(1-2), 1-9. doi:10.1007/s00024-010-0179-9

111. Parvez, I. A., & Ram, A. (1997). Probabilistic Assessment of Earthquake Hazards in the North-East Indian Peninsula and Hindukush Regions. *Pure and Applied Geophysics, 149*(4), 731-746. doi:10.1007/s000240050049

112. Parvez, I. A., Vaccari, F., & Panza, G. F. (2003). A deterministic seismic hazard map of India and adjacent areas. *Geophysical Journal International, 155*(2), 489-508. doi:10.1046/j.1365-246x.2003.02052.x

113. Paul, J., Bürgmann, R., Gaur, V. K., Bilham, R., Larson, K. M., Ananda, M. B., Jade, S., Mukal, M., Anupama, T. S., Satyal, G., & Kumar, D. (2001). The motion and active deformation of India. *Geophysical Research Letters, 28*(4), 647-650. doi:10.1029/2000gl011832

114. Phanikanth, V. S., Choudhury, D., Reddy, & G. R. (2011). Equivalent linear seismic ground response analysis of some typical sites in Mumbai. *Geotechnical and Geological Engineering, 29*(6),1109–1126

115. Pollitz, F. F., Nyst, M., & Nishimura, T. (2005). Coseismic slip distribution of the 1923 Kanto earthquake, Japan. *Journal of Geophysical Research: Solid Earth, 110*(11), 1–16.

116. Raghukanth, S. T. G., & Iyengar, R. N. (2006). Seismic hazard estimation for Mumbai city. *Current Science, 91*(11),1486–94

117. Raghukanth, S. T. G., & Iyengar, R. N. (2007). Estimation of seismic spectral acceleration in Peninsular India. *Journal of Earth System Science, 116*(3), 199-214. doi:10.1007/s12040-007-0020-8

118. Raghukanth, S. T. G., Singh, K. D. & Pallav, K. (2009). Deterministic Seismic Scenarios for Imphal City. *Pure and Applied Geophysics, 166*, 641-672

119. Raghukanth, S. T. G., & Dash, S. K. (2010). Deterministic seismic scenarios for northeast India. *Journal of Seismology, 14*,143–167

120. Raghukanth, S. T. G., Kumari, K. L., & Kavitha, B. (2011). Estimation of ground motions during the 18th September 2011 Sikkim earthquake. *Geomatics Natural Hazards and Risk, 3*(1), 9–34

121. Rajendran, C. P., Rajendran, K., Duarah, B. P., Baruah, S., & Earnest, A. (2004). Interpreting the style of faulting and paleoseismicity associated with the 1897 Shillong, northeast India, earthquake: Implications for regional tectonism. *Tectonics,23*(4).doi:10.1029/2003tc001605

122. Rao, N. P., & Kumar, M. R. (1997). Uplift and tectonics of the Shillong plateau, northeast India. *Journal of Physics of the Earth, 45*, 167-176.

123. Rastogi, B. K., Chadha, R.K., & Rajgopalan, G. (1993). Palaeoseismicity studies in Meghalaya. *Current Science*, 64(11&12), 933-935

124. Reasenberg, P. (1985). Second-order moment of central California seismicity, 1969-1982. *Journal of Geophysical Research: Solid Earth, 90*(B7), 5479-5495. doi:10.1029/jb090ib07p05479

125. Reiter, L. (1990). *Earthquake hazard analysis: Issues and Insights*. Columbia University

126. Ristau, J., Rogers, G. C., & Cassidy, J. F. (2005). Moment Magnitude-Local Magnitude Calibration for Earthquakes in Western Canada. *Bulletin of Seismological Society of America, 95*(5), 1994-2000. doi:10.1785/0120050028

127. Romero, S. M., & Rix, G. J. (2005). *Ground motion amplification of soils in the upper Mississippi embayment*. National Science Foundation Mid America Earthquake Center

128. Sabri, M. S. A. (2002). *Earthquake intensity-attenuation relationship for Bangladesh and its surrounding region* (Master's thesis). Bangladesh University of Engineering and Technology, Dhaka, Bangladesh

129. Sanjay, K. P., Ashok, K., Sumer, C., & Bansal, B. K. (2013). Intensity mapping of Mw 6.9 2011 Sikkim–Nepal border earthquake and its relationship with PGA: distance and magnitude. *Natural Hazards, 69,*1781–1801

130. Scherbaum, F., Delavaud, E., & Riggelsen, C. (2009). Model Selection in Seismic Hazard Analysis: An Information-Theoretic Perspective. *Bulletin of Seismological Society of America, 99*(6), 3234-3247. doi:10.1785/0120080347

131. Scordilis, E. M. (2006). Empirical Global Relations Converting M_S and m_b to Moment Magnitude. *Journal of Seismology, 10*(2), 225-236. doi:10.1007/s10950-006-9012-4

132. Seeber, L., Armbruster, J. G. & Jacob, K. H. (1999). *Probabilistic Assessment of Seismic Hazard for Maharashtra*. Government of Maharashtra, unpublished report

133. SEISAT. (2000). *Seismotectonic Atlas of India and its environs*. Geological Survey of India, India

134. Shanker, D., & Sharma, M. L. (1998). Estimation of Seismic Hazard Parameters for the Himalayas and its Vicinity from Complete Data Files. *Pure and Applied Geophysics, 152*(2), 267-279. doi:10.1007/s000240050154

135. Sharma, M. L., & Malik, S. (2006). *Probabilistic seismic hazard analysis and estimation of spectral strong ground motion on bedrock in northeast India*. 4th International conference on earthquake Engineering, Taipei, Taiwan. Retrieved from http://conf.ncree.org.tw/proceedings/i0951012/data/pdf%5C4ICEE-0015.pdf

136. Sharma, M. L. & Bungum, H. (2006). *New strong ground motion spectral attenuation relations for the Himalayan region*. 1st European Conference on Earthquake Engineering and Seismology, Switzerland September, 2006

137. Sharma, M. L., Douglas, J., Bungum, H., & Kotadia, J. (2009). Ground-Motion Prediction Equations Based on Data from the Himalayan and Zagros Regions. *Journal of Earthquake Engineering, 13*(8), 1191-1210. doi:10.1080/13632460902859151

138. Sikder, A. M., & Alam, M. (2003). 2-D modelling of the anticlinal structures and structural development of the eastern fold belt of the Bengal Basin, Bangladesh. *Sedimentary Geology, 155*(3-4), 209-226. doi:10.1016/s0037-0738(02)00181-1

139. Sil, A., Sitharam, T. G., & Kolathayar, S. (2013). Probabilistic seismic hazard analysis of Tripura and Mizoram states. *Natural Hazards, 68*(2), 1089-1108. doi:10.1007/s11069-013-0678-y

140. Sitharam, T. G., & Sil, A. (2014). Comprehensive seismic hazard assessment of Tripura and Mizoram states. *Journal of Earth System Science, 123*(4), 837-857. doi:10.1007/s12040-014-0438-8

141. Socquet, A., Vigny, C., Chamot-Rooke, N., Simons, W., Rangin, C., & Ambrosius, B. (2006). India and Sunda plates motion and deformation along their boundary in Myanmar determined by GPS. *Journal of Geophysical Research: Solid Earth, 111*(B5). doi:10.1029/2005jb003877

142. Sokolov, V., & Ismail-Zadeh, A. (2015). Seismic hazard from instrumentally recorded, historical and simulated earthquakes: Application to the Tibet–Himalayan region. *Tectonophysics, 657*, 187-204. doi:10.1016/j.tecto.2015.07.004

143. Srinivasan, V. (2003) Deciphering differential uplift in Shillong Plateau using remote sensing. *Journal of Geological Society of India*,*612*, 773 – 777

144. Srivastava, H., Verma, M., Bansal, B., & Sutar, A. K. (2015). Discriminatory characteristics of seismic gaps in Himalaya. *Geomatics, Natural Hazards and Risk, 6*(3), 224-242. doi:10.1080/19475705.2013.839483

145. Stein, S., Geller, R. J., & Liu, M. (2012). Why earthquake hazard maps often fail and what to do about it. *Tectonophysics, 562-563*, 1-25. doi:10.1016/j.tecto.2012.06.047

146. Stepp, J.C. (1972). *Analysis of completeness of the earthquake sample in the Puget sound area and its effect on statistical estimates of earthquake hazard*. International conference on microzonation, Seattle, USA. Retrieved from http://www.resolutionmineeis.us/sites/default/files/references/stepp-1972.pdf

147. Strahan, G. (1891). *Synoptical Volume 32*. Great Trigonometrical Survey of India, Assam Valley Triangulation, Calcutta.

148. Sukhija, B. S., Rao, M. N., Reddy, D. V., Nagabhushanam, P., Hussain, S., Chadha, R. K., & Gupta, H.K. (1999a). Timing and return period of major paleoseismic events in the Shillong Plateau, India. *Tectonophysics*, *208*, 53–65.

149. Sukhija, B. S., Rao, M. N., Reddy, D. V., Nagabhushanam, P., Hussain. S., Chadha, R.K., & Gupta, H.K. (1999b). Paleoliquefaction evidence and periodicity of large pre-historic earthquakes in Shillong Plateau, India. *Earth Planet Science Letters*, *167*, 269–282.

150. Sukhija, B., Reddy, D., Kumar, D., & Nagabhushanam, P. (2006). Comment on "Interpreting the style of faulting and paleoseismicity associated with the 1897 Shillong, northeast India, earthquake: Implications for regional tectonism" by C. P. Rajendran et al. *Tectonics*, *25*, 1-4.

151. Tandon, A. N. (1956). Zoning of India liable to earthquake damage. *Indian Journal of Meteorology and Geophysics*, *10*, 137–146.

152. Tavakoli, B., & Ghafory-Ashtiany, M. (1999). Seismic hazard assessment of Iran. *Annals of Geophysics, 42*, 1013-1021. doi:10.4401/ag-3781

153. Thakur, V. C., Sriram, V., & Mundepi, A. K. (2000). Seismotectonics of the great 1905 Kangra earthquake meizoseismal region in Kangra-Chamba, NW Himalaya. *Tectonophysics*, *326*(3-4), 289–298.

154. Thingbaijam, K. K., & Nath, S. K. (2008). Estimation of Maximum Earthquakes in Northeast India. *Pure and Applied Geophysics, 165*(5), 889-901. doi:10.1007/s00024-008-0334-8

155. Toro, G.R. (2002) *Modification of the Toro et al. (1997) attenuation equations for large magnitudes and short distances*. Risk Engineering Inc.

156. Toro, G. R., Abrahamson, N. A., & Schneider, J. F. (1997). Model of Strong Ground Motions from Earthquakes in Central and Eastern North America: Best Estimates and Uncertainties. *Seismological Research Letters, 68*(1), 41-57. doi:10.1785/gssrl.68.1.41

157. Trifunac, M. D., & Brady, A. G. (1975). On the correlation of seismic intensity scales with peaks of recorded strong ground motion. *Bulletin of Seismological Society of America, 65*,139–162

158. Umut, D. (2004). *Sensitivity analysis of soil site response modelling in seismic microzonation for Lalitpur, Nepal* (M.Sc. Thesis). International Institute of Geo-information Science and Earth Observation, Enschede, Netherlands

159. Vere-Jones, D., Robinson, R., & Yang, W. (2001). Remarks on the accelerated moment release model: Problems of model formulation, simulation and estimation. *Geophysical Journal International, 144*(3), 517-531. doi:10.1046/j.1365-246x.2001.01348.x

160. Vernant, P., Bilham, R., Szeliga, W., Drupka, D., Kalita, S., Bhattacharyya, A. K., Gaur, V. K., Pelgay, P., Cattin, R., & Berthet, T. (2014). Clockwise rotation of the Brahmaputra Valley relative to India: Tectonic convergence in the eastern Himalaya, Naga Hills, and Shillong Plateau. *Journal of Geophysical Research: Solid Earth, 119*(8), 6558-6571. doi:10.1002/2014jb011196

161. Wald, D. J., Quintoriano, V., Heaton, T.H., & Kanamori, H. (1999). Relationship between peak ground acceleration, peak ground velocity and modified Mercalli intensity in California. *Earthquake Spectra, 15*,557–564

162. Walter, D. M., Vijaya, V. R., Reddy, P. R., Gary, S. C., & Shane, T. D. (2005). Comparison of the deep crustal structure and seismicity of North America with the Indian subcontinent. *Current Science, 88*(10),1639–1651

163. Wang, Y., Sieh, K., Tun, S. T., Lai, K., & Myint, T. (2014). Active tectonics and earthquake potential of the Myanmar region. *Journal of Geophysical Research: Solid Earth, 119*(4), 3767-3822. doi:10.1002/2013jb010762

164. Wells, D. L, & Coppersmith, K. J. (1994). New Empirical Relationships among Magnitude, Rupture Length, Rupture Width, Rupture Area, and Surface Displacement. *Bulletin of Seismological Society of America*, *84*(4), 974–1002

165. Wiemer, S. & Wyss, M. (2000). Minimum Magnitude of Completeness in Earthquake Catalogs: Examples from Alaska, the Western United States, and Japan. *Bulletin of Seismological Society of America, 90*(4), 859-869. doi:10.1785/0119990114

166. Wilson, C. A. K. (1939). *Triangulation of the Assam Valley Series*. Geodetic Report, Survey of India,10-22, Dehra Dun.

167. Xio. G. R., Gan, W. J., Chen, W. T., Cheng, J. (2010) Present-Day Movement of Bangong Co-Nujiang Suture Zone, Tibetan Plateau, Inferred from GPS Measurements. *Journal of Jilin University (Earth Science Edition)*, 40(6), 1496-1502

168. Yin, A. (2000). Mode of Cenozoic east-west extension in Tibet suggesting a common origin of rifts in Asia during the Indo-Asian collision. *Journal of Geophysical Research: Solid Earth, 105*(B9), 21745-21759. doi:10.1029/2000jb900168

169. Yin, A. (2006). Cenozoic tectonic evolution of the Himalayan orogen as constrained by along-strike variation of structural geometry, exhumation history, and foreland sedimentation. *Earth-Science Reviews, 76*(1-2), 1-131. doi:10.1016/j.earscirev.2005.05.004

170. Youngs, R. R., Chiou, S. J., Silva, W. J. & Humphrey, J. R., (1997). Strong ground motion attenuation relationship for subduction zone earthquakes, *Seismological Research Letters, 68*(1), 58-73.

171. Zhou, S., Qiu, R., Sun, K., & Zhang, L. (2011). *The Dynamic Process Mesozoic-cenozoic Igneous in Tibetan Plateau, China*. New Frontiers in Tectonic

Research - General Problems, Sedimentary Basins and Island Arcs. doi:10.5772/25236

172. Zitellini, N., Chierici, F., Sartori, R., & Torelli, L. (1999). The tectonic source of the 1755 Lisbon earthquake and tsunami. Annals of Geophysics. https://doi.org/10.4401/ag-3699

Appendix I: List of Publications from this research work

Journal Papers

1. **Baro O**, Kumar A, Alik IZ (2018) Seismic hazard assessment of the Shillong Plateau, India. **Geomatics Natural Hazard and Risk** doi: 10.1080/19475705.2018.1494043

2. **Baro O**, Kumar A (2017) Seismic source characterization for the Shillong plateau in northeast India. **Journal of Seismology** 10.1007/s10950-017-9664-2

3. Kumar A, Harinarayan N H, **Baro O** (2017) Nonlinear soil response to ground motions during different earthquakes in Nepal, to arrive at surface response spectra.**Natural Hazards** 87(1): 13-33

4. **Baro O**, Kumar A (2015) A review on the tectonic setting and seismic activity of the Shillong plateau in the light of past studies. **Disaster Advances** 8(7):34-45

Conference Papers

1. **Baro O** and Kumar A (2018) Effect of the Size of Shillong Plateau on Relative Weightage of Selected Attenuation Relations for Seismic Hazard Analysis. Geotechnical Earthquake Engineering and Soil Dynamics V, ASCE special Publication, Austin, Texas, USA

2. Kumar A, **Baro O** (2016) In-direct estimation of local soil response in the light of past as well as recent earthquakes in the Shillong plateau. In Indian Geotechnical Conference, Chennai, India

3. **Baro O**, Kumar A (2015) An insight into the Shillong plateau seismicity: a review. In 50th Indian Geotechnical Conference, Maharashtra, India

Appendix II: List of earthquakes considered in this study

(Note: NDMA (2010) reported EQ data in M_W scale, IMD reported data in M_L scale and as per Baruah and Baruah (2011) this data is taken as M_W, USGS reported data in m_b scale which is converted to M_W)

Longitude	Latitude	Magnitude	Year	Month	Date	Depth	Hrs	Mins
90.2	30	7.7	1411	9	29	0	0	0
94.9	26.75	6.5	1548	2	1	0	0	0
94.9	26.75	6.5	1596	2	1	0	0	0
91.75	26.18	4.3	1663	2	7	0	0	0
94.6	27.75	7.2	1697	2	13	0	0	0
88.4	22.6	7.2	1737	10	11	0	0	0
92	22	7.5	1762	4	2	0	7	30
88.4	22.6	4.3	1762	7	13	0	0	0
88	24	6	1764	6	4	0	0	0
89.75	24.5	7.8	1787	6	1	0	0	0
92	28.5	7.7	1806	6	11	0	0	0
88.4	22.6	4.3	1808	4	13	0	0	0
88.4	22.6	4.5	1811	2	1	0	0	0
89.4	25.8	4.5	1816	9	12	0	0	0
91	23.5	6	1822	4	3	0	0	0
88.4	22.6	4.5	1822	8	16	0	0	0
88.4	22.6	4.3	1823	4	3	0	0	0
91.2	23.5	4.5	1825	1	9	0	0	0
90.4	24.8	4.3	1825	1	8	0	0	0
88.4	22.6	4.5	1827	1	16	0	0	0
94.5	24.5	5	1828	7	8	0	0	0
88.4	22.6	4.5	1829	9	18	0	0	0
91	22	5	1830	12	31	0	0	0
89.4	25.8	6.3	1834	7	8	0	0	0
88.4	22.9	4.3	1836	1	24	0	0	0
95	28	4.3	1840	1	14	0	0	0
91.8	26.2	5.6	1841	2	9	0	0	0
94.7	27	4.3	1842	1	4	0	0	0

Longitude	Latitude	Magnitude	Year	Month	Date	Depth	Hrs	Mins
87	25	5.5	1842	2	5	0	21	15
87	25	4.9	1842	5	21	0	0	0
88.3	27	4.3	1842	9	18	0	0	0
90	25	6.5	1842	11	11	0	0	0
91.8	26.2	5	1842	10	23	0	0	0
95	28	5.7	1843	4	6	0	0	0
95.4	27.2	5.7	1843	6	16	0	0	0
94.7	27	5.7	1843	6	17	0	0	0
88.3	27	5.5	1843	8	10	0	0	0
93	26	5	1843	9	2	0	0	0
91.8	26.2	4.3	1843	11	14	0	1	0
91.8	26.2	5.7	1843	12	18	0	16	20
91.8	26.2	5.7	1845	8	22	0	12	30
88.4	22.7	4.9	1845	8	6	0	23	30
91.9	24.9	4.3	1845	10	28	0	0	0
90.4	24.8	6.3	1846	10	17	0	0	0
90	24	6	1846	10	18	0	8	45
92.7	26.3	6.3	1847	0	0	0	0	0
94	27	6	1846	12	10	0	0	0
88.4	22.6	4.7	1847	5	5	0	17	0
88.4	22.6	4.2	1848	2	20	0	17	0
88.4	22.6	4.3	1848	11	30	0	0	2
92	26	5.7	1849	1	22	0	0	0
91	26.3	5	1849	1	23	0	8	15
88.3	27	6	1849	2	27	0	21	0
88.4	22.6	4.2	1850	5	7	0	0	0
91.8	22.3	5.5	1851	1	8	0	0	0
88.4	22.6	5.7	1851	2	9	0	0	0
91.7	25.3	5	1851	10	15	0	0	0
88.4	22.6	4.3	1852	2	9	0	13	55
88.3	27	7	1852	5	1	0	0	0
88	27	6.5	1852	5	0	0	0	0

Longitude	Latitude	Magnitude	Year	Month	Date	Depth	Hrs	Mins
90.4	23.7	5.7	1852	8	9	0	4	37
92.8	26.6	4.3	1858	8	22	0	8	0
88.4	22.6	5	1861	2	16	0	0	0
88.3	27	5	1862	6	18	0	0	0
88.3	27	5.7	1863	3	29	0	22	0
88.3	27	5	1863	7	8	0	20	15
88.3	27	5	1863	8	11	0	14	15
90.4	23.7	4.5	1864	1	5	0	0	0
88.3	27	5	1865	12	16	0	22	0
89.2	23.2	4.3	1865	11	17	0	0	0
92.5	22.2	6	1865	12	19	0	0	0
88.5	23.4	4.7	1865	12	25	0	4	0
90.3	22.7	4.3	1865	12	27	0	19	15
91.9	24.9	5.5	1868	6	30	0	0	0
92.5	24.5	7.5	1869	1	10	0	0	0
91.9	25.6	5	1869	4	17	0	0	0
88.3	27	4.3	1869	3	23	0	2	15
88.4	22.6	4.2	1869	6	9	0	15	15
88.3	27	5.7	1869	8	9	0	0	0
90.4	23.7	4.3	1870	4	22	0	0	0
88.3	27	4.3	1875	4	26	0	0	0
93	26.5	5.7	1875	9	3	0	0	0
94	24.5	6.3	1880	6	19	0	0	0
92.8	24.8	5	1882	10	13	0	0	0
90	24	7	1885	7	14	0	0	55
89.2	25	4.9	1885	7	24	0	0	0
87.7	23.2	4.2	1886	5	19	0	0	0
88.4	22.6	4.2	1888	12	23	0	0	0
91	25.9	8.1	1897	6	12	0	11	6
92.8	24.8	6.3	1898	4	20	0	0	0
88.3	27	6	1899	9	25	0	0	0
87	27	5	1909	2	17	0	0	0

Longitude	Latitude	Magnitude	Year	Month	Date	Depth	Hrs	Mins
88	23	5	1911	12	7	0	0	0
91.5	29.5	7.1	1915	2	3	0	2	39
92	26	5	1915	11	14	0	0	0
91	24.5	7.6	1918	7	8	0	10	22
93.2	22.2	6	1920	8	15	0	6	59
91	25.3	7.1	1923	9	9	0	22	3
93.4	22.6	6	1923	8	10	0	15	58
93	25	6	1924	1	30	0	0	5
90	29.5	5.8	1924	8	13	35	23	57
94.5	24.5	5.5	1926	8	18	0	23	58
93	25	5.5	1926	10	23	0	14	30
95	24.5	6.5	1927	3	15	130	16	56
94.5	24.5	5.5	1927	5	20	0	10	51
90	22	5.5	1927	8	25	0	22	56
90.2	25.8	7.1	1930	7	2	0	21	3
90.8	25.8	5.5	1930	7	4	0	21	34
93.5	25	5.5	1930	7	11	0	7	6
93.8	25.3	6	1930	9	22	0	14	19
92	24.5	5.8	1932	3	27	35	8	44
90.2	25.8	5.5	1932	3	24	0	16	8
92.5	25.5	5	1932	3	6	0	0	18
95.7	25.8	7	1932	8	14	120	4	39
92	26.5	5.5	1932	11	9	0	18	30
90.5	25.7	5.8	1933	3	6	0	13	5
95.7	25.8	5.2	1933	12	4	0	14	40
95	24.5	6.5	1934	6	2	130	5	54
89.4	25.8	5.5	1934	7	21	0	0	0
89.5	24.4	6.2	1935	3	21	0	0	4
89.3	28.8	6.3	1935	5	21	140	4	22
94.7	25.1	6	1935	4	23	0	16	45
90.3	26.6	5.8	1936	6	18	0	14	56
90.5	25.7	5.3	1936	5	30	0	7	8

Longitude	Latitude	Magnitude	Year	Month	Date	Depth	Hrs	Mins
94	25.5	5.9	1937	3	21	0	16	12
92	27	5.7	1937	3	9	0	20	19
94.7	24.9	5.7	1937	9	9	0	23	37
90.5	28	5.7	1938	2	26	0	12	10
95	23.5	6.8	1938	4	14	130	1	16
95	24.5	6	1938	5	6	100	3	41
91	26	5.2	1938	4	13	0	1	10
94.7	24.9	5	1938	5	6	0	3	40
94.25	23.5	7.2	1938	8	16	35	4	27
94.1	24.3	6.5	1939	5	27	70	3	45
94	23.5	5.8	1939	6	19	35	21	56
92	27	5.7	1940	2	13	0	11	46
94.25	23.75	6.5	1940	5	11	80	21	0
90.5	28	5.2	1940	8	2	0	3	3
92	30	6.1	1940	10	4	35	4	35
92	27.2	6.8	1941	1	21	180	12	41
92.5	26.5	6.5	1941	1	27	180	2	30
93	27.5	5.8	1941	5	22	35	1	0
92	27	5.8	1941	9	6	0	3	17
90.3	24	5.9	1942	2	21	0	21	46
92	27	6	1943	2	8	0	21	5
93	26	7.2	1943	10	23	35	17	23
92.2	24.7	5.9	1944	12	24	0	14	46
90.9	25.1	6.1	1945	5	19	0	5	2
92.6	26.4	5.6	1946	3	16	0	14	15
92	30	5.7	1946	7	2	0	11	12
94.7	24.9	5.5	1947	3	8	0	14	33
94.8	23.8	6.2	1947	5	8	0	18	44
93.7	28.8	7.7	1947	7	29	0	13	43
94.8	23.8	6.2	1947	8	23	0	4	34
91.9	27.9	5.9	1947	11	29	0	17	56
94.8	23.8	6	1948	2	4	0	4	45

Longitude	Latitude	Magnitude	Year	Month	Date	Depth	Hrs	Mins
94	26.8	5.5	1948	3	1	0	16	50
94.1	22.3	6	1948	9	28	0	21	36
91.9	27.9	5.5	1948	10	7	0	1	18
94	26.8	6	1948	11	28	0	21	43
93	24	6	1949	7	15	0	11	0
89	26	6	1949	12	10	0	19	37
90.5	28	6	1950	2	26	0	3	35
95	26.8	7	1950	8	26	0	6	33
91.9	27.9	6.7	1950	8	16	0	17	51
94.2	28.7	6.3	1950	8	22	0	6	43
93	25	6	1950	8	15	0	21	42
93.7	28.8	6	1950	8	21	0	22	55
94.2	28.7	6.7	1950	9	30	0	7	28
92	29.3	5.5	1950	9	5	0	20	18
93	24	5.5	1950	9	25	0	12	25
94.7	24.9	6.7	1950	11	18	0	0	44
95	26.8	6.4	1950	11	12	0	21	30
94.2	28.7	6.6	1951	1	3	0	21	14
91.8	24	6.3	1950	12	29	0	22	35
94.2	28.7	6.5	1951	3	12	0	14	52
90.5	25.9	6.8	1951	4	7	0	20	29
94.2	28.7	6.5	1951	4	22	0	3	37
93.7	28.1	6.4	1951	4	14	0	23	40
94.1	22.3	6	1951	10	1	0	23	59
93.7	28.8	6	1951	10	18	0	5	2
92	30	5.5	1951	12	3	0	6	57
94.8	23.8	6	1952	1	15	0	2	31
90.8	29.6	5.5	1952	3	6	0	9	11
92	30	5.5	1952	3	14	0	18	19
94.5	25.5	6	1952	4	30	0	1	49
94.5	28.5	6	1952	5	26	0	2	46
94	28	6	1952	8	25	0	1	44

Longitude	Latitude	Magnitude	Year	Month	Date	Depth	Hrs	Mins
92	30	5.5	1952	9	15	0	17	59
94	25.5	6	1952	11	7	0	4	33
95.2	25	6	1952	11	28	0	5	34
95.1	24.2	7.3	1954	3	21	0	23	42
91.7	27.8	6.5	1954	2	23	0	6	40
90.2	29.9	6.3	1955	3	27	0	14	38
92.7	21.6	6.7	1955	12	14	0	10	51
94.2	23.4	6	1956	2	29	0	20	51
94.2	23.1	6	1956	3	3	0	10	13
93.95	22.6	6.3	1956	7	12	0	15	1
90.9	24.8	6	1956	6	12	0	3	12
94.79	23.88	6	1956	9	19	0	23	47
94.17	23.37	6	1956	12	30	0	21	59
94	23	5.2	1956	12	31	0	21	59
95	25.5	6	1957	5	28	0	0	0
93.76	24.38	7.2	1957	7	1	41	19	30
93	24.5	5.5	1957	12	12	0	0	0
92	27	5	1958	1	4	0	0	0
92.53	27.62	5.5	1958	2	13	0	0	11
90.86	24.93	5	1958	2	9	36	9	31
93.8	23.53	6.5	1958	3	22	51	10	11
91.5	28.5	5.7	1959	2	22	0	3	30
94.76	25.7	5.2	1959	4	9	0	17	8
91	30	5.7	1959	6	10	0	4	25
94	24	5.4	1959	6	7	0	8	33
95.5	25.5	5	1959	5	22	0	8	31
92.38	21.51	5.9	1959	11	2	30	13	15
93	28	5	1959	11	2	0	5	9
93	27	4.9	1960	5	26	160	20	5
90.3	26.9	6.8	1960	7	29	11	10	42
88.5	27	5.5	1960	8	21	29	3	29
94.32	23.65	5.5	1960	11	15	56	9	5

Longitude	Latitude	Magnitude	Year	Month	Date	Depth	Hrs	Mins
95.34	24.86	5.4	1961	2	4	141	8	51
94.8	24.7	5.7	1961	6	14	62	0	41
91.9	26.7	4.9	1961	11	6	67	7	59
90	27	5.5	1961	12	25	0	11	19
95.1	25.7	4.8	1962	4	17	165	11	51
95	26	4.5	1962	5	3	0	20	37
93.3	26.6	5.5	1962	10	30	33	16	13
94.5	24.25	4	1962	11	30	0	16	1
87.1	27.2	5.2	1963	2	22	0	1	32
90.5	24.9	6.4	1963	6	19	0	10	47
90.9	24.8	6.4	1963	6	21	0	0	0
92.09	25.13	4.8	1963	6	21	47	15	26
92	28	4	1963	7	5	0	7	19
94	23	5.6	1963	9	28	0	6	0
95.3	25.2	5.3	1963	10	14	33	2	1
93.58	22.33	6.1	1964	1	22	60	15	58
87.78	27.3	4.7	1964	2	1	33	11	28
95.41	25.64	4.4	1964	1	15	0	17	39
91.18	27.4	5.3	1964	2	18	22	3	48
95.71	25.82	5.3	1964	3	27	115	4	30
90.17	27.52	5.2	1964	4	13	1	3	19
94.39	23.47	4.9	1964	3	20	94	19	0
89.36	27.13	4.9	1964	3	27	29	23	3
95.69	25.88	5.4	1964	6	3	121	2	49
95.31	24.88	5.5	1964	7	12	152	20	15
94.67	23.51	5.4	1964	7	13	110	10	58
93.95	23	5.2	1964	6	13	60	17	35
92.26	27.12	5.5	1964	9	1	33	13	22
88.21	27.36	5	1964	8	30	21	2	35
94.18	24.32	4.7	1964	8	17	158	14	42
93.75	28.04	6	1964	10	21	37	23	9
88.6	27.9	5.1	1964	10	25	0	15	40

Longitude	Latitude	Magnitude	Year	Month	Date	Depth	Hrs	Mins
94.5	27.9	4.6	1964	10	6	413	2	55
92.2	29.84	4.8	1964	11	10	85	17	13
87.84	27.4	5.9	1965	1	12	23	13	32
94.21	24.97	5.4	1965	2	18	45	4	26
94.64	23.63	5.2	1965	2	25	94	10	34
92.33	26.82	4.8	1965	4	11	70	22	33
93.67	24.94	5.2	1965	6	18	48	8	17
95.33	24.68	4.7	1965	6	11	149	15	43
94.46	23.34	4.9	1965	12	5	97	22	1
91.7	27.1	4.7	1965	11	6	40	16	4
92.5	26.7	4.9	1965	12	9	8	20	26
90.04	25.91	4.8	1966	3	23	0	22	52
91.44	26.35	4.6	1966	2	24	47	0	16
92.8	22.1	5	1966	5	6	0	0	8
95.54	24.21	5	1966	5	23	0	7	48
92.84	26.14	4.7	1966	6	26	74	10	56
92.6	27.84	4.7	1966	7	5	33	10	1
93.5	24.6	4.1	1966	6	5	45	8	29
92.61	27.49	5.4	1966	9	26	20	5	10
95.6	26.9	4.8	1966	9	11	26	15	55
94.28	23.04	5	1966	10	22	72	3	3
94.81	24.41	4.8	1966	10	2	75	4	31
93.72	23.84	4.2	1966	10	27	38	17	32
89	28	5.2	1966	12	28	33	3	59
90.54	25.4	5.1	1967	1	30	55	7	9
94.19	23.55	4.8	1967	1	4	54	11	26
93.8	23.13	4.8	1967	2	8	51	17	17
94.72	23.94	4.7	1967	1	13	84	14	4
94.29	28.41	5.7	1967	3	14	20	6	58
92.52	27.38	4.6	1967	2	25	33	11	56
95	24.04	5	1967	4	15	0	0	19
94.95	24.76	4.5	1967	4	23	53	20	18

Longitude	Latitude	Magnitude	Year	Month	Date	Depth	Hrs	Mins
94.68	23.05	4.9	1967	6	17	122	13	14
94.8	23.5	4.8	1967	6	26	0	12	28
92.14	27.87	4.7	1967	7	7	33	22	56
91.86	27.42	5.9	1967	9	15	19	10	32
87	27	5.2	1967	9	13	33	19	37
91.9	24	4.8	1967	9	6	2	1	43
94.27	23.2	4.6	1967	8	27	66	11	11
91.61	24.05	4.8	1967	11	14	24	0	4
91.75	25.46	4.6	1967	11	10	44	6	4
94.89	23.38	4.5	1967	10	18	58	0	55
93.2	23.64	5	1968	1	18	75	19	57
92.2	29.8	5	1968	1	31	25	11	45
95.65	26.01	4.7	1968	1	23	96	3	22
95	24.51	4.6	1968	4	13	119	23	31
92.28	26.23	4.5	1968	5	2	51	0	26
91.94	24.83	5.3	1968	6	12	39	4	29
90.62	26.42	5	1968	8	18	22	14	18
94.23	25.28	4.5	1968	8	9	45	2	24
92.9	26.9	4.2	1968	11	18	51	8	49
92.4	22.98	5.2	1969	1	25	49	23	34
91.61	24.12	5	1968	12	27	27	14	38
94.14	27.46	5.3	1969	2	7	0	9	25
95.37	24.53	4.6	1969	2	18	164	21	3
92.36	26.54	4.5	1969	2	22	38	20	37
95.2	25.93	5.3	1969	4	28	68	12	50
92.71	26.93	5.3	1969	6	30	44	8	51
91.77	25.72	5.1	1969	6	1	33	8	35
94.7	23.09	6.2	1969	10	17	124	1	25
94.38	23.61	5	1969	10	29	70	22	24
95.37	24.8	4.7	1969	9	29	118	19	57
94.8	25.2	4.7	1969	9	30	50	23	13
91.8	26.6	5.3	1969	11	11	0	5	50

Longitude	Latitude	Magnitude	Year	Month	Date	Depth	Hrs	Mins
90.24	27.66	4.9	1969	11	5	13	20	25
93.64	24.43	4.7	1969	12	19	57	14	41
93.96	27.4	5.4	1970	2	19	12	7	10
93.99	24.91	4.7	1970	3	13	59	18	24
94.06	23.96	5	1970	5	29	49	10	33
95.37	26.02	6.7	1970	7	29	68	10	16
95.1	26.24	5.3	1970	7	29	52	10	31
88.58	25.72	5	1970	7	25	32	1	35
94.64	24.34	4.3	1970	7	7	95	4	13
91.55	24.78	4.8	1970	8	28	39	1	24
93.87	24.62	4.6	1970	8	13	42	7	0
91.66	23.71	5.4	1971	2	2	37	7	59
94.82	24.34	4.6	1971	5	17	163	8	43
94.78	24.6	4.9	1971	6	26	74	2	16
94.31	23.78	4.5	1971	6	16	18	20	6
93.15	26.41	5.4	1971	7	17	52	15	0
95.29	24.97	4.6	1971	10	10	133	19	2
90.65	26.18	4.6	1971	10	31	33	15	54
94.72	25.17	5.6	1971	12	29	46	22	27
87.95	27.92	5.2	1971	12	4	29	8	38
95.34	25.58	4.7	1972	4	17	110	10	35
93.55	25.79	4.3	1972	3	26	88	6	10
94.83	22.94	4.3	1972	4	1	155	21	34
92.44	29.59	4.5	1972	6	8	73	23	10
94.6	24.24	4.5	1972	7	11	61	20	46
88.01	27.33	4.4	1972	8	21	33	14	4
95.58	24.75	4.7	1972	11	11	172	1	47
88.43	26.88	4.3	1972	11	6	59	10	56
94.53	24.43	4.2	1973	2	10	67	4	25
95.39	26.1	4.4	1973	3	19	64	13	40
93.52	24.31	5.9	1973	5	31	1	23	39
94.91	24.61	4.1	1973	5	23	62	1	57

Longitude	Latitude	Magnitude	Year	Month	Date	Depth	Hrs	Mins
94.49	23.27	5.4	1973	7	27	60	20	23
94.86	23.6	4.9	1973	7	4	126	21	4
92.6	27.49	4.8	1973	7	4	30	16	44
89.17	29.59	4.8	1973	8	1	63	14	5
95.06	24.05	4.2	1973	7	12	115	21	31
92.61	27.08	4.7	1973	9	11	54	15	56
95.52	26.41	4.3	1973	8	15	61	9	0
93.55	27.69	4.8	1973	10	9	33	4	1
91.7	25.72	4.5	1973	11	2	21	12	9
92.45	25.21	4.2	1973	10	31	33	12	6
94.08	22.65	4.4	1973	12	4	63	12	48
92.9	22.8	4.8	1974	1	20	20	20	5
93.38	22.43	4.7	1973	12	26	31	1	42
94.72	23.43	4.6	1974	1	7	108	5	18
93.6	25.68	4.3	1974	1	28	42	14	17
94.07	23.88	4	1974	1	1	285	13	53
94.83	23.1	4.9	1974	3	5	0	3	12
91.91	25.66	4.4	1974	5	15	34	3	51
93.54	25.79	4.6	1974	6	22	50	18	10
95.08	24.56	4.4	1974	5	25	111	16	7
92.32	27.34	4.5	1974	7	9	53	7	17
94.78	23.09	4.3	1974	6	22	107	18	48
93.31	22.01	4.6	1974	7	23	35	3	6
91.04	25.63	4.6	1974	9	21	27	6	27
94.63	24.14	4.5	1974	9	21	109	17	53
94.62	22.97	4.4	1974	8	30	107	20	2
95.31	24.44	4.8	1974	12	2	107	1	8
93.69	23.88	4.6	1974	12	7	78	13	55
95.43	24.9	4.5	1974	11	16	128	22	7
94.55	25.13	4.8	1975	1	13	0	3	45
87.67	27.95	4.6	1975	2	6	63	6	39
94.04	22.79	4.4	1975	1	17	16	15	9

Longitude	Latitude	Magnitude	Year	Month	Date	Depth	Hrs	Mins
88.37	27.44	4.4	1975	1	23	33	1	37
93.5	24.11	4.7	1975	3	3	42	19	24
94.09	23.86	5.3	1975	5	21	51	3	16
87.5	27.74	4.7	1975	6	24	33	15	38
94.22	22.29	4.6	1975	9	17	69	3	0
94.34	22.92	4.8	1975	10	21	52	7	10
94.27	23.62	5.2	1975	12	13	62	22	35
87.8	28.15	4.9	1975	11	26	33	15	2
93.5	24.41	4.4	1976	2	1	59	15	38
92.09	26.55	4.6	1976	3	11	68	0	32
93.26	24.44	4.3	1976	3	16	59	4	55
94.38	24.31	4.3	1976	3	30	54	6	48
95.39	25.1	4.5	1976	5	25	130	4	48
94.64	22.76	4.4	1976	6	30	97	23	15
92.4	28.06	4.7	1976	8	5	55	10	24
89.57	29.81	5.4	1976	9	14	75	6	43
95.07	24.21	4.9	1976	9	24	138	0	9
94.54	24.26	4.6	1976	12	6	66	16	13
92.44	27.75	5	1976	12	17	33	10	21
94.61	23.1	4.8	1976	12	15	103	4	35
95.18	26.12	4.8	1976	12	25	54	1	7
95.15	25.49	4.6	1977	1	5	104	14	10
92.95	24.33	4.6	1977	2	6	0	16	53
92.96	21.68	5.4	1977	5	12	0	12	20
88.43	26.07	4.6	1977	6	5	0	19	21
93.11	26.58	5.1	1977	7	10	0	9	48
93.33	23.47	5.2	1977	10	13	0	11	32
93	26.51	5	1977	11	13	52	21	2
92.31	23.71	5	1977	12	23	33	21	0
94.7	23.02	5	1978	2	3	91	23	46
95.2	24.73	4.9	1978	1	8	97	6	32
94.7	23.08	5.3	1978	2	23	112.9	23	18

Longitude	Latitude	Magnitude	Year	Month	Date	Depth	Hrs	Mins
94.13	23.3	4.8	1978	2	22	83	9	7
94.76	23.92	4.7	1978	2	9	85	5	36
94.74	24.31	4.6	1978	2	11	87	14	45
94.62	24.91	4.9	1978	3	31	33	19	20
92.74	23.15	4.7	1978	3	28	33	12	37
93	24.38	4.4	1978	3	18	60	18	41
92.59	27.65	4.9	1978	4	19	0	18	58
94.54	24.46	4.4	1978	3	28	52	10	24
92.38	22.8	4.4	1978	4	7	48	23	32
94.64	23.68	4.4	1978	4	27	60	10	18
94.65	22.88	4.4	1978	6	10	113	11	18
94.63	22.89	4.5	1978	7	23	149	10	17
94.72	23.72	4.9	1978	9	22	101.8	4	54
87.33	27.66	4.7	1978	10	14	0	18	48
94.97	24.04	4.6	1978	10	6	0	23	5
93.69	24.37	4.5	1978	10	10	49	18	14
94.67	22.69	4.2	1978	9	18	110	19	29
92.1	26.24	4.8	1978	11	18	55	13	24
94.68	24.18	4.7	1978	10	20	98	17	21
93.73	22.68	4.7	1978	12	14	74.9	4	11
92.85	23.47	4.6	1978	12	29	33	8	53
94.17	24.81	4.4	1978	12	30	33	23	33
95.49	25.15	4.4	1979	1	14	33	16	57
91.89	27.39	4.3	1979	1	13	33	3	27
92.49	24.96	4.2	1979	1	9	64	2	39
91.02	24.87	4.8	1979	1	28	0	6	6
94.09	22.3	4.8	1979	3	25	0	3	48
94.52	24.48	4.5	1979	3	3	89	12	25
93.5	24.56	4.5	1979	3	4	33	17	40
91.23	25.98	4.2	1979	2	26	53	6	54
94.62	24.94	4.6	1979	4	10	0	17	29
88.84	25.98	4.6	1979	4	11	33	16	8

Longitude	Latitude	Magnitude	Year	Month	Date	Depth	Hrs	Mins
90.68	26.46	4.3	1979	4	2	33	1	16
94.82	24.61	4.2	1979	3	28	71	13	16
92.43	23.95	4.5	1979	5	12	27	6	10
94	24.19	4.1	1979	4	18	73	8	4
94.74	24.5	5.2	1979	5	29	82	0	39
87.48	26.74	5.2	1979	6	19	1	16	29
92.79	22.31	4.9	1979	5	19	60.7	18	23
95.16	25.28	4.1	1979	5	31	101	19	40
91.81	26.81	4.9	1979	7	29	67.8	14	15
95.11	25.73	4.9	1979	8	1	155	8	58
95.22	24.88	4.8	1979	7	13	108	23	20
94.93	24.2	4.9	1979	8	11	113	20	32
95.15	25.95	4.4	1979	8	21	137	5	56
87.62	27.97	4.5	1979	10	17	33	1	44
94.35	23.04	4.5	1979	10	19	91	15	13
94.9	24.41	4.8	1979	12	3	0	7	24
88.69	27.95	4.5	1979	11	16	39	19	17
93.94	22.1	4.3	1979	11	7	80	6	42
95.04	24.65	4.2	1979	12	17	131.9	7	21
95.17	24.69	4.2	1980	1	27	166	3	25
94.61	23.37	4.2	1980	2	23	85	17	28
94.69	23.87	4.7	1980	3	28	97	16	15
94.41	28.63	4.4	1980	3	26	48	22	24
94.19	23.72	4.7	1980	5	20	83	13	19
94.12	22.27	4.1	1980	5	6	167	22	23
90.31	25.79	4.8	1980	6	11	68	5	25
93.71	22.51	4.4	1980	7	17	77	10	7
94.95	26.65	4.9	1980	8	18	56.6	14	17
94.62	24.81	4.8	1980	8	12	52	16	44
95.33	24.89	4.2	1980	9	14	109	16	3
88.8	27.4	6.1	1980	11	19	1	19	0
93.92	22.74	5.2	1980	11	20	30	18	14

Longitude	Latitude	Magnitude	Year	Month	Date	Depth	Hrs	Mins
91.46	23.9	4.5	1980	10	30	29	5	29
90.94	22.06	5	1980	12	1	0	20	33
89.59	26.67	4.3	1980	12	22	33	4	36
88.88	29.08	4.4	1980	12	26	66	5	19
89.76	27.2	4.8	1981	2	9	16	15	49
93.66	26.03	4.7	1981	2	28	40	1	58
94.88	24.66	4.7	1981	3	7	80.9	22	16
90.48	26.29	5.1	1981	3	19	0	13	52
95.34	24.9	5.7	1981	4	25	146	11	32
89.07	22.35	4.8	1981	3	26	0	2	47
94.56	22.94	4.7	1981	5	1	97	4	8
95.04	24.63	4.4	1981	4	11	136	1	24
93.87	22.47	4.3	1981	5	6	76	15	32
93.15	23.7	4.2	1981	5	6	33	19	8
87.14	27.16	4.4	1981	6	21	0	9	51
93.68	23.72	4.2	1981	6	17	66	11	12
94.65	24.79	4.6	1981	7	18	81	9	0
94.68	22.95	4.5	1981	7	30	112	21	12
94.26	22.59	4.2	1981	7	15	101	11	52
94.43	22.89	4.7	1981	8	23	89	9	29
94.91	24.68	4.4	1981	8	23	90	1	24
95.47	26.6	4.9	1981	9	27	0	1	3
94.44	23.67	4.5	1981	10	9	117	5	23
95.54	25.15	4.1	1981	10	6	164	10	40
93.23	22.7	4.7	1981	11	21	44	1	52
89.12	29.52	4.7	1981	11	21	50	4	25
90.76	21.71	4.5	1981	11	20	0	11	14
95.13	25.65	4.4	1981	11	15	69	23	45
94.35	24.69	4.5	1982	1	3	84	11	37
92.51	27.5	4.4	1981	12	9	33	10	52
92.06	24.7	4.8	1982	1	11	40	20	53
95.08	25.02	4.3	1981	12	11	121	11	22

Longitude	Latitude	Magnitude	Year	Month	Date	Depth	Hrs	Mins
90.62	25.79	4.5	1982	2	26	48	0	5
92.29	26.3	4.5	1982	2	26	33	8	14
90.89	25.47	4.3	1982	1	28	33	7	18
94.82	24.07	4.1	1982	2	26	140	16	52
88.84	27.38	4.9	1982	4	5	9	2	19
92.92	28.31	4.7	1982	4	24	52	2	4
94.47	24.35	4.4	1982	4	6	102	5	44
94.65	22.78	4.4	1982	5	13	143.1	12	38
94.99	25.34	4.4	1982	5	17	94	23	17
93.96	24.1	4.4	1982	5	22	76	9	2
89.97	26.24	4.4	1982	6	20	33	15	29
94.72	24.65	4.3	1982	6	1	79	2	49
90.31	25.88	4.9	1982	7	6	8	6	13
94.45	23.06	4	1982	6	25	102	4	42
91.46	25.38	4.9	1982	8	31	32	10	42
95.31	25.93	4.9	1982	9	14	88	6	1
89.26	27.04	4.5	1982	8	18	51	18	1
91.27	25.15	4.8	1982	9	21	43	12	38
92.23	25.16	4.5	1982	8	21	50	4	26
94.4	23.42	4.5	1982	10	7	102	1	52
94.87	27.78	5	1982	11	26	28	13	26
91.75	26.38	4.7	1982	11	18	0	6	2
94.69	24.83	5.1	1982	12	12	0	1	18
94.48	24.52	4.7	1982	12	11	65	20	55
95.03	24.67	5.4	1983	1	13	109	23	0
94.45	24.23	5	1983	1	3	84	11	28
91.69	26.01	4.8	1982	12	30	61	8	37
94.07	23.92	4.5	1983	1	1	0	1	52
95.15	24.95	4.3	1982	12	17	116	5	45
91.36	25.46	4.7	1983	1	19	10	12	9
92.87	26.9	5.2	1983	2	2	42	20	44
95.04	24.72	4.9	1983	1	31	70	3	26

Longitude	Latitude	Magnitude	Year	Month	Date	Depth	Hrs	Mins
94.55	23.94	4.4	1983	2	5	140.1	1	31
94.24	24.01	4.3	1983	1	29	90	17	52
93.89	22.83	4.6	1983	3	5	49	16	41
93.41	25.61	5	1983	4	13	0	20	14
94.48	22.85	4.5	1983	4	13	119	21	7
93.69	21.86	4.3	1983	4	1	67	4	24
94.76	22.89	4.5	1983	5	7	99	10	24
92.24	25.09	4.2	1983	5	1	0	0	19
93.87	23.06	4.9	1983	6	26	80	2	31
95.62	26.03	4.6	1983	6	16	98	10	50
95.12	24.55	5.2	1983	8	23	128	12	12
94.43	22.73	4.7	1983	8	21	123	8	31
91.25	25.37	4.6	1983	7	23	58	7	28
94.67	25.04	5.7	1983	8	30	60	10	39
95.12	24.77	4.8	1983	9	23	115	20	18
94.79	23.05	4.7	1983	9	18	61	17	27
94.07	23.73	4.3	1983	9	7	92	22	24
92.52	28.05	4.9	1983	10	2	38	21	3
94.42	24.89	4.7	1983	10	21	71	23	32
90.31	29.51	4.4	1983	10	16	33	22	3
91.73	25.15	4.3	1983	11	17	41	21	20
87.91	25.87	4.2	1983	12	23	33	19	35
94.26	22.69	4.1	1983	12	5	0	6	16
94.71	22.72	4.6	1984	2	5	93	10	3
94.21	24.19	4.6	1984	2	12	81.6	3	5
94.62	24.52	5.2	1984	3	5	67	21	26
94.79	24.99	4.9	1984	2	19	50	9	29
93.29	26.75	4.9	1984	3	21	15	23	6
93.53	24.22	5.7	1984	5	6	31	15	19
91.51	23.66	5.2	1984	5	21	12	9	59
95.7	26.03	4.9	1984	4	25	108	14	58
94.57	24.87	4.3	1984	5	7	88	9	17

Longitude	Latitude	Magnitude	Year	Month	Date	Depth	Hrs	Mins
92.61	26.91	4.4	1984	6	9	72	23	7
94.96	24.72	4.3	1984	5	16	118	18	29
94.82	24.81	4.7	1984	7	5	79	22	46
92.74	25.8	4.5	1984	7	4	33	13	29
94.33	24.81	4.4	1984	7	7	73	22	39
94.35	22.94	4	1984	6	22	131	6	42
94.32	23.47	4.7	1984	8	5	80	1	7
92.15	26.49	5.2	1984	9	22	28	9	10
91.51	25.44	4.9	1984	9	30	34	21	35
94.34	23.04	4.8	1984	9	28	55	18	21
93.58	24.65	4.7	1984	9	16	36	1	26
93.44	25.37	4.5	1984	10	3	59	21	46
94.69	28.09	4.3	1984	9	28	55	18	21
92.72	26.72	4.5	1984	11	15	83	21	9
94.5	24.03	4.4	1984	10	18	117	19	47
94.84	24.33	4.7	1984	12	8	107	23	47
95.02	24.61	4.6	1984	11	28	114	19	35
94.18	24.04	4.1	1984	11	13	76	1	41
92.85	24.66	5.5	1984	12	30	3	23	33
91.96	27.14	5.4	1985	1	7	12	16	13
94.38	24.7	4.7	1985	1	21	94	12	57
94.52	23.32	4.6	1985	1	25	107	20	58
95.24	25.54	4.7	1985	2	17	85	0	24
94.54	25.42	4.5	1985	2	3	62	2	40
94.46	24.31	4.7	1985	4	2	97	19	48
94.6	23.7	4.2	1985	3	4	99	23	46
94.08	27.72	4.2	1985	3	5	52	10	10
91.8	28.33	4.8	1985	4	6	33	12	8
88.48	27.6	4.5	1985	5	25	33	0	28
90.21	26.87	4.7	1985	6	7	33	18	23
90.2	25.65	4.5	1985	6	17	22	21	52
95.65	25.31	4.2	1985	8	22	83.7	17	4

Longitude	Latitude	Magnitude	Year	Month	Date	Depth	Hrs	Mins
92.52	27.1	5.3	1985	10	12	14	18	22
95.18	24.79	4.9	1985	10	12	108.3	5	50
89.73	27.19	4.3	1985	10	2	45	16	33
91.52	23.61	5	1985	11	3	9	3	57
93.96	22.65	4.4	1985	11	8	47	1	0
94.7	25.1	4.3	1985	11	26	33	17	19
88.32	26.93	5.3	1986	1	7	69	20	20
92.07	27.09	4.7	1985	12	26	11	18	4
93.24	24.1	4.6	1985	12	22	52	21	35
92.63	22.4	4.6	1986	1	2	28	9	32
93.96	23.38	4.5	1986	1	8	82	19	4
94.3	22.75	4.6	1986	1	17	62	5	31
93	23.87	5.2	1986	2	8	30	0	28
91.13	25.1	5.2	1986	2	19	7	17	34
87.86	28.15	4.6	1986	2	10	87	12	56
93.88	22.06	4.1	1986	2	8	76	22	0
94.7	24.43	4.5	1986	3	13	0	9	45
94.74	24.43	5.3	1986	4	17	85.8	13	15
94.51	22.85	5.2	1986	4	26	102.4	0	25
95.36	25.05	4.5	1986	4	20	112	0	3
94.19	23.71	5.2	1986	7	26	38	20	24
95.54	26.75	4.7	1986	7	23	68.2	5	18
91.6	27.6	4.4	1986	7	16	33	6	37
92.14	25.38	5.3	1986	9	10	47	7	50
94.11	22.6	4.9	1986	8	16	89.1	22	44
94.02	23.41	4.2	1986	9	30	72	0	1
91.97	25.03	4.5	1986	10	14	33	14	3
94.8	25.3	4.3	1986	11	22	65	13	7
92.21	27.17	4.2	1986	11	8	48	18	24
92.91	26.47	5	1986	12	31	46	15	49
92.69	27.63	4.9	1987	1	24	24	10	34
94.75	23.68	4.6	1987	2	7	107	4	39

Longitude	Latitude	Magnitude	Year	Month	Date	Depth	Hrs	Mins
94.08	23.1	4.6	1987	2	13	47	19	20
94.83	24.25	4.6	1987	2	15	109	19	26
93.7	22.6	5	1987	4	29	48	0	15
94.64	24.07	4.9	1987	4	29	107	5	15
95.18	24.87	4.6	1987	4	3	140	5	48
94.21	25.23	5.7	1987	5	18	53	1	53
94.39	23.6	4.6	1987	6	10	33	3	15
94.58	22.7	4.4	1987	5	30	111	15	21
93.59	26.15	4.3	1987	6	11	62	17	29
95.19	24.95	4.7	1987	7	19	123	22	49
92.68	27.76	4.6	1987	7	17	9	21	12
92.3	23.6	4.2	1987	7	16	33	2	19
93.41	26.64	5.2	1987	9	6	58	23	38
94.41	23.05	5	1987	8	24	86	9	24
93.81	23.84	4.7	1987	9	5	76	8	41
94.3	23.5	4.6	1987	8	6	110	17	48
95.27	24.78	5	1987	9	9	122.2	12	45
90.37	29.84	5	1987	9	25	19	23	16
94.9	23.7	4.6	1987	9	28	100	13	1
90.42	29.9	4.6	1987	10	6	10	22	18
92.8	27.3	4.3	1987	9	13	33	21	4
92.76	27.38	4.8	1987	10	15	27	16	22
89.06	27.07	4.1	1987	10	22	19	21	23
93.22	26.33	4.8	1987	12	1	59	8	50
90.01	29.63	4.6	1987	11	1	0	14	37
90.4	29.8	4.7	1987	12	12	45	5	49
90.92	26.04	4.5	1987	12	11	57	6	39
91.56	24.67	5.9	1988	2	6	33	14	50
90.29	29.75	4.6	1988	1	10	50	6	18
91.43	24.52	4.9	1988	2	17	39	1	2
94.4	24.3	4.8	1988	2	17	111	17	52
92.11	27.11	4.7	1988	2	17	2	6	30

Longitude	Latitude	Magnitude	Year	Month	Date	Depth	Hrs	Mins
92.99	26.73	4.4	1988	2	17	46	1	1
93.9	25.1	4.3	1988	2	12	33	5	51
88.8	27.8	4.2	1988	1	19	33	11	23
93.7	23.4	4.2	1988	1	20	92	7	10
94.08	23.33	4.7	1988	2	24	72	14	7
91.56	24.72	4.5	1988	2	28	22	5	55
95.41	25.97	4.2	1988	3	6	106	4	43
93.88	24.9	4.2	1988	4	18	60	5	18
88.42	27.1	4	1988	3	27	70	5	56
91.6	25.9	4.1	1988	4	30	33	3	27
92.47	28.27	4	1988	4	6	33	11	28
88.61	27.45	4.6	1988	5	26	42	16	30
90.88	25.32	4.3	1988	5	10	33	7	16
93.21	22.53	4.3	1988	5	12	57.5	2	45
95.38	25.03	4.8	1988	7	10	125	3	31
91.24	28.11	4.7	1988	7	5	66	7	36
94.8	24.7	4.4	1988	6	28	139	20	52
95.15	25.13	7	1988	8	6	100	0	36
94.57	24.47	4.9	1988	8	8	139	11	55
93.9	22.5	4.3	1988	7	11	33	5	53
95.29	25.7	4.2	1988	8	7	33	13	4
95.13	25.29	4.9	1988	8	13	91	19	59
94.52	25.28	4.3	1988	8	12	0	0	8
94.5	23.5	4.1	1988	7	19	128	6	55
95.1	25.27	4.8	1988	8	21	92	13	16
88.37	27.19	4.9	1988	9	27	28	19	10
87.5	26.39	4.4	1988	8	29	33	12	12
91.75	26.3	4.3	1988	9	4	7	8	1
92.89	22.44	4.9	1988	10	22	33	4	23
94.72	24.68	4.4	1988	10	9	46	22	5
95.7	24.9	4.2	1988	10	12	33	18	54
93.36	23.15	5.5	1988	11	27	33	7	12

Longitude	Latitude	Magnitude	Year	Month	Date	Depth	Hrs	Mins
94.74	23.25	5	1988	12	27	123	18	15
91.12	27.66	4.8	1988	12	20	39	9	45
94.56	24.09	4.7	1988	11	30	83	3	9
95.02	25.12	4.5	1988	12	4	100	19	43
87.86	27.98	4.5	1988	12	27	38	2	56
93.92	22.42	4.5	1988	12	30	65	10	49
92.46	24.1	4.7	1989	1	10	33	19	21
87.97	27.14	4.3	1988	12	13	52	6	29
94.26	24.72	4.3	1989	1	22	72.6	19	41
93.34	24.74	4.2	1988	12	29	79	17	21
94.95	25.32	4.1	1989	1	27	93	16	14
92.64	27.1	4.6	1989	2	28	42	0	26
92.77	26.93	5	1989	3	8	59	20	2
89.2	23.5	4	1989	2	14	33	15	52
94.66	25.15	5.3	1989	4	3	58	19	39
90.02	29.11	5	1989	4	9	10	2	31
92.43	24.4	4.9	1989	4	13	10	7	25
95.1	25	4.2	1989	4	6	103	5	47
92	22.66	4	1989	3	13	31	13	6
94.63	23.43	4.6	1989	5	18	112	2	56
94.84	24.38	4.5	1989	4	24	119	18	11
87.86	27.38	4.9	1989	5	22	4	19	24
92.51	22.89	4.3	1989	5	9	0	16	17
91.58	25.6	4.2	1989	4	29	33	12	55
89.78	21.83	5.7	1989	6	12	6	0	4
94.37	23.79	4.8	1989	6	28	66	12	8
90.7	26.39	4.4	1989	6	11	50	13	42
94.3	22.5	4.3	1989	5	31	110	17	24
94.37	23.53	4.3	1989	7	10	72	14	46
95.2	24.8	4.2	1989	6	12	33	22	30
94.54	22.79	5.4	1989	7	15	96	0	9
94.55	24.51	5	1989	8	9	80	16	1

Longitude	Latitude	Magnitude	Year	Month	Date	Depth	Hrs	Mins
92.55	27.55	4.9	1989	7	25	0	0	31
94.03	24.46	4.9	1989	7	30	33	13	17
94.03	24	4.3	1989	7	30	109.4	18	32
92.7	26.9	4.3	1989	8	3	33	11	10
94.5	23.7	4	1989	7	15	33	22	33
92.65	26.88	4.5	1989	9	19	25	17	7
94.37	22.69	4.3	1989	9	25	112.7	2	9
95.52	24.34	4.3	1989	10	12	33	14	37
94.58	22.88	4.7	1989	12	9	114	11	32
95.3	25.3	4.4	1989	12	4	146	11	3
89.7	29	4.3	1989	11	19	33	22	11
95.26	24.74	6.2	1990	1	9	121	18	51
88.11	28.15	5.7	1990	1	9	35	2	29
94.63	24.46	5.3	1990	1	10	87	6	37
94.27	24.13	4.1	1989	12	29	99	21	26
90.02	29.14	4.8	1990	2	22	54	13	33
94.2	25.3	4.7	1990	2	26	51	1	31
93.13	24.9	4.6	1990	2	22	52	22	7
92.41	24.85	4.2	1990	2	5	33	2	6
88.4	28.7	4.1	1990	3	1	33	18	47
94.3	23.7	4.1	1990	3	15	151	15	19
94.01	23.02	4	1990	2	26	93	6	20
93.32	26.44	5.5	1990	4	30	33	1	55
94.35	23.85	4.5	1990	4	8	82	15	15
95.23	26.5	4.5	1990	4	30	150	1	56
90.23	29.76	4.3	1990	5	22	33	9	0
94	24.98	4.4	1990	6	14	58	15	28
92.62	22.78	4.2	1990	5	14	26	4	28
94.5	23.64	4.2	1990	6	4	85	21	40
95.52	26.5	4.1	1990	5	24	94	9	3
94.44	23.64	4.2	1990	7	13	114	3	24
94.1	23	4.1	1990	6	24	89	2	35

Longitude	Latitude	Magnitude	Year	Month	Date	Depth	Hrs	Mins
93.8	23.6	4.1	1990	6	30	155	2	28
92.74	27.18	4.8	1990	8	29	25	2	41
92.67	26.58	5.2	1990	9	2	57	6	29
95.23	24.9	4.5	1990	8	2	159	2	31
94.65	22.67	4.5	1990	8	2	132	19	8
95.4	24	4.1	1990	9	10	75	14	48
92.44	26.47	4.7	1990	10	29	37	11	32
94.3	23.2	4	1990	10	3	77	10	7
93	23.81	4.8	1990	11	15	26	3	28
94.64	24.37	4.8	1990	11	29	82	10	20
94.84	25.4	4.3	1990	11	10	102	9	53
92.59	26.68	4.8	1990	12	29	27	19	24
95.2	24.32	4.6	1991	1	3	33	7	5
93.8	22.97	4.5	1990	12	28	49	8	11
94.42	23.36	4.3	1990	12	10	79.1	11	56
92.3	27.8	4.2	1990	12	11	33	18	38
95.22	24.72	5.4	1991	1	23	118	6	7
91.17	25.51	4.9	1991	2	2	25	0	15
95.39	26.08	4.5	1991	1	28	0	22	24
93.29	23.81	4.4	1991	1	31	33	12	9
95.26	25.04	4.3	1991	2	6	142.3	19	38
92.5	24.4	4.2	1991	1	23	33	14	3
91.67	25.5	4	1991	2	3	19	13	22
94.7	25.8	4.9	1991	3	11	33	10	24
95.06	24.73	4.7	1991	3	7	133.1	20	58
92.96	26.4	4.4	1991	4	9	50	22	59
93.68	24.26	4.9	1991	5	11	44	2	15
91.35	24.44	4.4	1991	4	13	33	4	58
93.81	23.92	4	1991	4	15	33	16	3
93.19	26.59	5.4	1991	6	23	46	10	4
94.36	24.65	5	1991	5	28	142	20	4
94.48	23.26	4.4	1991	6	25	104	6	8

Longitude	Latitude	Magnitude	Year	Month	Date	Depth	Hrs	Mins
95.2	25.3	4.2	1991	5	25	84	17	7
95.21	25.14	4.7	1991	7	19	110	7	5
95.16	24.59	4.4	1991	7	29	128	0	40
88.66	25.27	4.6	1991	8	7	10	11	36
91.18	25.29	4.6	1991	8	22	45	3	53
93.89	24.15	4.6	1991	9	7	64	3	0
90.47	24.5	4.4	1991	9	2	78	17	20
90.27	25.59	5.1	1991	9	26	0	5	4
92.14	26.23	4.9	1991	9	19	0	4	23
90.41	30	4.2	1991	9	27	0	11	56
94.6	22.83	4	1991	8	28	182.4	11	18
94.4	22.7	4.6	1991	9	30	75	18	35
93.18	24.68	4.6	1991	11	17	60	5	17
94.3	22.7	4.5	1991	11	9	107	11	28
94.74	23.5	4.3	1991	11	17	91	3	39
93.83	24	5	1991	12	7	52	13	57
93.8	22.9	4.7	1991	12	7	79	11	19
92.86	26.14	4.2	1991	11	11	33	13	42
93.12	24.69	5.3	1991	12	20	39	2	6
87.96	27.79	4.6	1991	12	21	65	19	52
94.58	23.74	4.3	1991	12	14	94	7	4
93.52	23.55	4.2	1991	12	4	0	4	30
92.6	24.4	4.4	1992	1	13	33	18	36
92.63	24.95	4.3	1992	1	10	0	2	46
92.2	25.2	4.9	1992	2	25	33	1	57
90.9	23.48	4.2	1992	2	1	0	4	52
93.6	22.7	4.1	1992	1	30	73	17	54
95.2	24.9	5.3	1992	3	25	106	22	32
88	28.1	4.8	1992	4	4	33	17	43
94	22.9	4.6	1992	3	24	129	2	2
94.7	23.2	4.5	1992	3	8	83	11	25
95.52	26.09	4.5	1992	3	12	0	19	11

Longitude	Latitude	Magnitude	Year	Month	Date	Depth	Hrs	Mins
92.09	27.04	4.4	1992	3	25	95.9	22	59
89.4	29.4	4.2	1992	3	7	113	22	41
94.9	24.3	5.6	1992	4	15	116	1	32
94.03	23.46	4.9	1992	4	26	108.1	0	53
90.52	25.32	4.7	1992	4	15	0	17	28
95.2	26.7	4.5	1992	4	20	47	7	29
92.1	27.3	4.5	1992	4	20	33	18	50
87.1	27.4	4.2	1992	4	1	33	13	41
90.6	25.8	4.1	1992	4	20	55	19	22
94.1	22.6	4.5	1992	5	27	33	2	47
94.7	22.9	4.5	1992	5	28	90	14	8
92	23.2	4.4	1992	5	28	33	9	53
89.3	26.91	4.3	1992	5	11	0	14	43
93.9	23.6	4.2	1992	5	9	60	12	59
91.1	23.9	4.1	1992	5	3	33	21	11
94	23.1	4.5	1992	6	8	117	2	39
94.1	28.5	4.4	1992	6	8	10	0	25
93.59	24.22	4.3	1992	6	4	81.5	19	44
93.22	22.7	4.9	1992	7	9	0	2	9
93	21.6	4.3	1992	6	13	33	22	44
93.44	23.61	4.8	1992	7	14	0	17	26
94.81	24.47	4.2	1992	7	2	144.4	22	10
92.77	27.05	4.1	1992	6	14	0	11	12
94.9	23	4.1	1992	6	15	71	3	57
93.5	22.6	4	1992	6	14	68	14	19
90.2	29.6	6	1992	7	30	14	8	24
90.2	29.3	4.7	1992	7	24	33	6	24
90.4	30	4.4	1992	7	30	33	17	28
91.9	25.4	4.2	1992	8	8	50	12	7
92.4	21.5	4	1992	7	19	33	13	48
93.1	23.4	4.7	1992	9	21	33	12	17
95	24.5	4.4	1992	9	6	122	23	7

Longitude	Latitude	Magnitude	Year	Month	Date	Depth	Hrs	Mins
93.5	22.6	4.2	1992	8	21	33	21	57
94.6	24.21	4.8	1992	10	5	0	23	1
94.22	23.59	4.5	1992	10	24	124	15	19
94.7	25.08	4.5	1992	10	25	0	16	16
94.3	24.4	4.3	1992	10	4	60	21	18
92.9	27.6	4.4	1992	11	11	68	5	27
93.2	27.6	4.3	1992	10	31	33	1	56
94.5	22.7	4.3	1992	11	11	88	23	9
91.39	25.48	4.9	1992	12	12	0	14	20
95.52	26.03	4.3	1992	12	18	121.4	23	52
94.73	24.53	4.2	1992	12	22	102.6	0	19
94.8	23.2	4.2	1993	1	1	96	23	49
92.16	27.58	4.2	1993	1	4	0	5	54
89.74	21.92	4.1	1992	12	10	12	0	23
92.6	23.4	4	1992	12	16	33	14	38
87.5	25.9	4.9	1993	2	15	30	14	29
92.35	23.51	4.7	1993	2	12	0	12	44
95.7	25.8	4.4	1993	1	23	109	9	39
94.4	22.7	4.3	1993	2	17	125	2	28
94.43	23.03	4.1	1993	2	4	138.6	3	23
92.8	26.3	4.1	1993	2	17	28	23	27
93.7	24.1	4	1993	1	27	65	0	39
94.5	23.2	5.3	1993	4	1	105	16	30
92.98	22.81	4.9	1993	3	1	0	4	10
94.14	23.93	4.9	1993	3	18	77.4	23	0
95.1	24.7	4.9	1993	3	27	115	9	42
90.75	28.9	4.7	1993	3	5	0	7	28
93.6	24.36	4.6	1993	3	22	122.3	22	1
90.2	25.4	4.4	1993	3	3	33	5	17
94.1	23.9	4.5	1993	4	11	75	5	34
94.2	22.4	4.6	1993	4	13	9	15	59
90.1	29.84	4.4	1993	3	22	0	14	56

Longitude	Latitude	Magnitude	Year	Month	Date	Depth	Hrs	Mins
95.35	24.73	4.3	1993	4	4	157.1	19	44
93.54	26.56	4.2	1993	4	9	0	20	29
94.7	24.6	4.2	1993	4	14	125	6	18
93.6	23.56	4.1	1993	4	4	0	0	21
93.58	23.17	4.1	1993	4	11	0	23	55
94.27	22.27	4.8	1993	5	11	96.7	12	5
93.5	21.8	4.6	1993	5	27	48	17	50
91.69	22.9	4	1993	4	27	0	23	14
92.45	27.3	4.9	1993	6	18	0	22	46
95.12	25.45	4.7	1993	6	19	0	10	30
93.3	26.8	4.5	1993	5	28	33	14	20
93.56	23.83	4.8	1993	7	8	73.6	5	9
93.8	23.1	4.6	1993	7	14	69	4	49
92.6	27.5	4.5	1993	6	23	33	17	19
94.58	23.43	4.5	1993	6	24	110.6	21	59
91.87	27.34	4.7	1993	7	31	71	19	29
93.5	22.8	4.7	1993	8	2	75	14	41
94.08	23.37	4.7	1993	8	6	104.1	6	49
94.2	23.5	4.6	1993	9	6	85	20	14
87.3	27.2	4.4	1993	9	5	33	6	5
95.18	24.87	4.3	1993	9	6	133.9	14	28
95.6	26	4.2	1993	8	17	106	22	56
95.32	25.45	4.9	1993	10	17	0	18	20
92.9	27.8	4.6	1993	9	20	33	7	40
94.41	23.67	4.3	1993	10	10	108.5	5	24
95.04	24.94	4.2	1993	9	19	130.3	21	0
92.04	27.29	5	1993	12	12	29.9	23	34
95	25.2	4.4	1993	12	2	96	22	4
94.12	23.3	4.4	1993	12	15	133.4	1	2
93.1	24.5	4.3	1993	11	26	0	18	4
92.25	23.67	4.2	1993	12	5	0	4	42
94.7	24.3	4	1993	11	17	113	19	26

Longitude	Latitude	Magnitude	Year	Month	Date	Depth	Hrs	Mins
94.36	24.41	4.9	1993	12	22	132	4	9
93.87	22.48	4.6	1993	12	20	85.9	18	36
91.97	28.18	4.6	1994	1	6	39.1	21	12
93.5	25.2	4.6	1994	1	20	33	23	30
87.67	27.34	4.5	1993	12	30	27.8	10	18
94.7	24.6	4.4	1994	1	29	45	18	28
93.91	24.94	4.2	1994	2	8	93	16	31
89.12	26.4	4	1994	1	16	33	14	22
94.94	24.69	4.9	1994	3	5	108.1	20	44
94.8	24.6	5	1994	4	9	90	11	19
93.1	22.2	4.5	1994	3	11	34	6	23
95.5	25	4.9	1994	4	14	183	17	32
93.21	24.3	4.9	1994	4	24	0	8	44
92.9	26.3	4.3	1994	4	18	33	14	40
94.3	23.75	4.3	1994	4	21	242.9	3	41
91.3	26.4	4.2	1994	3	24	33	13	51
94.5	24.8	4.9	1994	5	5	76	10	43
95.6	25.9	4.7	1994	5	5	104	6	4
93.15	24.19	4.3	1994	5	1	0	13	3
93.6	26.4	4.2	1994	5	6	33	17	52
90.5	25.9	4.1	1994	4	15	33	14	28
92.96	23.04	4.7	1994	6	1	0	2	15
92.19	24.34	4.7	1994	6	9	53.1	22	53
94.5	24.6	4.6	1994	5	28	99	7	12
87.8	26.6	4.5	1994	5	25	48	7	38
94.7	24.9	4.4	1994	6	2	113	13	26
95.3	25.62	4.3	1994	5	19	107.6	3	46
94.67	28.34	4.4	1994	6	25	33	4	18
92.21	29.18	4.4	1994	6	26	0	6	6
95.14	24.79	4.8	1994	6	28	172.9	3	11
92.7	25	4.6	1994	7	24	33	23	39
95.2	24.7	6.1	1994	8	8	127	21	8

Longitude	Latitude	Magnitude	Year	Month	Date	Depth	Hrs	Mins
92.5	26.7	4.6	1994	8	5	33	11	19
94.7	24.8	4.6	1994	9	3	92	15	46
91.66	26.58	4.6	1994	9	6	0	15	17
88.55	23.34	4.9	1994	9	28	33	16	46
91.9	30.1	4.7	1994	10	11	33	5	32
90.73	25.63	4.6	1994	9	28	33.1	4	4
93.68	23.37	4.5	1994	9	15	43	15	43
92.96	26.68	4.4	1994	9	21	0	3	39
92.03	22.36	4.1	1994	9	17	0	8	41
93.07	22.27	4.9	1994	10	21	0	4	48
94.6	24.2	4.8	1994	10	18	87	17	0
92.4	27.2	4.8	1994	10	25	33	7	29
95.4	24.9	4.6	1994	11	2	137	9	51
87.71	27.94	4.9	1995	1	1	58.4	19	56
93.7	24	4.5	1995	1	17	33	11	18
92.5	27.42	4.4	1995	1	20	40.3	21	12
94.32	24.02	4.4	1995	1	27	64.3	19	27
95.3	25.3	4.4	1995	2	8	33	16	31
92.3	27.6	5.2	1995	2	17	33	2	44
94.51	24.11	4.6	1995	3	11	113.5	12	23
92.5	28.1	4.6	1995	3	26	33	18	22
94.22	22.49	4.3	1995	3	20	107.4	3	12
94.71	24.52	4.8	1995	4	9	71.7	10	16
95.41	24.9	4.7	1995	4	28	132	8	3
94.3	24.7	4.3	1995	3	29	33	2	46
91.3	26.3	4.1	1995	4	3	33	1	59
95.3	25	6.7	1995	5	6	33	1	59
95.3	25.3	5.2	1995	5	9	33	9	54
94.97	25.4	5	1995	5	4	169.5	13	26
90.81	26.11	4.9	1995	5	9	0	11	30
94.52	22.78	4.7	1995	5	13	115.6	6	35
94.5	23.9	4.4	1995	6	7	33	17	27

Longitude	Latitude	Magnitude	Year	Month	Date	Depth	Hrs	Mins
95.42	24.17	4.3	1995	5	10	100	0	51
88	23.8	4	1995	5	14	33	19	10
94.2	23.2	4.8	1995	6	17	33	21	9
92.26	23.08	4.8	1995	7	20	27.1	20	6
91.91	28.38	4.7	1995	6	28	0	20	4
93.72	23.08	4.7	1995	7	5	84.2	9	33
92.3	27.5	4.6	1995	7	3	33	0	59
94.58	24.25	4.6	1995	7	11	164.7	19	28
94.7	23.7	4.4	1995	6	26	33	7	21
93.57	23.21	4.8	1995	7	29	61.1	20	1
94.4	28.81	4.3	1995	7	10	112.2	16	48
94.6	23.1	4.3	1995	7	30	33	2	1
90.4	26.4	4.3	1995	8	8	33	16	52
95.3	24.8	4.2	1995	7	19	33	18	10
95.04	25.29	4.7	1995	8	30	58.4	6	19
95.26	24.99	4.3	1995	8	21	113.4	17	52
92.6	26.9	4.2	1995	7	30	33	12	54
93.93	27.83	4.6	1995	9	4	0	1	44
94.7	24.5	4.2	1995	8	13	33	22	15
88.1	26.82	4.5	1995	9	20	83.8	9	32
92.62	27.54	4.8	1995	9	29	0	9	47
93.94	28.44	4.8	1995	10	23	0	22	57
95	24	4.6	1995	10	19	33	22	42
93.08	23.87	4.6	1995	11	18	0	3	41
95.1	24.5	4.1	1995	10	22	33	19	1
92.85	27.34	4.5	1995	11	30	0	12	36
91.54	24.76	4.5	1995	12	6	47.4	0	50
91.94	24.25	4.4	1995	12	1	0	2	28
91.6	26.2	4.4	1995	12	1	33	20	9
93.08	22.61	4.4	1995	12	6	104	0	14
94.47	24.5	4.3	1995	12	1	69.4	23	27
89.25	25.47	5	1996	1	3	33	16	4

Longitude	Latitude	Magnitude	Year	Month	Date	Depth	Hrs	Mins
92.22	27.6	4.2	1995	12	27	0	14	32
94.06	22.76	4.9	1996	1	28	0	13	49
94.7	23.41	4.9	1996	2	8	119.2	21	38
94.26	22.49	4.6	1996	1	10	39.7	12	19
93.22	23.81	4.4	1996	2	8	75.8	15	54
95.2	24.8	4.1	1996	1	9	33	19	45
92.06	28.76	4.8	1996	2	16	0	3	2
87.94	28.16	4.6	1996	2	12	84	9	32
90.6	26.08	4.6	1996	2	17	44.6	6	59
95.2	24.2	4.1	1996	2	11	33	11	56
93.63	24.41	4.7	1996	2	23	0	11	36
92.66	23.56	4.7	1996	3	4	0	8	30
94.07	22.69	4.7	1996	3	20	129	18	40
93.09	24.94	4.5	1996	3	20	21.1	18	12
93.2	23.65	4.3	1996	3	6	50.1	23	51
94.38	23.18	4.3	1996	3	9	0	1	40
91.98	29.16	4.3	1996	3	21	0	14	24
94.73	24.53	4.1	1996	3	6	88	5	24
87.6	27.8	5.2	1996	4	26	33	16	31
92.02	30.04	4.7	1996	4	22	16.6	4	43
92.65	24.84	4.3	1996	4	8	0	18	11
94.76	25.12	4.4	1996	4	28	87.7	8	17
92.27	26.44	5.3	1996	5	14	57.6	19	5
94.62	22.72	4.6	1996	5	11	119.9	7	57
92.77	26.79	4.6	1996	5	21	33	19	51
94.2	24.35	4.2	1996	5	7	79.6	22	28
92.2	28.3	5	1996	6	9	0	23	15
94.03	28.19	4.2	1996	5	31	0	17	35
93.95	23.48	4.2	1996	5	31	68	18	38
91.09	23.44	4.2	1996	6	12	0	17	14
93.35	21.62	4.5	1996	6	15	43.2	8	24
94.6	22.8	4.2	1996	6	18	0	17	32

Longitude	Latitude	Magnitude	Year	Month	Date	Depth	Hrs	Mins
91.99	29.2	4	1996	5	21	0	0	35
95.39	24.9	4.7	1996	6	28	124.7	9	25
92.2	27.18	4.6	1996	6	27	0	16	0
94.7	24.1	4.5	1996	6	30	0	23	42
94.17	23.12	4.2	1996	6	27	0	11	58
93.8	27.9	4	1996	6	3	0	4	17
92.28	26.32	4.7	1996	7	17	41	5	23
94.1	23.6	4.6	1996	7	28	0	7	8
92.1	27	4.4	1996	7	12	0	12	38
95.4	25.9	4.4	1996	7	28	0	14	26
90.99	23.82	4.3	1996	7	26	33	12	47
93.16	26.43	4.7	1996	8	4	43.4	13	51
92.5	21.8	4	1996	7	5	0	14	1
95.27	24.89	4.4	1996	8	6	0	3	4
95.17	25.25	4.4	1996	8	6	90.2	6	21
94.87	24.41	4.3	1996	8	16	104.5	23	39
90.1	25.8	4.3	1996	8	18	0	2	48
92.6	27.6	4.6	1996	9	14	33	2	9
92.5	27	4.5	1996	9	12	33	18	4
94.48	22.51	4.4	1996	9	3	122.9	12	49
95.05	25.09	4.4	1996	9	7	80.3	15	18
88.2	27	4.4	1996	9	13	33	3	41
94.9	24.1	4.3	1996	8	20	120	8	30
88.6	23.3	4.5	1996	9	24	36	3	28
88.5	27.4	4.9	1996	9	25	33	17	41
94.7	23.54	4.4	1996	9	30	126.8	2	56
93.79	24.21	4.3	1996	9	1	73.7	21	28
93.68	23.21	4.3	1996	9	6	67.1	23	43
92.23	22.07	4.2	1996	8	30	0	5	6
94.55	26.69	4.5	1996	10	1	0	8	43
94.65	24.98	4.4	1996	10	13	0	14	36
94.25	28.1	4.3	1996	10	25	115.6	17	22

Longitude	Latitude	Magnitude	Year	Month	Date	Depth	Hrs	Mins
91.76	25.38	4.3	1996	10	25	61	18	31
92.93	29.31	4.1	1996	9	25	0	19	29
94.1	23.2	4.1	1996	9	30	33	16	4
94.58	23.04	4.9	1996	10	31	102.8	4	47
95.2	24.3	4.8	1996	11	17	137	22	48
92.6	24.6	4.7	1996	11	19	0	0	12
94.18	23.58	4.5	1996	11	13	43.2	11	15
92.4	21.8	4.4	1996	11	12	0	0	32
93.25	26.46	4.4	1996	11	19	40.1	10	37
92.57	26.72	4.4	1996	11	24	33	0	52
91.8	28.93	4.3	1996	11	11	0	20	23
94.9	25.3	4.6	1996	12	10	0	12	8
92.73	22.26	4.2	1996	11	10	0	14	55
94	23.5	4.4	1996	12	15	71	20	58
92.47	23.94	4.3	1996	12	18	118.4	7	24
94.46	24.68	4.2	1996	11	18	89.6	13	4
94.1	22.8	4.2	1996	12	17	33	23	40
87.74	27.65	4.1	1996	11	18	0	9	7
92.5	26.8	4.4	1996	12	23	33	9	39
91.25	26.53	5	1997	1	12	16	8	19
92.5	26.7	4.4	1996	12	24	33	0	52
90.31	25.59	4.4	1997	1	22	0	11	12
90.2	26.34	4.3	1996	12	30	0	15	57
94.62	24.14	4.2	1997	2	9	116.5	23	41
93.6	23	4.1	1997	1	10	100	21	22
94.4	23.86	4.2	1997	2	15	102	14	21
91.78	24.67	4.2	1997	2	17	40.1	16	48
94.4	24.9	4	1997	1	30	100	15	55
92.41	27.21	4.4	1997	3	10	33	17	55
92.71	27.38	4.3	1997	3	10	33	17	50
94.15	24.17	4	1997	2	15	64.3	4	19
94.6	22.7	4.8	1997	4	15	120	0	13

Longitude	Latitude	Magnitude	Year	Month	Date	Depth	Hrs	Mins
94.39	23.39	4.3	1997	3	17	93.7	11	1
94.9	23.4	4.5	1997	4	21	120	14	22
92.59	27.13	4.3	1997	4	4	63.7	18	5
92.16	24.79	4.3	1997	4	20	48.4	12	27
90.38	23.09	4.1	1997	4	4	0	10	8
92.25	24.8	5.6	1997	5	8	35	2	53
92.53	27.54	4.3	1997	5	4	23.9	7	31
93.6	25.15	4.3	1997	5	6	51.7	2	57
93.45	25.83	4.3	1997	5	12	0	14	41
93.9	25.1	4.3	1997	5	19	33	15	32
95.24	24.33	4.1	1997	4	29	152.3	12	34
89.91	23.98	4.9	1997	6	15	35	1	5
92.63	28.05	4.7	1997	6	2	33	19	30
91.81	27.5	4.5	1997	6	15	11	22	56
94.08	24.19	4.4	1997	6	6	94.9	3	8
92.32	25.06	4.3	1997	6	24	66.9	14	9
89.93	25.72	4.2	1997	6	24	0	13	0
95.55	24.6	4.6	1997	7	17	0	11	8
91.8	26.83	4.6	1997	7	18	0	19	39
95.38	25	4.4	1997	7	1	123.6	11	55
95.72	26.07	4.4	1997	7	24	92	23	19
92.76	26.69	4.3	1997	6	27	33.5	16	37
94.45	23.23	4.3	1997	7	15	84.6	18	45
93.08	27.66	4.3	1997	7	18	0	21	34
93.16	23.88	4.7	1997	7	31	33	15	59
92.02	24.4	4.5	1997	8	14	0	5	5
91.44	28.23	4.4	1997	8	4	33	22	31
92.77	23.06	4.4	1997	8	13	0	4	22
92.93	26.02	4.3	1997	8	6	58	8	58
93.59	22.02	4.3	1997	8	8	68	10	27
93.05	26.93	4.2	1997	8	5	0	7	5
94.72	24.38	4.2	1997	8	5	100	23	48

Longitude	Latitude	Magnitude	Year	Month	Date	Depth	Hrs	Mins
89.52	29.17	4.2	1997	8	10	0	11	53
93.04	24.31	4.1	1997	7	15	0	2	57
87.53	28.14	4.3	1997	8	17	0	20	3
95.04	24.85	4.2	1997	8	18	102	6	37
93.82	24.09	4.1	1997	7	28	0	12	35
94.95	23.89	4.1	1997	8	23	204.8	20	31
94.51	24.47	4.4	1997	9	4	114.4	2	2
93.12	23.41	4.3	1997	8	27	0	4	7
90.98	23.2	4	1997	8	5	33	15	59
88.1	28.84	4.7	1997	9	18	70.7	7	37
94.91	25.23	4.5	1997	9	28	129	14	32
90.66	26.35	4.4	1997	9	13	0	21	21
93.95	22.88	4.4	1997	9	27	93.4	10	43
93.3	24.96	4.4	1997	10	8	52	3	2
89.7	29.5	5.3	1997	10	30	33	2	2
89.4	29.2	4.8	1997	10	30	0	20	3
93.5	23.9	4.7	1997	10	26	70	0	55
95.06	25.09	4.3	1997	10	25	0	9	19
94.38	23.87	4.2	1997	10	2	118.8	20	43
92.7	22.2	6	1997	11	21	54	11	23
87.34	27.6	5	1997	11	27	33	16	11
94.18	27.09	4.5	1997	11	4	0	11	5
95.45	25.61	4.5	1997	11	27	0	15	30
93.87	23.1	4.4	1997	11	20	60	20	55
89.43	24.22	4.3	1997	11	10	0	6	31
92.22	26.49	4.3	1997	11	27	0	12	56
87.17	27.48	4.9	1997	12	8	33	2	3
87.76	27.7	4.1	1997	11	27	33	16	55
94.45	24.71	4.1	1997	11	27	0	23	2
95.16	25.1	4.1	1997	12	2	100	11	6
92.36	23.04	4	1997	11	10	0	9	12
93.2	22.7	4.8	1998	1	2	33	21	12

Longitude	Latitude	Magnitude	Year	Month	Date	Depth	Hrs	Mins
94.77	23.53	4.7	1997	12	29	120.1	9	8
91.8	26	4.4	1998	1	6	33	3	9
93.48	28.56	4.4	1998	1	13	68.7	20	48
91.3	25.51	4.3	1997	12	27	41.5	12	5
95.06	25.05	4.3	1998	1	10	106.5	2	28
93.55	21.91	4.1	1997	12	19	81.7	17	12
93.77	22.54	4	1997	12	17	95.6	19	35
94.1	23	4.6	1998	2	18	45	9	2
88.1	26.5	4.5	1998	2	12	33	2	40
94.35	23.29	4.4	1998	1	27	0	4	2
94.43	24.31	4.3	1998	2	6	84.4	20	15
91.4	24.14	4.3	1998	2	20	0	10	14
87.5	27	4.3	1998	2	28	33	4	59
90.04	26.14	4.2	1998	2	15	0	5	43
94.5	23.5	4.2	1998	3	1	100	15	12
94.7	23.2	4	1998	2	5	100	6	36
94.4	24.5	4.6	1998	3	6	67	12	50
95	25.2	4.4	1998	3	11	98	15	34
94.98	24.91	4.3	1998	4	10	122.7	4	59
90.16	27.28	4.1	1998	3	16	0	10	35
95.31	24.93	5	1998	5	2	122	8	36
95.75	25.03	4.8	1998	4	18	20	19	46
90.36	28.6	4.5	1998	5	13	27.9	1	24
94.67	24.93	4.3	1998	4	23	39.2	21	37
90.68	29.14	4.3	1998	5	13	0	1	59
93.3	28.9	4.1	1998	4	25	33	22	50
90.51	28.71	4.3	1998	6	6	0	14	19
92.4	23.33	4.3	1998	6	9	27.2	7	9
94.71	22.98	4.5	1998	6	30	117	8	0
94.22	23.92	4.3	1998	6	30	79.7	13	8
93.74	27.69	4	1998	6	2	87.1	12	15
91.02	27.32	5.2	1998	7	8	33	3	44

Longitude	Latitude	Magnitude	Year	Month	Date	Depth	Hrs	Mins
94.49	22.85	4.5	1998	7	17	100	21	13
94.3	25.84	4.3	1998	7	3	0	17	21
93.8	23.8	4	1998	6	19	100	3	54
93.55	24.22	4.7	1998	7	27	58	19	3
90.98	27.55	5.2	1998	8	18	22	4	10
93.94	26.06	4.5	1998	8	19	151.6	7	21
95.57	25.65	4.3	1998	8	11	0	21	40
94.32	23.24	4.3	1998	8	16	105.2	19	46
94.58	23.6	4.2	1998	8	4	33	5	50
93.27	22.09	4	1998	7	30	67.3	20	54
87.73	28.01	4	1998	7	31	33	17	50
92.81	27.77	5.4	1998	9	26	33	18	27
88.34	27.2	4.6	1998	9	10	33	22	57
94.43	23.39	4.6	1998	9	24	109.3	2	20
94.68	23.74	5.2	1998	10	16	101	0	5
94.4	24.39	4.6	1998	10	21	86.7	3	26
93.42	25.31	4.3	1998	10	6	0	12	42
90.75	25.62	4.3	1998	10	16	46.1	22	22
95.33	24.66	4.3	1998	10	17	124.4	17	1
95.15	23.78	4.1	1998	10	25	134.4	8	40
93.32	24.18	4.1	1998	10	26	161.4	23	20
94.91	24.69	4	1998	9	27	140.4	16	58
94.15	23.9	4.3	1998	10	30	105.1	2	50
95.05	25.42	4.2	1998	11	17	127.8	15	31
87.89	27.75	5	1998	11	26	73	10	14
93.49	26.34	4.9	1998	12	2	33	13	25
92.29	26.6	4.8	1998	12	4	40.4	4	42
95.15	24.72	4.4	1998	12	11	147.5	9	49
94.25	22.75	4.3	1998	12	19	103.9	23	53
95.15	25.02	4.2	1998	12	2	136	1	4
92.76	22.31	4.2	1998	12	21	33	15	4
94.63	26.37	4	1998	11	24	60	16	22

Longitude	Latitude	Magnitude	Year	Month	Date	Depth	Hrs	Mins
92.63	26.43	4.7	1999	1	20	57.2	7	58
94.55	23.92	4.3	1998	12	31	101.2	3	5
93.86	23.02	4.2	1999	1	7	59	10	15
93.66	22.45	4.2	1999	1	12	0	5	40
93.19	22.95	4	1999	1	5	33	21	17
92.85	22.16	4.8	1999	2	8	9.3	9	2
93.69	23.35	4.8	1999	2	22	21	11	37
94.59	25.34	4.5	1999	2	19	99.3	9	45
92.04	22.59	4.4	1999	2	8	18	9	3
93.67	26.45	4.3	1999	2	21	40.8	21	4
93.94	23.81	4	1999	1	28	108.5	17	57
93.31	22.03	4.4	1999	3	4	71.5	7	12
94.06	25.93	4.4	1999	3	11	0	22	12
93.4	23.38	4.3	1999	3	6	69.5	17	20
95.37	25.71	4	1999	2	16	91	1	57
94.26	23.14	4.8	1999	3	29	0	12	41
93.51	25	4.8	1999	4	5	33	22	32
89.04	24.79	4.6	1999	4	14	0	23	21
93.81	24.73	4.4	1999	4	14	33	6	9
93.33	25.8	4.4	1999	4	15	110	6	48
93.99	25.24	4.4	1999	4	30	58.3	3	39
95.51	24.93	4.2	1999	5	9	165.1	8	8
87.85	28.04	4.1	1999	4	10	33	20	42
94.93	25.47	4.6	1999	6	9	58	15	21
92.85	26.56	4.4	1999	5	11	0	16	39
94.47	23.37	4.4	1999	5	25	113.8	8	9
94.78	24.31	4.2	1999	5	15	0	20	17
92.61	26.95	4.1	1999	5	17	0	13	56
91.95	26.81	4.6	1999	6	26	48.5	21	36
93.66	24.13	4.3	1999	6	26	85.7	17	57
93.43	25.77	4.6	1999	7	28	72	17	55
92.02	21.53	4.2	1999	7	22	10	10	42

Longitude	Latitude	Magnitude	Year	Month	Date	Depth	Hrs	Mins
93.78	23.14	4	1999	7	5	122	21	44
89.15	22.88	4.4	1999	8	28	79.7	20	2
91.93	26.26	5.3	1999	10	5	33	17	4
94.12	24.3	4.7	1999	10	1	0	6	9
88.79	24.98	4.5	1999	9	21	0	13	54
87.53	28.07	4.4	1999	9	5	33	2	28
94.48	22.75	4.7	1999	10	8	115.4	12	18
94.76	23.67	4.5	1999	10	6	134.3	10	23
94.68	23.4	4.3	1999	9	9	136	0	25
88.3	28.51	4.2	1999	9	8	0	18	8
95.24	24.8	4.7	1999	10	19	145	17	34
91.78	26.18	4.3	1999	10	9	70.1	1	39
90.06	29.61	4.3	1999	10	15	33	7	33
93.72	21.89	4.3	1999	10	17	13.1	0	45
87.98	27.24	4	1999	9	20	23	7	28
92.02	26.07	4.5	1999	10	23	62.7	16	32
93.53	21.85	4.5	1999	11	24	58	3	53
94.02	22.64	4.3	1999	10	24	85.4	20	48
91.55	28.59	4.3	1999	11	13	44.6	19	44
94.77	24.11	4.7	1999	12	22	116.1	0	28
94.61	23.16	4.4	1999	12	24	102	14	40
92.51	28	5.3	2000	1	2	33	10	23
88.36	27.68	4.7	2000	1	25	32.2	12	7
92.49	27.57	4.7	2000	1	26	33	21	11
92.05	27.47	4.7	2000	1	26	33	21	12
94.56	24.68	4.5	1999	12	26	99.5	2	44
91.76	29	5	2000	1	30	33	6	35
91.77	21.45	4.5	1999	12	31	29.9	0	53
92.74	22.2	4.5	2000	1	3	8	22	34
93.8	22.3	4.7	2000	2	14	38.2	17	43
92.06	23.65	4.3	2000	1	23	75	0	33
92.69	27.36	4.3	2000	1	28	0	0	16

Longitude	Latitude	Magnitude	Year	Month	Date	Depth	Hrs	Mins
94.18	22.87	4.2	2000	2	27	48	17	21
91.86	26.71	4.6	2000	3	17	70.1	15	44
94.92	25.24	4.3	2000	3	18	93.8	16	38
94.31	24.03	4.3	2000	3	28	99	16	40
94.82	24.32	4.3	2000	4	8	90.3	2	8
93.69	22.26	4.1	2000	3	28	70.7	18	59
94.57	24.63	4.1	2000	3	30	66	15	12
87.85	27.43	4	2000	3	13	108	20	44
91.42	28.03	5.2	2000	5	14	15	17	18
94.41	25.38	4.7	2000	5	11	58	16	51
94.51	23.85	4.4	2000	5	3	0	15	42
92.44	24.67	4.3	2000	4	16	33	11	40
89.76	25.94	4.3	2000	4	18	46.4	7	53
93.16	26.3	4.3	2000	4	21	0	6	35
94.42	22.47	4.3	2000	4	27	34.6	12	28
95.15	26.41	4.1	2000	4	22	78	15	41
95.14	24.73	4.9	2000	6	1	130	23	48
89.6	25.79	4.4	2000	6	20	0	7	16
93.63	24.73	4.3	2000	6	28	90.7	8	16
94.25	23.42	4.1	2000	5	31	194	2	40
94.64	24.51	5	2000	7	2	60	4	27
90.67	24.11	4.7	2000	7	4	100.2	22	21
92.71	26.52	4.5	2000	8	16	33	23	6
94.72	23.95	4.3	2000	7	17	0	16	5
93.61	21.98	4.3	2000	8	2	33	17	58
94.74	24.68	4.3	2000	8	13	75.4	14	59
95.16	26.48	4.2	2000	7	20	90	5	54
94.31	22.28	4.2	2000	7	31	95.8	3	15
92.94	21.95	4.1	2000	7	20	0	11	2
94.16	23.98	4.4	2000	8	29	54.2	14	51
94.43	22.63	4.4	2000	9	9	92.9	19	40
94.18	22.29	4.2	2000	9	1	76.8	3	48

Longitude	Latitude	Magnitude	Year	Month	Date	Depth	Hrs	Mins
94.34	24.26	4.2	2000	9	28	40	16	29
92.45	28.31	4.1	2000	9	10	33	23	32
94.4	23.95	5	2000	10	11	130	9	42
91.8	26.22	4	2000	9	17	13	19	46
94.45	23.41	4.6	2000	10	27	119.3	10	8
92.69	22.43	4.6	2000	11	9	33	8	37
90.67	25.86	4.5	2000	11	3	0	0	33
91.41	25.31	4.5	2000	11	9	48.4	17	31
94.41	24.42	4.4	2000	11	15	77	6	18
94.48	23.68	4.7	2000	12	5	33	9	53
95.58	26.34	4.3	2000	11	24	82.6	1	22
94.45	26.76	4.2	2000	11	18	0	18	55
93.83	23.75	4.1	2000	12	6	0	1	48
92.51	21.84	4	2000	11	13	33	8	56
94.6	23.42	4.3	2000	12	14	75	9	0
94.15	22.79	4.3	2000	12	15	102.2	19	44
90.02	25.73	4.3	2001	1	16	0	8	6
95.12	26.52	4.2	2000	12	30	51.7	14	33
93.4	28.62	4.1	2000	12	17	261	20	31
93.7	23.3	4.6	2001	1	20	35.7	12	49
95.16	25.48	4.4	2001	1	30	0	11	30
94.28	23.91	4.4	2001	2	4	95	13	3
92.18	25.23	4.4	2001	2	11	96	1	20
93.5	24.57	4.4	2001	2	20	0	5	21
94.71	23.9	4.3	2001	1	22	135.7	13	33
94.35	23.01	4.3	2001	1	28	85.8	11	55
92.71	27.64	4.2	2001	1	24	10	23	57
90.55	26.48	4.6	2001	2	27	20	1	46
93.76	23.99	4.6	2001	3	3	96	22	56
89.53	27.05	4.1	2001	2	9	81.5	10	20
91.87	27.81	4.6	2001	3	10	33	0	20
92.09	26.38	4.4	2001	4	6	55	3	32

Longitude	Latitude	Magnitude	Year	Month	Date	Depth	Hrs	Mins
94.73	23.98	4.3	2001	3	12	115.7	17	10
94.15	22.77	4.3	2001	4	2	139.5	9	58
88.12	27.6	4.3	2001	4	8	0	18	35
94.93	24.73	4.2	2001	4	5	133.3	11	3
94.42	23.31	4.1	2001	3	8	0	2	48
94.97	25.08	5	2001	4	10	96	22	8
94.76	24.72	4.9	2001	4	26	35.8	21	1
90.67	26.13	4.5	2001	4	20	33	18	35
93.53	23.41	4.4	2001	4	29	68	21	52
89.17	22.59	4.3	2001	4	16	15	0	31
91.58	24.08	4.3	2001	4	18	13.4	20	47
90.55	27.65	4.3	2001	5	3	59.8	16	3
93.95	23.58	4.3	2001	5	7	83.4	1	6
93.91	21.98	4.2	2001	4	12	84.2	13	27
94.69	23.56	4.5	2001	5	13	124.5	15	55
93	27.89	4.4	2001	5	13	9.5	17	32
91.4	25.88	4.1	2001	4	27	33	12	28
92.07	22.78	4	2001	4	14	33	5	59
93.92	23	4.5	2001	5	16	33	16	17
94.11	23.5	4.5	2001	5	30	49.9	9	34
94.43	23.07	4.5	2001	6	17	120.9	18	43
92.94	26.46	4.4	2001	5	18	33	19	26
91.97	23.41	4.3	2001	5	21	51.7	23	37
94.72	25.78	4.3	2001	5	26	90	14	51
89.97	29.66	4.3	2001	6	7	0	2	37
94.45	23.53	4.3	2001	6	13	104.9	12	9
93.72	23.32	4.2	2001	6	1	65.5	10	40
91.44	26.16	4.2	2001	6	7	33	5	36
95.26	23.71	4.2	2001	6	13	33	7	55
91.87	26.5	4.2	2001	6	20	33	14	44
90.39	24.1	4	2001	5	26	0	1	22
93.58	23.27	4.8	2001	6	29	41.8	12	13

Longitude	Latitude	Magnitude	Year	Month	Date	Depth	Hrs	Mins
93.38	23.89	4.6	2001	6	29	86	12	14
95.44	24.84	4.5	2001	6	30	161	0	21
89.21	26.97	4.2	2001	7	3	32.2	19	16
93.82	22.56	4.5	2001	8	1	156.9	8	37
93.76	23.24	4.4	2001	7	17	0	2	44
95.3	26.7	4.4	2001	7	23	0	7	32
94.43	24.19	4.3	2001	7	9	142.6	9	8
94.64	24.62	4.9	2001	8	12	141	1	58
93.9	23.53	4.3	2001	7	28	83.3	6	59
92.79	23	4.3	2001	7	29	0	8	29
87.69	28.05	4.3	2001	8	6	0	6	23
92.03	24.58	4.3	2001	8	8	0	10	0
90.87	25.35	4.4	2001	9	4	51.6	22	8
94.29	25.81	4.3	2001	8	26	136.1	18	5
92.26	27.37	4.3	2001	8	29	33	19	26
93.25	26.52	4.3	2001	9	11	0	2	8
93.99	23.97	4.2	2001	9	1	128.5	2	43
90.92	22.49	4.2	2001	9	16	0	15	56
94.98	24.39	4.1	2001	8	21	117	16	41
94.67	24.29	4.5	2001	9	23	50.6	14	47
91.97	23.37	4.3	2001	9	26	25.1	1	46
94.37	24.36	4	2001	9	3	104.5	14	45
93.36	23.58	4.8	2001	10	7	43	13	56
92.7	21.36	4.7	2001	10	19	60	7	4
94.47	22.75	4.4	2001	10	25	116	17	5
92.04	26.07	4.2	2001	10	6	41.9	19	27
93.11	26.07	4.1	2001	10	26	33	8	22
87.76	26.99	4	2001	9	27	2	22	40
92.24	27.54	4.7	2001	11	6	135	14	9
88.33	27.18	4.7	2001	12	2	15	22	41
94.76	25.3	4.8	2001	12	24	100	5	49
93.54	22.41	4.5	2001	12	25	61	17	53

Longitude	Latitude	Magnitude	Year	Month	Date	Depth	Hrs	Mins
95.27	26.4	4.2	2001	11	27	0	11	15
94.09	23.29	4.3	2002	1	3	78.5	23	55
94.5	24.24	4.3	2002	1	7	149	14	16
91.92	27.43	4.3	2002	1	12	66.8	10	1
90.36	23.74	4.1	2001	12	19	5	7	54
93.33	23.08	4.6	2002	1	27	0	6	27
92.85	22.73	4.3	2002	1	27	46.9	13	41
94.7	24.25	4.3	2002	2	4	113	17	25
92.27	21.54	4.1	2002	1	29	144.9	21	56
90.49	24.67	4	2002	1	9	0	6	54
94.25	22.87	4.5	2002	3	17	107.5	14	40
92.15	25.21	4.3	2002	3	12	59.1	7	33
87.43	27.2	4.3	2002	3	15	10	20	6
90.52	25.88	4.4	2002	3	24	37.3	3	48
92.5	26.76	4.4	2002	3	27	33	16	49
93.14	29.75	4.3	2002	3	30	51.5	23	22
94.61	24.2	4.3	2002	3	31	90.5	6	11
94.19	23.29	4.3	2002	4	11	117.4	3	28
91.91	25.09	4.3	2002	4	12	27.4	15	48
94.24	22.38	4	2002	3	15	108.9	16	47
91.85	22.59	4.9	2002	5	5	33	4	54
94.73	24.24	4.2	2002	4	17	23	20	17
88.12	27.21	4.2	2002	5	3	0	4	1
95.03	25.42	4.3	2002	5	17	0	22	12
93.7	23.78	4	2002	4	22	0	7	20
94.84	25.31	4.2	2002	5	25	111.4	16	43
88.96	26.03	4.9	2002	6	20	15	5	40
91.28	25.32	4.4	2002	6	20	22.7	14	46
89.52	29.75	4.4	2002	6	20	41.8	16	46
93.54	23.95	4.5	2002	7	14	33	2	17
92.31	26.63	4.4	2002	7	10	0	14	32
87.47	27.77	4.4	2002	7	16	33	18	39

Longitude	Latitude	Magnitude	Year	Month	Date	Depth	Hrs	Mins
92.13	25.15	4.4	2002	7	20	33	7	37
93.19	26.8	4.3	2002	7	5	99.6	8	39
90.8	25.81	4.3	2002	7	11	0	19	16
94.39	23.92	4.3	2002	7	14	33	1	15
92.09	24.75	4.3	2002	7	23	45.1	20	21
94.44	22.74	4.2	2002	7	4	33	1	3
88.03	28.09	4.1	2002	7	18	98.3	23	24
94.3	24.68	4.1	2002	7	22	76.7	12	26
93.5	23.38	4.1	2002	7	29	0	12	35
94.22	22.42	4.1	2002	7	30	112.5	10	35
92.97	27.21	4.4	2002	8	20	33	8	46
93.22	22.17	4.3	2002	8	3	51.9	16	28
94.95	24.25	4.3	2002	8	23	0	2	44
94.91	24.8	4.3	2002	8	29	125.3	6	29
93.16	26.8	4	2002	8	7	0	15	23
94.22	22.54	4	2002	8	17	86.9	19	38
94.21	24.67	4	2002	8	20	78.2	18	26
93.86	23.16	5	2002	9	27	0	15	20
92.57	23.64	4.7	2002	9	27	33	15	21
92.09	24.68	4.7	2002	10	14	33	13	27
95.27	24.85	4.3	2002	10	5	158.7	12	14
90.18	26.5	4.3	2002	10	24	33	23	25
93.58	23.06	4.3	2002	11	3	0	15	30
94.46	24.9	4.2	2002	10	5	33	5	18
90.83	30.01	5.2	2002	11	16	10	8	52
92.47	26.28	5.1	2002	11	16	26.3	22	39
90.45	29.79	4.5	2002	11	16	10.6	9	40
94.76	24.46	4.4	2002	11	13	128.2	18	32
92.38	27.64	4.4	2002	11	14	33	2	59
93.94	23.54	4.2	2002	10	22	33	9	44
94.16	24.59	4.4	2002	11	21	66.8	19	33
88.08	27.43	4	2002	10	23	0	18	4

Longitude	Latitude	Magnitude	Year	Month	Date	Depth	Hrs	Mins
90.39	29.68	4.8	2002	11	29	10	16	49
87.64	27.97	4	2002	10	29	33	17	26
93.87	24.19	4	2002	10	29	0	21	35
95.07	24.62	4.6	2002	12	28	122.9	10	57
90.26	29.72	4.4	2002	11	30	60.5	7	11
90.01	29.37	4.4	2002	12	4	0	15	59
94.07	22.76	4.4	2002	12	29	115.1	10	8
93.66	23.52	4.3	2002	12	12	69.2	10	55
93.62	22	4.3	2002	12	12	38.5	18	4
94.85	25	4.3	2002	12	19	127.1	22	41
93.98	23.23	4.3	2002	12	25	75.9	12	14
90.66	29.88	4.2	2002	12	21	0	22	26
94.68	24.41	4.4	2003	1	15	138.5	10	41
93.43	24.48	4.4	2003	2	8	0	11	26
94.41	24.12	4.3	2003	1	20	77	20	37
90.58	25.65	4.3	2003	2	12	0	7	8
90.41	29.58	4.2	2003	1	31	10	6	4
94.64	25.01	4	2003	1	12	117.7	0	39
91.03	25.73	4.3	2003	2	20	43	14	22
90.51	26.12	4.2	2003	2	15	96	21	37
94.17	24.84	4	2003	1	26	99.6	4	27
94.96	25.69	4.1	2003	3	5	0	19	34
89.76	27.21	4	2003	2	5	0	2	13
89.47	27.43	5.4	2003	3	25	10	18	51
95	25.26	4.6	2003	3	18	70	8	20
94.07	23.04	4.6	2003	3	20	55.3	7	2
93.97	24.03	4.4	2003	3	15	0	3	59
93.9	22.71	4.4	2003	3	31	81.4	7	23
93.98	23.46	4.3	2003	3	10	83.6	3	40
91.95	26.62	4.3	2003	3	31	74.2	5	32
92.72	27.54	4.3	2003	4	6	0	14	7
95.04	24.73	4.2	2003	3	6	75	9	41

Longitude	Latitude	Magnitude	Year	Month	Date	Depth	Hrs	Mins
95.17	26.45	4.1	2003	3	14	62.5	20	23
94.42	22.56	4.1	2003	3	17	0	8	15
92.15	29.45	4.5	2003	4	18	17.3	21	21
94.62	24.85	4.1	2003	4	1	121.2	14	21
94.2	23.29	4.2	2003	5	2	118.9	21	25
92.71	26.37	4	2003	4	8	14	16	55
92.77	27.02	4.9	2003	5	30	57.5	10	27
92.29	26.91	4.7	2003	5	23	86.1	2	27
93.92	24.05	4.3	2003	5	12	0	16	0
94.18	22.65	4.3	2003	5	18	113.9	16	7
88.96	27.17	4.3	2003	5	25	0	4	57
93.73	23.23	4.3	2003	6	4	0	13	16
94.66	24.41	4.3	2003	6	9	121.7	14	43
91.3	27.16	4.2	2003	6	2	75.6	15	14
92.87	22.47	4.1	2003	5	9	0	19	29
93.16	24.9	4.3	2003	6	21	41.1	0	11
90.41	27.13	4.3	2003	6	26	13.8	11	18
94.05	22.84	4.3	2003	6	30	65	0	7
92.51	27.26	4.2	2003	6	28	0	13	31
95.06	24.66	4.1	2003	6	5	0	18	32
88.13	27.73	4.1	2003	6	23	80	12	30
92.44	22.92	5.6	2003	7	26	10	23	18
91.83	23.05	4.7	2003	8	1	10	3	19
92.2	22.62	4.5	2003	7	27	48.8	0	17
92.07	27.01	4.3	2003	7	26	0	17	3
93.57	23.4	4.3	2003	7	29	0	19	53
91.28	22.29	4.1	2003	7	27	0	13	12
94.62	24.62	4.1	2003	8	4	0	21	13
89.9	25.74	4	2003	7	5	0	19	41
94.63	23.41	4.3	2003	8	8	109	2	38
88.22	27.43	4	2003	7	8	15	12	30
94.19	23.89	4.6	2003	8	19	101.4	15	46

Longitude	Latitude	Magnitude	Year	Month	Date	Depth	Hrs	Mins
92.13	22.65	4.3	2003	8	13	0	8	11
92.74	27.44	4.3	2003	8	20	0	14	6
95.68	25.09	4	2003	7	20	94.3	4	51
95.06	24.87	4.6	2003	8	24	22	19	7
93.89	25.29	4.4	2003	8	26	61	20	54
93.76	22.86	4.4	2003	8	27	42	1	44
94.4	23.83	4.3	2003	8	22	154.8	11	55
93.29	22.71	4.2	2003	8	28	64.2	6	8
94.02	24.63	4	2003	7	30	0	14	36
94.54	23.48	4.6	2003	9	21	118.1	12	33
92.96	24.77	4.5	2003	9	1	42.3	5	53
94.35	24.2	4.4	2003	9	13	85.6	20	57
93.71	23.98	4.4	2003	10	10	85.6	14	11
95.06	23.45	4.3	2003	10	10	0	7	4
94.65	25.01	4.5	2003	10	15	119.3	9	10
93.37	23.65	4.5	2003	11	8	33	5	59
94.13	23.51	4.4	2003	10	12	47.2	21	33
94.87	24.6	4.4	2003	10	15	125.3	18	20
95.71	25.88	4.4	2003	11	3	33	19	27
94.1	22.97	4.4	2003	11	11	80.5	20	11
93.75	23	4.3	2003	10	12	0	8	28
92.21	29.09	4.3	2003	11	3	0	7	39
92.99	21.92	4.3	2003	11	9	12	19	36
94.08	23.86	4.1	2003	10	14	98.2	12	20
91.9	22.45	4.1	2003	10	17	35.8	6	26
94.96	24.61	4.6	2003	11	19	144.6	10	52
93.95	22.81	4.5	2003	11	17	39.7	15	43
93.36	25.84	4.5	2003	11	29	0	18	34
90.26	25.8	4.4	2003	12	2	17	21	14
88.44	29.01	4.3	2003	11	30	88.5	12	57
93.55	23.75	4.1	2003	12	6	62	15	24
92.31	22.8	4.5	2003	12	19	0	15	30

Longitude	Latitude	Magnitude	Year	Month	Date	Depth	Hrs	Mins
94.07	23.23	4.3	2003	12	18	106.5	8	48
93.25	22.05	4.2	2003	12	13	59.9	15	15
88.11	27.28	4.3	2003	12	27	66.5	14	12
95.14	26.14	4	2003	11	29	160.9	2	46
93.98	23.01	4.3	2004	1	3	91	15	44
92.36	22.75	4.2	2003	12	30	0	5	36
94.9	25.3	4	2003	12	2	33	10	29
92.85	23.64	4.2	2004	1	6	0	7	40
93.9	23.45	4.5	2004	1	19	73.8	1	42
94.27	22.82	4.6	2004	2	19	149.9	4	58
93.2	21.84	4.3	2004	1	28	61.3	13	6
89.54	27.04	4.3	2004	2	17	46.3	2	4
87.55	28.05	4.6	2004	2	27	10	12	53
94.09	23.45	4.6	2004	3	14	38.1	19	43
95.03	23.8	4.4	2004	3	1	0	12	9
93.49	22.41	4.3	2004	3	13	79.3	16	36
87.86	27.47	4.1	2004	2	18	10	1	23
94.95	23.54	4.7	2004	3	20	75	19	20
94.55	23.53	4.6	2004	3	25	110.5	12	57
95.47	25.27	4.5	2004	3	27	113	18	28
92.05	29.92	4.1	2004	2	28	0	3	16
95.03	24.62	4.7	2004	4	9	105.4	10	27
88.03	27.47	4.5	2004	3	31	25.7	22	32
93.54	25.12	4.4	2004	4	1	119.1	4	16
94.75	24.41	4.1	2004	3	13	146.7	18	21
93.7	23.32	4	2004	3	11	0	23	57
95.22	24.7	4.5	2004	4	13	83	21	10
88.36	27.6	4	2004	3	14	0	13	42
94.39	28.87	4.4	2004	4	20	0	8	17
93.43	29.2	4.4	2004	4	20	0	21	56
94.04	23.01	4.3	2004	4	24	99.5	13	54
94.2	23.25	4.4	2004	5	2	100.5	1	14

Longitude	Latitude	Magnitude	Year	Month	Date	Depth	Hrs	Mins
93.84	23.01	4.2	2004	5	10	0	9	21
93.76	27.77	4	2004	4	11	39.8	1	47
93.58	22.74	4.9	2004	5	24	163	2	34
95.05	24.85	4.6	2004	5	24	106	1	39
94.38	23.43	4.5	2004	5	16	92.7	4	57
93.61	25.29	4.4	2004	5	12	95	20	26
94.27	24.19	4.3	2004	5	21	121.5	6	15
93.87	24.18	4.2	2004	5	14	103.9	4	16
94.57	24.24	4.1	2004	5	24	131.8	8	1
89.22	26.28	4.9	2004	5	27	0	0	22
94.85	25.58	4.5	2004	6	3	81	13	1
88.19	28.05	4.4	2004	5	26	0	14	55
89.62	29.86	4.1	2004	6	5	33	8	47
92.07	26.73	4	2004	5	5	62.3	9	7
88.36	25.19	4.8	2004	6	7	39	5	28
93.89	22.21	4	2004	5	7	134.1	4	41
94.08	23.31	4.7	2004	6	14	33	11	38
94.37	24.19	4.5	2004	6	19	99.5	7	55
95.18	25.25	4.4	2004	6	19	33	10	24
89.75	24.66	4.3	2004	6	16	0	23	36
88.53	28.52	4.2	2004	6	17	93.1	21	46
94.21	24.85	4.1	2004	6	25	104.7	23	3
93.95	22.29	4	2004	6	11	167	23	44
95.35	25.22	4.3	2004	7	24	57.8	6	29
94.57	23.32	4.5	2004	8	6	119.5	7	8
94.15	22.54	4.5	2004	8	7	96.5	10	26
94.34	23.84	4.3	2004	8	11	91.1	20	40
93.92	23.22	4.2	2004	8	8	58.6	15	35
91.72	27.55	4.2	2004	8	9	14	8	18
90.33	25.86	4.1	2004	8	4	20	2	9
90.81	25.47	4.3	2004	8	12	0	18	8
93.8	23.27	4.1	2004	8	12	63.4	18	58

Longitude	Latitude	Magnitude	Year	Month	Date	Depth	Hrs	Mins
93.03	26.23	4	2004	7	13	71.2	19	31
94.24	23.38	4.9	2004	8	24	79	0	16
93.1	23.75	4.5	2004	9	17	0	0	16
94.67	24.38	4.3	2004	8	20	157.5	10	30
93.33	24.54	4.5	2004	9	18	33	12	37
94.98	24.9	4.5	2004	10	1	117.8	20	24
95.73	25.05	4.9	2004	10	8	33	6	28
94.05	24.32	4.7	2004	10	8	72	21	48
93.68	23.48	4.3	2004	9	24	61.7	15	58
94.82	25.46	4.3	2004	10	11	138	13	38
93.6	23.82	4.2	2004	9	24	86.6	14	33
92.09	26.35	4.1	2004	9	27	34	2	23
93.53	24.07	4.7	2004	11	5	33	21	15
94.96	23.58	4.3	2004	10	27	0	19	43
94.5	23.39	4.3	2004	11	4	121.4	10	2
94.35	24.9	4.2	2004	10	31	82	12	26
94.59	23.91	4.2	2004	10	31	128.8	22	42
93.13	23.63	4.2	2004	11	2	26	0	48
92.55	26.43	4.1	2004	11	2	19	8	23
87.73	27.73	4	2004	10	10	10	11	48
92.6	24.85	5.3	2004	12	9	35	8	48
91.07	27.29	4.5	2004	11	24	63.6	22	35
91.99	27.16	4.3	2004	11	12	72.5	1	59
94.31	25.2	4.3	2004	12	16	137.3	17	15
91.26	27.49	4.3	2004	12	16	45.8	17	29
93.81	22.87	4	2004	11	19	0	20	57
94.02	23.32	4.6	2004	12	28	78.3	11	27
94.14	22.35	4.5	2004	12	28	126.8	8	44
94.53	24.62	4.3	2004	12	24	82.3	5	46
94.69	23.47	4.2	2005	1	7	61	3	53
95.61	26.22	5.2	2005	2	3	90	20	13
92.4	24.66	5.2	2005	2	15	11	11	15

Longitude	Latitude	Magnitude	Year	Month	Date	Depth	Hrs	Mins
94.31	22.96	4.8	2005	1	18	15	3	2
94.68	24.32	4.7	2005	2	15	94	13	5
94.8	25.45	4.4	2005	2	21	77	23	7
92.85	27.41	4.1	2005	1	21	72.4	13	50
94.82	23.78	4.4	2005	2	22	83	7	46
94.79	25.45	5.2	2005	3	25	67	13	34
95.21	26.43	4.9	2005	3	23	69	5	59
87.9	28.22	4.8	2005	3	26	33	20	32
94.69	23.11	4.3	2005	2	28	123.5	13	54
94.59	24.5	4.2	2005	3	11	88.1	16	39
94.06	22.42	4.6	2005	4	12	0	14	12
93.5	22.36	4.5	2005	4	2	0	18	52
90.5	26.14	4.4	2005	4	28	0	14	20
94.56	24.34	4.3	2005	4	2	95.8	1	55
94.63	23.81	4.2	2005	4	19	93	14	4
95.3	24.42	4.3	2005	5	2	0	8	57
91.03	26.08	4.2	2005	5	3	33	0	38
92.35	22.7	4.1	2005	4	5	4	3	23
93.39	25.33	4.5	2005	5	6	103.6	13	55
92.17	22.81	4.4	2005	5	24	0	21	6
92.53	26.98	4.3	2005	5	29	69	10	46
95.57	26.25	4.5	2005	6	14	30	11	37
94.22	22.6	4.4	2005	6	5	110.1	21	40
87.97	27.46	4.3	2005	6	14	10	14	23
94.99	24.34	4.1	2005	5	25	93.7	9	24
94.6	24.29	4	2005	5	14	150.5	4	31
94.74	24.86	4	2005	5	19	0	5	18
93.08	26.57	4.6	2005	6	24	44.6	1	46
94.51	22.54	4.3	2005	6	20	102.1	18	22
87.21	26.14	4	2005	5	27	57	22	12
93.45	26.62	4.9	2005	7	17	30	6	12
92.25	22.97	4.8	2005	7	21	34	11	40

Longitude	Latitude	Magnitude	Year	Month	Date	Depth	Hrs	Mins
91.42	23.19	4.3	2005	7	26	24.3	18	27
93.61	22.82	4.2	2005	7	9	0	4	11
93.96	22.7	4.4	2005	8	17	15	6	25
91.9	23.02	4.2	2005	7	21	0	12	45
94.08	23.44	4.3	2005	8	24	146.3	20	32
92.55	27.56	4.2	2005	8	5	0	20	41
95.11	24.6	4	2005	7	27	152.3	16	50
94.67	24.79	5.5	2005	9	18	86	7	25
90.53	25.88	4.6	2005	9	12	35	16	59
87.29	27.66	4.4	2005	8	28	10	13	14
94	23.82	4.3	2005	9	2	66.2	15	36
94.51	25.24	4	2005	9	1	0	7	26
93.97	22.79	4.5	2005	10	29	128.9	17	29
95.43	24.58	4.4	2005	10	14	172.4	0	13
92.34	24.43	4.3	2005	11	8	0	4	51
92.35	27.1	4.3	2005	11	8	0	13	28
95.32	25.22	4.1	2005	10	9	96.7	18	40
95.58	25.94	4.1	2005	10	9	122.2	19	14
93.94	24.49	4.3	2005	11	22	108.7	15	28
93.06	25.43	4.1	2005	11	11	67	23	18
88.92	28.35	4.1	2005	11	25	0	12	50
95.64	26.7	4.1	2005	11	25	0	20	11
94.15	24.67	4.6	2005	12	13	77.9	3	30
90.38	25.73	4.6	2005	12	31	0	6	31
93.52	21.78	4.3	2005	12	17	94.1	11	2
92.24	25.5	4.2	2005	12	12	66.3	7	12
95.24	24.7	4.2	2006	1	9	144	1	28
92.17	26.48	4.1	2005	12	9	0	13	36
88.28	27.45	5.4	2006	2	14	30	0	55
92.28	27.44	4.8	2006	2	11	33	5	4
94.39	23.06	4.5	2006	1	27	61.4	23	58
91.59	24.03	4.3	2006	2	12	0	4	54

Longitude	Latitude	Magnitude	Year	Month	Date	Depth	Hrs	Mins
89.24	24.23	4.3	2006	2	19	18	1	2
94.27	24.41	4.2	2006	2	16	16	7	1
94.66	24.32	4.1	2006	1	26	0	6	54
91.24	27.59	4	2006	1	21	76.8	12	31
91.58	27.13	5.6	2006	2	23	10	20	4
94.4	24.4	4.8	2006	3	2	66	17	16
93.76	24.66	4.3	2006	3	21	92.7	7	29
94.55	24	4.3	2006	3	24	0	4	7
92.44	26.21	4	2006	2	24	30	2	36
92.38	26.89	5	2006	3	25	10	5	51
94.09	23.1	4.7	2006	3	25	96	20	13
94.24	23.62	4	2006	2	26	0	19	16
94.73	23.88	4.7	2006	4	14	33	16	24
94.21	24.12	4.5	2006	5	1	81.2	1	56
95.6	25.67	4.4	2006	5	9	33	23	17
94.43	25.59	4.2	2006	4	25	33	13	18
91.06	28.4	4.2	2006	5	7	0	6	11
95.38	25.11	4.1	2006	4	10	49.7	7	7
94.37	23.15	5.6	2006	5	11	30	17	22
95.04	24.76	4.9	2006	5	11	0	9	49
91.22	24.48	4.1	2006	4	11	0	1	7
92.35	27.54	4.1	2006	4	11	33	3	54
92.99	22.56	4.1	2006	5	11	0	17	42
87.74	28.03	4	2006	4	11	0	14	15
95.05	23.66	4.4	2006	5	17	240.7	11	22
94.27	23.34	4.3	2006	5	14	100	4	36
95.15	24.9	4.1	2006	5	15	96	23	58
91.78	21.26	4.9	2006	6	2	10	8	51
94.18	22.32	4.7	2006	6	19	10	14	53
94.57	24.84	4.5	2006	6	22	15	19	15
94.31	23.73	4.3	2006	5	30	134.4	13	42
94.22	22.67	4.3	2006	6	3	118.9	19	44

Longitude	Latitude	Magnitude	Year	Month	Date	Depth	Hrs	Mins
95.57	25.01	4.1	2006	6	3	0	13	11
94.47	24.49	4.6	2006	7	14	0	19	2
94.65	23.26	4.5	2006	7	12	0	1	3
91.13	27.63	4.3	2006	7	15	10.4	6	44
90.7	25.64	4.1	2006	6	19	33	16	57
95.04	25.62	4.1	2006	7	7	0	22	7
91.57	26.75	4	2006	6	19	0	11	57
95.08	24.53	4	2006	6	23	0	2	45
88.69	27.47	4	2006	6	23	0	22	7
92.7	24.45	4.8	2006	8	12	33	20	46
94.38	24.27	4.6	2006	8	2	91.7	13	6
93.16	23.72	4.3	2006	8	3	102.8	12	32
93.86	23.22	4.3	2006	8	13	99.6	15	10
89.21	26.97	4	2006	7	17	10	13	47
94.13	23.86	4	2006	7	18	0	20	12
93.05	27.16	4.2	2006	8	21	115	3	34
89.89	23.5	4	2006	8	5	38	14	39
94.48	24.73	4.1	2006	9	10	93	6	12
94.76	26.44	4	2006	8	10	0	16	21
94.3	22.61	4.8	2006	9	24	99.4	8	45
94.2	23.65	4.4	2006	9	29	93	12	13
92.55	25.74	4	2006	9	5	0	1	40
92.44	27.65	4.9	2006	10	14	33	1	18
87.79	23.81	4	2006	9	18	36	12	45
93.14	22.11	4.3	2006	10	19	33	17	35
92.3	27.44	4.3	2006	10	20	41.3	1	25
94.33	23.43	4.6	2006	10	24	128.6	14	0
93.74	22.38	4	2006	10	1	0	18	47
95.17	24.77	4.9	2006	11	6	96	1	19
92.35	24.53	4.9	2006	11	10	33	13	21
93.48	21.83	4.8	2006	11	3	33	14	43
94.06	24.08	4.3	2006	11	16	79	18	11

Longitude	Latitude	Magnitude	Year	Month	Date	Depth	Hrs	Mins
94.77	23.2	4.2	2006	11	19	69.2	6	41
90.29	25.04	4.3	2006	12	20	10	10	30
89.91	26.86	4.1	2006	11	26	0	18	3
91.69	25.24	4.3	2007	1	4	5.3	11	58
91.71	24.15	4.2	2007	1	2	0	13	0
92.18	23	4.1	2006	12	6	41.2	14	42
89.6	27.17	4.7	2007	1	20	10	7	33
94.55	22.95	4.4	2007	1	12	118.6	12	17
92.97	22.66	4.3	2007	1	21	50.5	2	48
94.01	23.55	4.3	2007	1	21	74	16	15
91.09	27.66	4.1	2006	12	24	0	17	21
92.47	26.18	4.1	2007	1	17	0	6	13
94.24	22.47	4	2006	12	21	0	17	56
94.28	24.97	4.6	2007	1	24	38	11	3
89.86	25.69	4.5	2007	1	24	19	10	29
94.05	28.21	4.5	2007	2	2	35.2	0	41
94.63	24.33	4.4	2007	2	17	105.1	23	52
91.34	26.33	4.2	2007	2	14	35	11	44
94.85	24.65	4.1	2007	1	31	109.6	2	3
87.66	27.98	4.1	2007	2	6	59	21	38
93.32	27.63	5.1	2007	3	8	10	17	33
94.73	24.34	4.5	2007	3	9	90.2	14	50
90.25	24.73	4.5	2007	3	9	0	23	36
95.17	25.21	4.1	2007	3	1	100.6	3	40
94.47	23.69	4.6	2007	3	13	87.2	22	46
91.28	27.16	4.4	2007	3	14	57.1	1	9
92.97	26.25	4	2007	2	15	0	10	2
92.52	24.52	4	2007	2	15	16	18	13
95.5	26.29	4.4	2007	3	18	81.7	21	55
93.76	22.51	4.3	2007	3	19	40.2	5	11
88.69	28.86	4.1	2007	3	22	0	18	29
92.93	22.16	4	2007	2	23	0	7	3

Longitude	Latitude	Magnitude	Year	Month	Date	Depth	Hrs	Mins
95.08	24.88	4.4	2007	4	5	100	8	42
87.72	28.23	4.3	2007	4	17	63.4	7	4
94.3	23.36	4.6	2007	5	7	94	5	58
94.46	22.55	4.2	2007	4	10	85.3	16	10
92.65	27.55	4.2	2007	4	11	73.5	5	21
87.32	27.17	4.1	2007	5	6	11.5	23	53
94.59	24.17	4	2007	4	11	0	0	31
88.42	27.45	5	2007	5	20	43	14	18
87.78	27.34	4.3	2007	5	16	33.9	7	17
87.38	24.45	4.3	2007	5	25	60	9	21
87.57	27.77	4.3	2007	5	28	0	3	29
94.5	25.08	4.3	2007	6	4	108.5	8	31
94.64	25.97	4.8	2007	6	25	15	18	9
94.62	25.07	4.3	2007	6	21	108	14	26
88.09	27.33	4.1	2007	5	26	0	10	28
94.5	23.78	4.3	2007	7	2	104.4	16	38
94.62	24.38	4	2007	6	3	208	4	26
88.86	25.42	4.9	2007	7	22	39	14	3
94.26	23.93	4.4	2007	7	20	104.7	17	1
94.91	24.63	4.3	2007	7	17	131.1	11	42
87.89	27.47	5	2007	8	11	35	14	35
92.05	22.98	4.9	2007	7	28	33	0	48
93.98	23.06	4.7	2007	8	16	37	5	16
94.39	24.25	4.4	2007	8	10	90.9	1	47
94.5	22.99	4.2	2007	8	18	122	0	56
92.39	22.84	4.1	2007	7	28	0	1	0
92.59	23.19	4.1	2007	8	4	74.8	5	36
93.97	23.9	4.1	2007	8	13	33	8	28
93.67	23.01	4.3	2007	8	26	131	3	20
90.25	23.08	4.3	2007	8	31	65.4	12	6
95.11	24.65	4	2007	8	4	159.9	20	16
95.33	25.93	4.8	2007	9	25	123.6	3	2

Longitude	Latitude	Magnitude	Year	Month	Date	Depth	Hrs	Mins
94.64	23.91	4.8	2007	9	26	54.9	16	17
92.71	23	4.6	2007	9	7	38	20	14
93.95	22.56	4.4	2007	9	25	97	2	43
95.45	25.03	4.2	2007	9	22	39	22	57
91.16	25.37	4.1	2007	9	18	40	19	49
92.45	27.05	4	2007	8	31	15.4	3	44
87.8	27.59	4	2007	9	1	73	1	33
93.81	23.83	4.1	2007	10	2	56.6	6	2
90.76	26.44	4	2007	9	7	17.7	3	44
94.94	24.56	4	2007	9	12	127.4	12	51
92.39	22.22	4.9	2007	11	7	10	7	10
92.11	29.4	4.4	2007	10	29	0	4	54
93.41	22.11	4.3	2007	10	14	50.2	0	46
91.73	23.7	4.3	2007	10	20	0	10	10
93.16	26.32	4.3	2007	11	17	48.4	3	59
93.9	23.91	4.2	2007	11	1	64.7	4	9
94.42	23.23	4.1	2007	11	7	99.6	2	27
92.13	29.66	4.6	2007	11	18	8	5	49
92.1	23.54	4	2007	10	18	35.3	22	9
94.37	23.58	4.8	2007	11	29	115	19	0
95.27	26.07	4.6	2007	11	30	95.9	8	44
94.19	22.2	4.2	2007	11	27	41.9	23	37
92.32	22.78	4.1	2007	11	25	35.5	17	39
94.04	23.53	4	2007	10	30	71.7	22	35
92.6	24.01	4	2007	11	3	0	6	13
90.96	25.75	4	2007	11	5	44.6	1	0
93.71	24.07	4.6	2007	12	7	97	6	56
94.54	23.53	4.3	2007	12	13	0	10	56
94.19	24.26	4.2	2007	12	11	80.3	13	45
95.65	24.63	4	2007	11	14	0	13	59
93.7	23.48	4.5	2007	12	15	50.6	4	24
94.43	23.62	4.3	2007	12	23	106.7	3	36

Longitude	Latitude	Magnitude	Year	Month	Date	Depth	Hrs	Mins
94.3	23.33	4.1	2007	12	23	103.6	4	25
92.51	22.91	4.9	2008	1	12	34	22	44
94.52	22.67	4.5	2008	1	14	88.6	22	54
94.09	27.82	4.4	2008	1	25	9.5	15	10
93.09	26.83	4.3	2008	1	1	27	7	1
95.12	24.72	4.2	2008	1	13	136	15	5
92.5	22.88	4.8	2008	1	31	45	13	22
94.8	25.67	4.7	2008	2	14	67.6	1	35
94.05	23.19	4.4	2008	2	26	71	22	20
92.65	27.52	4.3	2008	1	29	50.2	12	23
95.4	26.39	4.3	2008	2	10	68.5	8	38
94.13	22.56	4.3	2008	2	25	92.6	9	46
89.93	25.92	4.1	2008	2	17	0	14	42
87.64	25.61	4.1	2008	2	21	0	6	57
90.47	27.69	4.1	2008	2	23	18.8	13	39
87.89	27.46	4.1	2008	2	23	60.2	14	49
93.99	24.09	4	2008	2	4	74	14	18
95.13	24.6	4.4	2008	3	10	103.4	0	1
91.94	26.75	4.4	2008	3	13	38	15	42
94.98	24.93	4.3	2008	3	8	35	16	51
92.86	25.08	4.1	2008	3	14	16.3	13	27
88.57	27.47	4	2008	2	18	53.8	8	56
92.25	26.25	4.6	2008	4	17	44	1	12
93.29	24.04	4.5	2008	3	26	35	4	38
93.98	23.81	4.5	2008	4	20	88.4	0	30
94.56	24.05	4.4	2008	3	28	121.2	6	1
93.01	26.4	4.4	2008	4	3	46	19	5
94.4	22.58	4.3	2008	4	6	101.5	2	23
92.08	22.72	4.3	2008	4	8	40	19	10
92.61	22.96	4.1	2008	4	8	43.5	15	49
95.02	24.65	4	2008	3	25	112.2	23	26
95.48	24.56	4	2008	4	5	74.3	18	42

Longitude	Latitude	Magnitude	Year	Month	Date	Depth	Hrs	Mins
92.7	27.53	4.5	2008	5	10	71.2	5	58
95.59	24.46	4.4	2008	6	7	45.8	10	34
91.17	23.97	4.3	2008	5	8	42.4	22	20
93.34	28.23	4.6	2008	6	9	0	8	27
94.23	22.31	4.3	2008	5	27	57	1	46
91.84	26.35	4.3	2008	5	29	46	10	34
94.6	23.49	4.3	2008	5	29	131.7	13	5
94.22	23.37	4.3	2008	6	2	53.1	11	43
94.35	24.37	4.2	2008	5	17	81.3	8	8
95.12	24.35	4.2	2008	5	21	133	7	59
89.2	29.04	4.2	2008	5	25	10	10	28
92.89	27.1	4.1	2008	5	13	0	20	44
89.62	29.85	4.2	2008	6	14	0	11	38
94.54	23.46	4.4	2008	6	24	110.2	20	49
94.97	24.07	4.2	2008	6	28	0	0	59
94.14	22.81	4.1	2008	5	28	0	3	38
94.36	23.68	5.2	2008	7	27	105	22	42
95.44	25.98	4.8	2008	7	7	38	2	50
90.56	24.79	4.6	2008	7	26	15	18	51
94.16	22.83	4.5	2008	7	25	91.9	18	9
91.97	27.38	4.3	2008	7	14	60.5	13	28
94.91	24.96	4.2	2008	7	18	105.2	13	10
93.31	24.57	4.1	2008	7	22	69.9	2	20
88.46	24.41	4	2008	7	5	39	16	55
89.05	22.15	4.9	2008	8	22	650	18	7
92.72	22.31	4.7	2008	8	22	35	18	6
87.95	28.25	4	2008	8	1	0	8	50
95.08	26.19	4.3	2008	9	4	74	20	33
94.27	23.19	4	2008	8	7	95.8	20	0
90.14	29.08	5	2008	9	23	10	19	57
90.69	23.39	4.6	2008	9	20	0	12	0
90.61	29.87	4.1	2008	9	21	0	6	35

Longitude	Latitude	Magnitude	Year	Month	Date	Depth	Hrs	Mins
92.14	27.32	4	2008	8	27	33	5	35
90.36	29.84	6.2	2008	10	6	10	8	30
91.05	29.75	4.9	2008	10	6	24.5	14	26
91.37	29.42	4.8	2008	10	6	0	10	45
91.66	29.59	4.8	2008	10	7	0	21	48
89.68	28.92	4.7	2008	10	9	10	3	28
90.75	30.06	4.6	2008	10	10	10	21	18
93.91	23.56	4.5	2008	10	8	66	6	46
90.47	28.78	5	2008	11	6	10	15	4
90.67	29.65	4.3	2008	10	6	0	8	59
87.84	27.47	4.3	2008	10	7	3.3	18	9
92.33	29.58	4.2	2008	10	7	0	19	58
89.92	29.67	4.2	2008	10	9	0	4	39
94.57	23.02	5	2008	11	10	108	20	55
90.45	29.84	4.8	2008	11	23	0	13	22
87.36	23.64	4.6	2008	11	8	0	16	51
92.46	27.5	4.5	2008	11	24	10	14	58
92.85	25.82	4.3	2008	11	7	50.8	0	29
91.14	23.77	4.3	2008	11	18	0	23	0
92.78	27.75	4.2	2008	11	14	81.7	4	26
88.05	27.37	5.5	2008	12	2	24.7	5	11
94.05	22.82	4.9	2008	11	29	87.1	6	54
93.64	23.14	4.6	2008	12	5	73.9	12	59
94.66	24.9	4.4	2008	12	14	79.6	16	54
95.04	24.03	4.3	2008	12	18	0	12	15
91.59	23.98	4.1	2008	11	18	0	23	15
94.53	22.58	4.9	2008	12	19	108.1	11	52
95.32	24.89	4.1	2008	11	22	133.4	8	4
88.63	27.22	5.3	2008	12	25	33	0	26
94.73	24.61	4.8	2008	12	23	87.2	16	2
91.97	25	4.4	2008	12	23	41.7	13	20
94.3	25.9	4.8	2009	2	24	10	17	46

Longitude	Latitude	Magnitude	Year	Month	Date	Depth	Hrs	Mins
90.2	26	4.4	2009	2	15	30	19	35
94.5	24.7	4.5	2009	5	15	15	15	6
91.7	26.4	4	2009	4	25	10	14	29
94.6	24.3	5.9	2009	9	3	100	19	51
94.8	25.2	5.3	2009	8	30	66	19	27
92.5	26.6	4.9	2009	8	19	20	10	45
93.4	22.3	4.8	2009	8	5	29	2	58
91.5	27.3	6.2	2009	9	21	8	8	53
91.4	27.3	5.2	2009	10	29	5	17	0
94.5	23.5	4.9	2009	10	11	10	18	26
92.6	27.7	4.5	2009	11	17	30	17	39
90.3	27.6	4.3	2009	11	18	54	0	49
90	26.6	4.2	2009	10	29	10	19	56
94.8	24.5	5.5	2009	12	29	80	9	1
91.4	27.3	5.5	2009	12	31	7	9	57
91.8	22	5.1	2009	12	13	10	14	41
94.5	23	5.6	2010	3	12	96	23	19
92.8	27.8	4	2010	2	16	8	20	57
93.2	25.8	4	2010	2	23	30	6	55
93.8	24.2	4.3	2010	4	27	45	14	20
94.1	24.3	4.1	2010	4	28	11	18	54
91.2	27.6	4.3	2010	7	21	10	2	57
91.3	26.5	4.1	2010	7	26	31	19	43
90.2	25.9	5	2010	9	11	20	7	2
90.7	23.6	4.8	2010	9	10	15	17	54
94.9	25.2	4.6	2010	8	30	93	9	39
93.3	25	4.8	2010	12	12	15	1	40
93.8	28.6	4.6	2010	11	17	33	4	37
94.6	24.8	6.4	2011	2	4	72	13	53
94.4	24.3	4.6	2011	1	27	75	22	40
91	23.5	4	2011	2	12	10	10	22
92.5	25.5	4.3	2011	4	26	70	17	0

Longitude	Latitude	Magnitude	Year	Month	Date	Depth	Hrs	Mins
94.7	25.9	4.3	2011	4	29	10	2	39
88	27.5	4.9	2011	6	3	26	0	53
91.1	23.9	4.2	2011	6	23	30	12	39
89.7	23.7	4.1	2011	6	9	10	7	34
88.6	25.3	4.5	2011	7	28	18	17	53
88.1	27.8	6.9	2011	9	18	46	12	40
88.5	27.6	5	2011	9	18	16	13	11
94.9	23.7	4.8	2011	9	22	128	14	17
93.8	24.4	4.5	2011	9	23	33	13	23
94.3	25.2	4.2	2011	9	4	20	20	52
95.3	25.1	5.8	2011	11	21	80	3	15
94	24.8	4.5	2011	10	21	36	14	40
88	27.7	4.5	2011	12	14	50	20	20
91.8	23.5	4.2	2012	1	1	12	2	35
93.7	26.6	4.4	2012	2	10	10	15	45
94.7	25.3	4	2012	1	11	10	22	23
93.7	24.7	4.5	2012	2	26	36	15	55
87.8	26.1	4.9	2012	3	27	12	23	40
93	26.6	5.4	2012	5	11	20	12	41
91.6	26.7	4.5	2012	5	27	18	15	1
95.1	27.5	4.4	2012	5	4	15	20	9
94.4	25.2	4	2012	5	22	63	12	19
88	27.4	4	2012	5	30	10	1	54
94.6	25.7	5.8	2012	7	1	50	4	13
94.2	23	6	2012	7	29	70	2	21
94.2	25.5	5.5	2012	7	14	35	19	55
93.2	26.5	4.5	2012	7	10	56	13	3
92.5	26.7	5	2012	8	19	35	9	24
91.8	24.8	4.3	2012	8	5	19	6	36
92.8	26.9	5.1	2012	10	2	35	18	37
91.1	25.7	4.2	2012	9	6	10	18	27
88.5	27.4	4.1	2012	9	18	10	12	26

Longitude	Latitude	Magnitude	Year	Month	Date	Depth	Hrs	Mins
95.2	26.2	4.1	2012	9	21	96	14	20
94	23.9	4	2012	9	11	10	11	9
93.6	24.7	4.2	2012	10	12	10	23	16
94.3	28.4	4.2	2012	10	28	10	5	44
94.2	28.8	4	2012	10	24	80	21	7
95.7	25.9	4.7	2012	11	30	10	3	52
91.5	23.7	4.2	2012	11	25	15	6	1
91.6	24.2	4.2	2012	12	30	30	8	16
88.3	27.3	4.1	2012	11	30	10	19	39
94.8	25.1	4.1	2012	12	5	85	8	5
94.9	25.4	5.9	2013	1	9	89	1	41
94.3	28.1	4.5	2013	1	7	10	5	32
92.2	24.8	5.2	2013	3	2	10	1	30
89.1	25.4	4.5	2013	2	19	10	21	5
91.4	26.1	4.1	2013	3	4	5	16	5
92.5	27.5	4.7	2013	4	27	10	5	16
92	26.3	4.6	2013	4	16	16	1	23
94.8	24.2	5	2013	8	2	15	12	4
91.4	24.1	4.2	2013	7	8	10	3	44
94.9	25.3	4.8	2013	9	7	90	3	24
92.4	27.4	4.8	2013	9	9	33	11	58
92.5	26.7	4.2	2013	8	21	30	6	57
88.5	27.4	5	2013	10	3	10	6	12
93.5	26.5	5.5	2013	11	6	20	4	16
94.2	22.9	4.7	2013	10	29	46	7	51
89.5	26.6	4.7	2013	12	4	10	13	5
94.5	24.6	4	2013	11	12	90	19	52
93.2	24.3	4.5	2013	12	30	10	9	44
94.9	24.9	4.2	2013	12	17	118	7	34
93.9	23.9	5.1	2014	1	29	33	13	46
92.5	27.2	4.8	2014	2	23	10	17	4
94.3	22.9	4.7	2014	1	30	66	12	17

Longitude	Latitude	Magnitude	Year	Month	Date	Depth	Hrs	Mins
93.7	24.5	4.2	2014	2	26	10	20	58
91.2	24.3	4	2014	2	28	10	13	11
92.4	26.4	4.4	2014	4	1	33	17	45
93.6	25.4	4.3	2014	4	6	28	6	38
93.1	23.3	4	2014	4	4	10	6	57
94.5	24.4	4.8	2014	5	29	10	3	23
94.8	25.2	4.6	2014	5	28	35	3	19
90.4	26.5	4.5	2014	5	30	10	6	37
93.4	22.3	4.2	2014	6	4	41	7	20
94.6	24.7	4.8	2014	8	16	10	16	39
93.1	22.1	5.2	2014	9	9	7	9	28
95.2	25.1	4.6	2014	9	6	139	17	12
92.8	27.8	4.4	2014	9	13	10	3	31
91.4	23.9	4.2	2014	8	17	98	20	34
90.2	26.1	4.2	2014	9	12	10	7	56
92.3	27.6	4.1	2014	8	20	10	8	4
93.9	24.1	4.8	2014	10	24	10	0	5
94.7	23.7	4	2014	10	24	80	5	11
94.5	24.3	5	2014	12	21	80	5	37
92.5	27	4.8	2014	12	4	10	23	53
94.4	23.5	4.2	2014	12	27	10	2	2
92.9	22.3	4.1	2014	12	22	10	23	24
95	25.1	4.8	2015	1	24	10	16	11
89.9	26.4	4.1	2014	12	25	10	7	40
92	26.4	4	2014	12	29	10	17	26
94	24.2	5	2015	2	12	90	14	32
93.2	26.4	4.1	2015	2	1	10	16	0
92.5	22.6	4	2015	1	15	5	1	33
92.7	26.8	4.8	2015	4	16	10	22	5
89.5	21.9	4.5	2015	4	8	10	1	43
94.5	24.5	4	2015	3	17	96	15	28
92.9	22	4	2015	3	22	10	12	6

Longitude	Latitude	Magnitude	Year	Month	Date	Depth	Hrs	Mins
88.1	26.7	5.1	2015	4	27	10	12	35
94.3	26.5	4.7	2015	4	30	10	19	21
88.1	27.3	4	2015	4	23	10	20	26
93.8	24.4	4.1	2015	5	26	30	17	24
90.1	26.5	5.6	2015	6	28	10	1	5
93.4	28.1	4	2015	5	28	10	11	46
90.4	26.8	4.5	2015	7	10	10	12	53
90.6	25.6	4.2	2015	7	10	10	22	27
91	27.3	4.3	2015	7	27	10	7	33
87.9	27.6	4.2	2015	9	7	15	12	55
91.8	26.6	4.6	2015	9	25	15	16	57
94.5	24.7	4.5	2015	9	17	72	18	34
89.4	25.5	4	2015	8	28	10	19	21
92.8	26.3	4	2015	9	5	10	5	39
88.8	27.2	4.5	2015	10	10	15	1	48
93.8	25.1	4.1	2015	10	11	21	8	34
92.3	24.6	4.9	2015	10	29	15	22	15
93.2	22.5	4	2015	10	2	5	11	29
92.8	26.4	4.9	2015	11	25	10	21	45
91.8	25.5	4	2015	10	31	10	5	16
93.5	24.8	6.7	2015	1	3	17	23	5
93.2	26.4	4.2	2015	12	23	30	9	22